# ENGINEERING ANTI-BACTERIAL ANTIBODIES FOR THERAPEUTIC AND DIAGNOSTIC PURPOSES

**Thae Thae Min**

**A Thesis Submitted in Partial Fulfillment of the Requirement for the Degree of Doctor of Philosophy Program in Biotechnology**

**Suranaree University of Technology**

**Academic Year 2020**

# วิศวกรรมแอนติบดีต่อเชื้อแบคทีเรีย เพื่อการรักษาและตรวจวินิจฉัย

**นางสาว เธ เธ มิน**

มหาวิทยาลัยเทคโนโลยีสุรนารี

**วิทยานิพนธ์นี้เป็นส่วนหนึ่งของการศึกษาตามหลักสูตรปริญญาวิทยาศาสตรดุษฎีบัณฑิต**
**สาขาวิชาเทคโนโลยีชีวภาพ**
**มหาวิทยาลัยเทคโนโลยีสุรนารี**
**ปีการศึกษา 2563**

**ENGINEERING ANTI-BACTERIAL ANTIBODIES FOR THERAPEUTIC AND DIAGNOSTIC PURPOSES**

Suranaree University of Technology has approved this thesis submitted in partial fulfillment of the requirements for the Degree of Doctor of Philosophy.

Thesis Examining Committee

(Assoc. Prof. Dr. Apichat Boontawan)

Chairperson

(Prof. Dr. Montarop Yamabhai)

Member (Thesis Advisor)

(Prof. Dr. Watchara Kasinrerk)

Member

(Assoc. Prof. Dr. Griangsak Eumkeb)

Member

(Dr. Poochit Nonejuie)

Member

(Assoc.Prof. Flt. Lt. Dr. Kontorn Chamniprasart)

Vice Rector for Academic Affairs and Internationalization

(Prof. Dr. Neung Teaumroong)

Dean of Institute of Agricultural Technology

มหาวิทยาลัยเทคโนโลยีสุรนารี

เธ เธ มิน : วิศวกรรมแอนติบอดีต่อเชื้อแบคทีเรีย เพื่อการรักษาและตรวจวินิจฉัย (ENGINEERING ANTI-BACTERIAL ANTIBODIES FOR THERAPEUTIC AND DIAGNOSTIC PURPOSES) อาจารย์ที่ปรึกษา : ศาสตราจารย์ ดร. มณฑารพ ยมาภัย, 229 หน้า.

แอนติบอดีสามารถใช้เป็นยารักษาโรค ตั้งแต่ในช่วงคริสตศักราช 1980 ที่มีการใช้เซรั่มซึ่งประกอบด้วยแอนติบอดีแบบโพลีโคลนอลในการรักษา ก่อนที่จะไม่ได้รับความนิยมเนื่องจากความซับซ้อนของเซรั่ม และมีการค้นพบยาปฏิชีวนะ จนเมื่อมีการพัฒนาเทคโนโลยีในการผลิตแอนติบอดีแบบโมโนโคลนอล (monoclonal antibody) ในปี 1975 และการใช้เทคโนโลยีเฟจ ซึ่งได้เริ่มขึ้นตั้งแต่ปี 1990 เพื่อการตรวจวิเคราะห์ และรักษา จนถึงในปัจจุบัน โมโนโคลนอลแอนติบอดีได้ถูกใช้กันอย่างแพร่หลาย โดยเฉพาะในการรักษาโรคมะเร็ง และกลุ่มโรคไม่ติดต่อเรื้อรัง แต่แอนติบอดีสำหรับใช้ในการรักษาโรคติดต่อ (infectious diseases) ชนิดต่าง ๆ นั้นยังมีไม่มากนัก ดังนั้น ในการศึกษานี้ จึงมีวัตถุประสงค์เพื่อพิสูจน์ว่าแอนติบอดีชนิดเส้นเดี่ยวส่วนแปรผันสูง (scFv) ที่ได้จากการคัดเลือกด้วยเทคโนโลยีเฟจนั้น สามารถใช้ในการรักษา และการตรวจวินิจฉัยการติดเชื้อแบคทีเรียทั้งชนิดแกรมบวก คือ โพรพิโอนิแบคทีเรียม แอคเน่ (*Propionibacterium acnes*) และแบคทีเรียแกรมลบ คือ ซูโดโมแนส เอโรจิโนซ่า (*Pseudomonas aeruginosa*) จากการคัดเลือกแอนติบอดีโดยใช้คลังย่าโม 1 ซึ่งเป็นคลังที่แสดงชิ้นแอนติบอดีมนุษย์ส่วน scFv บนโปรตีนปกคลุมผิว เป็นแหล่งในการคัดเลือกแอนติบอดีนั้น พบว่าสามารถคัดเลือกแอนติบอดี scFv ที่จับจำเพาะต่อเชื้อ *P. acnes* และ *P. aeruginosa* จำนวน 3 และ 1 โคลน ตามลำดับ โดยแอนติบอดี ต่อเชื้อ *P. acnes* ชื่อโคลน yPac1A8 และ แอนติบอดี ต่อเชื้อ *P. aeruginosa* ชื่อโคลน yPgi3G4 ได้ถูกนำมาศึกษาเพื่อยืนยันคุณสมบัติการจับจำเพาะด้วยวิธีการต่าง ๆ 6 วิธีคือ วิธีอีไลซ่า, เวสเทอร์นบลอต, โฟลไซโตเมตรี, การส่องดูผ่านกล้องจุลทรรศน์คอนโฟคอล กล้องจุลทรรศน์ เดลต้าวิชั่น อัลตร้า และกล้องจุลทรรศน์อิเลคตรอน จากนั้นเมื่อนำแอนติบอดีต่อเชื้อ *P. acnes* yPac1A8 มาทดสอบด้วยวิธีการตกตะกอนด้วยอิมมูน พบว่าแอนติบอดีจับกับโปรตีนชื่อ แคมพ์ แฟคเตอร์ 1 ของเชื้อแบคทีเรีย *P. acnes* จากนั้นแอนติบอดีทั้งสองโคลนนี้ได้ถูกนำมาตัดต่อทางพันธุวิศวกรรมเพื่อเชื่อมต่อกับโปรตีนเรืองแสงสีเขียว ชนิด EmGFP เพื่อใช้การในการทดลองย้อมสีทางอิมมูนแบบขั้นตอนเดียว นอกจากนี้แล้วแอนติบอดียังถูกนำมาเชื่อมต่อกับโปรตีน ไบโอติน ของเชื้อแบคทีเรีย เอสเชอริเชียโคไล (*Escherichia coli*) ได้สำเร็จ ซึ่งสามารถนำไปใช้ในการศึกษาต่อได้ในอนาคต สุดท้ายนี้แอนติบอดี scFv ทั้งสองโคลนนี้ได้ถูกทำพันธุวิศวกรรมแอนติบอดีเป็นแอนติบอดีชนิดเต็มรูปแบบ คือ IgG แล้วนำไปใช้ในการศึกษาผลทางชีววิทยาของแอนติบอดีต่อเชื้อแบคทีเรีย ในรูปแบบต่างๆ คือ กระบวนการเกาะกลุ่มของเซลล์ การทำลายเซลล์ผ่านกระบวนการกระตุ้นปฏิกิริยาคอมพลีเมนต์

และการตรึงแบคทีเรียให้เซลล์เม็ดเลือดขาวมนุษย์ชนิด แมโครเฟจ กิน ผลการศึกษาเหล่านี้แสดงว่า แอนติบอดี yPac1A8 และ yPgi3G4 มีศักยภาพที่จะถูกนำไปพัฒนาต่อเพื่อใช้ในการรักษาในอนาคต

มหาวิทยาลัยเทคโนโลยีสุรนารี

สาขาวิชาเทคโนโลยีชีวภาพ ลายมือชื่อนักศึกษา_____

ปีการศึกษา 2563 ลายมือชื่ออาจารย์ที่ปรึกษา_____

THAE THAE MIN : ENGINEERING ANTI-BACTERIAL ANTIBODIES FOR THERAPEUTIC AND DIAGNOSTIC PURPOSES. THESIS ADVISOR : PROF. MONTAROP YAMABHAI, Ph.D., 229 PP.

SINGLE CHAIN FRAGMENT VARIABLE/AFFINITY SELECTION/GRAM-POSITIVE/GRAM-NEGATIVE BACTERIA/SCFV LIBRARY

Antibodies have been used as therapeutic agents. Polyclonal serum therapy started in the 1890s and soon became obsolete because of its complications and the discoveries of antibiotics. After the introduction of monoclonal antibody technology in 1975 and that of phage display antibody technology in 1990, antibodies are once again regarded as therapeutic agents. Nowadays, monoclonal antibodies for cancer and non-communicable diseases are the best-selling drugs on pharmaceutical market. But there are very few antibody biologics available for infectious diseases. This study aimed to prove that single chain fragment variables (scFv) obtained by affinity selection (biopanning) can be engineered into therapeutic and diagnostic agents for bacterial infections using one Gram-positive (*Propionibacterium acnes*) and one Gram-negative (*Pseudomonas aeruginosa*) model bacteria and the Yamo-I phage display human scFv library. Three anti-*P. acnes* scFv and one anti-*P. aeruginosa* scFv were identified. Two scFv, yPac1A8 (anti-*P. acnes* scFv) and yPgi3G4 (anti-*P. aeruginosa* scFv) were further studied. Their specific binding property was confirmed by ELISA, Western Blot, flow cytometry, confocal microscopy, deltavision ultra microscopy, and electron microscopy. Anti-*P. acnes* scFv, yPac1A8, was used to immunoprecipitate its target, CAMP factor 1, from *P. acnes*. Both scFv were subcloned to conjugate with EmGFP

and used as a one-step immunostaining reagent. Moreover, both scFv were engineered to couple with the biotin carboxyl carrier protein of *Escherichia coli* and successfully biotinylated for future applications. Finally, both scFv were engineered to become full-length IgG for three functional assays; namely, agglutination of live target bacteria, enhancement of complement-mediated bacteriolysis, and opsonization of target bacteria for phagocytosis by human macrophage cells. The results indicated that both yPac1A8 and yPgi3G4 IgG have the potential to be further developed into antibody therapeutics in the future.

มหาวิทยาลัยเทคโนโลยีสุรนารี

School of Biotechnology

Academic Year 2020

Student's Signature _____

Advisor's Signature _____

# ACKNOWLEDGEMENT

First of all, I would like to express my sincere gratitude to my advisor Professor Dr. Montarop Yamabhai for the continuous support of my PhD study and related research, for her patience, motivation, and immense knowledge. I could not have imagined having a better advisor and mentor for my PhD study.

I am deeply thankful to Assoc. Professor Dr. Griangsak Eumkeb, Suranaree University of Technology, Thailand, Professor Dietmar Haltrich, University of Natural Resources and Life Sciences, Vienna, Austria, and Asst. Prof. Pattra Suntornthiticharoen, Rangsit University, Thailand for kindly sharing bacteria for my research.

My sincere thanks go to Dr. Poochit Nonejuie and Mr. Htut Htut Htoo, The Microbe Lab, Mahidol University, Thailand for helping me with Deltavision Ultra microscpy. I wish to acknowledge the staff of Confocal and Electron microscopy sections of Suranaree University of Technology, Electron microscopy section of Chulalongkorn University and Electron microscopy section of Kasetsart University for helping me with immunoelectron microscopy work.

I am grateful to all the faculty members and Ms. Prangkhaw Prukhett of School of Biotechnology, Suranaree University of Technology, Thailand for their kind support throughout my studies. I would like to give special thanks to MY LAB members for their kind help. I would like to thank SUT-ASEAN PhD Scholarship programme 2014 for giving me the opportunity to study at Suranaree University of Technology.

Thae Thae Min

# TABLE OF CONTENTS

**Page**

ABSTRACT (THAI)..... I

ABSTRACT (ENGLISH)..... III

ACKNOWLEDGEMENT..... V

TABLE OF CONTENTS..... VI

LIST OF TABLES..... XIII

LIST OF FIGURES..... XVII

LIST OF ABBREVIATIONS..... XXII

**CHAPTER**

**I INTRODUCTION**……... 1

1.1 Rationale of the study…… 1

1.2 Research objective…… 3

1.2.1 Main Objective……... 3

1.2.2 Specific objectives……... 3

**II LITERATURE REVIEW**……... 4

2.1 Serum therapy in pre-antibiotic era……... 4

2.2 Antibiotic era and antimicrobial resistance (AMR)…….. 6

2.3 Return of antibodies as therapeutic agents…… 8

2.3.1 Hybridoma technology……... 8

2.3.2 Phage display technology……... 8

2.3.3 Antibody therapeutics..... 9

# TABLE OF CONTENTS (Continued)

**Page**

2.4 Full-length immunoglobulin G (IgG) and Single Chain Fragment Variable (scFv)…… 12

2.5 Production of scFv fragments……. 13

2.6 Usefulness of scFv fragments……. 14

2.7 Model bacteria of this study…… 15

2.7.1 *Pseudomonas aeruginosa* (Gram-negative bacilli)……...15

2.7.2 *Propionibacterium acnes* (Gram-positive bacilli)…… 17

**III ISOLATION AND IDENTIFICATION OF SCFV AGAINST *P. ACNES* AND *P. AERUGINOSA* BY AFFINITY SELECTION**……... 19

3.1 Abstract……... 19

3.2 Introduction……. 20

3.3 Materials and methods…… 20

3.3.1 Bacterial strains…… 20

3.3.2 Affinity selection (Biopanning) against *P. acnes* and *P. aeruginosa*…….……... 21

3.3.3 Expression of hexa-histidine-tagged scFv (6xHis-tagged scFv)……. 24

3.3.4 Purification of hexa-histidine-tagged scFv…….. 25

3.3.5 Enzyme linked immunosorbent assay (ELISA)……... 26

3.3.6 Western Blotting (WB)…… 28

3.3.7 Flow Cytometry……... 29

# TABLE OF CONTENTS (Continued)

**Page**

3.3.8 Confocal laser scanning microscopy (CLSM)……. 30

3.3.9 Transmission electron microscopy (TEM)…….. 31

3.4 Results and discussion…… 32

3.4.1 Affinity selection against *P. acnes* and *P. aeruginosa*……. 32

3.4.2 DNA and amino acid sequence analysis of selected bacteriophage clones…… 34

3.4.3 Expression and purification of 6xHis-tagged scFv…….. 38

3.4.4 Specific binding of antibacterial scFv by whole cell ELISA…….…….. 40

3.4.5 Detection of bacterial targets by WB…….. 40

3.4.6 Checkerboard titration (Dilution) ELISA…… 43

3.4.7 Detection of live bacteria by flow cytometry…….. 43

3.4.8 Immunofluorescent staining of planktonic bacteria……. 45

3.4.9 Immunofluorescent staining of biofilms…….. 49

3.4.10 Transmission Electron Microscopy……. 51

3.5 Conclusion and future perspectives…… 52

**IV IDENTIFICATION OF TARGET LIGAND OF YPAC1A8 BY IMMUNOPRECIPITATION AND MASS SPECTROMETRY**……. 53

4.1 Abstract……... 53

4.2 Introduction……. 54

4.3 Materials and methods…… 54

4.3.1 Bacterial strains…… 54

# TABLE OF CONTENTS (Continued)

**Page**

4.3.2 Identification of target antigen in boiled *P. acnes* preparation……... 54

4.3.3 CAMP (Christie-Atkins-Munch-Peterson) factor production by *P. acnes*……..... 58

4.3.4 Identification of target antigen in *P. acnes* broth culture supernatant……... 60

4.4 Results and discussion……. 61

4.4.1 Identification of target antigen in boiled *P. acnes* preparation……... 61

4.4.2 CAMP (Christie-Atkins-Munch-Peterson) factor production by *P. acnes*……...……... 66

4.4.3 Identification of target antigen in *P. acnes* broth culture supernatant……... 70

4.5 Conclusion and future perspectives…… 78

**V FROM SINGLE CHAIN FRAGMENT VARIABLE (SCFV) TO SCFV-BCCP, SCFV-EMGFP, AND SCFV-LL37 FORMATS**…… 80

5.1 Abstract……... 80

5.2 Introduction……. 80

5.3 Biotin carboxyl carrier protein (BCCP) and scFv conjugation……... 82

5.3.1 bccp PCR…….. 82

# TABLE OF CONTENTS (Continued)

**Page**

5.3.2 Restriction enzyme digestion of PCR products and vectors…….. 85

5.3.3 Ligation of recipient vectors and inserts…….. 86

5.3.4 Transformation of scFv-bccp and scFv-bccp-6xHis constructs……. 86

5.3.5 Confirmation of presence of inserts in scFv-bccp and scFv-bccp-His constructs……. 88

5.3.6 DNA sequence checking of scFv-bccp and scFv-bccp-His constructs……. 90

5.3.7 Predicted three-dimensional structure of scFv-bccp-His constructs……. 92

5.3.8 Expression and purification of scFv-bccp-His constructs… 92

5.3.9 Biotinylated scFv ELISA……. 94

5.4 EmGFP and scFv conjugation……. 98

5.4.1 Restriction enzyme cloning of scFv-EmGFP conjugates…. 98

5.4.2 Expression of EmGFP conjugates……. 100

5.4.3 Purification of scFv-EmGFP conjugates…… 100

5.4.4 Western Blot analysis of scFv-EmGFP conjugates…… 102

5.4.5 Predicted 3D-structure of scFv-EmGFP constructs……... 104

5.4.6 Fluorometric detection of yPac1A8-EmGFP……. 104

5.4.7 Direct immunofluorescence staining with scFv-EmGFP... 106

# TABLE OF CONTENTS (Continued)

**Page**

5.5 Antimicrobial peptide LL-37 and scFv conjugation……. 108

5.5.1 LL-37……. 108

5.5.2 scFv-LL-37 constructs……... 109

5.6 Conclusion and future perspectives……... 111

**VI FROM SINGLE CHAIN FRAGMENT VARIABLE (SCFV) TO FULL-LENGTH IMMUNOGLOBULIN G (IGG)**……..... 112

6.1 Abstract……. 112

6.2 Introduction……... 113

6.3 Materials and methods…….. 114

6.3.1 Generation of IgG heavy chain and light chain plasmids... 114

6.3.2 Recombinant full-length IgG expression system……... 120

6.3.3 Quantitation of IgG in crude supernatant by using ForteBio Octet K2 Platform…….. 123

6.3.4 Recombinant IgG purification……... 123

6.3.5 Crude supernatant IgG ELISA……... 126

6.3.6 Slide agglutination test using crude supernatant IgG……. 126

6.3.7 Slide agglutination test using purified IgG…… 127

6.3.8 Complement mediated bacteriolysis of *P. aeruginosa* enhanced by yPgi3G4 IgG……. 127

6.3.9 Antibody-dependent cellular phagocytosis assay……..... 131

6.3.10 Interleukin-8 (IL-8) ELISA…… 137

6.4 Results and discussion…….. 138

# TABLE OF CONTENTS (Continued)

**Page**

6.4.1 Generation of IgG heavy chain and light chain plasmids... 138

6.4.2 Recombinant full-length IgG expression system……... 146

6.4.3 Quantitation of IgG in crude supernatant by using ForteBio Octet K2 Platform…….….. 147

6.4.4 Recombinant IgG purification……... 149

6.4.5 Crude supernatant IgG ELISA……... 153

6.4.6 Slide agglutination test using crude supernatant IgG……. 154

6.4.7 Slide agglutination test using purified IgG…… 154

6.4.8 Complement-mediated bacteriolysis of *P. aeruginosa* enhanced by yPgi3G4 IgG……. 155

6.4.9 Antibody-dependent cellular phagocytosis assay…...…... 166

6.4.10 Interleukin-8 (IL-8) ELISA……... 178

6.5 Conclusion and future perspectives…….. 182

**VII CONCLUSION**..... 184

REFERENCES…… 185

APPENDIX..... 214

BIOGRAPHY..... 229

# LIST OF TABLES


**Table** **Page**

Table 2.1 Anti-bacterial sera, target bacteria and indications to use…… 5

Table 2.2 Antibacterial mAb undergoing clinical trials…….. 10

Table 2.3 Anti-Pseudomonal peptides and scFv identified by phage display technology……... 16

Table 2.4 Invasive infections caused by *P. acnes*..…… 17

Table 3.1 Summary of biopanning against *P. acnes* and *P. aeruginosa*……. 33

Table 3.2 Summary of DNA and amino acid sequence analysis of isolated scFv……..……. 35

Table 4.1 Protein hits of POI-1 and POI-2 of boiled antigen IP at p<0.05……. 63

Table 4.2 Protein hits of POI-1 and POI-2 of supernatant IP at p<0.05……. 71

Table 4.3 Protein sequence coverage between IP sequences and protein hit….. 73

Table 5.1 Primers for bccp PCR…….. 83

Table 5.2 bccp PCR components…… 83

Table 5.3 bccp PCR cycles…….. 83

Table 5.4 bccp PCR products…….. 84

Table 5.5 Restriction digestion reaction ……..……... 85

Table 5.6 Concentration of restriction enzyme digested vectors and inserts….. 85

Table 5.7 Ligation reaction set up……... 86

Table 5.8 Transformation results of scFv-bccp, scFv-bccp-His constructs…..... 88

# LIST OF TABLES (Continued)

**Table** **Page**

Table 5.9 Length of vectors, inserts and ligated scFv-bccp and scFv-bccp-His constructs……..……. 90

Table 5.10 Length of recombinant products of scFv-EmGFP cloning……. 99

Table 5.11 Properties of scFv-LL37 recombinant proteins……. 110

Table 6.1 Primers for VH, VL insert PCR…… 115

Table 6.2 VH, VL insert PCR components……... 115

Table 6.3 VH, VL insert PCR cycles…… 116

Table 6.4 Restriction digestion reaction for HC pTT28 vector and VH inserts…… 117

Table 6.5 Restriction digestion reaction for LC pTT28 vector and VL inserts…… 117

Table 6.6 Ligation reaction for HC pTT28 vector and VH inserts, and LC pTT28 vector and VL inserts…… 118

Table 6.7 IgG constructs DNA sequence check …… 119

Table 6.8 IgG expression system (2 mL transfection volume)…… 121

Table 6.9 IgG expression system (30 mL transfection volume)…….. 122

Table 6.10 Materials used for yPac1A8 IgG purification……... 124

Table 6.11 Materials used for yPgi3G4 IgG purification…… 125

Table 6.12 Complement-mediated bacteriolysis assay set up……..129

Table 6.13 Final concentration of reaction components in one reaction tube…. 130

# LIST OF TABLES (Continued)

**Table** **Page**

Table 6.14 Antibody-dependent cellular phagocytosis (*P. acnes* experiment)……..……. 134

Table 6.15 Antibody-dependent cellular phagocytosis (*P. aeruginosa* experiment)..…… 134

Table 6.16 Final concentration of reaction components……. 134

Table 6.17 Reagents for IL-8 ELISA…….. 137

Table 6.18 VH, VL PCR products…….. 138

Table 6.19 Concentration of restriction enzyme digested vectors and inserts after gel-purification…….. 140

Table 6.20 Length of vectors, inserts and ligated IgG constructs……... 140

Table 6.21 Transformation results of ligation controls and IgG constructs…… 142

Table 6.22 IgG constructs DNA sequence check result…….. 145

Table 6.23 Calculation of IgG concentration in crude supernatant……..…….. 148

Table 6.24 Summary of recombinant IgG yield in this study……. 152

Table 6.25 Number of viable *P. aeruginosa* in seed cultures and input bacterial number (inoculum) in each assay set…… 158

Table 6.26 Number of *P. aeruginosa* left in reaction tubes (six assay sets)…... 159

Table 6.27 *P. aeruginosa* survival relative to input (inoculum)……. 163

Table 6.28 Tukey's multiple comparisons test result of complement-mediated bacteriolysis assay……..……... 164

Table 6.29 Tukey's multiple comparisons test result of THP-1 and *P. acnes* experiment (six repeats)…….…… 179

# LIST OF TABLES (Continued)

**Table** **Page**

Table 6.30 Tukey's multiple comparisons test result of THP-1 and *P. aeruginosa* experiment (six repeats)……. 181

มหาวิทยาลัยเทคโนโลยีสุรนารี

# LIST OF FIGURES

**Figure** **Page**


Figure 2.1 Timeline of successful development of therapeutic mAbs…….. 9

Figure 3.1 DNA and amino acid sequence analysis of yPac1A8 and yPgi3G4... 37

Figure 3.2 Expression and purification of 6xHis-tagged scFv……. 39

Figure 3.3 Cross-reactivity analysis of scFv by whole-cell ELISA and WB…... 41

Figure 3.4 Checkerboard titration and flow cytometry analysis…….. 44

Figure 3.5 CLSM of yPac1A8 and planktonic bacteria…… 46

Figure 3.6 CLSM of yPgi3G4 and planktonic bacteria…… 47

Figure 3.7 *P. acnes* DMST 14916 stained with yPac1A8 scFv……... 48

Figure 3.8 *P. aeruginosa* DMST 37186 stained with yPgi3G4 scFv……... 49

Figure 3.9 CLSM of biofilms stained by indicated scFv…….. 50

Figure 3.10 TEM of *P. acnes* DMST 14916 and *P. aeruginosa* DMST 37186…. 51

Figure 3.11 Summary of Chapter III…….. 52

Figure 4.1 Immunoprecipitation of boiled *P. acnes* antigen……... 62

Figure 4.2 Mascot Score Histogram of POI-1 of boiled antigen IP……. 64

Figure 4.3 Mascot Score Histogram of POI-2 of boiled antigen IP……. 64

Figure 4.4 WB analysis of POI-1 and POI-2 of boiled antigen IP……... 65

Figure 4.5 Classic CAMP test result…… 67

Figure 4.6 Modified CAMP test result……. 68

Figure 4.7 CAMP factor ELISA result……. 69

Figure 4.8 Immunoprecipitation of *P. acnes* broth culture supernatant…… 70

# LIST OF FIGURES (Continued)

**Figure** **Page**

Figure 4.9 Mascot Score Histogram of POI-1 of supernatant IP……. 72

Figure 4.10 Mascot Score Histogram of POI-2 of supernatant IP……. 72

Figure 4.11 Protein sequence coverage between IP sequences and protein hit….. 73

Figure 4.12 Phylogenetic tree view of amino acid sequence alignment…… 75

Figure 4.13 Summary of chapter IV……... 78

Figure 5.1 bccp PCR products…….. 84

Figure 5.2 Transformation results of ligation controls, scFv-bccp, and scFv-bccp-His constructs…… 87

Figure 5.3 Restriction enzyme cut-check result of scFv-bccp and scFv-bccp-His constructs…… 89

Figure 5.4 The vector maps of scFv-bccp and scFv-bccp-His constructs…… 91

Figure 5.5 Predicted 3D-structure of yPac1A8-bccp-6xHis construct……. 92

Figure 5.6 SDS-PAGE gels of scFv-bccp-6xHis protein purification…… 93

Figure 5.7 Biotinylated yPac1A8 scFv (yPac1A8-bccp-6xHis) ELISA…….. 95

Figure 5.8 Biotinylated yPac1E4 scFv (yPac1E4-bccp-6xHis) ELISA……... 96

Figure 5.9 Biotinylated yPgi3G4 scFv (yPgi3G4-bccp-6xHis) ELISA……... 97

Figure 5.10 The vector maps of scFv-EmGFP constructs……..… 99

Figure 5.11 Examination of scFv-EmGFP elutes……. 101

Figure 5.12 Analysis of scFv and scFv-EmGFP by Western Blot……... 103

Figure 5.13 3D model of (A) yPac1A8-EmGFP and (B) yPgi3G4-EmGFP…… 104

Figure 5.14 Fluorometric immunoassay of yPac1A8-EmGFP……. 105

Figure 5.15 Confocal microscopy of *P. acnes* and *P. aeruginosa*……... 107

# LIST OF FIGURES (Continued)

**Figure** **Page**

Figure 5.16 The vector maps of scFv-LL37 constructs…… 109

Figure 5.17 Predicted 3D structure of (A) yPac1A8-LL37 (B) yPgi3G4-LL37... 110

Figure 5.18 Summary of chapter V…….. 111

Figure 6.1 Determination of viable count (cfu/mL) in *P. aeruginosa* seed cultures…….. 130

Figure 6.2 Determination of viable count (cfu/mL) in reaction tubes…… 131

Figure 6.3 Bird-eye view of experiment plan for 3 reaction sets……... 135

Figure 6.4 VH and VL PCR products……. 139

Figure 6.5 IgG heavy chain and light chain vector maps of yPac1A8 and yPgi3G4……. 141

Figure 6.6 Transformation results of ligation controls and IgG constructs…… 142

Figure 6.7 Restriction enzyme cut-check result of yPac1A8 and yPgi3G4 heavy chain vectors (6 clones each)……..…… 143

Figure 6.8 Restriction enzyme cut-check result of yPac1A8 and yPgi3G4 light chain vectors (3 clones each)…… 144

Figure 6.9 Binding curve graph of standard IgG and samples……... 147

Figure 6.10 Standard curve showing standard IgG (blue) and samples (red)….. 148

Figure 6.11 Chromatogram showing the purification profile of yPac1A8 IgG… 149

Figure 6.12 Chromatogram showing the purification profile of yPgi3G4 IgG… 151

Figure 6.13 Reduced SDS-PAGE analysis of purified IgG…….. 152

Figure 6.14 *P. acnes* and *P. aeruginosa* and crude supernatant IgG ELISA…... 153

# LIST OF FIGURES (Continued)

**Figure** **Page**

Figure 6.15 *P. acnes* slide agglutination test using crude supernatant IgG…….. 154

Figure 6.16 *P. acnes* slide agglutination test using purified IgG……. 154

Figure 6.17 *P. aeruginosa* slide agglutination test using purified IgG……. 155

Figure 6.18 Culture plates and colony counts of seed cultures of assay set 1, 2, and 3…….……..…….. 157

Figure 6.19 Culture plates and colony counts of seed cultures of assay set 4, 5, and 6……..…….. 158

Figure 6.20 Culture plates and colony counts of assay set 1…… 160

Figure 6.21 Culture plates and colony counts of assay set 2…… 160

Figure 6.22 Culture plates and colony counts of assay set 3…… 161

Figure 6.23 Culture plates and colony counts of assay set 4…… 161

Figure 6.24 Culture plates and colony counts of assay set 5…… 162

Figure 6.25 Culture plates and colony counts of assay set 6…… 162

Figure 6.26 *P. aeruginosa* survival relative to inoculum (%) in four different treatment settings……..…….. 165

Figure 6.27 Phase-contrast pictures of THP-1 cells (thick arrow) challenged with *P. acnes* (thin arrows)……..……... 168

Figure 6.28 Phase-contrast pictures of THP-1 cells (thick arrow) challenged with *P. aeruginosa* (thin arrows)……..…….. 169

Figure 6.29 First set of confocal microscopy images of THP-1 and *P. acnes* experiment…….……. 171

# LIST OF FIGURES (Continued)

**Figure** **Page**

Figure 6.30 Second set of confocal microscopy images of THP-1 and *P. acnes* experiment……..……. 172

Figure 6.31 Third set of confocal microscopy images of THP-1 and *P. acnes* experiment……..……. 173

Figure 6.32 First set of confocal microscopy images of THP-1 and *P. aeruginosa* experiment……. 174

Figure 6.33 Second set of confocal microscopy images of THP-1 and *P. aeruginosa* experiment……. 175

Figure 6.34 Third set of confocal microscopy images of THP-1 and *P. aeruginosa* experiment……. 176

Figure 6.35 Comparison of IL-8 response (*P. acnes* experiment)……... 178

Figure 6.36 Comparison of IL-8 response (*P. aeruginosa* experiment)…..…… 180

Figure 6.37 Summary of chapter VI……. 182

มหาวิทยาลัยเทคโนโลยีสุรนารี

# LIST OF ABBREVIATIONS

| | | |
|---|---|---|
| 2xYT medium | = | Yeast Extract Tryptone medium |
| 6xHis | = | 6 x Histidine |
| ABTS | = | 2,2'-Azino-bis (3-ethylbenzothiazoline-6-sulfonic acid) |
| ADCP | = | Antibody-dependent cellular phagocytosis |
| AMR | = | Antimicrobial Resistance |
| BCCP | = | Biotin Carboxyl Carrier Protein |
| BHI broth | = | Brain Heart Infusion broth |
| BSA | = | Bovine Serum Albumin |
| CAMP factor | = | Christie-Atkins-Munch-Peterson factor |
| CDR | = | Complementarity-determining regions |
| cfu | = | colony forming unit |
| CHO cell | = | Chinese Hamster Ovary cell |
| CLSM | = | Confocal Laser Scanning Microscopy |
| DAPI | = | 4′,6-diamidino-2-phenylindole |
| DMST | = | Department of Medical Sciences Thailand |
| DSM | = | German Collection of Microorganisms and Cell Cultures |
| *E. coli* | = | *Escherichia coli* |
| ELISA | = | Enzyme-Linked Immunosorbent Assay |
| EmGFP | = | Emerald Green Fluorescence Protein |
| GDP | = | Gross Domestic Product |

มหาวิทยาลัยเทคโนโลยีสุรนารี

# LIST OF ABBREVIATIONS (Continued)

| | | |
|---|---|---|
| HEK 293 cell | = | Human Embryonic Kidney 293 cell |
| HRP | = | Horseradish Peroxidase |
| IgG | = | Immunoglobulin G |
| IGHV | = | human immunoglobulin heavy variable |
| IGLV | = | human immunoglobulin λ variable |
| IL-8 | = | Interleukin-8 |
| IP | = | immunoprecipitation |
| IPTG | = | isopropyl-β-D-thiogalactopyranoside |
| LB broth | = | Luria-Bertani broth |
| mAb | = | monoclonal antibody |
| MS | = | Mass Spectrometry |
| MWCO | = | Molecular Weight Cut Off |
| Ni-NTA | = | Nickel-Nitrilotriacetic Acid |
| OD | = | Optical Density |
| *P. acidipropionici* | = | *Propionibacterium acidipropionici* |
| *P. acnes* | = | *Propionibacterium acnes* |
| *P. aeruginosa* | = | *Pseudomonas aeruginosa* |
| *P. fluorescens* | = | *Pseudomonas fluorescens* |
| *P. freudenreichii* | = | *Propionibacterium freudenreichii* |
| *P. putida* | = | *Pseudomonas putida* |
| PBS | = | Phosphate Buffer Saline |
| PCR | = | Polymerase Chain Reaction |

# LIST OF ABBREVIATIONS (Continued)

| | | |
|---|---|---|
| PFA | = | paraformaldehyde |
| pfu | = | plaque forming unit |
| POI | = | Protein Of Interest |
| PVDF membrane | = | Polyvinylidene Difluoride membrane |
| RBC | = | Red Blood Cell |
| rpm | = | rate per minute |
| RPMI 1640 medium | = | Roswell Park Memorial Institute (RPMI) 1640 Medium |
| *S. aureus* | = | *Staphylococcus auerus* |
| scFv | = | single chain fragment variable |
| SDS-PAGE | = | sodium dodecyl sulfate–polyacrylamide gel electrophoresis |
| SEM | = | Standard Error of the Mean |
| SOC medium | = | Super Optimal broth with Catabolites repression medium |
| TB | = | Terrific Broth |
| TEM | = | Transmission Electron Microscopy |
| THP-1 cell | = | Tohoku Hospital Pediatrics-1 cell |
| TISTR | = | Thailand Institute of Scientific and Technological Research |
| TMB substrate | = | 3,3',5,5'-tetramethylbenzidine substrate |
| USD | = | U.S. Dollar |
| $V_H$ | = | Variable region of heavy chain of an immunoglobulin |
| $V_L$ | = | Variable region of light chain of an immunoglobulin |
| WB | = | Western Blot |
| WHO | = | World Health Organization |

# CHAPTER I

# INTRODUCTION

## 1.1 Rationale of the study

In 19th century, polyclonal antibodies of animal origin were used to treat infectious diseases of human and it was the treatment of choice in pre-antibiotic era. Serum therapy saved human lives although there were concerns about injection-related complications and immune reaction against foreign serum (Hewlett, 1910). Later on, serum therapy was succeeded by antibiotics which have saved millions of human lives. The antibiotic era started with the discovery of penicillin in 1928, followed by introduction of several new antibiotic classes (Fleming, 1929). Unfortunately, antibiotic administration caused natural selection of antibiotic resistant mutants among microbes which resulted in emergence of antimicrobial resistance (AMR). Once curable infections became incurable with recommended antibiotics and human death attributable to AMR will surpass that to cancer in 2050 (O'Neill, 2016).

Reports on multidrug-resistant and pandrug-resistant superbugs appeared and WHO has declared the list of most important resistant bacteria for which new treatments are in urgent need (WHO, 2017). AMR problem is superimposed by the shortage of new antibiotics. Up to September 2019, there are 50 antibiotics in clinical development pipeline but majority of them are analogues of existing ones (WHO, 2019a). Not only new antibiotics but also new therapeutic options are needed for antibiotic-resistant infections. Antibodies can be a solution to AMR problem.

Unlike the polyclonal antibodies present in animal sera which was used in the past, antibodies of human origin can be produced in laboratories nowadays after introduction of monoclonal antibody technology, antibody phage display technology and recent advances in molecular biology (Clackson, Hoogenboom, Griffiths, & Winter, 1991; Kohler & Milstein, 1975). Moreover, antibody engineering has reached a whole new level with the production of chimeric and humanized antibodies, immunoglobulin fragments, antibody libraries, and antibody fusion proteins. There is hope on antibody biologics for bacterial infections since monoclonal antibodies have made successful debut as autoimmune biologics, anti-cancer biologics and anti-viral biologics.

Developing antibody biologics for bacterial infections is an exciting research field. This study has initiated the process of antibody therapeutics and diagnostics development for two model bacteria; starting from isolating scFv antibody fragments from a phage display human scFv antibody library to the construction of full-length IgG antibody and their functional assays *in-vitro*. The methodology and the outcomes are described as this thesis book.

Chapter II is the literature review on serum therapies, antimicrobial resistance, antibody biologics, scFv antibody fragment and full-length IgG. Chapter III describes about the isolation of antibody fragments from Yamo-I scFv library by affinity selection against model bacteria. Chapter IV is about the identification of target ligand in model bacteria by using isolated scFv. Chapter V focusses on engineering of scFv into scFv-EmGFP, scFv-biotin carboxyl carrier protein, and scFv-antimicrobial peptide conjugates. Chapter VI highlights the engineering of scFv into full-length IgG and IgG functional assays *in-vitro*.

## 1.2 Research objective

### 1.2.1 Main Objective

This study aimed to prove that single chain fragment variable (scFv) obtained by affinity selection (biopanning) can be engineered into therapeutic and diagnostic agents for bacterial infections by using one Gram-positive (*Propionibacterium acnes*) and one Gram-negative (*Pseudomonas aeruginosa*) model bacteria and Yamo-I phage display human scFv library.

### 1.2.2 Specific objectives

1. To identify scFv from Yamo-I phage display human scFv library by affinity selection against *Propionibacterium acnes* and *Pseudomonas aeruginosa*
2. To identify target ligands of identified scFv
3. To engineer isolated scFv into different formats, such as, biotinylated scFv, EmGFP tagged scFv, and anti-microbial peptide conjugated scFv
4. To engineer isolated scFv into full-length IgG and do functional assays

# CHAPTER II

# LITERATURE REVIEW

## 2.1 Serum therapy in pre-antibiotic era

Antibody therapeutics for infectious diseases started as serum therapy for diphtheria and tetanus in 1890s. Emil von Behring, who was a medical doctor, immunized animals against diphtheria and tetanus, identified specific antibodies (antitoxins) in blood of immunized animals and successfully used antitoxins as effective prophylaxis and curative treatment for human. He won the very first Nobel Prize for Medicine or Physiology in 1901 (Linton, 2005; Nobel-Prize-Organisation, 1901).

Two types of serum were available at that time: antibacterial serum which causes the destruction of target bacteria and antitoxic serum that causes the neutralization of exotoxin secreted by the target bacteria. Both types were prepared by immunizing animals, e.g., horses, goats, rabbits. Horses were most commonly used and about 6-12 litres of blood was withdrawn from one horse at a time. The obtained serum was preserved by adding 0.2% carbolic acid or 0.3% trikresol and stored in liquid or desiccated form. Notably, 1g of dried serum corresponds to 10 $cm^3$ of fluid serum. Although the production and preservation processes are more or less the same, the stability of serum varies. For example, diphtheria anti-toxin retained its activity for more than one year while anti-microbial and anti-endotoxin sera lost their activity rapidly. The dose of serum given to human patients ranged from 5 to 60 mL (Hewlett, 1910; Lindsay, 1933).

**Table 2.1 Antibacterial sera, target bacteria and indications to use**

| Serum | Target bacteria | Indication | References |
|---|---|---|---|
| anti-streptococcal serum | *Streptococcus pyogenes* | septic and puerperal infections | (Eason, 1935; Lindsay, 1933; Sheplar, Spence, & Macneal, 1934; C. P. Thomas, 1897) |
| anti-pneumococcal serum | *Streptococcus pneumoniae* | pneumonia | (Armstrong & Johnson, 1931; Macleod, 1939) |
| anti-meningococcal serum | *Neisseria meningitidis* | meningitis | (Flexner & Jobling, 1908) |
| anti-plague serum | *Yersinia pestis* | plague | (Calmette, 1900; Dawson, 1927) |
| anti-endotoxic serum, O+Vi anti-typhoid serum | *Salmonella typhi* | enteric fever | (Bruce, 1909; Felix, 1954) |
| anti-anthrax serum | *Bacillus anthracis* | human anthrax | (Knudson, 1986; Ladwig, 1943; Smyth & Higgins, 1945; Turnbull & Shadomy, 2011) |
| anti-toxin serum | *Clostridium botulinum* | human botulism | (Bronfenbrenner & Weiss, 1923) |
| anti-toxin serum | *Vibrio cholerae* | cholera | (Ghosh, 1935) |
| anti-dysenteric serum | *Shigella sonnei, S. boydii, S. flexneri, S. dysenteriae* | bacillary dysentery | (Klein, 1919; Roy, 1935; Waller & Oxon, 1919) |
| anti-Hansen bacilli serum | *Mycobacterium leprae* | Hansen's disease | (Reenstierna, 1942) |
| anti-staphylococcal serum | *Staphylococcus aureus* | Staphylococcal infections | (Maynard & Bushnell, 1905; B. A. Thomas, 1913) |
| anti-tuberculosis serum | *Mycobacterium tuberculosis* | tuberculosis | (Bassan, 1905; Hemsted, 1909; Latham, 1904; Mitchell, 1912) |

Available case reports on antibacterial serum therapy are summarized in **Table 2.1** above. During the pre-antibiotic era, serum therapy played key role in treating infectious diseases. Specific sera against several pathogens, including not only bacteria

but also viruses (anti-rabies serum, anti-polio serum, anti-malta fever serum) and parasites (anti-trypanosomiasis serum) were produced (Faber, 1941; Nattan-larrier & Noyer, 1931; Rodet & Galavielle, 1902; Stableforth, 1954).

The outcome of serum therapy depends on the timing of the treatment, and the quality and quantity of the serum given. To obtain the best outcome, serum therapy must be given to the patient as early as possible and the dose must be sufficient enough to stop the detrimental effect of bacteria or its toxin. It was administered via intramuscular or subcutaneous or intravenous or intraperitoneal route and was repeated as needed. Serum therapy can be followed by injection-related complications, e.g., abscess formation and haemorrhage at the site of inoculation. Septic infection due to contaminated serum, albuminuria, pyrexia, skin rashes, joint pains and anaphylaxis due to foreign serum administration can happen (Cecil, 1937; Hewlett, 1910). Moreover, serum therapy has the animal farm maintenance issues, and batch to batch variation in effectiveness. When the antibiotics were introduced, the demand for serum therapy decreased rapidly.

## 2.2 Antibiotic era and antimicrobial resistance (AMR)

Starting from the introduction of arsphenamine (Salvarsan) for treatment of syphilis and African trypanosomiasis in 1907 (Williams, 2009) and of penicillin in 1928 (Fleming, 1929), antibiotics have saved millions of lives. Antibiotic discoveries were regarded as important medical achievement milestones and more than 20 new classes of antibiotics had successfully launched into the market until 1962. Later on, new antibiotics discoveries have nearly stopped not only because it is time-consuming and expensive but also because it is extremely difficult (Buckland, 2017; Coates, Halls, &

Hu, 2011). Up to September 2019, there are 50 antibiotics in clinical development pipeline but majority of these antibiotics are analogues of existing ones (WHO, 2019a).

The introduction of antibiotic to microbes is followed by emergence of microbial resistance to that antibiotic. Penicillin was discovered by Alexander Fleming, Professor of Bacteriology, at St. Mary's Hospital in London in 1928 and it became available for medical use by the 1940s and since then, it has been widely used. The first penicillin-resistant *Streptococcus pneumoniae* was isolated in Australia in 1967 and 34% of isolated *S. pneumoniae* were resistant to penicillin by 1998 (Doern, 2001). Reports on multidrug-resistant bacteria are on a rise which further jeopardize the antibiotic scarcity problem. In the US alone, more than 2.8 million antibiotic-resistant infections occur, and more than 35,000 people die from AMR related problems each year (CDC, 2019). In European Union and European Economic Area countries, more than 670,000 antibiotic-resistant infections occur and approximately 33,000 people die from that each year (ECDC, 2019).

In 2050, human death attributable to AMR is estimated to surpass that to cancer and global GDP loss related to AMR will be in trillions of USD (O'Neill, 2014). Antimicrobial resistance is an urgent issue which needs coordinated interaction at national and global levels to control emergence and spread of multidrug-resistant bacteria. At the same time, antibiotics research and development, which has been hindered by scientific and economic challenges, should be welcomed and encouraged.

## 2.3 Return of antibodies as therapeutic agents

### 2.3.1 Hybridoma technology

The return of antibodies as therapeutic agents became possible when monoclonal antibody technology was introduced in 1975 (Kohler & Milstein, 1975). The first monoclonal antibody (mAb) developed was against sheep red blood cells. The spleen cells of mouse immunized with sheep RBC were fused with myeloma cell line of mouse origin and finally, hybridoma cells producing monoclonal antibody against sheep RBC were obtained. Georges J.F. Köhler and César Milstein received the Nobel Prize in Physiology or Medicine 1984 for hybridoma technology development (Nobel-Prize-Organization, 1984). With hybridoma technology, antibodies having the same target specificity can be produced in cell cultures and in mice peritoneal cavities. It has been applied for medical and industrial use (Tami, Parr, Brown, & Thompson, 1986). Moreover, mAbs are also widely used in molecular research laboratories as an essential research tool.

### 2.3.2 Phage display technology

Phage display technology (biopanning / affinity maturation), in which *E. coli* bacteriophage M13 was genetically modified to carry peptide or scFv gene sequence and display corresponding peptide or scFv unit as a part of its protein coat, was introduced in late 20$^{th}$ century by George P. Smith (Parmley & Smith, 1988) and Sir Gregory P. Winter (McCafferty, Griffiths, Winter, & Chiswell, 1990). George P. Smith and Sir Gregory P. Winter received the Nobel Prize in Chemistry 2018 for phage display and antibody display technologies (Nobel-Prize-Organization, 2018). Phage display technology has been used to construct random peptide display or antibody

fragments display phage libraries, from which biopharmaceuticals have been successfully developed.

### 2.3.3 Antibody therapeutics

Nowadays, monoclonal antibodies have become the best-selling drugs in the pharmaceutical market. Global therapeutic monoclonal antibody market reached USD 115.2 billion in 2018 and it is expected to reach USD 300 billion by 2025 as shown in **Figure 2.1** below (Lu et al., 2020). Moreover, the size of global cancer monoclonal antibody market is estimitated to be USD 41.3 billion in 2019 and is estimated to reach USD 70.6 billion at the end of 2024 (Market-Data-Forecast, 2019).

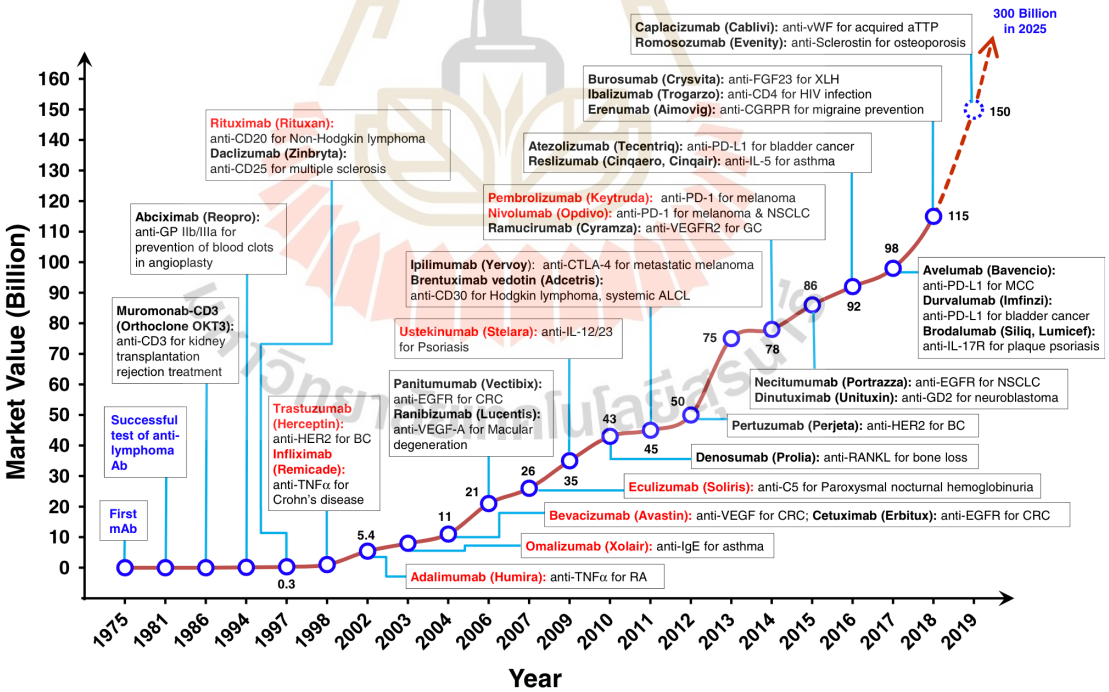


**Figure 2.1 Timeline of successful development of therapeutic mAbs** (Lu et al., 2020).

Monoclonal antibodies are important treatment option for cancer and non-communicable diseases. Unlike that, only a handful of mAbs are available to use for infectious diseases. For example, palivizumab is used for prophylaxis against respiratory syncytial virus infection (DiGiandomenico & Sellman, 2015; Marston, Paules, & Fauci, 2018; Zurawski & McLendon, 2020). By 2018, three mAbs have been approved for bacterial infections by US Food and Drug Administration. Raxibacumab is from GlaxoSmith Kline and is human IgG1(λ) for *Bacillus anthracis*. Obiltoxaximab is from Elusys and is chimeric IgG1(κ) for *Bacillus anthracis* and bezlotoxumab is from Merck & Co. and is human IgG1 for *Clostridium difficile* (Fernebro, 2011; Hauser, Mecsas, & Moir, 2016; Wang-Lin & Balthasar, 2018; Zurawski & McLendon, 2020).

A number of antibacterial mAb are undergoing clinical trials. Many of them are ongoing but some have already been terminated. The available information on antibacterial mAb are summerized in **Table 2.2** below.

**Table 2.2 Antibacterial mAb undergoing clinical trials**

| **mAb** | **Target bacteria** | **Clinical trial status** | **References** |
|---|---|---|---|
| Anthim (ETI-204) | *Bacillus anthracis* | not mentioned | (Fernebro, 2011) |
| Valortim (MDX-1303) | *Bacillus anthracis* | not mentioned | (Fernebro, 2011) |
| CDA1/CDB1 | *Clostridium difficile* | not mentioned | (Fernebro, 2011) |
| PolyCAb | *Clostridium difficile* | Phase 1 | (Zurawski & McLendon, 2020) |
| Cd-ISTAb | *Clostridium difficile* | Preclinical | (Zurawski & McLendon, 2020) |
| DSTA4637 (antibody-antbiotic conjugate) | *Staphylococcus aureus* | Phase Ib | (Motley, Banerjee, & Fries, 2019) |

**Table 2.2 Antibacterial mAb undergoing clinical trials (continued)**

| mAb | Target bacteria | Clinical trial status | References |
|---|---|---|---|
| MED 14893 mAb | *Staphylococcus aureus* | Phase 2 | (Francois, Barraud, & Jafri, 2017; Hauser et al., 2016; Speziale, Rindi, & Pietrocola, 2018; Zurawski & McLendon, 2020) |
| RG7861 | *Staphylococcus aureus* | | (Zurawski & McLendon, 2020) |
| F598 | *Staphylococcus aureus* | Phase 2 terminated | (Motley et al., 2019) |
| MEDI4892 (Suvratoxumab) | *Staphylococcus aureus* | Phase 2 | (Motley et al., 2019) |
| Tefibazumab, | *Staphylococcus aureus* | Phase 2 terminated | (Zurawski & McLendon, 2020) |
| AR-301 (Salvecin) | *Staphylococcus aureus* | Phase 3 | (Francois et al., 2017; Motley et al., 2019; Zurawski & McLendon, 2020) |
| Pagibaximab | *Staphylococcus aureus* | terminated | (Fernebro, 2011; Speziale et al., 2018) |
| ASN100 (2 mAb Cocktail) | *Staphylococcus aureus* | Phase 2 terminated | (Francois et al., 2017; Motley et al., 2019; Speziale et al., 2018; Zurawski & McLendon, 2020) |
| 514G3 | *Staphylococcus aureus* | Phase 2 | (Francois et al., 2017; Motley et al., 2019; Speziale et al., 2018; Zurawski & McLendon, 2020) |
| Mukoviszidos (IgY polyclonal) | *Pseudomonas aeruginosa* | Phase 3 | (Fernebro, 2011; Motley et al., 2019) |
| KB001 | *Pseudomonas aeruginosa* | Phase 2 terminated | (Fernebro, 2011; Zurawski & McLendon, 2020) |
| Panobacumab (KBPA101) | *Pseudomonas aeruginosa* | not mentioned | (Fernebro, 2011) |
| MEDI3902 | *Pseudomonas aeruginosa* | Phase 2 | (Ali et al., 2019; DiGiandomenico et al., 2014; DiGiandomenico et al., 2012; Motley et al., 2019; Tabor et al., 2018; Thanabalasuriar et al., 2017; Warrener et al., 2014; WHO, 2019a; Zurawski & McLendon, 2020) |
| AR-105 (Aerucin) | *Pseudomonas aeruginosa* | Phase 2 | (Motley et al., 2019) |

**Table 2.2 Antibacterial mAb undergoing clinical trials (continued)**

| mAb | Target bacteria | Clinical trial status | References |
|---|---|---|---|
| AR101 | *Pseudomonas aeruginosa* | Phase 2 | (WHO, 2019a; Zurawski & McLendon, 2020) |
| AR401 | *Acinetobacter baumannii* | Preclinical | (Zurawski & McLendon, 2020) |
| VXD-003 | *Acinetobacter baumannii* | Preclinical | (Zurawski & McLendon, 2020) |
| ASN-4 | *Escherichia coli* | Preclinical | (Zurawski & McLendon, 2020) |
| Shigamab | *Escherichia coli* | Phase 2 | (Fernebro, 2011; Hauser et al., 2016) |
| Urtoxazumab | *Escherichia coli* | not mentioned | (Fernebro, 2011) |
| A1102 mAb | multi-drug resistant *Klebsiella pneumoniae* | not mentioned | (Babb & Pirofski, 2017) |
| ASN-5 | *Klebsiella pneumoniae* | Preclinical | (Zurawski & McLendon, 2020) |
| TRL1068 | Biofilms | Phase 1 | (Zurawski & McLendon, 2020) |

## 2.4 Full-length immunoglobulin G (IgG) and Single Chain Fragment Variable (scFv)

One IgG molecule is a tetramer, having two heavy chains (50 kDa each) and two light chains (25 kDa each). It has a molecular weight of approximately 150 kDa and is 20-40 nm in diameter and about 2 nm in height (Chen, Cai, Xu, & Chen, 2004; Murphy, 2012; Saber, Sarkar, Gill, Nazari, & Faridani, 2011). A recombinant scFv antibody fragment is a single protein which contains antigen binding domains ($V_H$ and $V_L$) of lgG joined covalently by a flexible peptide linker. One scFv fragment has a molecular weight of about 30 kDa and a diameter of 5 nm, which is about one-fifth the size of parental IgG molecule (Vallet-Courbin et al., 2017).

The carboxy terminus of scFv fragment ends with Amber stop codon. The whole scFv DNA sequence is inserted into phagemid vector of M13 bacteriophage, precisely in between the leader sequence and Gene III protein DNA sequence. As a result, scFv fragment is incorporated into bacteriophage coat protein III and displayed on phage particle surface, in such a way that scFv can bind to its specific target without compromising the attachment of phage to its host *E. coli* (Petrenko & Smith, 2015; Russel, Lowman, & Clackson, 2004).

## 2.5 Production of scFv fragments

The success of scFv production depends on the structure of scFv protein itself. For example, CDR and framework sequence patterns of scFv can modify the folding process. Presence of disulfide bond in both $V_H$ and $V_L$ domains of scFv is essential for correct folding. In comparison, $V_L$ domain became less stable than $V_H$ domain if there is no intra-domain disulfide bridge (Berkmen, 2012; Gaciarz & Ruddock, 2017; Glockshuber, Schmidt, & Pliickthun, 1992; Montoliu-Gaya, Martinez, & Villegas, 2017).

Secondly, production of functional scFv depends on expression system. It can be carried out in *E. coli* expression system (Gaciarz & Ruddock, 2017; Glockshuber et al., 1992), mammalian cell expression system like HEK cells and CHO cells (Weatherill et al., 2012) and plant cell system like transgenic tobacco plants (Schouten, Roosien, Bakker, & Schots, 2002). Several *E. coli* strains are available for scFv production. SHuffle *E. coli* is genetically engineered to be able to catalyze disulfide bond formation in cytoplasm by deleting thioredoxin and glutaredoxin pathways and mutating peroxidase AhpC. It also favors disulfide bond shuffling by intracytoplasmic expression

of DsbC which is important for correct folding of recombinant proteins (Berkmen, 2012). Usefulness of SHuffle *E. coli* has been evaluated for varieties of recombinant protein production (Fathi-Roudsari, Akhavian-Tehrani, & Maghsoudi, 2016; Lamppa, Tanyos, & Griswold, 2013; Lobstein et al., 2012; Nguyen et al., 2018; Ren, Ke, & Berkmen1, 2016).

## 2.6 Usefulness of scFv fragments

One scFv molecule binds to its specific target through CDR regions of $V_H$ and $V_L$ domains. In addition, through available tag sequence attached to them, scFv antibody fragments can bind to tag detection systems. The scFv fragments can be used as therapeutic agents after some modifications. For example, pexelizumab (C5 inhibitor monoclonal antibody), which is under clinical trial for treatment of patients with acute myocardial infarction or undergoing coronary artery bypass graft surgery, is developed from a recombinant scFv fragment (Evans et al., 1995; Fitch et al., 1999; Mahaffey et al., 2006; Theroux et al., 2005).

The scFv fragments can function as biosensors after being coupled to chemical ligands or nanoparticles. They have been used for atherosclerotic plaque imaging (Dietrich et al., 2007), studying the kinetics and thermodynamics of antigen/scFv antibody binding (Shen et al., 2005), development of microcantilever-based immunosensor (Backmann et al., 2005), and intracellular targeting and functional analysis of scFv in mammalian cells (Cardinale, Filesi, Mattei, & Biocca, 2004). Moreover, scFv with certain tag systems, e.g., VSV tag (Lensen et al., 2005), HA tag (Kitidee et al., 2010), and Myc tag (Kleymann, Ostermeier, Heitmann, Haase, & Michel, 1995), were used to study kidney morphology and virus particles.

## 2.7 Model bacteria of this study

### 2.7.1 *Pseudomonas aeruginosa* (Gram-negative bacilli)

*P. aeruginosa* has a cosmopolitan distribution. It can cause sepsis, septicemia, pneumonia, post-surgical infections and biofilm-forming infections. Patients on ventilators, catheterized patients and patients with burns and wounds are particularly at risk of *P. aeruginosa* infections. This bacterium is intrinsically resistant to antibiotics and carbapenem-resistant *Pseudomonas aeruginosa* has been listed as critically important antibiotic-resistant bacteria for research, discovery, and development of new antibiotics by WHO (WHO, 2017).

The multidrug-resistant *P. aeruginosa* is estimated to cause 32,600 infections among hospitalized patients, 2,700 estimated deaths and USD 767 million healthcare costs in the US alone in 2017. About 32.1% of reported *P. aeruginosa* isolates were resistant to at least one of the antimicrobial groups under regular surveillance in European Union and European Economic Area countries in 2018 (CDC, 2019; ECDC, 2019). Several studies have been done to identify anti-Pseudomonal peptides and scFv antibody fragments which are summerized in **Table 2.3** below.

According to 2019 updates on antibacterial agents in clinical developments by WHO, one antibiotic (cefiderocol) and two biologicals (MEDI-3902 and AR-101) under development are active against *P. aeruginosa* (WHO, 2019b). MEDI-3902 (gremubamab) is anti-*P. aeruginosa* IgG monoclonal antibody and is in clinical development phase 2. It has been developed by MedImmune Pharmaceuticals, U.S.A. AR-101 (panobacumab, aerumab) is anti-*P. aeruginosa* serotype O11 IgG monoclonal antibody and is in clinical development phase 2. It has been jointly developed by Aridis Pharmaceuticals, U.S.A and Shenzhen Hepalink Pharmaceutical

Group Co., Ltd, China. MEDI-3902 targets the virulence factors: Psl and PcrV, whereas AR-101 binds to surface polysaccharide alginate of *P. aeruginosa*.

**Table 2.3 Anti-Pseudomonal peptides and scFv identified by phage display technology**

| Library used | Biopanning Target | Result | References |
|---|---|---|---|
| PHD-12 and PHD-C7C peptide libraries (New England Biolabs, U.S.A) | recombinant MurA transferase | anti-*P. aeruginosa* peptide | (Molina-Lopez, Sanschagrin, & Levesque, 2006) |
| PHD-12 and PHD-C7C peptide libraries (New England Biolabs, U.S.A) | recombinant *MurC* amide ligase | anti-*P. aeruginosa* peptide | (El Zoeiby, Sanschagrin, Darveau, Brisson, & Levesque, 2003) |
| PHD-12 peptide library (New England Biolabs, U.S.A) | recombinant *MurF* amide ligase | anti-*P. aeruginosa* peptide | (Paradis-Bleau et al., 2008) |
| PHD-12 peptide library (New England Biolabs, U.S.A) | recombinant *MurE* amide ligase | anti-*P. aeruginosa* peptide | (Paradis-Bleau et al., 2009) |
| PHD-12 and PHD-C7C peptide libraries (New England Biolabs, U.S.A) | recombinant FtsA and FtsZ cell division proteins | anti-*P. aeruginosa* peptide | (Paradis-Bleau, Sanschagrin, & Levesque, 2005) |
| Self-constructed peptide phage library (DIP3) | whole *Escherichia coli* cells | anti-*P. aeruginosa* peptide | (Pini et al., 2005) |
| PHD-12 peptide library (New England Biolabs, U.S.A) | whole *Escherichia coli* cells | anti-*P. aeruginosa* peptide | (Rao, Mohan, & Atreya, 2013) |
| self-constructed human scFv antibody phage display libraries | heat-killed *P. aeruginosa* | scFv against Psl exopolysaccharide of *P. aeruginosa* | (DiGiandomenico et al., 2012) |
| self-constructed human scFv antibody phage display library | recombinant *P. aeruginosa* exotoxin A | scFv against *P. aeruginosa* exotoxin A | (Kulkeaw et al., 2009; Santajit et al., 2019) |

### 2.7.2 *Propionibacterium acnes* (Gram-positive bacilli)

*P. acnes* is anaerobic skin commensal which plays a major role in pathogenesis of acne. It can persist intracellularly in human macrophage cells (Achermann, Goldstein, Coenye, & Shirtliff, 2014; Fischer et al., 2013). It has the ability to form biofilm and give implant-associated infections (Sowmiya et al., 2015). Some of the *P. acnes* related infections are summarized in **Table 2.4** below.

**Table 2.4 Invasive infections caused by *P. acnes***

| ***P. acnes* is the causal agent** | **References** |
|---|---|
| *P. acnes*: an agent of prosthetic joint infection and colonization | (Zeller et al., 2007) |
| Intravascular device infections epidemiology, diagnosis, and management | (Gandelman et al., 2007) |
| Management and outcome of permanent pacemaker and implantable cardioverter-defibrillator infections | (Sohail et al., 2007) |
| Characteristics and treatment outcome of cerebrospinal fluid shunt–associated infections in adults: a retrospective analysis over an 11-year period | (Conen et al., 2008) |
| Risk factors for infections related to external ventricular drainage | (Hoefnagel, Dammers, Ter Laak-Poort, & Avezaat, 2008) |
| Microbiologic diagnosis of prosthetic shoulder infection by use of implant sonication | (Piper et al., 2009) |
| Sonication of removed breast implants for improved detection of subclinical infection | (Rieger, Pierer, Luscher, & Trampuz, 2009) |
| Pilot study of association of bacteria on breast implants with capsular contracture | (Pozo et al., 2009) |
| Bacterial colonization and infection of electrophysiological cardiac devices detected with sonication and swab culture | (Rohacek et al., 2010) |
| Peri-prosthetic infections after shoulder hemiarthroplasty | (Singh, Sperling, Schleck, Harmsen, & Cofield, 2012) |
| Characteristics and outcome of 16 periprosthetic shoulder joint infections | (Achermann et al., 2013) |
| *P. acnes*: an underestimated etiology in the pathogenesis of osteoarthritis? | (Levy et al., 2013) |
| Characteristics of infections associated with external ventricular drains of cerebrospinal fluid | (Walti, Conen, Coward, Jost, & Trampuz, 2013) |

**Table 2.4 Invasive infections caused by *P. acnes* (continued)**

| ***P. acnes* is the causal agent** | **References** |
|---|---|
| Infection rates of external ventricular drains are reduced by the use of silver-impregnated catheters | (Lajcak, Heidecke, Haude, & Rainov, 2013) |
| Bacterial biofilms and capsular contracture in patients with breast implants | (Rieger et al., 2013) |
| Nonpyogenic degenerated intervertebral discs | (Yuan et al., 2017) |
| Prosthetic valve endocarditis due to P. acnes | (Valen, Wijngaarden, Verkaik, Mokhles, & Bogers, 2016) |
| Shoulder infections after orthopedic implantation | (Lim, Na, & Joo, 2017) |
| 18% of infectious keratitis | (Kadler, Mehta, & Funk, 2015) |
| *P. acnes* endophthalmitis in a glaucoma patient | (Gutiérrez-Díaz, Montero-Rodríguez, Mencía-Gutiérrez, Fernández-González, & Pérez-Blázquez, 2001) |
| Patients with prosthetic heart valves or annuloplasty ring are vulnerable to *P. acnes* endocarditis | (Banzon et al., 2017) |

*P. acnes* has been used as biopanning target by one study group (Jung et al., 2008). They generated scFv display phage library from human peripheral blood mononuclear cells which were immunized in vitro with heat-killed *P. acnes*. Although three anti-*P. acnes* scFv clones were identified, there was no known further development from them.

Our study was performed to identify scFv from Yamo-I phage display human scFv library by affinity selection against *P. acnes* and *P. aeruginosa*. The isolated scFv were used to identify target ligands. The selected scFv were engineered into different formats, such as, biotinylated-scFv, EmGFP-tagged scFv, and anti-microbial peptide-conjugated scFv. Finally, scFv were engineered into full-length IgG. These scFv are expected to be developed into antibody therapeutics for antibiotic-resistant *P. acnes* and *P. aeruginosa* infections, and diagnostics for implantation infections caused by *P. acnes* in the future.

# CHAPTER III

# ISOLATION AND IDENTIFICATION OF SCFV AGAINST *P. ACNES* AND *P. AERUGINOSA* BY AFFINITY SELECTION

## 3.1 Abstract

Globally, the Nobel-prize winning antibody phage display technology has been used to isolate and identify antibody fragments specific against the target of interest. In this study, to identify scFv specific against *Propionibacterium acnes* and *Pseudomonas aeruginosa* from Yamo-I phage display human scFv library, affinity selection (biopanning) was performed. Three scFv clones specific against *P. acnes* were identified after first round and one scFv clone specific against *P. aeruginosa* was obtained after third round of affinity selection. The best anti-*P. acnes* clone, yPac1A8 scFv, and anti-*P. aeruginosa* clone, yPgi3G4 scFv were studied further. Their target binding activity was confirmed by whole cell ELISA, Western Blot and flow cytometry. More in detail, the cell surface binding porperty of yPac1A8 and yPgi3G4 scFv were confirmed by confocal laser scanning microscopy, deltavision ultra microscopy and transmission electron microscopy. Both scFv were selected to be engineered for therapeutic and diagnostic purposes.

## 3.2 Introduction

A recombinant scFv antibody fragment is a single polypeptide chain which contains antigen binding domains ($V_H$ and $V_L$) of lgG joined covalently by a flexible peptide linker. One scFv fragment has a molecular weight of about 30 kDa and a diameter of 5 nm, which is about one-fifth the size of parental IgG molecule. MY LAB has developed a human scFv display phage library, named as Yamo-I library, from 140 healthy blood donors. Yamo-I library has 1.5 x $10^8$ clonal strength (Pansri, Jaruseranee, Rangnoi, Kristensen, & Yamabhai, 2009). From Yamo-I library, scFv specific against model bacteria of this study (*P. acnes* and *P. aeruginosa*) were isolated by affinity selection.

## 3.3 Materials and methods

### 3.3.1 Bacterial strains

*Propionibacterium acnes* DMST 14916 and *Pseudomonas aeruginosa* DMST 37186 were kindly provided by Assoc. Professor Griangsak Eumkeb, Thailand. Species identity of both strains were confirmed by 16S rRNA gene sequencing at Macrogen, Inc., South Korea. *P. acnes* DSM strains 1897, 16379, 30738, 30753 and 30919 were kindly provided by Professor Dietmar Haltrich, Austria. *Propionibacterium freudenreichii* TISTR 446, *Pseudomonas fluorescens* TISTR 358, *Pseudomonas putida* TISTR 1522, and *P. aeruginosa* TISTR strains 357, 781 and 1287 were purchased from Thailand Institute of Scientific and Technological Research (TISTR). *Propionibacterium acidipropionici* TISTR 442 and *P. aeruginosa* TISTR 1101 were kindly provided by TISTR for academic research purpose. TG1 strain *Escherichia coli and* HB2151 strain *E. coli* were obtained from Medical Research

Council Laboratory, Cambridge, UK. SHuffle T7 B strain *E. coli* (NEB#C3029J, U.S.A) was purchased from New England Biolabs, U.S.A.

### 3.3.2 Affinity selection (Biopanning) against *P. acnes* and *P. aeruginosa*

#### 3.3.2.1 Biopanning antigen preparation

Estimation of colony forming units (cfu) in bacterial suspension at an optical density ($OD_{600}$) 2.0 was performed according to Miles and Misra method (Miles, Misra, & Irwin, 1938). *P. acnes* suspension at $OD_{600}$ 2.0 contained about $1.6x10^9$ cfu/mL and that of *P. aeruginosa* contained about $2.7x10^9$ cfu/mL. Bacterial antigens from *P. acnes* DMST 14916 and *P. aeruginosa* DMST 37186 were prepared as previously described with some modifications (Vu et al., 2017). Briefly, *P. aeruginosa* colonies, streaked from -80°C stock on an LB agar, were inoculated into LB broth and incubated overnight at 250 rpm, 37°C; while, *P. acnes* colonies, streaked from -80°C stock on BHI agar, were inoculated into BHI broth and incubated for 5 days at 37°C anaerobically in a GasPak system. Bacterial cells were washed with PBS for two times and resuspended in PBS and $OD_{600}$ was adjusted to 2.0. Cell suspensions were boiled for 1 h in a water bath and protein concentration was checked by Bradford standard microtiter plate assay (BioRad#500-0006, California, U.S.A).

#### 3.3.2.2 Affinity selection procedure

Biopanning was carried out according to previously published protocol (McCafferty & Johnson, 1996). Maxisorp immunotube (Nalgene Nunc International, Denmark) was coated with 25 µg of boiled bacterial antigen in 100 mM

$NaHCO_3$ (pH 8.5) at 4ºC overnight. After washing three times with PBS, the tube was blocked with 2% (w/v) skimmed milk protein in phosphate buffer saline (PBSM) for 2 h. After three times washing with PBS, $10^{12}$ plaque forming units (pfu) of bacteriophage virions from Yamo-I human phage display scFv library (Pansri et al., 2009) in 2% PBSM was added and incubated for 2 h. It was washed 5 times with 0.05% (v/v) Tween-20 in PBS (PBST), followed by 5 times with PBS. The bound bacteriophages were eluted with 1 mg/mL of trypsin in PBS followed by 100 mM glycine-HCl (pH 2.0) elution and neutralization was carried out with 200 mM $NaPO_4$ (pH 7.5). Eluted bacteriophages were used to infect log phase *E. coli* TG1 and were spread onto a 2×YT agar plate containing 100 µg/mL ampicillin and 1.0% (w/v) glucose. For the second and third round, eluted bacteriophages were pooled together, amplified and purified by PEG (polyethylene glycol)-8000/NaCl precipitation, as previously described (Rangnoi, Jaruseranee, O'Kennedy, Pansri, & Yamabhai, 2011).

**3.3.2.3 Amplification of the individual bacteriophage clone**

Discrete colonies of *E. coli* TG1, infected with eluted phages from biopanning, were randomly picked and cultured in U-shaped 96-well microplates (ThermoScientific#163320, U.S.A) containing 2xYT-AmpGlu medium (2×YT medium containing 100 µg/mL ampicillin, 1.0% (w/v) glucose). After overnight incubation at 37°C, 5 µL from each well was sub-cultured into 200 µL of 2×YT-AmpGlu medium in deep-well plate (ThermoScientific #278743, U.S.A) at 37°C for 3 h. Then, 100 µL of 2×YT-AmpGlu medium containing $10^{11}$ pfu/mL of helper phage KM13 was added and incubated at 37°C at 150 rpm for 1h. After centrifuging (3000 *g*, 10 min, 4°C), cell pellet was incubated in 400 µL of 2×YT medium (100 µg/mL

ampicillin, 50 µg/mL kanamycin, 0.1% (w/v) glucose) at 30°C at 250 rpm for 20 h. After centrifugation of deep-well plate, bacteriophage containing supernatant was used for monoclonal phage ELISA as described in ELISA section.

**3.3.2.4 DNA and amino acid sequence analysis of selected bacteriophage clones**

Phagemids from selected ELISA-positive bacteriophage clones were prepared and sent for automated DNA sequence analysis as previously described (Sompungaa, Pruksametanana, Rangnoia, Choowongkomonb, & Yamabhai, 2019). DNA sequencing was performed at Macrogen, Inc., South Korea by using primers: pMOD5′ (5′ CAG GAA ACA GCT ATG ACC 3′) and pMOD3′ (5′ CCC TCA TAG TTA GCG TAA CG 3'). Contig alignment of the sequences was performed by using Vector NTI software (Thermo Fisher Scientific, U.S.A) and the aligned sequences were further analyzed with IgBLAST tool (https://www.ncbi.nlm.nih.gov/igblast/) from National Center for Biotechnology Information (Ye, Ma, Madden, & Ostell, 2013) and IMGT/V-QUEST tool (http://www.imgt.org/IMGTindex/V-QUEST.php) from international ImMunoGene-Tics information system (Brochet, Lefranc, & Giudicelli, 2008). Three-dimensional structures of selected scFv were generated by using SWISS-MODEL server (https://swissmodel.expasy.org) from Swiss Institute of Bioinformatics (Waterhouse et al., 2018) and PyMOL molecular visualization system (www.pymol.org) from Schrödinger, LLC, U.S.A (DeLano & Bromberg, 2004). From SWISS-MODEL template library, template (PDB ID code: 1f3r.1.B) was chosen by performing sequence identity analysis. Models were built by target-template alignment using ProMod3 and visualized with the program PyMOL, a

molecular visualization system from Schrödinger, LLC, U.S.A (DeLano & Bromberg, 2004).

#### 3.3.2.5 Small-scale production of soluble scFv from *E. coli* HB2151

Soluble scFv clones were produced from non-suppressor strain *E. coli* HB2151 which read the amber codon between scFv and geneIII protein DNA sequences in phagemid vector as a stop codon instead of glutamic acid (McCafferty & Johnson, 1996). Log phase HB2151 *E. coli* was infected with supernatant containing bacteriophage for 30 min at 37°C without shaking, spread onto a 2×YT-AmpGlu agar and incubated overnight at 37°C. Single colony was picked and cultured overnight in 2×YT-AmpGlu medium at 37°C at 250 rpm. It was diluted (1:100) in 2×YT medium (100 µg/mL ampicillin, 0.1% (w/v) glucose) and incubated for 3 h at 37°C with shaking. Protein expression was induced by 0.85 mM isopropyl-β-D-thiogalactopyranoside (IPTG) for 16 h at 30°C with shaking. After centrifuging (8000 rpm, 15 min, 4°C), supernatant containing soluble scFv was used for scFv ELISA as described in ELISA section.

### 3.3.3 Expression of hexa-histidine-tagged scFv (6xHis-tagged scFv)

From phagemid pMOD, scFv DNA sequences were subcloned into pET-21d (+) expression vector by restriction digestion with NcoI-HF (NEB#R3193S, U.S.A) and NotI-HF (NEB#R3189S, U.S.A). Recombinant plasmids carrying scFv genes against *P. acnes* and *P. aeruginosa* were designated as pET21d+/yPac1A8 and pET21d+/yPgi3G4, respectively. The integrity of the constructs was confirmed by

DNA sequencing (Macrogen, Inc., South Korea), using universal T7 promotor and T7 terminator primers. The scFv genes were expressed in SHuffle T7 B strain *E. coli* (NEB#C3029J, U.S.A), which promotes disulfide bond formation in cytoplasm, according to previous publications (Bezabeh et al., 2017; Lobstein et al., 2012) with some optimization. Briefly, a colony of SHuffle *E. coli* C3029 harboring pET21d+/yPac1A8 or pET21d+/yPgi3G4 was inoculated into Terrific broth (Tryptone 12 g/L, yeast extract 24 g/L, glycerol 4 mL/L, 0.17 M monobasic potassium phosphate 50 mL/L and 0.72 M dibasic potassium phosphate 50 mL/L) containing 100 µg/mL ampicillin and incubated overnight at 30°C at 225 rpm. It was sub-cultured (1:100 dilution) in fresh Terrific broth containing 100 µg/mL ampicillin and incubated at 30°C in a bench-top bioreactor system or in a baffled flask at 225 rpm until $OD_{600}$ reached 1.0. Protein expression was induced with 0.85 mM IPTG for 24 h at 25°C. The culture was kept on ice for 5 min and centrifuged at 3000 *g*, 30 min, 4°C. The cell pellet was used for scFv purification.

### 3.3.4 Purification of hexa-histidine-tagged scFv

The cell pellet was resuspended in lysis buffer (pH 7.5 containing 50 mM Tris-HCl, 0.5 M NaCl, 20 mM imidazole, 1mg/mL lysozyme) and sonicated with 500Watt Ultrasonic Processor (CV334, Thomas Scientific, U.S.A) for 30 sec followed by incubation on ice for 30 sec alternatively for 5 min. Supernatant was separated from cell debris and unbroken cells by centrifugation at 3000 *g*, 30 min, 4°C. That supernatant was centrifuged again after adding equal amount of equilibration buffer (pH 7.5 containing 50 mM Tris-HCl, 0.5 M NaCl, 20 mM imidazole) and transferred into a gravity flow column containing Ni-NTA (Nickel-Nitrilotriacetic acid) agarose

affinity chromatography matrix (Qiagen#30230, Germany), pre-equilibrated with equilibration buffer, and incubated for 45 min at 4°C. The agarose resin was washed with washing buffer (pH 7.5 containing 50 mM Tris-HCl, 0.5 M NaCl, 100 mM imidazole) and scFv was eluted with elution buffer (pH 7.5 containing 50 mM Tris-HCl, 0.5 M NaCl, 500 mM imidazole). Purity of eluted scFv was checked by SDS-PAGE (sodium dodecyl sulfate–polyacrylamide gel electrophoresis). Desalting and buffer exchange was performed by dialysis in SnakeSkin Dialysis Tubing with 10 kDa MWCO (ThermoScientific#68100, U.S.A) against PBS at 4°C overnight. Purified scFv concentration was determined by Bradford standard microtiter plate assay (BioRad#500-0006, U.S.A). The purified scFv were kept at -80°C in 250 mg/mL BSA (bovine serum albumin) or at -40°C in 20% glycerol.

### 3.3.5 Enzyme linked immunosorbent assay (ELISA)

#### 3.3.5.1 Monoclonal phage ELISA

About 5 µg of biopanning bacterial antigen in 100 mM $NaHCO_3$ (pH 8.5) was used as target and 1% (w/v) BSA in PBS as negative control. Antigen immobilization was done overnight at 4°C in Maxisorp 96-well plate (ThermoScientific #44-2404-21, U.S.A). The wells were blocked with PBSM for 1 h, incubated for 2 h with 50 µL PBSM and 150 µL phage supernatant from deep-well plate, treated for 1 h with anti-M13 mouse monoclonal antibody-HRP conjugate (GE Healthcare#27-9421-01, UK) diluted at 1:5000 in PBS, and incubated for 30 min with 1.0 mg/mL ABTS substrate (Amresco#0400-10G, U.S.A) in citric acid-$H_2O_2$ buffer (0.05%$H_2O_2$, 50 mM citric acid, pH 4.0). ELISA plate was washed by hands for three times with PBS before and after the blocking step. It was washed three times with

0.05% PBST followed by two times with PBS by using HydroFlex microplate washer (Tecan, Switzerland) after phage supernatant and antibody-HRP conjugate incubation steps. The absorbance was measured at 405 nm with Sunrise microplate reader (Tecan, Switzerland). Bacteriophage clones which showed OD value of at least two times higher than those of negative control were selected for confirmation.

**3.3.5.2 scFv ELISA against boiled bacterial antigen**

About 2 μg of biopanning bacterial antigen in 100 mM $NaHCO_3$ (pH 8.5) was used as target and 1% (w/v) BSA in PBS as negative control. Supernatant containing soluble scFv from HB2151 *E. coli* (150 μL/well) was used as primary detection agent. HisProbe-HRP diluted at 1:5000 in PBS was used as secondary detection agent. The ELISA procedure was the same as above. Clones which showed at least two times higher absorbance signal with target than negative control were selected for further study.

**3.3.5.3 scFv ELISA against whole cell bacteria**

For *Propionibacterium* species, colonies were sub-cultured into BHI broth and incubated for 5 days anaerobically at 37°C in case of *P. acnes* and at 30°C in case of *P. acidipropionici* and *P. freudenreichii*. For *Pseudomonas* species, colonies were sub-cultured into LB broth and incubated overnight at 250 rpm at 37°C in case of *P. aeruginosa* and at 30°C in case of *P. fluorescens* and *P. putida*. Cells were washed with PBS for two times and resuspended in PBS. $OD_{600}$ of cell suspensions were adjusted to 2.0 and it was heat-inactivated at 60°C for 30 min in water bath.

To check specificity of 6xHis-tagged scFv by ELISA, heat-inactivated bacteria ($10^9$ cells/mL) was used as target and purified scFv (10 μg/mL) was used as primary detection agent. ELISA procedure was the same as above except that immobilization step was performed overnight at 37°C and ELISA plate was incubated with purified scFv for 1 h.

**3.3.5.4 Checkerboard titration (dilution ELISA)**

To optimize the scFv ELISA and to determine the limit of detection of recombinant scFv, ELISA plate was coated with serial dilutions of heat-inactivated bacterial suspension from row A to F, where row A had the highest ($10^9$ cells/mL) bacterial concentration while row F had the lowest ($10^4$ cells/mL). ELISA procedure was carried out as described above except that the wells were incubated with six different dilutions of scFv in duplicate format from column 1 to 12, where column 1 and 2 had the highest scFv concentration (yPac1A8 scFv 10 μg/mL or yPgi3G4 scFv 40 μg/mL) while column 11 and 12 had the lowest (yPac1A8 scFv 0.1 μg/mL or yPgi3G4 scFv 1.0 μg/mL).

มหาวิทยาลัยเทคโนโลยีสุรนารี

**3.3.6 Western Blotting (WB)**

**3.3.6.1 WB of isolated 6xHis-tagged scFv**

Equal amount (1 μg) of purified scFv in SDS sample buffer were heat-treated at 90°C for 10 min and electrophoresed in 12.5% SDS-PAGE gel for 5 min at 50 V followed by 90 min at 100 V. Transfer of proteins from the gel to PVDF (polyvinylidene difluoride) membrane (Cytiva#10600021, U.S.A), which was activated with absolute methanol, was done at 30 V for 15 h at 4°C by wet-blotting using transfer

buffer (25 mM Tris, 192 mM glycine, 20% (v/v) methanol) and Mini Trans-Blot electrophoretic transfer cell (Biorad#1703930, U.S.A). The membrane was blocked with 3% (w/v) BSA in TBST (20 mM Tris-150 mM NaCl buffer containing 0.1% (v/v) Tween-20) for 1 h at room temperature followed by 3 times TBST washing, 5 min each. To detect scFv, the membrane was incubated with 10 mL of anti-histidine antibody-gold nanoparticle conjugate (Jena Bioscience#PS-110, Germany) for 3 h. The scFv bands became visible to the naked eyes.

**3.3.6.2 WB of bacterial targets using isolated 6xHis-tagged scFv**

About 30 µg of boiled bacterial antigen preparation was used as sample. The SDS-PAGE and wet-blotting procedures were the same as above. After blocking step, the membrane was incubated with 2 µg/mL of specific 6xHis-tagged scFv in TBST for 15 h at 4ºC, followed by washing 3 times with TBST (5 min per wash). It was then incubated with 1:5000 diluted HisProbe-HRP (a nickel $Ni^{2+}$-activated derivative of horseradish peroxidase) (Thermo Fisher Scientific#15165, U.S.A) in blocking buffer for 1 h at room temperature with slight rocking, followed by washing 3 times with TBST. Finally, the protein band was detected by chemiluminescence using Amersham ECL Prime Western blotting detection reagent (GE Healthcare#RPN2232, UK). Image analysis was performed by CCD camera-based imaging, using the ChemiDoc XRS Gel Documentation System (Bio-Rad, U.S.A).

**3.3.7 Flow Cytometry**

To check the binding of 6xHis-tagged scFv to live bacteria, a bacterial colony was suspended in 900 µL PBS and one third of it was diluted with PBS to 1 mL

and was centrifuged at 2000 *g*, 5 min. The cells were resuspended in 1 mL of 1% BSA - 0.1% PBST, blocked for 30 min at room temperature and washed two times with PBS. The cells were incubated with specific 6xHis-tagged scFv (200 µg/mL) for 1 h at room temperature. *P. acnes* cells were exposed to yPac1A8 scFv and *P. aeruginosa* cells to yPgi3G4 scFv. After two PBS washes, the cells were stained with a 1:500 dilution of Dylight 488-labelled anti-hexa-histidine mouse monoclonal antibody (Abcam# ab117512, UK) in PBS for 1 h in a dark place at room temperature. The cells were washed with PBS two times and resuspended in 500 µL PBS containing 4 µg/mL PI (Propidium Iodide) solution (Thermo Fisher Scientific#A28993, U.S.A). Sample reading was performed using Invitrogen Attune NxT Acoustic Focusing 3-Laser System Cytometer (Thermo Fisher Scientific# P3566, U.S.A).

### 3.3.8 Confocal laser scanning microscopy (CLSM)

#### 3.3.8.1 CLSM of planktonic bacteria

About 1 mL of broth culture was centrifuged (3000 *g*, 5 min), washed with PBS for two times and resuspended in PBS. About 5 µL of that was spread into a smear on a glass slide and dried completely at 37°C. The smear was fixed with 4% PFA (paraformaldehyde) in PBS (pH 7.4) for 30 min, blocked with 1% BSA-300 mM glycine-0.1% PBST for 30 min, treated with 2 µg of 6xHis-tagged scFv for 1 h, incubated with 1:500 dilution of Dylight 488-labelled anti-hexa-histidine mouse monoclonal antibody (Abcam#ab117512, UK) in PBS for 1 h, and counterstained with 300 µM DAPI (4′,6-diamidino-2-phenylindole) for 5 min. The smear was washed three times with PBS between above steps. The stained smear was covered with slow fade

gold mountant (Invitrogen#S36936, U.S.A) and examined with confocal microscope (Nikon A1R, Japan).

#### 3.3.8.2 Deltavision Ultra Microscopy of planktonic bacteria

The immunostaining procedure of *P. acnes* and *P. aeruginosa* with specific 6xHis-tagged scFv was carried out as above. The stained smears were examined with Deltavision Ultra Microscope (Cytiva, U.S.A) at the Microbe Lab, Institute of Molecular Biosciences, Mahidol University.

#### 3.3.8.3 CLSM of bacteria in biofilm

Bacterial biofilm was grown on coverslip by placing autoclaved glass coverslip at air-liquid interface of bacterial broth cultures as previously described (Schlapp, Scavone, Zunino, & Hartel, 2011). The incubation time for *P. acnes* and *P. aeruginosa* biofilms were 5 days anaerobically in GasPak system and overnight aerobically, respectively. Biofilms were washed with PBS for three times and dried completely at 37°C. The 6xHis-tagged scFv staining procedure was the same as above except that 20 µg of scFv was used for biofilm. One set of biofilms was used for crystal violet staining.

### 3.3.9 Transmission electron microscopy (TEM)

The procedure was carried out in a microcentrifuge tube. Bacteria in broth culture were centrifuged at 3000 *g*, 5 min and washed with 0.85% NaCl followed by PBS and fixed with 4% PFA (pH 7.4) in PBS for 30 min at room temperature. After washing with PBS for two times, the bacteria were blocked with 1% BSA - 300 mM

glycine in 0.1% PBST for 30 min at room temperature, followed by two PBS washes. Then, 50 µg of 6xHis-tagged scFv in PBS was added and incubated for 60 min at room temperature. After washing 2 times with PBS, a 1:20 dilution of 10 nm Ni-NTA nanogold (Nanoprobes#2084, U.S.A) in 0.05% TBST containing 1% BSA, which is the recommended dilution from the manufacturer, was added and incubated for 30 min at room temperature followed by two TBST-BSA washes. Then, the samples were resuspended in PBS, dehydrated by the graded ethanol dehydration method and polymerized in LR White medium grade resin and accelerator (EMS#14380, U.S.A) in a BEEM embedding capsule (EMS#69911-01, U.S.A) by a cold curing method. Finally, ultra-thin sections were examined with a transmission electron microscope (Hitachi Hi-Tech HT7700, Japan).

## 3.4 Results and discussion

### 3.4.1 Affinity selection against *P. acnes* and *P. aeruginosa*

Affinity selection of scFv fragments against *P. acnes* and *P. aeruginosa* was performed using Yamo-I human scFv library and a summary of biopanning results is shown in **Table 3.1** below.

After first round of biopanning against *P. acnes* (DMST 14916), 844 colonies of TG1 strain *E. coli* infected with eluted bacteriophages were obtained. Then, 576 colonies were manually picked and were subjected to monoclonal phage ELISA. Three bacteriophage clones, eventually designated as yPac1A8, yPac1E4, and yPac1E7 showed two folds higher OD signal against *P. acnes* than negative control (1%BSA), were selected for binding confirmation by phage ELISA and sent for DNA sequence analysis.

**Table 3.1 Summary of biopanning against *P. acnes* and *P. aeruginosa***

| **Biopanning target** | ***P. acnes* DMST 14916** | ***P. aeruginosa* DMST 37186** |
|---|---|---|
| round of selection done | 1 | 3 |
| colonies obtained | 844 colonies | $2.2 \times 10^4$ colonies |
| colonies picked up | 576 colonies | 96 colonies |
| positive clones at monoclonal phage ELISA | 3 clones | 61 clones |
| positive clones at scFv ELISA expressed in HB2151 *E. coli* | 1 out of 2 clones tested | 4 out of 15 clones tested |
| clones sent for DNA sequencing | 3 clones | 4 clones |
| DNA sequencing result | 3 unique scFv sequences | all 4 clones have same scFv sequence |
| scFv clone identity | yPac1A8, yPac1E4, yPac1E7 | yPgi3G4 |

The result revealed that they possessed unique scFv sequences. The clone yPac1E7 had an amber stop codon (TAG) within its open reading frame. Then, soluble scFv production in nonsuppressor strain *E. coli* (HB2151) was performed with yPac1A8 and yPac1E4 and the culture supernatant was used for scFv ELISA. Only yPac1A8 clone, which showed two times higher absorbance with target than 1%BSA control, was selected for expression in pET-21d (+).

For biopanning against *P. aeruginosa* (DMST 37186), 3 rounds of affinity selection were carried out and 96 colonies were randomly picked for monoclonal phage ELISA. Sixty-one bacteriophage clones showed two folds higher OD values against *P. aeruginosa* than negative control (1%BSA). After binding confirmation, 15 clones were selected to generate soluble scFv from non-suppressor strain *E. coli* HB2151. Out of 15, 4 clones that showed high signal by scFv ELISA were sent for DNA sequencing, and the result revealed that all clones possessed the same

scFv sequence. Among them, the clone which had the highest signal in HB2151 scFv ELISA (yPgi3G4) was selected for expression in pET-21d (+).

### 3.4.2 DNA and amino acid sequence analysis of selected bacteriophage clones

A diagram of recombinant scFv in this study is depicted in **Figure 3.1A**. Variable region of heavy chain ($V_H$) at N-terminus is connected to variable region of light chain ($V_L$) by GGGGSGGGGSGGGGS peptide linker sequence. C-terminus of scFv is linked with hexa-histidine tag (6xHis tag), followed by Myc tag. The gene of scFv and gene III protein sequence of bacteriophage are intervened by an Amber stop codon (TAG) which is recognized by the non-suppressor strain of *E. coli* HB2151 as a stop signal (Pansri et al., 2009). Comparison between DNA and amino acid sequences of isolated clones and human germline antibody variable region gene sequences are presented in **Table 3.2**.

Data analysis was performed by using IgBLAST (Ye et al., 2013) and IMGT/V-QUEST tools (Brochet et al., 2008). Out of the 7 existed IGHV (human immunoglobulin heavy variable) gene subgroups (IGHV-1 to 7), isolated scFv clones of this study belong to subgroup 3 and 6. Clones active against *P. acnes* (yPac1A8, yPac1E4, yPac1E7) are from IGHV subgroup 6 and derived from the same germline gene and allele IGHV6-1*01 with >91% sequence identity. Their sequences differ from germline by 13 to 17 amino acids. The highest amino acid variation frequency, 17 residues, is seen in yPac1E7 whose heavy chain variable domain is unproductive because of the presence of stop codon. All three clones share one CDR3 (complementary-determining region 3) amino acid sequence pattern ("-RG-S-FDM").

Clone active against *P. aeruginosa* (yPgi3G4) is from IGHV subgroup 3 and derived from IGHV3-7*01 with >90% sequence identity. Its sequence is different from germline by 15 amino acids.

**Table 3.2 Summary of DNA and amino acid sequence analysis of isolated scFv**

| **scFv clone** | **Germline** | **Identity to germline** | **Amino acid differences from germline** | **CDR3 sequence** |
|---|---|---|---|---|
| $V_H$ genes | | | | |
| yPac1A8 | Homsap IGHV6-1*01 | 92.59% | 13 | TRGKYSGFDM |
| yPac1E4 | Homsap IGHV6-1*01 | 92.59% | 13 | TRGKYSGFDM |
| yPac1E7 | Homsap IGHV6-1*01 | 91.92% | 17 | VRGQHSAFDM |
| yPgi3G4 | Homsap IGHV3-7*01 | 93.40% | 15 | ARVLWGFPFDL |
| $V_L$ genes | | | | |
| yPac1A8 | Homsap IGLV2-18*02 | 94.44% | 9 | SSFTSTISPSYV |
| yPac1E4 | Homsap IGLV2-14*01 | 98.96% | 1 | SSYTSSSPNWV |
| yPac1E7 | Homsap IGLV2-18*02 | 93.75% | 12 | SSYTSSSTWV |
| yPgi3G4 | Homsap IGLV2-8*01 | 97.57% | 8 | SSYGGSNNLV |

All isolated scFv clones, either active against *P. acnes* or *P. aeruginosa*, are members of IGLV (human immunoglobulin λ variable) gene subgroup 2 out of existing 11 (IGLV-1 to 11). The immunoglobulin light chain κ to λ ratio has been estimated to be 1.5 to 2, and the chance of isolating κ light chain antibodies is higher

than that of λ (Townsend et al., 2016). However, in our study, all scFv clones have λ light chain. Two of them (yPac1A8, yPac1E7) are derived from IGLV2-18*02 with >93% sequence identity and 9 to 12 amino acids difference. Another clone (yPac1E4) originates from IGLV2-14*01 with nearly 99% sequence identity and has only one amino acid difference. The last clone (yPgi3G4) is a derivative of IGLV2-8*01 with >97% sequence identity and has 8 amino acids difference. The amino acid sequence of the light chain CDR3 region of all isolated clones starts with "SS" and ends with "V".

Out of four scFv clones, the protein structure of yPac1A8 (anti-*P. acnes* clone) and yPgi3G4 (anti-*P. aeruginosa*) were studied further. Anti-*P. acnes* (yPac1A8) scFv is a 29.4 kDa protein of 279 amino acids. Anti-*P. aeruginosa* (yPgi3G4) scFv is a 28.7 kDa protein of 274 amino acids. The surface view of the predicted three-dimensional structure of yPac1A8 and yPgi3G4 were illustrated in **Figure 3.1B and 3.1C**, respectively. In addition, α-helix and β-sheet view of both clones were illustrated in **Figure 3.1D and 3.1E**. The intra-domain disulfide bond of yPac1A8 $V_H$ region was zoomed in and shown in **Figure 3.1D**.

มหาวิทยาลัยเทคโนโลยีสุรนารี

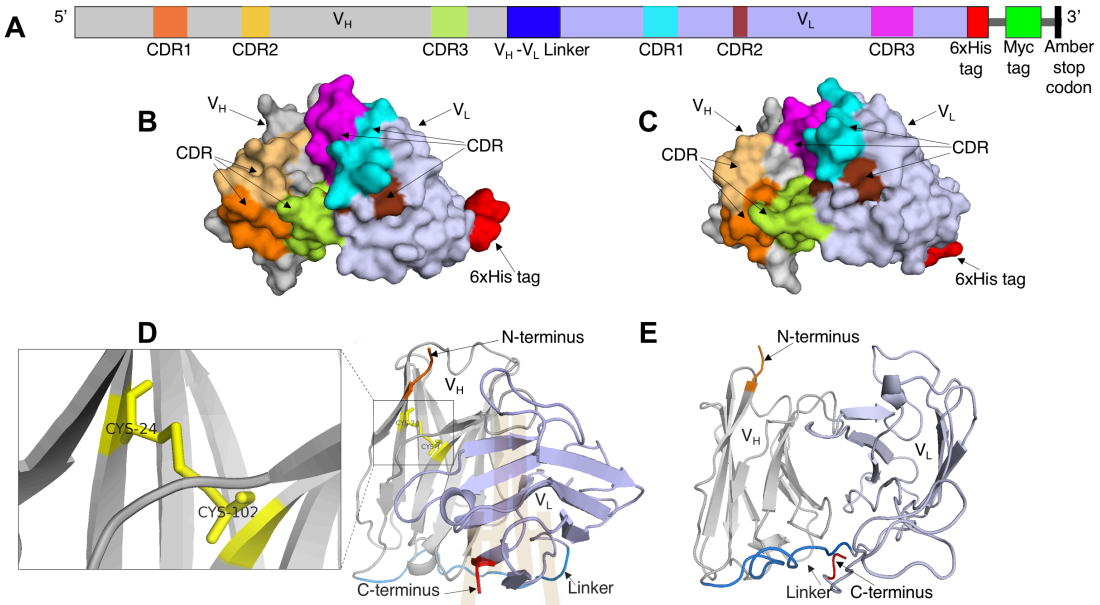


**Figure 3.1** **DNA and amino acid sequence analysis of yPac1A8 and yPgi3G4.** (A) Schematic arrangement of scFv primary structure from N-terminus (5') to C-terminus (3'): CDRs of $V_H$ domain, $V_H$-$V_L$ linker (blue), CDRs of $V_L$ domain, 6xHis tag (red), Myc tag (green), Amber stop codon (black). Surface view of (B) yPac1A8 scFv and (C) yPgi3G4 scFv: with same color coding as (A). A ribbon model of (D) yPac1A8 scFv and (E) yPgi3G4 scFv: N-terminus (orange), $V_H$ domain (grey), disulfide bridge (yellow), linker (blue), $V_L$ domain (violet) and C-terminus (red). Only yPac1A8 possesses intra-domain disulfide bridge between Cysteine 24 and Cysteine 102 residues of VH domain (shown in inset).

### 3.4.3 Expression and purification of 6xHis-tagged scFv

To further characterize, DNA sequences of yPac1A8 and yPgi3G4 scFv were sub-cloned into pET-21d (+), expressed in SHuffle T7 B strain *E. coli*, and purified by one-step Ni-NTA agarose affinity chromatography. Optimization of expression and purification processes were done and SDS-PAGE of the purification process of both scFv, before and after optimization are demonstrated in **Figure 3.2A to 3.2D**.

The majority of unwanted protein fractions could be removed after optimization. Elution fractions contained bands of scFv at expected molecular weight of approx. 29 kDa. About 3.0 mg of purified yPac1A8 scFv and 2.3 mg of purified yPgi3G4 scFv are routinely obtained from 1 L Terrific broth by baffled flask culture system. Discrepancy between the purity of the two scFv clones was observed under the same scFv expression and purification protocols (**Figure 3.2**). Clone yPac1A8, which has higher yield, appeared purer than clone yPgi3G4.

The two scFv clones were also observed by WB as shown in **Figure 3.2E**. About 1 µg of each scFv could be detected by anti-histidine antibody gold nanoparticle conjugate, indicating that hexa-histidine tag of both scFv fragments could interact with anti-6xhistidine detection system. Both yPac1A8 and yPgi3G4 scFv could be observed as bright red bands at expected size. Although equal amount of scFv as estimated by Bradford standard microtiter plate assay were loaded, yPgi3G4 WB band appeared slightly thinner than that of yPac1A8.

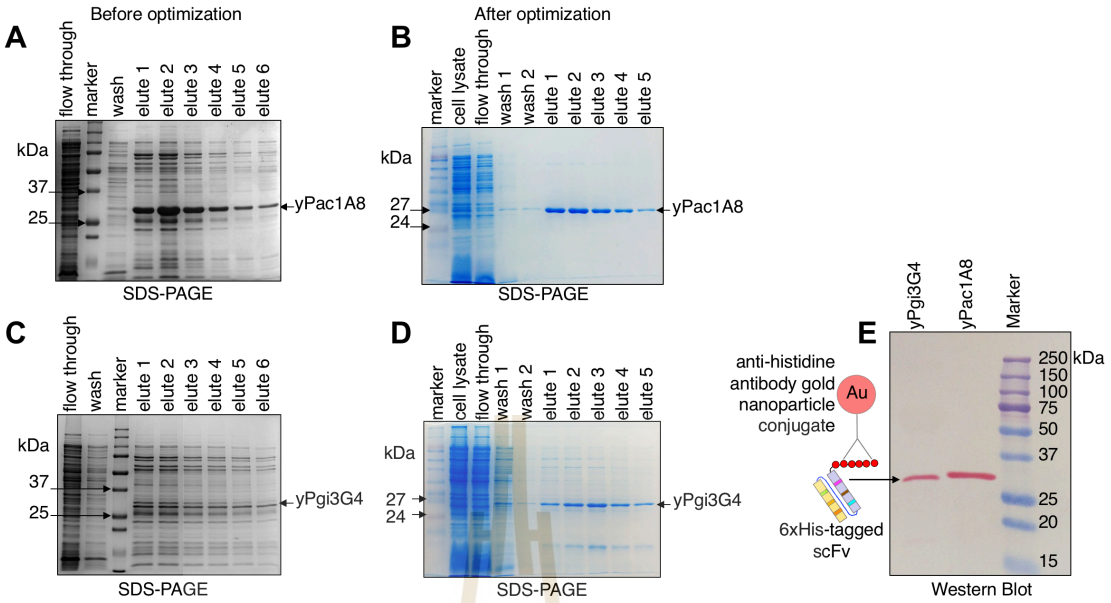


**Figure 3.2** **Expression and purification of 6xHis-tagged scFv.**

All gels were Coomassie Brilliant Blue-stained. (A) yPac1A8 scFv before optimization. (B) yPac1A8 scFv after optimization. (C) yPgi3G4 scFv before optimization (D) yPgi3G4 scFv after optimization. Precision Plus All Blue Prestained Protein Standards (BioRad#1610373, U.S.A) was used as a molecular weight marker in A and C. Prestained Protein Standards (Enzmart#APC-001, Thailand) was used as a molecular weight marker for B and D. (E) Purified yPac1A8 and yPgi3G4 scFv were resolved by SDS-PAGE and immunoblotted with anti-histidine antibody-gold nanoparticle conjugate. Solid arrow indicates scFv bands at correct size (about 30 kDa).

### 3.4.4 Specific binding of antibacterial scFv by whole cell ELISA

To evaluate the binding specificity of the two antibacterial scFv antibodies, ELISA against whole cell bacteria was performed. The binding of yPac1A8 and yPgi3G4 scFv were tested against a panel of Gram-positive bacteria (*P. acidipropionici, P. freudenreichii, P. acnes*) and Gram-negative bacteria (*P. putida, P. fluorescens, P. aeruginosa*). Heat-inactivated whole cell bacteria ($10^9$ cells/mL) were immobilized and incubated with 10 µg/mL of the two scFv clones.

Specific binding of yPac1A8 scFv to *P. acnes* and that of yPgi3G4 scFv to *P. aeruginosa* were demonstrated in **Figure 3.3A and 3.3B**. Anti-*P. acnes* scFv (yPac1A8) did not bind to five *P. acnes* strains tested other than its biopanning target. Anti-*P. aeruginosa* scFv (yPgi3G4) could bind to three out of four *P. aeruginosa* strains tested in addition to its biopanning target.

### 3.4.5 Detection of bacterial targets by WB

The preliminary detection of target antigens of the two scFv clones was performed by WB. As shown in **Figure 3.3C**, yPac1A8 scFv could detect its target antigen, located between 20 and 25 kDa regions, from denatured *P. acnes* DMST 14916 preparation but not from other *P. acnes* strains tested. Similarly, as shown in **Figure 3.3D**, yPgi3G4 scFv could detect its target antigen, located between 37 and 50 kDa regions, out of the boiled *P. aeruginosa* DMST 37186 preparation. Moreover, yPgi3G4 scFv could detect its target from three other *P. aeruginosa* strains tested (TISTR 357, 1101, 1287) except TISTR 781. These results are similar to the patterns obtained from ELISA assay.

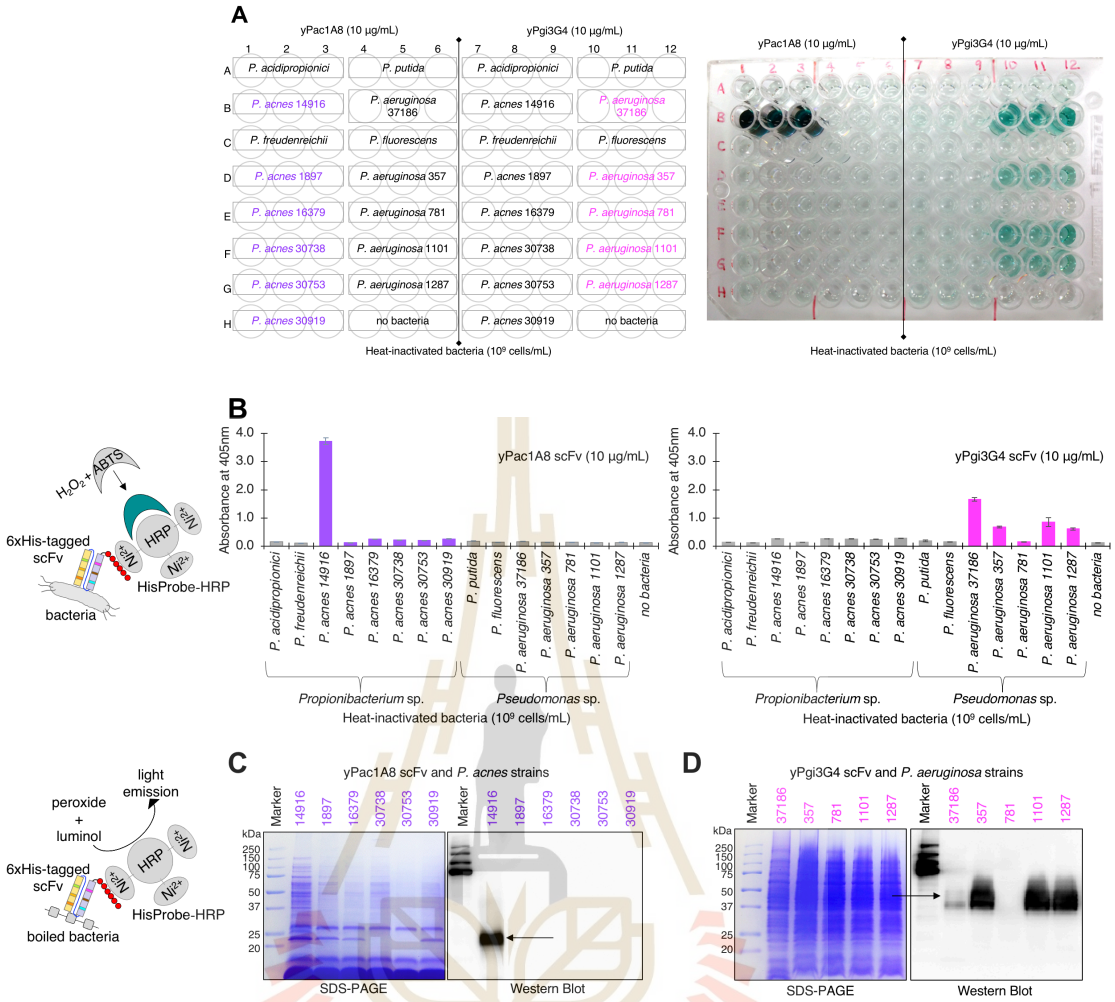


**Figure 3.3** **Cross-reactivity analysis of scFv by whole-cell ELISA and WB.**

Binding activity of yPac1A8 and yPgi3G4 scFv were determined by whole-cell ELISA on plate coated with indicated bacteria (A): *P. acidipropionici* TISTR 442, *P. freudenreichii* TISTR 446, *P. acnes* DMST 14916, *P. acnes* strains DSM 1897, 16379, 30738, 30753, 30919, *P. putida* TISTR 1522, *P. fluorescens* TISTR 358, *P. aeruginosa* DMST 37186, *P. aeruginosa* strains TISTR 357, 781, 1101, 1287. (B) The bars represent the average OD values of triplicate samples and error bars represent the standard error of the mean. (C) Coomassie Brilliant Blue-

stained SDS-PAGE and WB of boiled antigen preparation of *P. acnes* strains (DMST 14916, DSM 1897, 16379, 30738, 30753, 30919) immunoblotted with yPac1A8 scFv. *P. acnes* antigen located between 20 and 25 kDa (arrow pointed) was detected by yPac1A8 scFv. (D) SDS-PAGE and WB of boiled antigen preparation of *P. aeruginosa* strains (DMST 37186, TISTR 357, 781, 1101, 1287) immunoblotted with yPgi3G4. *P. aeruginosa* antigen located between 37 and 50 kDa (arrow pointed) was detected by yPgi3G4 scFv. Precision Plus All Blue Prestained Protein Standards (BioRad#1610373, U.S.A) was used as a molecular weight marker.

It has been shown that the level of expression and folding of different scFv fragments varied, depending on amino acid sequence and intracellular disulfide bond formation (Zarschler, Witecy, Kapplusch, Foerster, & Stephan, 2013). In this study, while there was one intra-domain disulfide in yPac1A8 scFv, there was no detectable disulfide bond formation in yPgi3G4. Consequently, we observed that the clone yPgi3G4 was less stable and this could be because the folding was disulfide-independent (Proba, WoÈrn, Honegger, & PluÈckthun, 1998). Even though both scFv antibodies could be expressed at relatively good yield from *E. coli* SHuffle strain, which favors disulfide bond formation inside cytoplasm (Berkmen, 2012; Ren, Ke, & Berkmen, 2016), it is possible to improve the stability, hence binding affinity, by introducing inter-domain disulfide bond (Weatherill et al., 2012; Zhao et al., 2010).

### 3.4.6 Checkerboard titration (Dilution) ELISA

A checkerboard titration was used to find the optimal concentration of target bacteria and corresponding scFv antibody for ELISA-based experiments and future applications (Bio-Rad, 2017; Boster-Bio, 2017; Fitzgerald, 2020). The results are shown in **Figure 3.4A and 3.4C**. For yPac1A8, the highest scFv concentration tested (10 μg/mL) could detect $1.6x10^5$ cells/mL and the lowest scFv concentration tested (0.1 μg/mL) could detect $1.6x10^9$ cells/mL. For yPgi3G4, as much as 40 μg/mL of scFv could detect $2.7x10^7$ cells/mL.

Based on checkerboard titration results, $10^9$ cells/mL of target bacteria and 10 μg/mL of scFv have been used in ELISA. In comparison, the binding affinity of scFv clone yPac1A8 to its target (*P. acnes*) is higher than that of the clone yPgi3G4 against its target (*P. aeruginosa*), at least in scFv ELISA. While apparent binding characteristic of the two isolated antibody seems sufficient for various assay formats, further improvement of binding affinity or specificity could be performed by different affinity maturation techniques as previously described (Rajpal et al., 2005; Rangnoi, Choowongkomon, O'Kennedy, Ruker, & Yamabhai, 2018).

มหาวิทยาลัยเทคโนโลยีสุรนารี

### 3.4.7 Detection of live bacteria by flow cytometry

To demonstrate the binding of yPac1A8 and yPgi3G4 to live target bacteria, flow cytometry analysis was performed. *P. acnes* and *P. aeruginosa* cells were exposed to corresponding specific scFv, followed by anti-polyhistidine Dylight 488 secondary antibody staining. Cells stained only with anti-polyhistidine Dylight 488 monoclonal antibody were used as negative control. From each sample, 10,000 events were collected and around 90% of them were bacteria which were gated in hierarchy

for Dylight 488 fluorescence signal. About 96.9% and 83.3% of *P. acnes* and *P. aeruginosa* were stained with their corresponding antibodies. Data analysis was performed using built-in Attune Cytometric Software. The results were presented in histogram overlay format in **Figure 3.4B and 3.4D**.

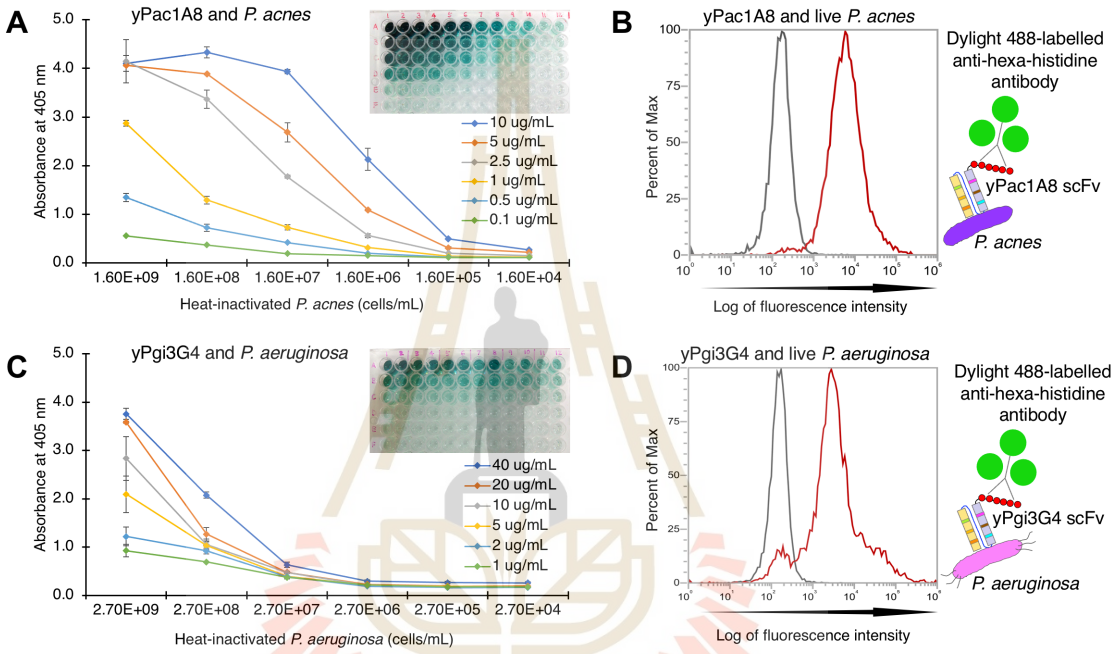


**Figure 3.4** **Checkerboard titration and flow cytometry analysis.**

Limit of detection of yPac1A8 for *P. acnes* DMST 14916 (A) and yPgi3G4 for *P. aeruginosa* DMST 37186 (C) were determined by checkerboard titration of whole-cell ELISA, using dilution series of scFv and serial dilutions of bacteria as indicated. The lines represent the average absorbance values of duplicate samples and error bars represent the standard error of the mean. Flow cytometry analysis of yPac1A8 (B) and yPgi3G4 scFv (D) binding to live *P. acnes* DMST 14916 and *P. aeruginosa* DMST 37186, respectively. Reactivity of 6xHis-tagged

scFv is indicated by red line. Secondary antibody alone control is indicated by black line.

### 3.4.8 Immunofluorescent staining of planktonic bacteria

#### 3.4.8.1 CLSM of planktonic bacteria

In addition to ELISA, WB, and flow cytometry, the binding of scFv antibodies was also revealed by confocal laser-scanning microscope technique as illustrated in **Figure 3.5 and 3.6**. *P. acidipropionici, P. freudenreichii* and *P. aeruginosa* were used as controls to demonstrate the species-specific binding of yPac1A8 to *P. acnes* (**Figure 3.5**). In bright field panel, bacterial cells were seen dispersed throughout the field. In DAPI panel, the nucleoid regions of bacteria were stained blue. In Dylight 488 panel, only *P. acnes* cells were bound by yPac1A8 hexa-histidine-tagged scFv which were detected by Dylight 488-labelled secondary detection agent and the cells appeared green. Some *P. acnes* cells showed green cell outline along unstained center suggesting the cell surface localization of yPac1A8 scFv-ligand.

Similar species-specific binding could be observed between 6xHis-tagged yPgi3G4 and its target bacteria, *P. aeruginosa* cells (**Figure 3.6**). *P. putida, P. fluorescens and P. acnes* were used as bacterial control. These results corresponded well with the ELISA as described in the previous section.

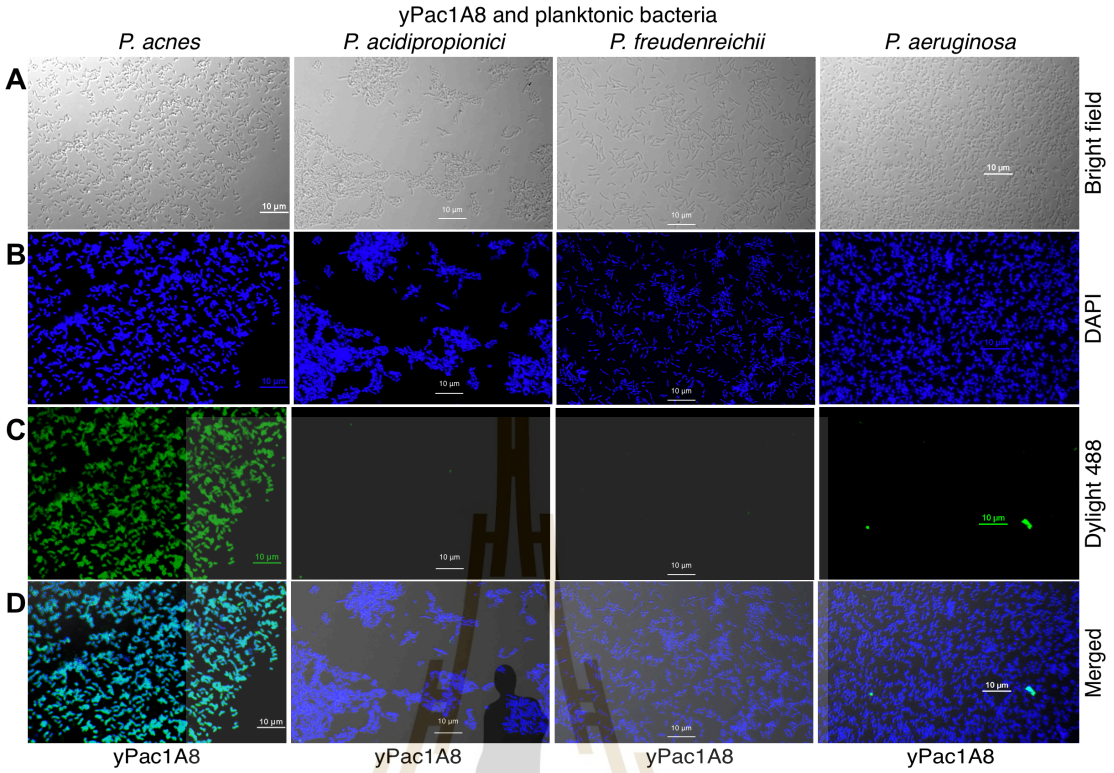


**Figure 3.5** **CLSM of yPac1A8 and planktonic bacteria**.

*P. acnes* DMST 14916, *P. acidipropionici* TISTR 442, *P. freudenreichii* TISTR 446 and *P. aeruginosa* DMST 37186 were incubated with yPac1A8 scFv, detected by Dylight 488-labelled anti-hexa-histidine mouse monoclonal antibody, and counterstained with DAPI. Photos were taken by Apo TIRF 60x Oil DIC N2 objective of Nikon A1R confocal laser microscope. Scale bar represents 10 μm. In bright field panel (A), individual bacterial cells were seen. In DAPI panel (B), nucleoids of bacteria were stained blue. In Dylight 488 panel (C), only *P. acnes* DMST 14916 was stained green. In merged panel (D), the blue nucleoids and the green cell surfaces of *P. acnes* overlapped. In case of

*P. acidipropionici, P. freudenreichii* and *P. aeruginosa*, only the blue nucleoids were seen.

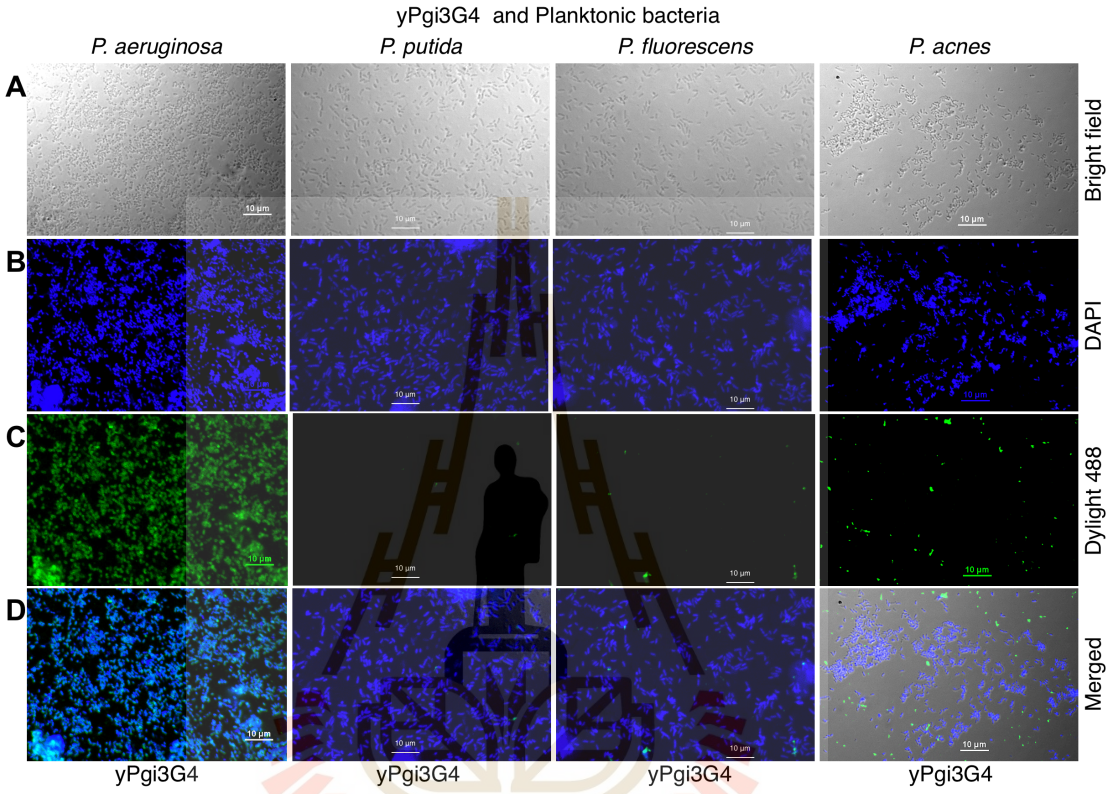


**Figure 3.6 CLSM of yPgi3G4 and planktonic bacteria.**

Photos of *P. aeruginosa* DMST 37186, *P. putida* TISTR 1522, *P. fluorescens* TISTR 358 and *P. acnes* DMST 14916 were taken at same specifications as Figure.5. Scale bar represents 10 µm. In bright field panel (A), bacterial cells are seen. In DAPI panel (B), nucleoids of bacteria are blue. In Dylight 488 panel (C), only *P. aeruginosa* is green. In merged panel (D), the blue nucleoids and the green cell surfaces of *P. aeruginosa* overlapped. In case of *P. putida, P. fluorescens* and *P. acnes*, only the blue nucleoids were seen.

#### 3.4.8.2 Deltavision Ultra Microscopy of planktonic bacteria

Moreover, the binding of scFv antibodies was also revealed by Deltavision Ultra Microscopy as illustrated in **Figure 3.7 and 3.8**. The cell surfaces of *P. acnes* and *P. aeruginosa* were stained green by Dylight 488-labelled secondary antibody, suggesting that the target ligands of yPac1A8 and yPgi3G4 scFv are located on the bacterial cell surface.

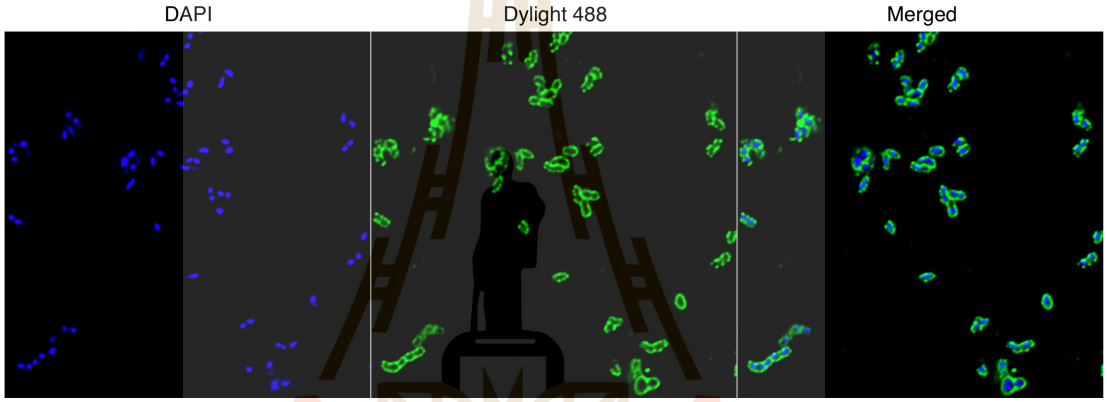


**Figure 3.7** ***P. acnes* DMST 14916 stained with yPac1A8 scFv**.

*P. acnes* DMST 14916 was incubated with yPac1A8 scFv, detected by Dylight 488-labelled anti-hexa-histidine mouse monoclonal antibody, and counterstained with DAPI. In DAPI panel, nucleoids of bacteria were stained blue. In Dylight 488 panel, *P. acnes* cell surfaces were stained green. When channels were merged, the blue nucleoid of *P. acnes* were surrounded by green cell margins. Photos were taken by Olympus 100X/1.40 objective of Deltavision Ultra Microscope (Cytiva, U.S.A).

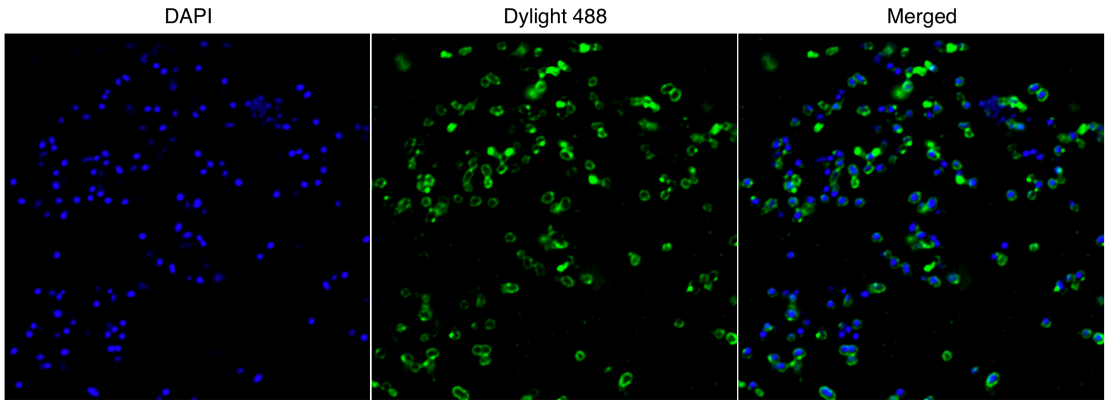


**Figure 3.8** ***P. aeruginosa* DMST 37186 stained with yPgi3G4 scFv**.

*P. aeruginosa* DMST 37186 was incubated with yPgi3G4 scFv, detected by Dylight 488-labelled anti-hexa-histidine mouse monoclonal antibody, and counterstained with DAPI. In DAPI panel, nucleoids of bacteria were stained blue. In Dylight 488 panel, *P. aeruginosa* cell surfaces were stained green. When channels were merged, the blue nucleoid of *P. aeruginosa* were surrounded by green cell margins. Photos were taken by Olympus 100X/1.40 objective of Deltavision Ultra Microscope (Cytiva, U.S.A).

### 3.4.9 Immunofluorescent staining of biofilms

Since bacterial biofilm may play a role in the pathogenesis and chronic infection (Vestby, Gronseth, Simm, & Nesse, 2020), the binding of selected scFv against target bacterial biofilms were also investigated. As demonstrated in **Figure 3.9**, *P. acnes* and *P. aeruginosa* biofilms cultured on glass coverslips were stained by yPac1A8 and yPgi3G4, respectively. Biofilms of *P. acidipropionici* TISTR 442 and *P. putida* TISTR 1522 were used as control. In bright field row, bacterial cell cluster was seen. In DAPI row, the nucleoid regions of bacteria were stained blue. In Dylight 488

row, *P. acnes* and *P. aeruginosa* cells were observed as green bacilli with obvious unstained central halo region. The results indicated that both scFv could bind to their target bacteria in biofilms.

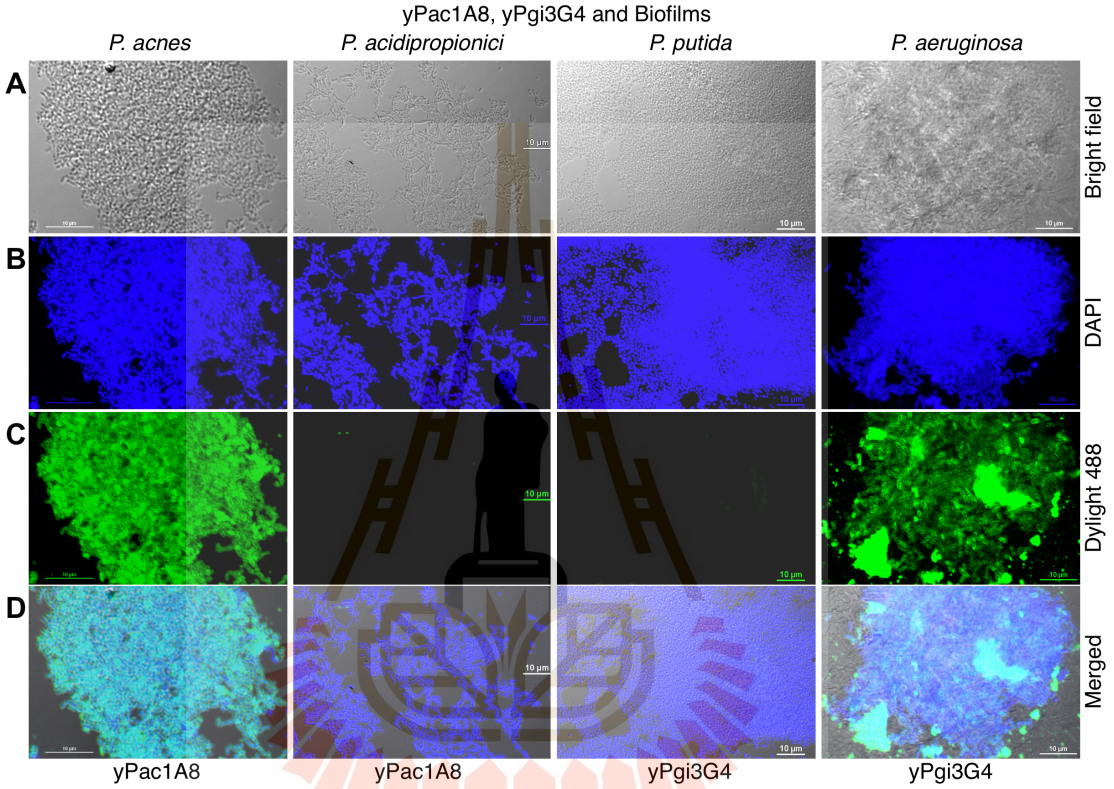


**Figure 3.9 CLSM of biofilms stained by indicated scFv.**

Biofilms of *P. acnes* DMST 14916, *P. acidipropionici* TISTR 442, *P. putida* TISTR 1522 and *P. aeruginosa* DMST 37186 were stained by yPac1A8 and yPgi3G4 scFv as indicated. Scale bar represents 10 µm.

### 3.4.10 Transmission Electron Microscopy

To confirm the cell surface location of target epitopes of both yPac1A8 and yPgi3G4 scFv, both scFv were used as primary detection agent in immunoelectron microscopy, which were visualized by Ni-NTA sensitized 10 nm nanogold particles. Under transmission electron microscope, nanogold particles were seen as dark dots along the cell outline of *P. acnes* and *P. aeruginosa* as shown in **Figure 3.10**. The result confirmed the cell surface localization of scFv ligands.

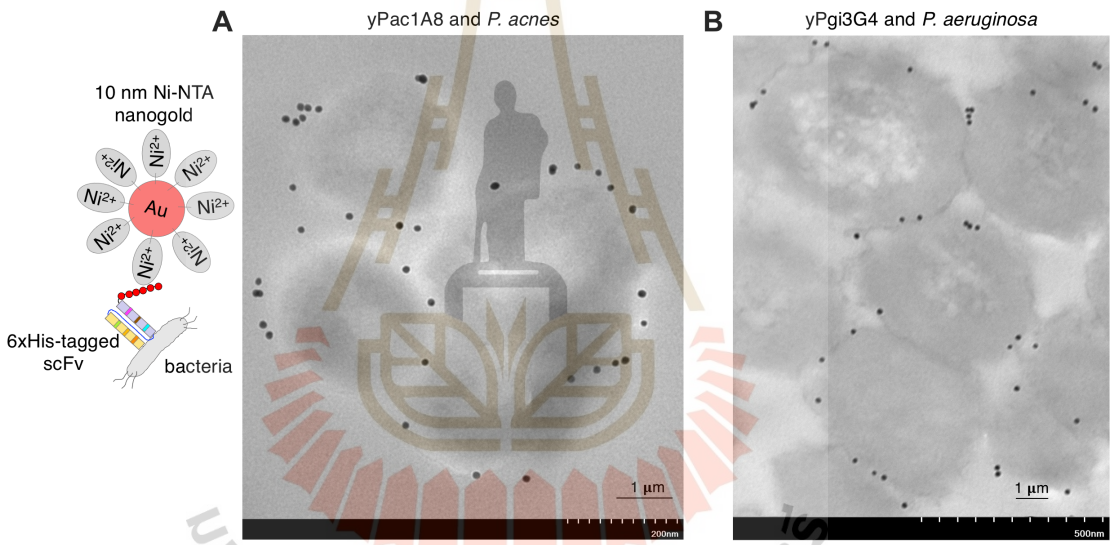


**Figure 3.10** **TEM of *P. acnes* DMST 14916 and *P. aeruginosa* DMST 37186.** (A) Four *P. acnes* DMST 14916 cells and (B) six *P. aeruginosa* DMST 37186 cells were treated with yPac1A8 and yPgi3G4 scFv, respectively. Big round structures are bacterial cells and small dense black dots are 10 nm Ni-NTA nanogold particles. Photos were taken by Hitachi Hi-Tech HT7700 transmission electron microscope at x25.0k magnification with Zoom-1 lens mode at accelerating voltage 80.0kV. Scale bar represents 1.0 µm.

## 3.5 Conclusion and future perspectives

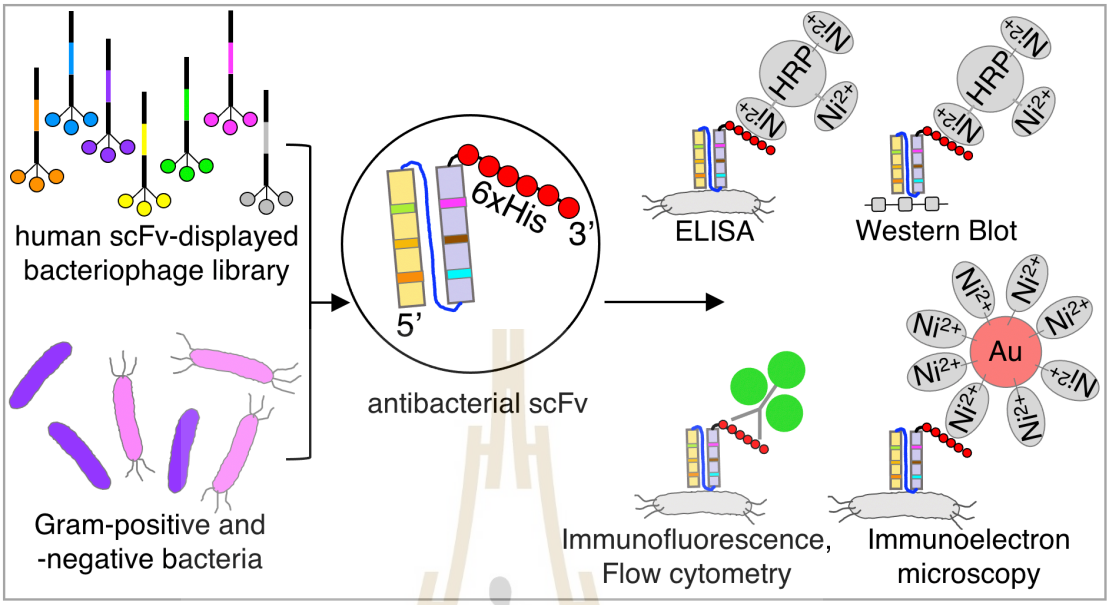


**Figure 3.11 Summary of Chapter III.**

The summary of chapter III is illustrated in **Figure 3.11**. *P. acnes* DMST 14916 and *P. aeruginosa* DMST 37186 were used as targets and Yamo-I human scFv display phage library of MY LAB was used as source of scFv antibody fragments in affinity selection. Three scFv clones for *P. acnes* were identified and the best of them (yPac1A8 scFv) was further characterized. One scFv clone for *P. aeruginosa* was identified and it was further analysed. Specific binding of scFv to target bacteria, both heat-inactivated and live forms, was confirmed by whole cell ELISA, Western Blot and flow cytometry. The cell surface location of yPac1A8 and yPgi3G4 scFv target ligands was confirmed by confocal laser scanning microscopy, deltavision ultra microscopy and transmission electron microscopy. The usefulness of scFv in bioimaging of bacteria was well-demonstrated. The methodology described in this chapter can be used to identifiy scFv for other bacteria of interest.

# CHAPTER IV

# IDENTIFICATION OF TARGET LIGAND OF YPAC1A8 BY IMMUNOPRECIPITATION AND MASS SPECTROMETRY

## 4.1 Abstract

The anti-*P. acnes* scFv (yPac1A8) was isolated from Yamo-I human scFv display phage library of MY LAB after affinity selection against *P. acnes* DMST 14916. The bacterial cell surface location of its target ligand was demonstrated in chapter III by confocal laser scanning microscopy, deltavision ultra microscopy and transmission electron microscopy. The Western Blot results of chapter III indicated that the target antigen of yPac1A8 scFv is located between 20 and 25 kDa regions and is abundant in heat-denatured *P. acnes* preparation. In this chapter, yPac1A8 scFv was used to immunoprecipitate its target from boiled *P. acnes* preparation. Not only from boiled preparation but also from the *P. acnes* broth culture supernatant, yPac1A8 scFv could pulldown its target which is the CAMP factor-1 of *P. acnes*. CAMP factor-1 is present on *P. acnes* cell surface and is also secreted as soluble toxin into the surrounding medium. The immunoprecipitated proteins were identified as CAMP factor-1 by mass spectrometry analysis at Proteomics International Laboratories Ltd., Australia. Reports on development of CAMP factor-based vaccines and immunotherapeutic for acnes vulgaris and related infections can be found, and some vaccines are undergoing clinical trials. Therefore, role of yPac1A8 scFv in *P. acnes* related infections should be explored more.

## 4.2 Introduction

In chapter III, human scFv antibody fragments against *P. acnes* (yPac1A8 scFv) and *P. aeruginosa* (yPgi3G4 scFv) has been identified and characterized. The presence of their targets on the surface of corresponding bacteria has also been confirmed. In this chapter, yPac1A8 scFv is used as a bait to pulldown and precipitate its target antigen from boiled *P. acnes* antigen preparation as well as from *P. acnes* broth culture supernatant by immunoprecipitation. The immunoprecipitated proteins are analysed by SDS-PAGE, Western Blot, and mass spectrometry.

## 4.3 Materials and methods

### 4.3.1 Bacterial strains

*Propionibacterium acnes* DMST 14916 was kindly provided by Assoc. Professor Griangsak Eumkeb, Suranaree University of Technology, Thailand. *P. acnes* DSM strains 1897, 16379, 30738, 30753 and 30919 were kindly provided by Professor Dietmar Haltrich, Austria. β-hemolytic strain *Staphylococcus aureus* was kindly provided by Assistant Professor Pattra Suntornthiticharoen from Rangsit University, Thailand. The source of materials used were described elsewhere.

### 4.3.2 Identification of target antigen in boiled *P. acnes* preparation

#### 4.3.2.1 *P. acnes* boiled antigen preparation

About 30 mL of 7 days old BHI broth culture of *P. acnes* DMST 14916 was washed two times with 0.85% NaCl solution and cells were resuspended in 1 mL of pulldown buffer (3.25 mM sodium phosphate pH 7.4, 70 mM

NaCl, 0.01% Tween-20). It was heat-treated at 99°C for 30 min and was used as *P. acnes* antigen source in immunoprecipitation.

#### 4.3.2.2 Immunoprecipitation (IP) of boiled *P. acnes* antigen

Cobalt-based magnetic beads (Dynabeads) for His-tagged protein isolation and pulldown (Invitrogen#10104D, U.S.A) were thoroughly resuspended. About 15 μL of beads was transferred into microcentrifuge tube. The beads were separated from storage buffer by using Dynal MPC-S magnetic particle concentrator (Dynal Biotech ASA#120.20, Norway) and resuspended in 700 μL of binding buffer (50 mM sodium phosphate pH 8.0, 300 mM NaCl, 0.01% Tween-20) containing 20 μg (28.5 mg/mL) of yPac1A8 scFv. It was incubated on a roller for 10 min at room temperature. The tube was then placed on Dynal MPC-S for 2 min and the beads were washed for four times with 0.05% PBST. After that, the beads were resuspended in 200 μL of boiled *P. acnes* antigen and incubated on a roller for 30 min at room temperature. The tube was then placed on Dynal MPC-S for 2 min and the beads were washed for eight times with 0.05% PBST. Finally, the beads were resuspended in 35 μL of SDS-sample buffer and heated for 10 min at 90°C. After cooling, the tube was placed on Dynal MPC-S for 2 min and supernatant (immunoprecipitation product) was collected.

#### 4.3.2.3 SDS-PAGE analysis of IP products

About 30 μL of IP products were electrophoresed by using 12.5% SDS-PAGE gel. Electrophoresis was done at 50 V for 5 min followed by 90 min at 100V. The gel was stained with Coomassie Brilliant Blue and checked for the

presence of immunoprecipitated protein by comparing with the Western Blot result which was discussed below.

#### 4.3.2.4 Western Blot (WB) analysis of IP products

About 5 µL each of IP products were electrophoresed by using 12.5% SDS-PAGE gel. Electrophoresis was done at 50 V for 5 min followed by 90 min at 100V. The PVDF (polyvinylidene difluoride) membrane of 0.2 µm pore size was activated with absolute methanol for 15 min and kept under cold WB transfer buffer (25 mM Tris, 192 mM glycine, 20% (v/v) methanol). When SDS-PAGE has finished, the gel was rinsed with cold WB transfer buffer and gel-PVDF membrane stack was prepared. Transfer of proteins from the gel to the membrane was done by wet-blotting using Mini Trans-Blot electrophoretic transfer cell (BioRad#1703930, U.S.A) at 30 V for 15 h at 4°C. Next day, the membrane was blocked with 3% (w/v) BSA in TBST (20 mM Tris, 150 mM NaCl buffer containing 0.1% (v/v) Tween-20) for 1 h at room temperature. It was washed with TBST for 3 times, 5 min each.

Then, the membrane was incubated with yPac1A8 scFv (2 µg/mL) in TBST for 15 h at 4°C. It was followed by washing 3 times with TBST, 5 min each. The membrane was then incubated with 1:5000 diluted HisProbe-HRP (Thermoscientific#15165, U.S.A) in blocking buffer for 1 h at room temperature. Finally, the membrane was washed three times with TBST. The presence of precipitated protein was detected by chemiluminescence, using Amersham ECL Prime Western blotting detection reagent (GE Healthcare#RPN2232, UK). Image analysis was performed by CCD camera-based imaging, using ImageQuant LAS 500 imager (GE Healthcare, UK).

#### 4.3.2.5 Mass spectrometry analysis of IP products

The immunoprecipitated protein bands in SDS-PAGE gel were compared with the WB result. Two proteins of interest (POI-1 and POI-2) having the same size as the WB band were identified. Both bands were excised and sent to Proteomics International Laboratories Ltd., Australia (https://www.proteomics.com.au) for mass spectrometry. At there, the excised gel bands were trypsin digested. The extracted peptides were analyzed by LC-MS using the Agilent 1260 Infinity HPLC system coupled to an Agilent 1260 Chipcube Nanospray interface on an Agilent 6540 mass spectrometer. Spectra were analyzed by using Mascot sequence matching software with MSPnr100 database.

#### 4.3.2.6 WB analysis of POI-1 and POI-2

To analyze the binding of POI-1 and POI-2 with yPac1A8, immunoprecipitation procedure was repeated as above. SDS-PAGE and WB procedures were also repeated, and the gel bands of POI-1 and POI-2 were excised. Then, POI-1 and POI-2 were extracted from the gel bands by passive diffusion technique with modification (Kurien & Scofield, 2012). Briefly, the gel bands were cut into small pieces and were incubated in 60 µL of SDS sample buffer for 4 h on a rotator at room temperature. After that, the supernatant was heated at 90°C for 10 min. About half of that was used for SDS-PAGE analysis and the remaining half was used for WB analysis.

### 4.3.3 CAMP (Christie-Atkins-Munch-Peterson) factor production by *P. acnes*

#### 4.3.3.1 Classic CAMP test

One-week old colonies of *P. acnes* DMST 14916, *P. acnes* DSM 1897, 16379, 30738, 30753 and 30919 on BHI agar were tested for CAMP factor production. Two-days old colonies of *P. acidipropionici* TISTR 442 and *P. freudenreichii* TISTR 446 on BHI agar and one-day old colonies of K12 strain *E. coli* C3026 on LB agar were used as negative controls. One-day old colonies of β-hemolytic strain of *S. aureus* was used as the source of β-hemolysin in CAMP test.

At the center of ready-to-use 5% sheep blood Columbia agar (RPD Ltd.#064-PA0004, Thailand), β-hemolysin-producing strain of *S. aureus* was streaked as a straight line. Bacterial strains to be tested were inoculated as straight lines perpendicular to the *S. aureus* streak. The plate was incubated anaerobically in a GasPak system at 37°C for 48 h. After that, the presence of characteristic arrowhead-shaped hemolytic pattern at points where *S. aureus* streak and the test strain streak were closest was checked.

มหาวิทยาลัยเทคโนโลยีสุรนารี

#### 4.3.3.2 Modified CAMP test

As CAMP factor is a soluble secretory protein of *P. acnes* into the surrounding medium, its presence in culture supernatant was tested by performing *P. acnes* culture supernatant CAMP test. *S. aureus* cell suspension of $OD_{600}$ 1.0 in PBS was applied to entire surface of 5% sheep blood Columbia agar by using sterile cotton swab. The plate was allowed to set for 15 min at room temperature. Three holes were made into the agar by using the base of the sterile disposable needle. One of the holes

was filled with 100 µL of BHI medium, second one with 100 µL of *P. acnes* DMST 14916 broth culture supernatant (72 h broth culture in BHI medium), and the last one with colony suspension of *P. acnes* DMST 14916 in 100 µL of BHI medium. The plate was then inoculated in upright position anaerobically in a GasPak system at 37°C for 48 h. The enhanced zone of hemolysis was checked around the agar holes.

#### 4.3.3.3 *P. acnes* broth culture supernatant ELISA

This time, the soluble CAMP factor presented in *P. acnes* broth culture supernatant was used as target of yPac1A8 scFv in ELISA. Triplicates of broth cultures were prepared from *P. acnes* DMST 14916, *P. acnes* DSM 1897, 16379, 30738, 30753 and 30919. They were incubated in BHI medium anaerobically in a GasPak system at 37°C. *P. acidipropionici* TISTR 442 and *P. freudenreichii* TISTR 446 were incubated in BHI medium anaerobically in a GasPak system at 30°C. K12 strain *E. coli* C3026 was incubated in LB medium aerobically at 37°C. The first set of broth cultures was taken out at 24 h incubation (Day 1 samples), second set at 72 h (Day 3 samples) and the last set at 5th day of incubation (Day 5 samples), respectively. After centrifugation, the broth culture supernatant samples were stored at 4°C.

Nunc Maxisorp 96-well plate (Thermoscientific#44-2404-21, U.S.A) was coated with 50 µL of bacterial broth culture supernatant samples in 50 µL of $NaHCO_3$ and incubated at 37°C overnight. Fresh BHI and LB medium were used as negative control. The plate was washed three times with PBS and blocked with 2% PBSM (2 % (w/v) skimmed milk protein in PBS) for 1 h at room temperature. After three times PBS washing, 10 µg/mL of yPac1A8 scFv was added and incubated at room temperature for 1 h. Three times 0.05% PBST washing and two times PBS washing

were performed with Tecan's HydroFlex automatic microplate washer (Tecan, Switzerland). Then, the wells were incubated with 1:5000 diluted HisProbe-HRP (Thermoscientific#15165, U.S.A) in PBS for 1 h at room temperature. It was followed by 0.05% PBST and PBS washing. Finally, the wells were incubated with ABTS substrate (Amresco#0400-10G, U.S.A) in citric acid-$H_2O_2$ buffer (0.05% $H_2O_2$ in 50 mM citric acid pH 4.0) for 30 min. The absorbance was measured at 405 nm with Tecan's Sunrise absorbance microplate reader (Tecan, Switzerland).

**4.3.4 Identification of target antigen in *P. acnes* broth culture supernatant**

**4.3.4.1 *P. acnes* broth culture supernatant preparation**

*P. acnes* DMST 14916 broth culture supernatant (72 h in BHI medium) was prepared as previously and used as antigen source for immunoprecipitation.

**4.3.4.2 Immunoprecipitation of *P. acnes* broth culture supernatant**

This time, 30 µL of cobalt-based magnetic beads (Dynabeads) for His-tagged protein isolation and pulldown (Invitrogen#10104D, U.S.A) was transferred into 5 mL Maxisorp immunotube (Nalgene Nunc International, Denmark). The beads were separated from storage buffer by using EasySep Magnet (STEMCELL Technologies#18000, Canada) and resuspended in 4 mL of binding buffer (50 mM sodium phosphate pH 8.0, 300 mM NaCl, 0.01% Tween-20) containing 30 µg (7.5 µg/mL) of yPac1A8 scFv. It was incubated on a roller for 10 min and the beads were

washed twice with 0.05% PBST as previously described. The beads were resuspended in 5 mL of BHI broth culture supernatant of *P. acnes* DMST 14916 and incubated on a roller for 1 h. The remaining steps were the same as previous immunoprecipitation experiment. The obtained IP products were checked by SDS-PAGE and WB analysis.

#### 4.3.4.3 Mass spectrometry analysis of *P. acnes* broth culture supernatant IP products

Like *P. acnes* boiled antigen IP result, two protein bands of interest (POI-1 and POI-2) were obtained. Both bands were excised and sent to Proteomics International Laboratories Ltd., Australia (https://www.proteomics.com.au) for mass spectrometry analysis.

## 4.4 Results and discussion

### 4.4.1 Identification of target antigen in boiled *P. acnes* preparation

#### 4.4.1.1 Immunoprecipitation (IP) of boiled *P. acnes* antigen

To immunoprecipitate its target from boiled *P. acnes* DMST 14916 antigen preparation, 6xHis-tagged yPac1A8 scFv was immobilized onto cobalt-based magnetic beads (Dynabeads). At the end of immunoprecipitation, scFv and its target antigen complexes were separated from Dynabeads and analyzed by SDS-PAGE. *P. aeruginosa* specific scFv (yPgi3G4) was used as scFv negative control. *P. aeruginosa* TISTR 357 was used as bacterial negative control.

#### 4.4.1.2 SDS-PAGE and WB analysis of boiled *P. acnes* IP products

As shown in **Figure 4.1A**, two protein bands (POI-1 and POI-2), which were present in *P. acnes* and yPac1A8 scFv IP product but not in *P. acnes* and yPgi3G4 scFv IP product (scFv negative control), and *P. aeruginosa* and yPac1A8 scFv IP product (bacterial negative control), were identified. Both POI-1 and POI-2 bands corresponded well with the thick band of WB **(Figure 4.1B)**. POI-1 was about 25 kDa and POI-2 was about 20-25 kDa. POI-2 band was darker than POI-1. Both of them were excised and sent for identification by mass spectrometry.

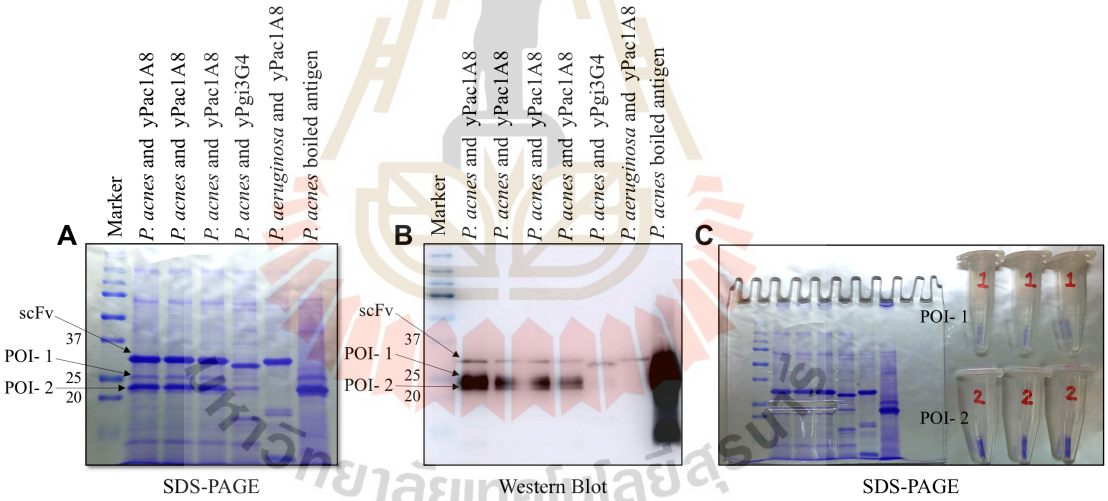


**Figure 4.1 Immunoprecipitation of boiled *P. acnes* antigen**

(A) SDS-PAGE gel of immunoprecipitation products. From left to right: triplicates of IP products (*P. acnes* antigen and yPac1A8 scFv), scFv negative control IP product (*P. acnes* antigen and yPgi3G4 scFv) and bacterial negative control IP product (*P. aeruginosa* antigen and yPac1A8 scFv). The last lane is *P. acnes* boiled antigen only. (B) WB analysis of immunoprecipitation products. (C) POI-1 and POI-2 samples

for mass spectrometry. All blue prestained protein standards (BioRad#1610373, U.S.A) was used.

#### 4.4.1.3 Mass spectrometry analysis of boiled *P. acnes* IP products

**Table 4.1** showed the protein hit (protein of extensive homology) of POI-1 and POI-2 at $p<0.05$. Both POI-1 and POI-2 are highly matched with protein ID W4UFP1, which is the CAMP factor of *P. acnes* JCM 18920. **Figure 4.2 and 4.3** showed the Mascot Score Histogram of POI-1 and POI-2, respectively. Protein sequence coverage between POI-1 and W4UFP1 is 54% and that of POI-2 and W4UFP1 is 60%. Protein sequence coverage data are collectively described in section 4.4.3.3 and **Figure 4.11**.

**Table 4.1 Protein hits of POI-1 and POI-2 of boiled antigen IP at $p<0.05$.**

| Sample name | Protein hit ($p<0.05$) | Detail identity of protein hit | Protein score obtained | Number of queries matched |
|---|---|---|---|---|
| POI-1 (25 kDa) | W4UFP1 (30.164 kDa) | CAMP factor of NCBI : txid 1302244 (*P. acnes* JCM 18920) | 939 | 67 |
| POI-2 (20-25 kDa) | W4UFP1 (30.164 kDa) | CAMP factor of NCBI : txid 1302244 (*P. acnes* JCM 18920) | 887 | 76 |

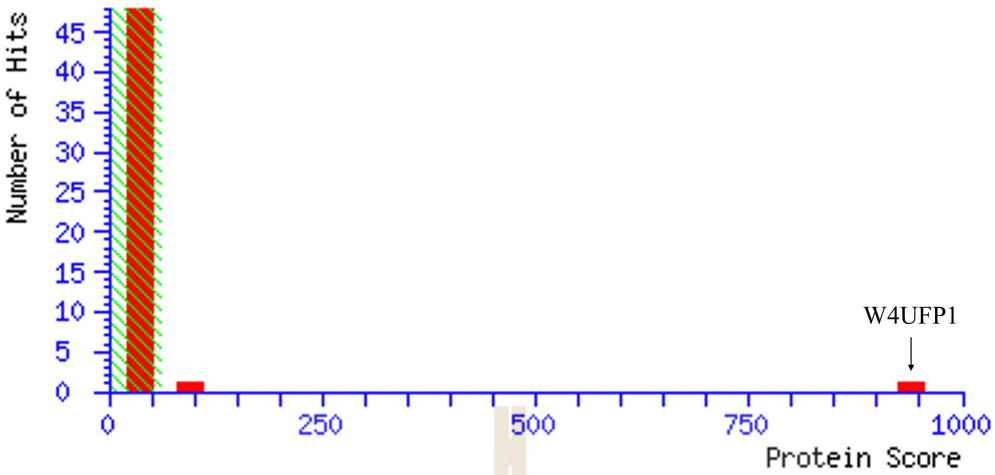


**Figure 4.2 Mascot Score Histogram of POI-1 of boiled antigen IP.**

The number of protein-matches at each scoring position is indicated by the height of the red bars. The non-significant protein-matches area is shaded in green. POI-1 of boiled *P. acnes* is confidently matched with W4UFP1 which is the CAMP factor of *P. acnes* JCM 18920.

**Figure 4.3 Mascot Score Histogram of POI-2 of boiled antigen IP.**

The number of protein-matches at each scoring position is indicated by the height of the red bars. The non-significant protein-matches area is shaded in green. POI-2 of boiled *P. acnes* is confidently matched with W4UFP1 which is the CAMP factor of *P. acnes* JCM 18920.

#### 4.4.1.4 WB analysis of POI-1 and POI-2 of boiled antigen IP

POI-1 and POI-2 extracted from the excised gel bands were analysed by WB. The result is shown in **Figure 4.4**. The POI-1 and POI-2 obtained from *P. acnes* boiled antigen and yPac1A8 scFv immunoprecipitation (**Figure 4.4A**) were excised from the gel (**Figure 4.4C**). Proteins were extracted from the gel slices and analyzed again by SDS-PAGE (**Figure 4.4D**). **Figure 4.4B** showed the WB result of IP products. **Figure 4.4E** showed the WB result of POI-1 and POI-2 separately. In comparison, POI-1 binds stronger with yPac1A8 scFv than POI-2.

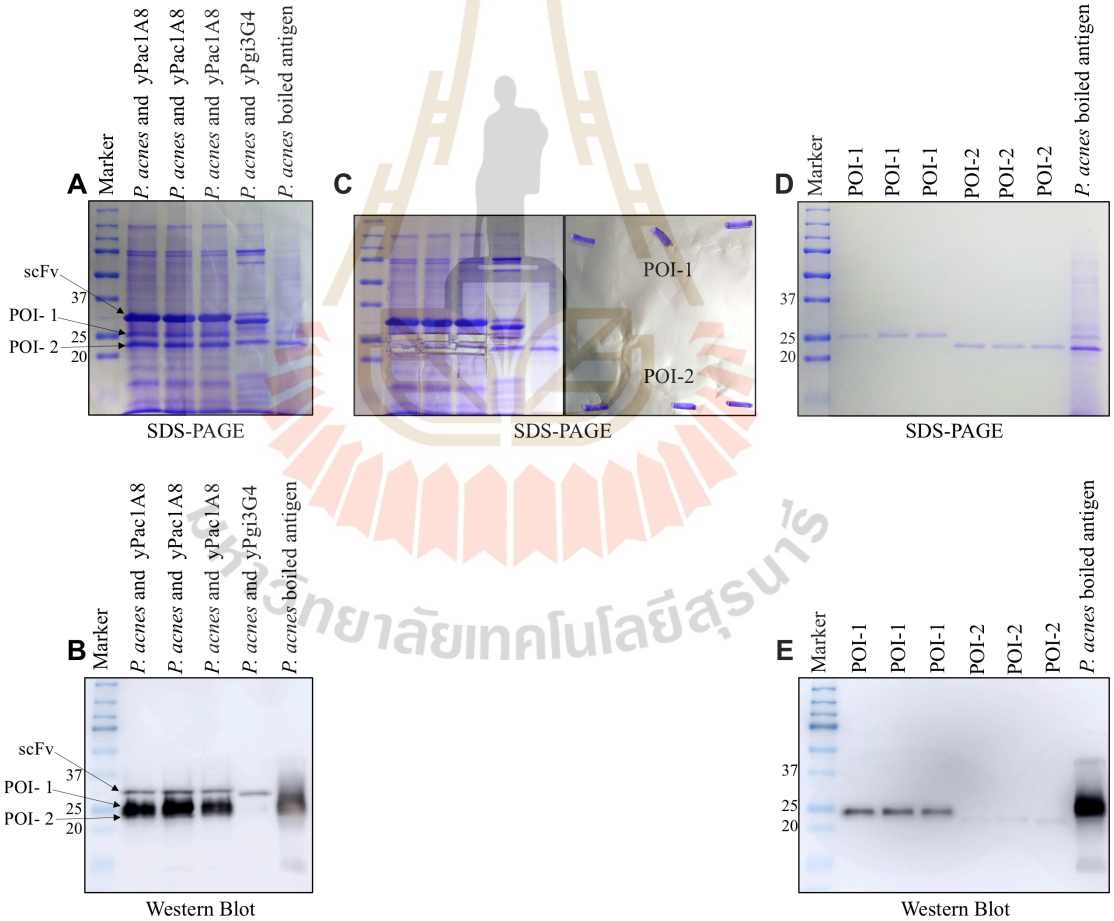


**Figure 4.4 WB analysis of POI-1 and POI-2 of boiled antigen IP**

(A) and (B) showed the SDS-PAGE and WB results of IP products. (C) showed the excision of POI-1 and POI-2. (D) and (E) are the SDS-PAGE

and WB results of POI-1 and POI-2. All blue prestained protein standards (BioRad#1610373, U.S.A) was used.

### 4.4.2 CAMP (Christie-Atkins-Munch-Peterson) factor production by *P. acnes*

#### 4.4.2.1 Classic CAMP test

The word "CAMP" is an acronym derived from the name of the researchers; Christie, Atkins, and Munch-Petersen, who first described the enhanced hemolysis phenomenon that occurred when β-hemolysin produced by *S. aureus* and hemolysin (CAMP factor) produced by Group-B streptococci came in contact (Christie, Atkins, & Munch-Petehsen, 1944; Mahon & Lehman, 2018). Originally, it was used for identification of Group-B streptococci. Later on, the test has been applied to other bacteria and fungus, such as, non Group-B streptococci, Vibrios, Candida (Chuzeville, Puymege, Madec, Haenni, & Payot, 2012; Köhler, 1988; Pakshir, Bordbar, Zomorodian, Nouraei, & Khodadadi, 2017). CAMP test has also been used to study CAMP factor of *P. acnes* (Valanne et al., 2005). The CAMP test can be performed in three ways depending on the source of β-hemolysin used. First is the use of β-hemolysin producing S. aureus and is the classic technique and a typical arrowhead shape can be seen (Darling, 1975; Guo, Xi, Wang, & Wang, 2019). Second is the use of β-hemolysin impregnated disk in which enhanced hemolysis is seen around the disk. Third is the use of extracted β-lysin drop (spot CAMP test) (Hansen & Sorensen, 2003; Khafri & Nazari, 2004; Ratner, Weeks, & Stratton, 1986; Zárate, Vargas, Pacheco, Canigia, & Smayevsky, 2005).

In this study, CAMP factor production in *P. acnes* strains was detected by performing classic CAMP test. An arrow-head shaped zone of augmented-hemolysis at the junction of *S. aureus* and test strains inoculation lines marked a positive CAMP reaction. All *P. acnes* strains tested produced CAMP factor detectable by classical CAMP test. The result is shown in **Figure 4.5**.

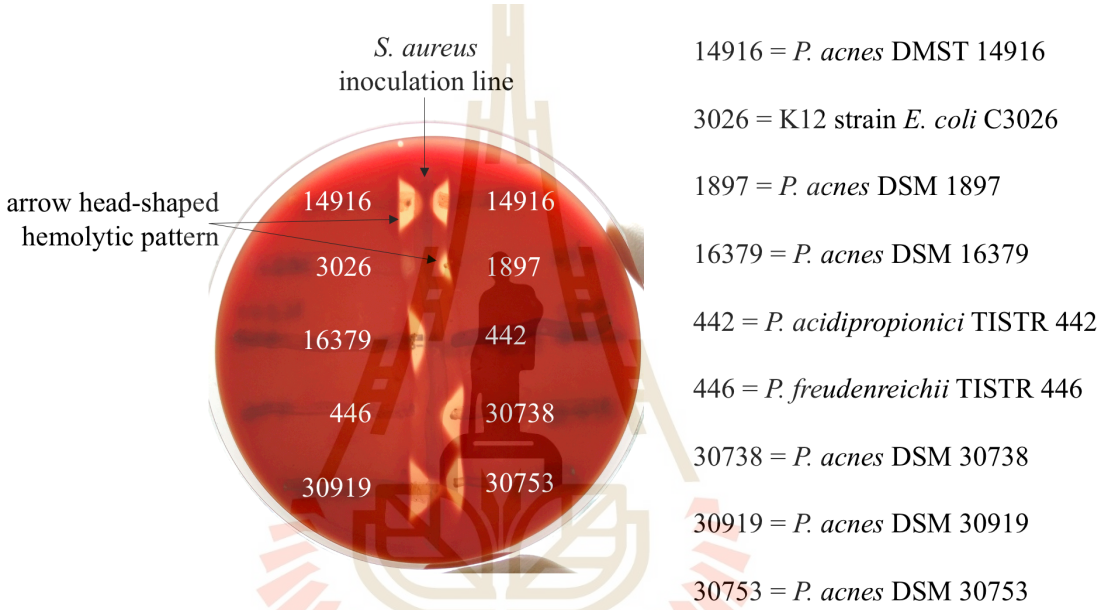


**Figure 4.5** **Classic CAMP test result.**

All *P. acnes* strains tested produced CAMP factor. K12 strain *E. coli* C3026, *P. acidipropionici* TISTR 442, and *P. freudenreichii* TISTR 446 were used as negative control.

#### 4.4.2.2 Modified CAMP test

Next, the presence of soluble CAMP factor in *P. acnes* broth culture supernatant was checked. As shown in **Figure 4.6**, *P. acnes* broth culture supernatant as well as *P. acnes* colony suspension could produce enhanced hemolysis zone around their corresponding wells. CAMP test results confirmed that *P. acnes*

strains in our laboratory can produce CAMP factor and soluble CAMP factor is present in *P. acnes* broth culture supernatant.

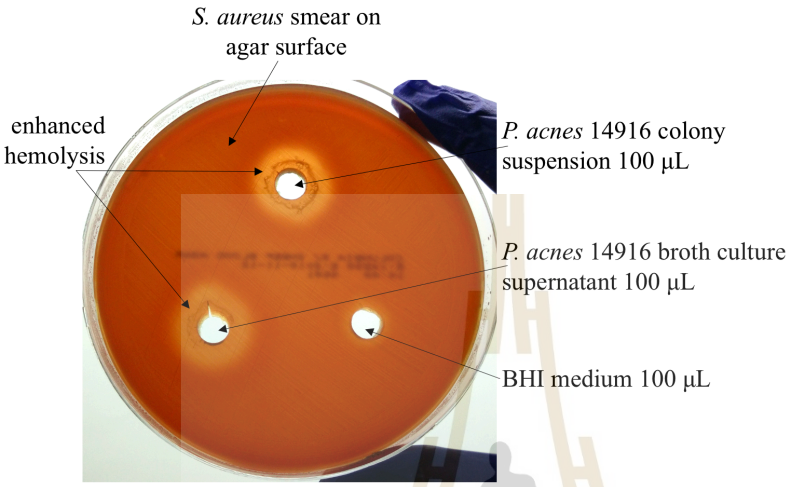


**Figure 4.6 Modified CAMP test result.**

Soluble CAMP factor is present in *P. acnes* broth culture supernatant.

#### 4.4.2.3 *P. acnes* broth culture supernatant ELISA

Based on the above CAMP test results, soluble CAMP factor in *P. acnes* broth culture supernatant was used as target for yPac1A8 scFv ELISA. The result is shown in **Figure 4.7**. A baseline was drawn and signals twice higher than baseline were regarded as positive. Out of 6 tested *P. acnes* strains, *P. acnes* DMST 14916, *P. acnes* DSM 1897, 30738, and 30753 are CAMP factor ELISA-positive.

*P. acnes* DMST 14916 showed high signal in all broth culture supernatant samples collected on day 1, day 3 and day 5. So, CAMP factor, detectable by yPac1A8 scFv, is secreted into the medium persistently throughout incubation period by *P. acnes* DMST 14916. In case of *P. acnes* DSM 1897, 30738, and 30753, CAMP factor ELISA is positive in day 1 samples but the signal waned out in Day 3 and

Day 5 samples. This result suggests that CAMP factor, detectable by yPac1A8 scFv, is secreted into the medium for a short period of time by *P. acnes* DSM 1897, 30738, and 30753.

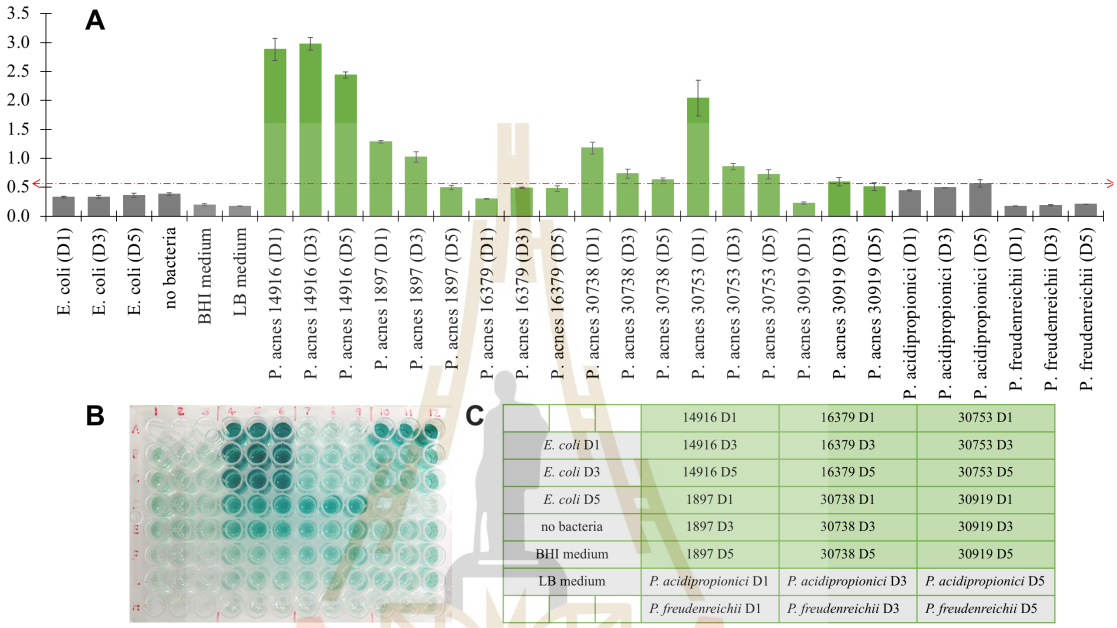


**Figure 4.7 CAMP factor ELISA result.**

(A) Bar diagram showing baseline cut-off and ELISA signals. The samples were tested in triplicates and error bars represent standard error of the mean (SEM) of triplicates. (B) CAMP factor ELISA plate. (C) ELISA sample guide.

### 4.4.3 Identification of target antigen in *P. acnes* broth culture supernatant

#### 4.4.3.1 Immunoprecipitation of *P. acnes* broth culture supernatant

Immunoprecipitation of target in *P. acnes* broth culture supernatant by yPac1A8 scFv was performed to prove that a soluble CAMP factor is present in *P. acnes* broth culture supernatant and it can be pulled down by yPac1A8 scFv. SDS-PAGE, WB, and mass spectrometry analysis of IP products were performed. The results obtained were shown in **Figure 4.8**.

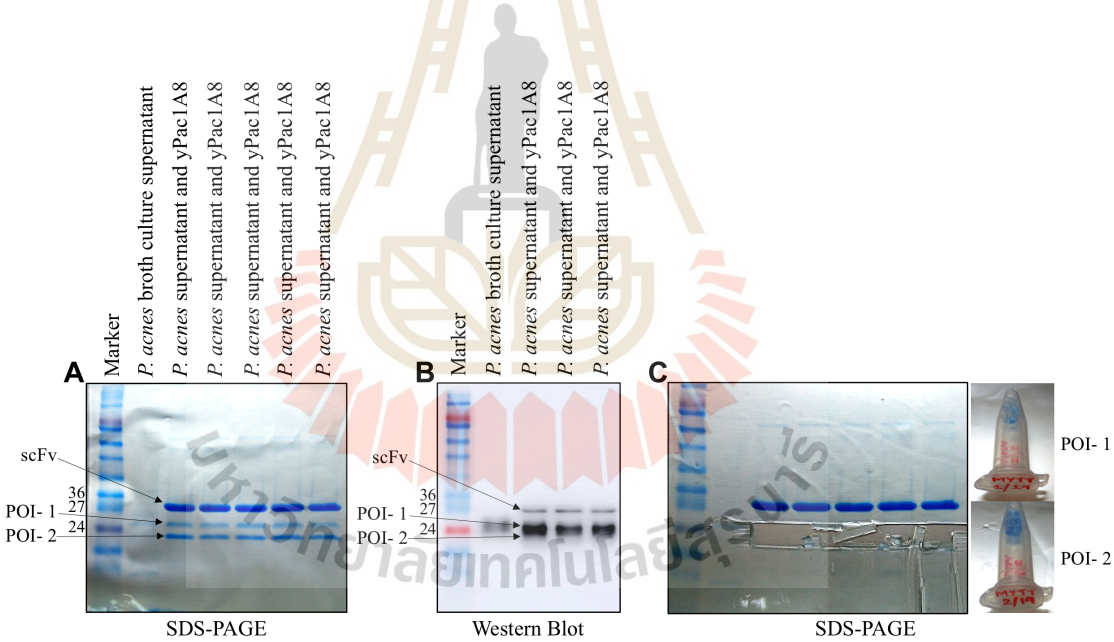


**Figure 4.8** **Immunoprecipitation of *P. acnes* broth culture supernatant.** (A) SDS-PAGE gel of IP products. From left to right, *P. acnes* broth culture supernatant and 5 repeats of IP products (*P. acnes* broth culture supernatant and yPac1A8 scFv IP). (B) WB analysis of IP products. (C) Excised POI-1 and POI-2 of IP products. Prestained Protein Standards (Enzmart#APC-001, Thailand) was used as a marker.

#### 4.4.3.2 Mass spectrometry analysis of *P. acnes* broth culture supernatant IP products

Two proteins of interest (POI-1 and POI-2), immunoprecipitated from *P. acnes* broth culture supernatant by yPac1A8 scFv, were sent for mass spectrometry analysis. **Table 4.2** showed the protein hit (protein of extensive homology) of POI-1 and POI-2 at $p<0.05$. Both POI-1 and POI-2 are highly matched with protein ID W4UFP1, which is the CAMP factor of *P. acnes* JCM 18920. **Figure 4.9 and 4.10** showed the Mascot Score Histogram of POI-1 and POI-2. Protein sequence coverage between POI-1 and W4UFP1 is 48% and that of POI-2 and W4UFP1 is 32%. Protein sequence coverage data are collectively described in section 4.4.3.3 and **Figure 4.11**.

**Table 4.2 Protein hits of POI-1 and POI-2 of supernatant IP at p<0.05.**

| Sample name | Protein hit (p<0.05) | Detail identity of protein hit | Protein score obtained | Number of queries matched |
|---|---|---|---|---|
| POI-1 (25 kDa) | W4UFP1 (30.164 kDa) | CAMP factor of NCBI : txid 1302244 (*P. acnes* JCM 18920) | 560 | 24 |
| POI-2 (20-25 kDa) | W4UFP1 (30.164 kDa) | CAMP factor of NCBI : txid 1302244 (*P. acnes* JCM 18920) | 485 | 24 |

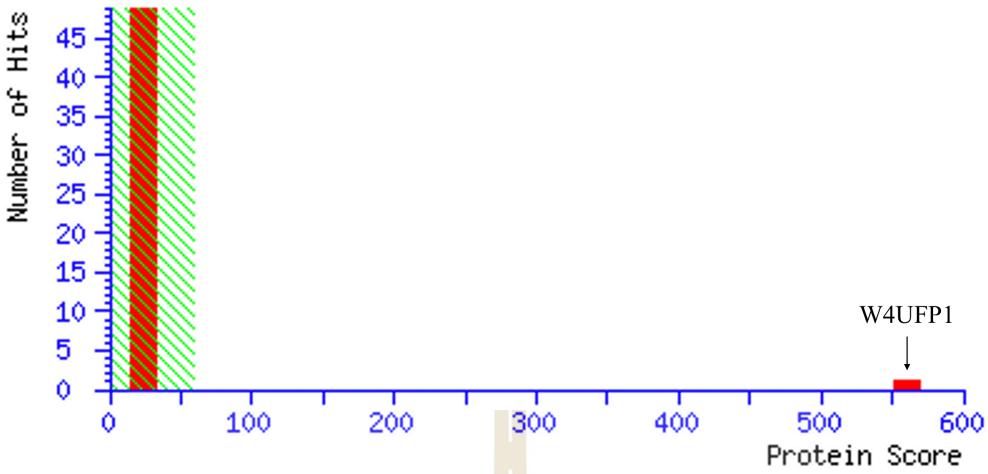


**Figure 4.9 Mascot Score Histogram of POI-1 of supernatant IP.**

The number of protein-matches at each scoring position is indicated by the height of the red bars. The non-significant protein-matches area is shaded in green. POI-1 of *P. acnes* broth culture supernatant is confidently matched with W4UFP1 which is the CAMP factor of *P. acnes* JCM 18920.

**Figure 4.10 Mascot Score Histogram of POI-2 of supernatant IP.**

The number of protein-matches at each scoring position is indicated by the height of the red bars. The non-significant protein-matches area is shaded in green. POI-2 of P. acnes broth culture supernatant is

confidently matched with W4UFP1 which is the CAMP factor of *P. acnes* JCM 18920.

#### 4.4.3.3 Analysis of sequence coverage between IP sequence queries and protein hit

**Table 4.3 Protein sequence coverage between IP sequences and protein hit**

| Sample name | Protein hit (p<0.05) | Protein sequence coverage (%) | Number of matched sequence segments |
|---|---|---|---|
| POI-1 (boiled *P. acnes* IP) | CAMP factor of *P. acnes* JCM 18920 | 54% | 6 |
| POI-2 (boiled *P. acnes* IP) | CAMP factor of *P. acnes* JCM 18920 | 60% | 4 |
| POI-1 (*P. acnes* supernatant IP) | CAMP factor of *P. acnes* JCM 18920 | 48% | 6 |
| POI-2 (*P. acnes* supernatant IP) | CAMP factor of *P. acnes* JCM 18920 | 32% | 5 |

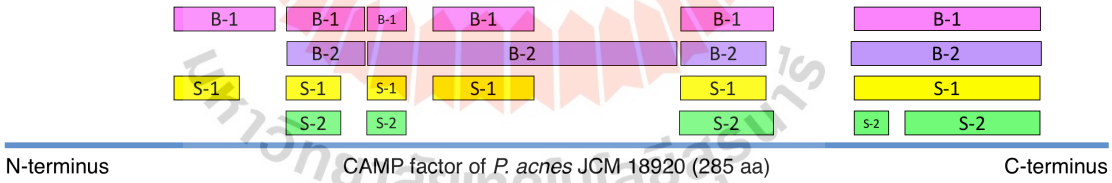


**Figure 4.11 Protein sequence coverage between IP sequences and protein hit** (W4UFP1 / CAMP factor of *P. acnes* JCM 18920).

The sequence alignment was made by using Snapgene software version 5.2.2 (www.snapgene.com).

In **Figure 4.11**, the backbone amino acid sequence (285 aa) is CAMP factor of *P. acnes* JCM 18920 (W4UFP1). The pink segments, named as B-1,

represent the matched-areas between sequence queries of POI-1 of boiled *P. acnes* antigen IP and the protein hit (CAMP factor of *P. acnes* JCM 18920). The purple segments represent the matched-areas between sequence queries of POI-2 of boiled *P. acnes* antigen IP and the protein hit. The yellow segments represent the matched-areas between sequence queries of POI-1 of *P. acnes* broth culture supernatant IP and the protein hit. The green segments represent the matched-areas between sequence queries of POI-2 of *P. acnes* broth culture supernatant IP and the protein hit. In section 4.4.1.4, WB analysis of POI-1 and POI-2 (**Figure 4.4**) showed that POI-1 binds stronger than POI-2 with yPac1A8 scFv. The sequence alignment indicated that the very first segment from N-terminus, which is present in POI-1 of both IP products (boiled IP and supernatant IP), is missing in POI-2. That segment of CAMP factor, close to N-terminus, probably is the main binding site (epitope) of yPac1A8 scFv. It has to be approved by epitope mapping and molecular docking in the future.

มหาวิทยาลัยเทคโนโลยีสุรนารี

#### 4.4.3.4 Analysis of protein hit (CAMP factor of *P. acnes* JCM 18920)

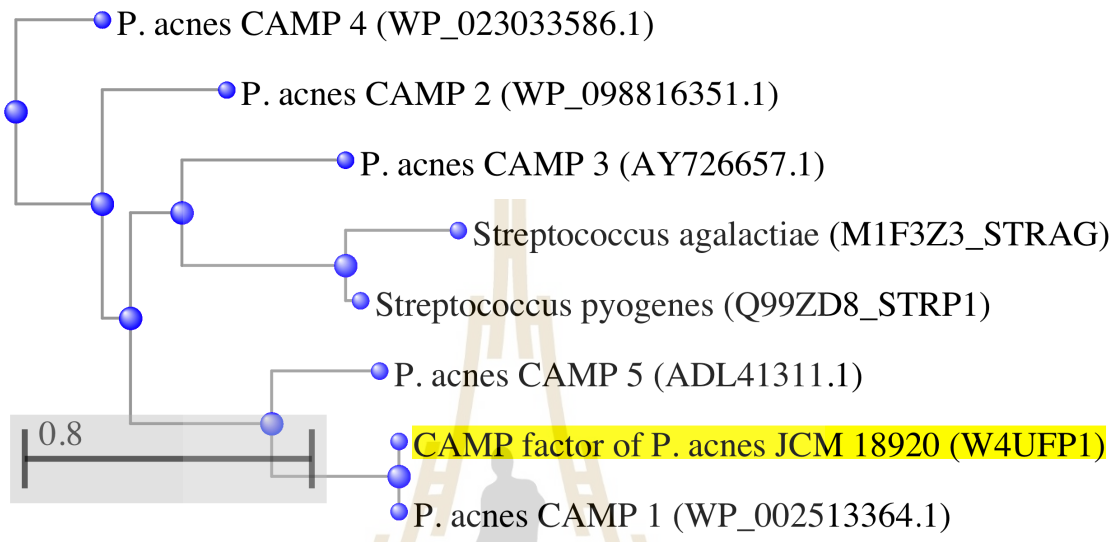


**Figure 4.12 Phylogenetic tree view of amino acid sequence alignment.** Amino acid sequences of CAMP factor of *P. acnes* JCM 18920 (W4UFP1), CAMP factor 1 of *P. acnes* (WP_002513364.1), CAMP factor 2 of *P. acnes* (WP_098816351.1), CAMP factor 3 of *P. acnes* (AY726657.1), CAMP factor 4 of *P. acnes* (WP_023033586.1), CAMP factor 5 of *P. acnes* (ADL41311.1), CAMP factor of *Streptococcus pyogenes* (Q99ZD8_STRP1), and CAMP factor of *Streptococcus agalactiae* (M1F3Z3_STRAG) are compared by using COBALT multiple sequence alignment tool from National Center for Biotechnology Information (Papadopoulos & Agarwala, 2007). The sequence alignment was made by using fast minimum evolution method, 0.85 maximum sequence difference, and Kimura's protein distance calculation.

According to the mass spectrometry analysis results, POI-1 and POI-2 of both boiled *P. acnes* IP and *P. acnes* broth culture supernatant IP have extensive amino acid sequence homology with CAMP factor of *P. acnes* JCM 18920 (W4UFP1). To the best of my knowledge, there are 5 CAMP factor gene loci and 5 types of predicted CAMP factor proteins in *P. acnes* (Valanne et al., 2005). CAMP factor of *P. acnes* JCM 18920 (W4UFP1) sequence is compared with *P. acnes* CAMP factor 1 to 5 reference sequences and also with prototype CAMP factors of *Streptococcus* species. The result is shown in **Figure 4.12**. The sequence of CAMP factor of *P. acnes* JCM 18920 (W4UFP1) is completely identical to that of *P. acnes* CAMP factor 1 (WP_002513364.1). Therefore, the ligand of yPac1A8 scFv is most likely to be the CAMP factor type 1 of *P. acnes*.

*P. acnes* is recently renamed as *Cutibacterium acnes* (Platsidaki & Dessinioti, 2018; UniProt). It is a Gram-positive, non-motile, non-spore-forming bacteria of approximately 0.4-0.5 x 0.8-0.9 µm. Its generation time is about 5.1 hours. There are three known phylotypes of *P. acnes*, designated as type I, II and III. Type I is subdivided into subtypes and clades, such as Type IA1 (Clade 1), Type IA1 (Clade 2), Type IA2, Type IB and Type IC. All *P. acnes* isolates of type IA, IB and II are CAMP factor positive on sheep blood agar (Dekio et al., 2015; Hall et al., 1994). *P. acnes* strains in MY LAB are CAMP factor positive on sheep blood agar and so, they are expected to be of type IA or IB or II.

*P. acnes* strains found on skin surfaces and associated with acne vulgaris are Type IA strains and they mainly produce CAMP factor 2 (Nazipi, Stodkilde-Jorgensen, Scavenius, & Bruggemann, 2017; Valanne et al., 2005). The target ligand of yPac1A8 scFv is CAMP factor 1. It may be the reason why yPac1A8

scFv does not cross-react with tested *P. acnes* strains isolated from acne lesions. In fact, CAMP factor 1 is abundantly produced by Type IB and II *P. acnes* isolates which are more often associated with soft and deep tissue infections (Nazipi et al., 2017; Valanne et al., 2005). The binding of yPac1A8 scFv to *P. acnes* strains of deep tissue origin should be tested in the future.

As majority of *P. acnes* studies focused on skin isolates, little is known about CAMP factor 1 or *P. acnes* strains producing it. Generally, the contribution of CAMP factor in *P. acnes* virulence is documented (Nakatsuji, Tang, Zhang, Gallo, & Huang, 2011). CAMP factor has been used as important target in cosmetic vaccine (acnes vaccine) development and the vaccine studies are ongoing (Elsevier, 2018; Huang, 2015; Liu, Nakatsuji, Zhu, Gallo, & Huang, 2011; Y. Wang et al., 2018). The potential role of each and every CAMP factor in *P. acnes* virulence remains to be explored.

มหาวิทยาลัยเทคโนโลยีสุรนารี

## 4.5 Conclusion and future perspectives

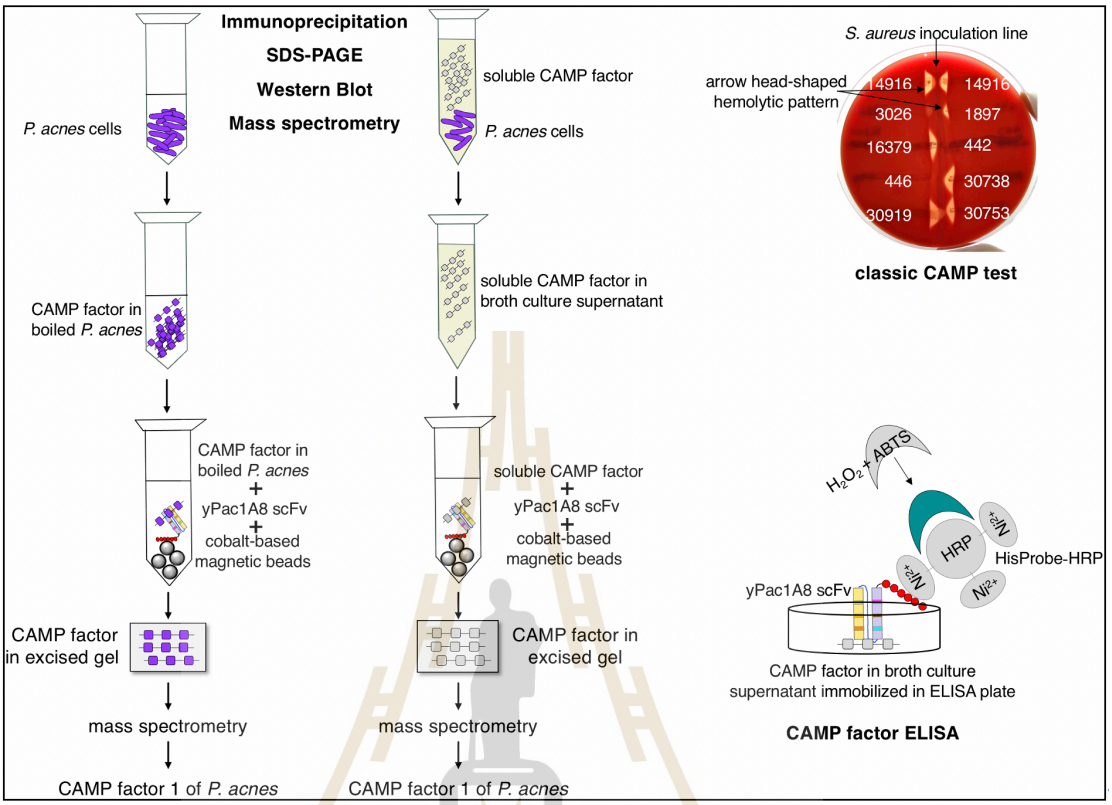


**Figure 4.13 Summary of chapter IV.**

The summary of chapter IV is illustrated in **Figure 4.13**. In this chapter, yPac1A8 scFv is used as a bait to immunoprecipitate its target antigen from boiled *P. acnes* antigen preparation (boiled IP) as well as from *P. acnes* broth culture supernatant (supernatant IP). The immunoprecipitated proteins are analysed by SDS-PAGE, Western Blot, and mass spectrometry. The protein band in WB corresponds to two protein bands (POI-1 and POI-2) in SDS-PAGE in both IP procedures. Both POI-1 and POI-2 from boiled *P. acnes* antigen IP are identified by mass spectrometry as CAMP factor 1. Similarly, Both POI-1 and POI-2 from *P. acnes* broth culture supernatant IP are CAMP factor 1. In immunoprecipitation SDS-PAGE, POI-2 band is darker than

POI-1. But, in WB, POI-1 binds stronger than POI-2 with yPac1A8 scFv. In mass spectrometry sequence alignment, the very first segment from N-terminus, which is present in POI-1 of both IP products (boiled IP and supernatant IP), is missing in POI-2. The CAMP factor secretion by *P. acnes* strains in MY LAB is confirmed by performing classic CAMP test, modified CAMP test and CAMP factor-ELISA. It can be concluded that yPac1A8 scFv binds with CAMP factor 1 of *P. acnes* which is present on the cell surface and is secreted into the surrounding medium as well. CAMP factors of *P. acnes* have not been studied much and there are many *P. acnes* CAMP factor types. Therefore, *P. acnes* CAMP factors and yPac1A8 scFv, both have to be explored more.

มหาวิทยาลัยเทคโนโลยีสุรนารี

# CHAPTER V

# FROM SINGLE CHAIN FRAGMENT VARIABLE (SCFV) TO SCFV-BCCP, SCFV-EMGFP, AND SCFV-LL37 FORMATS

## 5.1 Abstract

In chapter III, the anti-*Propionibacterium acnes* scFv (yPac1A8, yPac1E4, and yPac1E7) were isolated from Yamo-I human scFv display phage library of MY LAB after affinity selection against *P. acnes* DMST 14916. Similarly, anti-*Pseudomonas aeruginosa* scFv (yPgi3G4) was isolated after biopanning against *P. aeruginosa* DMST 37186. In this chapter, to broaden the scope of the use of isolated scFv, yPac1A8, yPac1E4, and yPgi3G4 are conjugated with biotin carboxyl carrier protein (BCCP) and biotinylated scFv are successfully obtained. Again, yPac1A8, and yPgi3G4 are conjugated with EmGFP protein and the constructs are used as one-step immunofluorescence staining reagent for target bacteria. Moreover, yPac1A8, and yPgi3G4 are planned to conjugate with human anti-microbial peptide (LL-37).

## 5.2 Introduction

In chapter III, Single Chain Fragment Variable (scFv) recombinant antibodies, yPac1A8, yPac1E4 and yPac1E7, all targeting *P. acnes* and yPgi3G4 targeting *P. aeruginosa* are generated. In this chapter, three scFv (yPac1A8, yPac1E4, and yPgi3G4) are conjugated with biotin carboxyl carrier protein (BCCP).

BCCP is intrinsically present in *E. coli*. It is naturally biotinylated by endogenous *E. coli* biotin ligase (Santala & Lamminmaki, 2004). Recombination of BCCP to scFv and expression of the construct in *E. coli* can give rise to biotinylated scFv.

Next, scFv is conjugated with EmGFP. Green fluorescent protein (GFP) is made up of 238 amino acids and has molecular weight of 27 kDa. It has 11 strands of β sheets arranged into a barrel shaped structure and the chromophore is located in the center of the β-barrel (Cubitt et al., 1995; Ilagan et al., 2010). For the discovery and development of GFP, Osamu Shimomura, Martin Chalfie, and Roger Y. Tsien received the Nobel Prize in Chemistry, 2008 (Nobel-Prize-Organisation, 2008). GFP is originated from the jellyfish, *Aequorea victoria*, and it has been modified and engineered to obtain variants with enhanced fluorescence and vibrant colours (Kumar & Pal, 2016). Nowadays, blue, cyan, green, yellow, orange, red, far-red, and infra-red fluorescent proteins are available for use (Addgene, 2017; Day & Davidson, 2009). GFP and the continually expanding family of fluorescent proteins are the essential toolkit for visualization of structures and dynamic processes in cells and organisms.

GFP has been conjugated with several fusion proteins and expressed in yeast, insects, plants, worms, several cell lines and transgenic animals (Cubitt et al., 1995). In this study, emerald GFP is used to conjugate with antibacterial scFv. EmGFP (emerald GFP) is derived from EGFP (enhanced GFP), which is originated from *Aequorea Victoria* GFP. EmGFP is a monomer and is made up of 240 amino acids. It is five-fold brighter than EGFP at 37°C and has excitation maximum at 487 nm and emission maximum at 509 nm (Cubitt, Woollenweber, & Heim, 1999; Cyagen, 2020).

Moreover, scFv has been planned to conjugate with a human antimicrobial peptide (LL-37). LL-37 is encoded by a single cathelicidin gene on chromosome 3p21.3 and contains 37 amino acids which starts with a pair of leucines. It has a net surface charge of (+6) and 35% hydrophobic amino acid content. It has a broad-spectrum antimicrobial, anti-biofilm, antiviral and anti-cancer activities but its actions are non-specific. LL-37 targets the anionic bacterial membranes and disrupts the bacterial membranes by micellization or by forming pores (Dürr, Sudheendra, & Ramamoorthy, 2006; Oren, Lerman, Gudmundsson, Agerberth, & Shai, 1999; G. Wang, Mishra, Epand, & Epand, 2014). LL-37 can be expressed in *E. coli* system (Li, Li, Li, Lockridge, & Wang, 2007). In this chapter, construction of scFv-BCCP, scFv-EmGFP, and scFv-LL37 are described.

## 5.3 Biotin carboxyl carrier protein (BCCP) and scFv conjugation

### 5.3.1 bccp PCR

DNA sequence of biotin carboxyl carrier protein (bccp) is obtained from *E. coli* K-12 NCBI reference sequence NC-000913.3. Based on that reference sequence, one forward and two reverse primers were constructed as shown in **Table 5.1**. The primer pair bccp FW and bccp RV produced PCR product with Not-I restriction site and the linker sequence (ASGAEFGGSG) at 5’ end and Xho I restriction site and stop codon (TAA) at 3’ end. The primer pair bccp FW and bccp-His RV produced PCR product with Not-I restriction site and the linker sequence (ASGAEFGGSG) at 5’ end and Xho I restriction site without stop codon at 3’ end. Heat-treated glycerol stock of *E. coli* K-12 strain C3026 or C3026 colony in deionized water was used as DNA template.

**Table 5.1 Primers for bccp PCR**

| Primer name | Sequences | Length and Tm |
|---|---|---|
| bccp FW | 5′-CTGTGCGCGGCCGCGTCTGGTGCGGAATTCGGTGGTTCTGGTATGGAAGCGCCAGCAGCAGCGGAAATC-3′ | 69-mer, Tm 64°C |
| bccp RV | 5′-GCACAGCTCGAGTTACTCGATGACGACCAGCGGCTCGTCAAATTC-3′ | 45-mer, Tm 65°C |
| bccp-His RV | 5′-GCACAGCTCGAGCTCGATGACGACCAGCGGCTCGTCAAATTC-3′ | 42-mer, Tm 67°C |

The bccp PCR components were prepared according to **Table 5.2** and PCR cycles were performed according to **Table 5.3** by using T-100 Thermal cycler (Bio-Rad#186-1096, U.S.A). PCR products were purified with Wizard SV Gel and PCR Clean-Up System (Promega#A9282, U.S.A).

**Table 5.2 bccp PCR components**

| Reaction components | Volume added per reaction |
|---|---|
| 10x KOD buffer | 5 µL |
| Ultrapure deionized water | X µL |
| KOD dNTP mixture (2 mM each) | 5 µL |
| 25 mM KOD $MgSO_4$ | 3 µL |
| Forward Primer (10 µM) | 1.5 µL |
| Reverse Primer (10 µM) | 1.5 µL |
| DNA Template | *E. coli* glycerol stock 10 µL or *E. coli* colony in deionized water (95°C x 5 min) |
| KOD hot start DNA polymerase (1 U/µL) (Toyobo#71086-3, U.S.A) | 1 µL |
| Total reaction volume | 50 µL/reaction |

**Table 5.3 bccp PCR cycles**

| PCR steps | Temperature | duration |
|---|---|---|
| Denaturation | 95°C | 5 min |
| Denaturation | 95°C | 20 sec |
| Annealing | 61°C | 10 sec 25 cycles repeat |
| Extension | 70°C | 15 sec |

Heat-treated (95°C x 5 min) glycerol stock of *E. coli* K-12 strain C3026 or C3026 colony in deionized water were used as DNA template. There was no amplified product from C3026 colony template PCR. Both bccp and bccp-His PCR products (white arrow pointed in **Figure 5.1**) were obtained from glycerol stock C3026 template PCR. The concentration of bccp and bccp-His PCR products after clean-up were shown in **Table 5.4**. The bccp PCR products were shown in **Figure 5.1**.

**Table 5.4 bccp PCR products**

| Lane no. in Figure 5.1 | PCR products | expected length (base pair) | DNA concentration after PCR clean up | 260/280 | 260/230 |
|---|---|---|---|---|---|
| Lane 4 | bccp | 318 bp | 52.7 ng/µL | 1.97 | 1.21 |
| Lane 5 | bccp-His | 315 bp | 53.6 ng/µL | 1.95 | 1.26 |

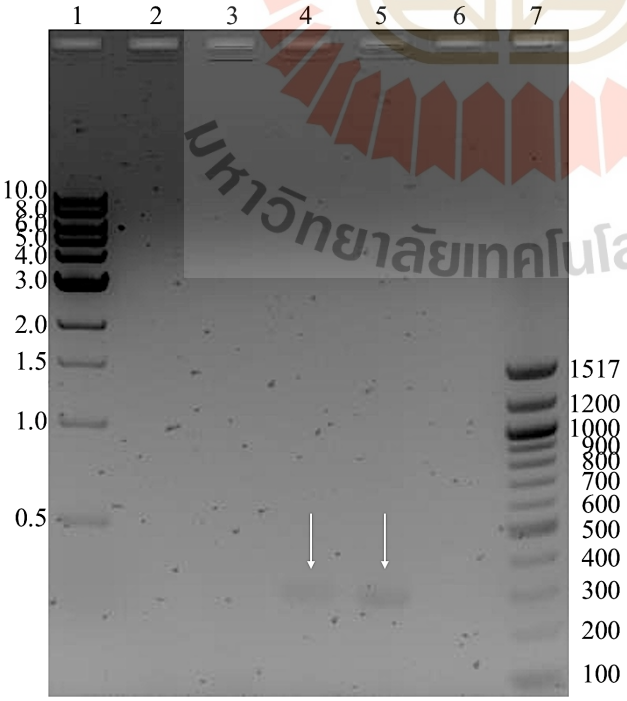


Lane 1= 1 kbp DNA ladder (NEB#N3232L, U.S.A)

Lane 2= bccp (*E. coli* colony)

Lane 3= bccp-His (*E. coli* colony)

Lane 4= bccp (*E. coli* glycerol stock)

Lane 5= bccp-His (*E. coli* glycerol stock)

Lane 6= negative control

Lane 7= 100 bp DNA ladder (NEB#N3231L, U.S.A)

**Figure 5.1 bccp PCR products.**

### 5.3.2 Restriction enzyme digestion of PCR products and vectors

The pET21(d+) vector carrying yPac1A8 or yPac1E4 or yPgi3G4 scFv, which were constructed in chapter II, were used as recipient vectors. The recipient vectors and bccp PCR products were restriction digested as follows. The reaction set up was shown in **Table 5.5**.

**Table 5.5 Restriction digestion reaction**

| Reaction components | Volume added per reaction | Concentration per reaction |
|---|---|---|
| 10x NEB cut smart buffer | 5 µL | 1x |
| Ultrapure deionized water | X µL | |
| DNA | X µL | 1 µg |
| Not-I HF (NEB# R3189S, U.S.A) (20U/µL) | 1 µL | 20 units |
| Xho I (NEB# R0146S, U.S.A) (20 U/µL) | 1 µL | 20 units |
| Total reaction volume | 50 µL/reaction | |

Restriction digestion was performed at 37°C overnight. Enzyme inactivation was done at 65°C for 20 min. After that, 5 units of (alkaline phosphatase, calf intestinal) (NEB# M0290S, U.S.A) was added and incubated at 37°C for 30 min. The gel purification of digestion products was performed by using ultrapure agarose (ThermoScientific#16500100, U.S.A) 1% gel at 100V for 75 min. After that, inserts and vectors with compatible overhangs/sticky ends were obtained as shown in **Table 5.6**.

**Table 5.6 Concentration of restriction enzyme digested vectors and inserts**

| gel-purified restriction digestion products | DNA concentration | 260/280 | 260/230 |
|---|---|---|---|
| bccp | 5.9 ng/µL | 1.78 | 0.48 |
| bccp-His | 6.9 ng/µL | 1.8 | 0.48 |
| pET21(d+)-yPac1A8 | 20.8 ng/µL | 2.06 | 0.98 |
| pET21(d+)-yPac1E4 | 17.4 ng/µL | 2.11 | 1.03 |
| pET21(d+)-yPgi3G4 | 22.3 ng/µL | 2.03 | 1.04 |

### 5.3.3 Ligation of recipient vectors and inserts

required mass of insert (g) = (desired insert/vector molar ratio) x mass of vector (g) x ratio of insert to vector lengths (NEBioCalculator version 1.12.0, NEB, U.S.A)

The above formula were used to calculate the required mass of inserts while vector : insert molar ratio was fixed at 1:3 and the mass of vector at 100 ng. Ligation reaction set up was shown in **Table 5.7**. Ligation reaction was performed at 16°C for 16 h and enzyme inactivation was done at 65°C for 10 min. Ligation reaction products were kept at 4°C until transformation was performed.

**Table 5.7 Ligation reaction set up**

| Ligation reaction components | Volume added per reaction | Concentration per reaction |
|---|---|---|
| 10x ligase reaction buffer | 2 µL | 1x |
| Ultrapure deionized water | X µL | |
| vector DNA | X µL | 100 ng |
| insert DNA | X µL | X ng |
| T4 DNA ligase (NEB#M0202S, U.S.A) | 1 µL | 400 units |
| Total reaction volume | 20 µL/reaction | |

### 5.3.4 Transformation of scFv-bccp and scFv-bccp-6xHis constructs

About 5 µL of each ligation product was mixed gently with 50 µL of chemically competent Top 10 *E. coli* and kept on ice for 30 min. It was exposed to 42°C for 30 sec and kept back on ice for 2 min. After that, 950 µL of SOC (Super Optimal broth with Catabolites repression) medium (pH 7.0, 0.5% (w/v) yeast extract, 2% (w/v) tryptone, 10 mM NaCl, 2.5 mM KCl, 20 mM MgSO4, 20 mM glucose and 10 mM MgCl2) was added and incubated at 37°C, 250 rpm for 1 h. Transformed *E. coli* were

collected by centrifuging at 2000 *g* for 5 min. They were spread onto LB agar plate containing 100 µg/mL ampicillin and incubated at 37°C overnight. Presence of *E. coli* colonies was checked on the next day. The results were shown in **Figure 5.2** and **Table 5.8**.

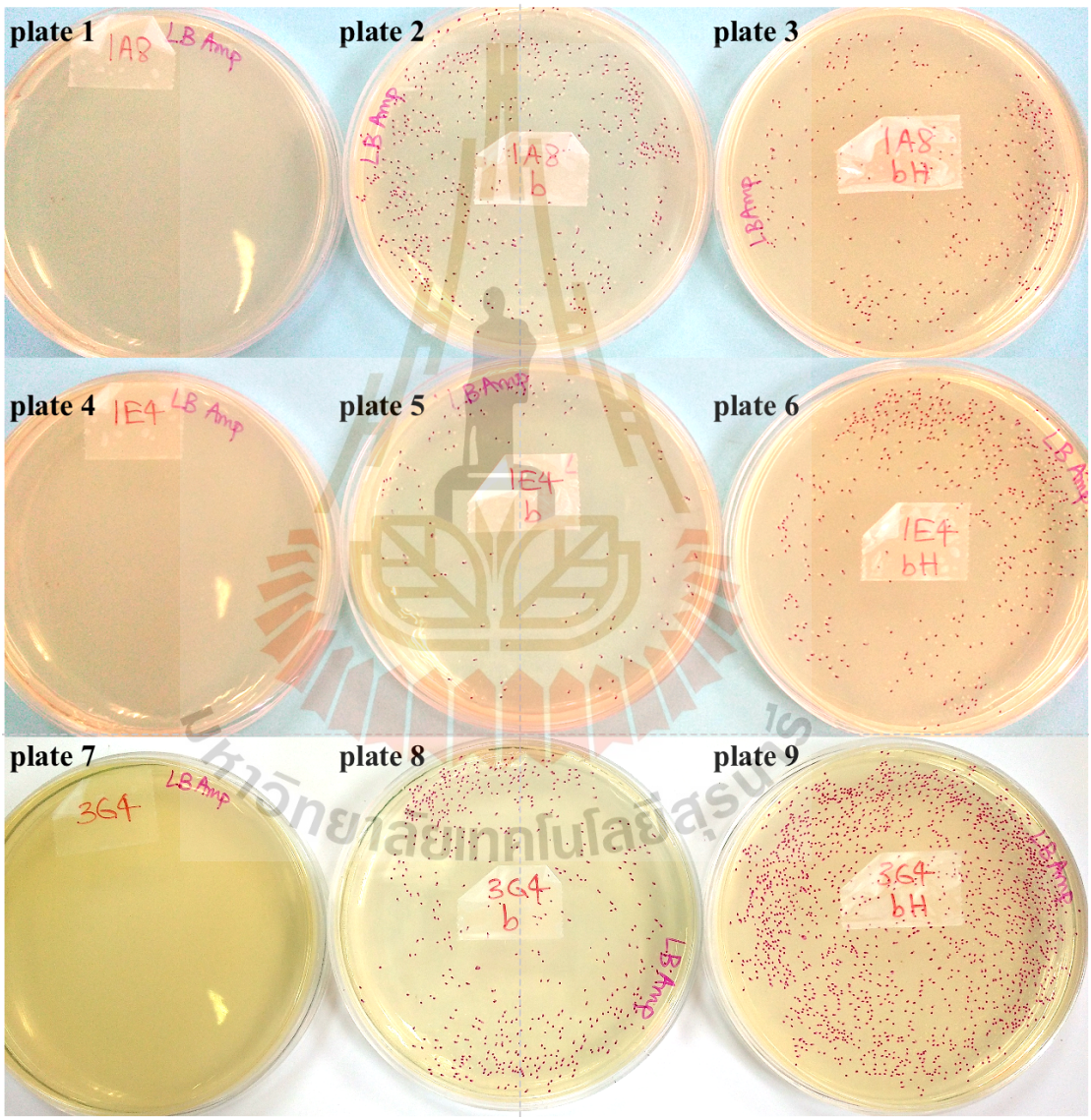


**Figure 5.2 Transformation results of ligation controls, scFv-bccp, and scFv-bccp-His constructs**

**Table 5.8 Transformation results of scFv-bccp, scFv-bccp-His constructs**

| Transformation of constructs | plate no. in Figure 5.2 | colony obtained | colony picked | clones sent for sequencing |
|---|---|---|---|---|
| Not-I HF and XhoI cut pET21(d+)-yPac1A8 | plate 1 | no colony | - | - |
| Not-I HF and XhoI cut pET21(d+)-yPac1E4 | plate 4 | no colony | - | - |
| Not-I HF and XhoI cut pET21(d+)-yPgi3G4 | plate 7 | no colony | - | - |
| yPac1A8-bccp | plate 2 | 483 colonies | 3 colonies | 2 clones |
| yPac1A8-bccp-His | plate 3 | 313 colonies | 3 colonies | 2 clones |
| yPac1E4-bccp | plate 5 | 110 colonies | 3 colonies | 2 clones |
| yPac1E4-bccp-His | plate 6 | 430 colonies | 3 colonies | 2 clones |
| yPgi3G4-bccp | plate 8 | 527 colonies | 3 colonies | 2 clones |
| yPgi3G4-bccp-His | plate 9 | 1600 colonies | 3 colonies | 2 clones |

### 5.3.5 Confirmation of presence of inserts in scFv-bccp and scFv-bccp-His constructs

On next day of transformation, *E. coli* colonies were picked up as shown in **Table 5.8** and overnight broth cultures in LB medium containing 100 µg/mL ampicillin were prepared. The scFv-bccp and scFv-bccp-His plasmids were prepared by using QIAprep Spin Miniprep Kit (Qiagen# 27106, Germany). Presence of inserts were checked by Not-1 HF and XhoI digestion. Restriction digestion was performed as described above (section 5.3.2) except that 250-300 ng of plasmid DNA was used to digest.

The restriction enzyme cut-check result of yPac1A8-bccp, yPac1A8-bccp-His, yPac1E4-bccp, yPac1E4-bccp-His, yPgi3G4-bccp, and yPgi3G4-bccp-His vectors were shown in **Figure 5.3** below. All the inserts cut and checked have inserts of expected length.

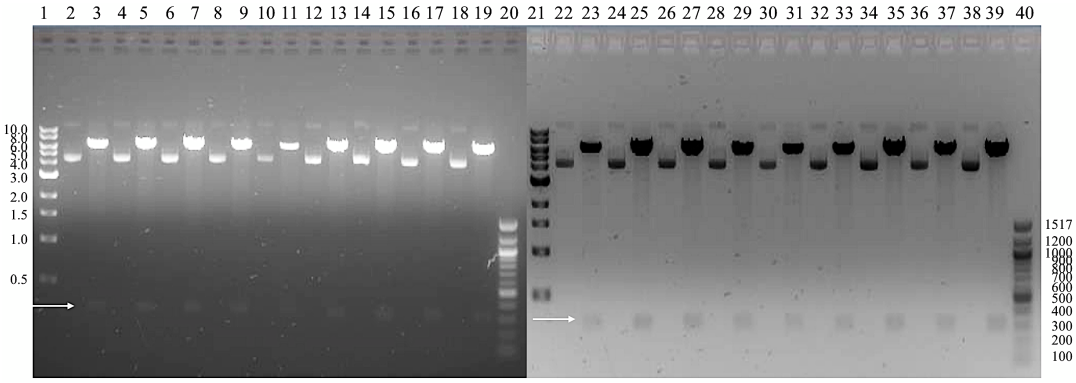


1 = 1kbp DNA ladder
2 = uncut yPac1A8-bccp no.1
3 = cut yPac1A8-bccp no.1
4 = uncut yPac1A8-bccp no.2
5 = cut yPac1A8-bccp no.2
6 = uncut yPac1A8-bccp no.3
7 = cut yPac1A8-bccp no.3
8 = uncut yPac1A8-bccp-His no.1
9 = cut yPac1A8-bccp-His no.1
10 = uncut yPac1A8-bccp-His no.2
11 = cut yPac1A8-bccp-His no.2
12 = uncut yPac1A8-bccp-His no.3
13 = cut yPac1A8-bccp-His no.3
14 = uncut yPac1E4-bccp no.1
15 = cut yPac1E4-bccp no.1
16 = uncut yPac1E4-bccp no.2
17 = cut yPac1E4-bccp no.2
18 = uncut yPac1E4-bccp no.3
19 = cut yPac1E4-bccp no.3
20 = 100 bp DNA ladder
21 = 1kbp DNA ladder
22 = uncut yPac1E4-bccp-His no.1
23 = cut yPac1E4-bccp-His no.1
24 = uncut yPac1E4-bccp-His no.2
25 = cut yPac1E4-bccp-His no.2
26 = uncut yPac1E4-bccp-His no.3
27 = cut yPac1E4-bccp-His no.3
28 = uncut yPgi3G4-bccp no.1
29 = cut yPgi3G4-bccp no.1
30 = uncut yPgi3G4-bccp no.2
31 = cut yPgi3G4-bccp no.2
32 = uncut yPgi3G4-bccp no.3
33 = cut yPgi3G4-bccp no.3
34 = uncut yPgi3G4-bccp-His no.1
35 = cut yPgi3G4-bccp-His no.1
36 = uncut yPgi3G4-bccp-His no.2
37 = cut yPgi3G4-bccp-His no.2
38 = uncut yPgi3G4-bccp-His no.3
39 = cut yPgi3G4-bccp-His no.3
40 = 100 bp DNA ladder

**Figure 5.3 Restriction enzyme cut-check of scFv-bccp and scFv-bccp-His constructs.**

1 kbp DNA ladder (NEB#N3232L, U.S.A) and 100 bp DNA ladder (NEB#N3231L, U.S.A) were used. The inserts were white-arrowed.

### 5.3.6 DNA sequence checking of scFv-bccp and scFv-bccp-His constructs

Two clones each of yPac1A8-bccp, yPac1A8-bccp-His, yPac1E4-bccp, yPac1E4-bccp-His, yPgi3G4-bccp, and yPgi3G4-bccp-His vectors were sent to Macrogen, Inc., South Korea for DNA sequence checking. Universal T7 promotor and T7 terminator primers were used for sequencing. The integrity of IgG constructs was checked by using Vector NTI software (ThermoScientific, U.S.A). The length of recipient vectors, inserts and scFv-bccp and scFv-bccp-His constructs were shown in **Table 5.9**.

**Table 5.9 Length of vectors, inserts and ligated scFv-bccp and scFv-bccp-His constructs**

| Name of vectors and inserts | length (base pair) |
|---|---|
| pET21(d+)-yPac1A8 | 6125 bp |
| pET21(d+)-yPac1E4 | 6122 bp |
| pET21(d+)-yPgi3G4 | 6110 bp |
| bccp insert with stop codon | 294 bp |
| bccp insert without stop codon | 291 bp |
| pET21(d+)-yPac1A8-bccp | 6419 bp |
| pET21(d+)-yPac1A8-bccp-6xHis | 6416 bp |
| pET21(d+)-yPac1E4-bccp | 6416 bp |
| pET21(d+)-yPac1E4-bccp-6xHis | 6413 bp |
| pET21(d+)-yPgi3G4-bccp | 6404 bp |
| pET21(d+)-yPgi3G4-bccp-6xHis | 6401 bp |

The vector maps of scFv-bccp and scFv-bccp-His constructs were made by using Snapgene software version 5.2. The vector maps are shown in **Figure 5.4** below.

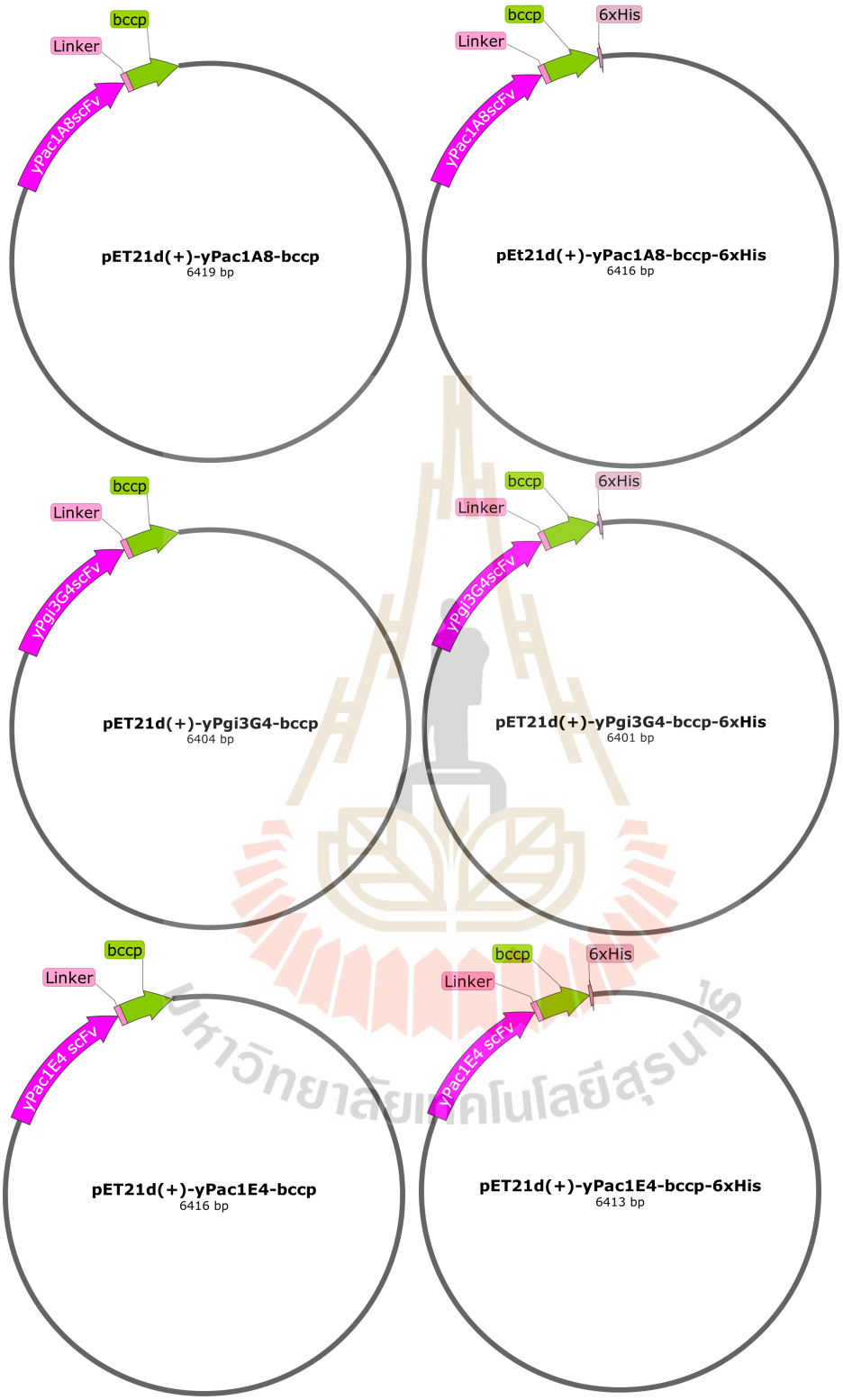


**Figure 5.4 The vector maps of scFv-bccp and scFv-bccp-His constructs.**

It is made by using Snapgene software version 5.2. The arrangement of recombinant genes can be seen.

### 5.3.7 Predicted three-dimensional structure of scFv-bccp-His constructs

The three-dimensional structural of yPac1A8-bccp is predicted by using Protein Homology/analogY Recognition Engine V 2.0 (Kelley, Mezulis, Yates, Wass, & Sternberg, 2015). It is shown in **Figure 5.5**, below.

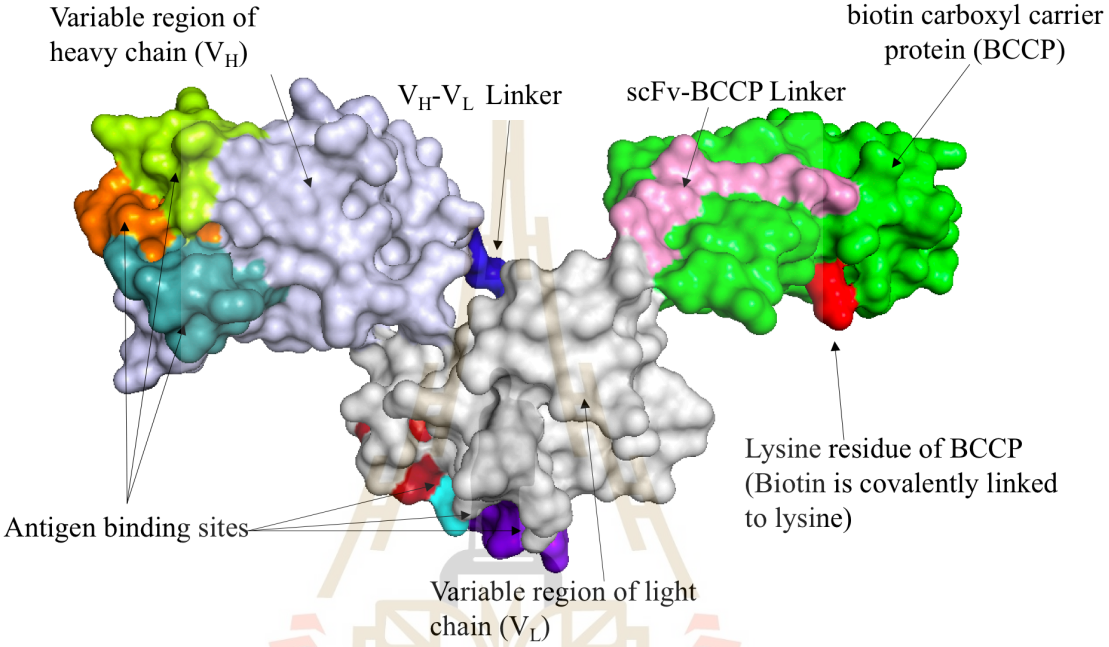


**Figure 5.5 Predicted 3D-structure of yPac1A8-bccp-6xHis construct.**

In our model, BCCP is attached to C-terminus of scFv by a 10-mer peptide linker (Ala-Ser-Gly-Ala- Glu-Phe-Gly-Gly-Ser-Gly) which is seen as the pink segment in the model (Santala & Lamminmaki, 2004). Naturally, biotin is covalently linked to lysine residue (red segment in the model) near the C-terminus of BCCP by intrinsic biotin ligase of *E. coli*.

### 5.3.8 Expression and purification of scFv-bccp-His constructs

The scFv-bccp-His constructs, pET21(d+)-yPac1A8-bccp-6xHis, pET21(d+)-yPac1E4-bccp-6xHis and pET21(d+)-yPgi3G4-bccp-6xHis were

transformed into SHuffle T7 B strain *E. coli* (NEB#C3029J, U.S.A), expressed in Terrific Broth (Tryptone 12 g/L, yeast extract 24 g/L, glycerol 4 mL/L, 0.17 M monobasic potassium phosphate 50 mL/L and 0.72 M dibasic potassium phosphate 50 mL/L) containing 100 µg/mL ampicillin. The medium was supplemented with 5 µM biotin, and expression was induced by 1 mM isopropyl-β-D-thiogalactopyranoside (IPTG). The expressed scFv-bccp-6xHis proteins were purified by using a gravity flow column containing Ni-NTA agarose affinity chomatography matrix (Qiagen#30230, Germany).

The purification process was monitored with SDS-PAGE and the gels were shown in Figure 5.6. The protein, bccp, is made up of 87 amino acids (9.3 kda). The recombinant proteins, yPac1A8-bccp-6xHis is made up of 358 amino acids (37.8 kDa), yPac1E4-bccp-6xHis is made up of 357 amino acids (37.68 kDa), and yPgi3G4-bccp-6xHis is made up of 353 amino acids (37.2 kDa), respectively.

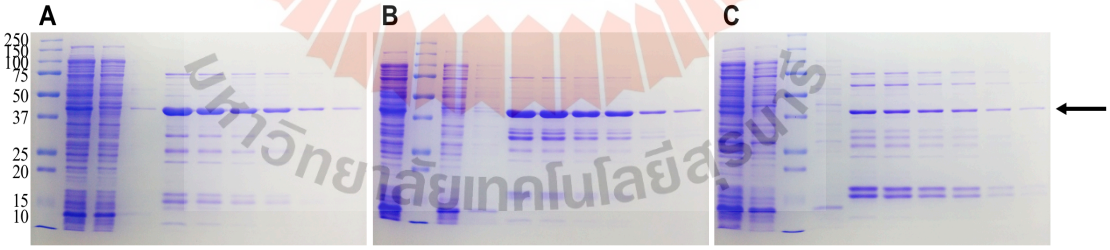


yPac1A8-bccp-6xHis purification SDS-PAGE | yPac1E4-bccp-6xHis purification SDS-PAGE | yPgi3G4-bccp-6xHis purification SDS-PAGE

**Figure 5.6 SDS-PAGE gels of scFv-bccp-6xHis protein purification.**

The expected size of the constructs was 37-38 kDa (arrow-pointed). All Blue Prestained Protein Standards (BioRad#1610373, U.S.A) is used.

### 5.3.9 Biotinylated scFv ELISA

To check functionality of biotinylated scFv, bacterial whole cell ELISA was performed. Heat-inactivated *P. acnes* DMST 14916 ($10^9$ cells/mL) was used as target for yPac1A8-bccp-6xHis and yPac1E4-bccp-6xHis scFv. Heat-inactivated *P. aeruginosa* DMST 37186 ($10^9$ cells/mL) was used as target for yPgi3G4-bccp-6xHis scFv. Purified yPac1A8-bccp-6xHis scFv (10 µg/mL), yPac1E4-bccp-6xHis scFv (20 µg/mL) and yPgi3G4-bccp-6xHis (20 µg/mL) were used as primary detection agent.

HisProbe-HRP (ThermoScientific#15165, U.S.A) (1:5000 dilution in PBS) and Streptavidin-HRP (ThermoScientific#N100, U.S.A) (1:5000 dilution in PBS) were used as secondary detection agent. ABTS substrate (Amresco#0400-10G, U.S.A) in citric acid-$H_2O_2$ buffer (0.05%$H_2O_2$ in 50 mM citric acid pH 4.0) was used as substrate for both HRP systems. ELISA procedure was the same as in chapter III. The absorbance was measured at 405 nm with Tecan's Sunrise absorbance microplate reader (Tecan, Switzerland). ELISA results are shown in **Figure 5.7, Figure 5.8,** and **Figure 5.9**.

มหาวิทยาลัยเทคโนโลยีสุรนารี

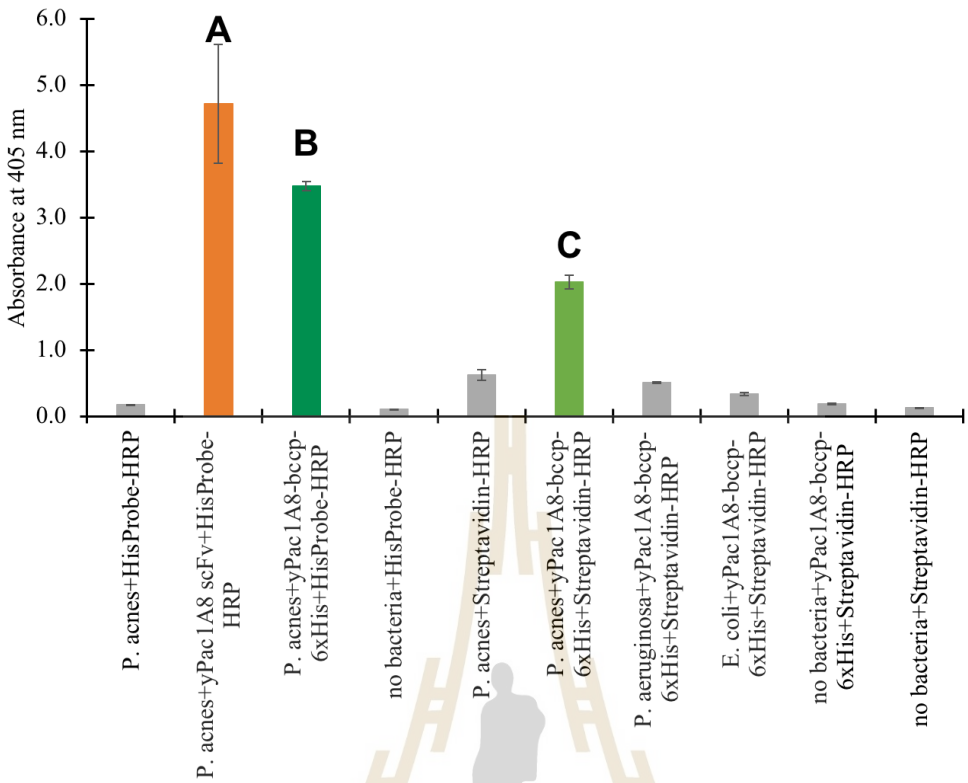


**Figure 5.7** **Biotinylated yPac1A8 scFv (yPac1A8-bccp-6xHis) ELISA.**

Bar A (orange) is positive control, which is 6xHis-tagged scFv detected by HisProbe-HRP. Bar B (dark green) is yPac1A8-bccp-6xHis detected by HisProbe-HRP. Bar C (light green) is yPac1A8-bccp-6xHis detected by Streptavidin-HRP. The remaining bars are bacterial controls and secondary antibody controls. ELISA is performed in triplicates and error bars represent SEM.

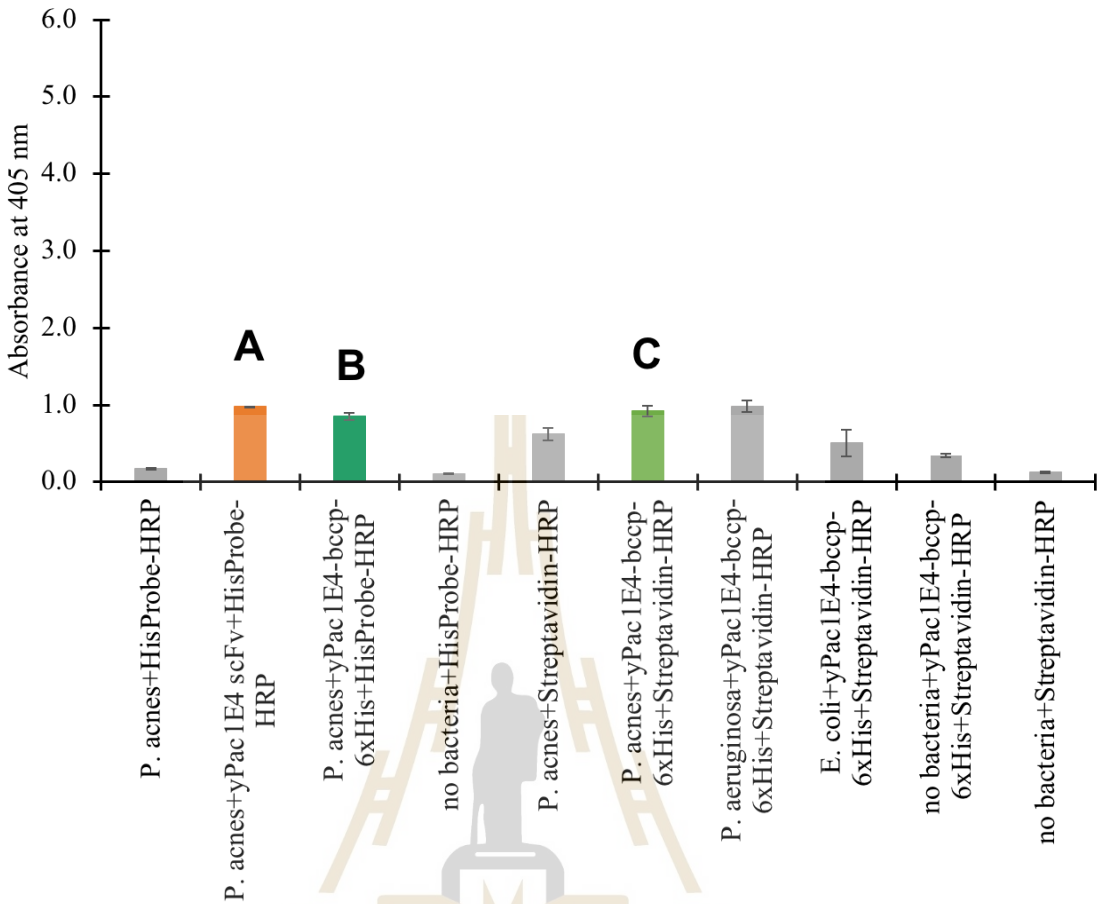


**Figure 5.8** **Biotinylated yPac1E4 scFv (yPac1E4-bccp-6xHis) ELISA.**

Bar A (orange) is positive control, which is 6xHis-tagged scFv detected by HisProbe-HRP. Bar B (dark green) is yPac1E4-bccp-6xHis detected by HisProbe-HRP. Bar C (light green) is yPac1E4-bccp-6xHis detected by Streptavidin-HRP. The remaining bars are bacterial controls and secondary antibody controls. ELISA is performed in triplicates and error bars represent SEM.

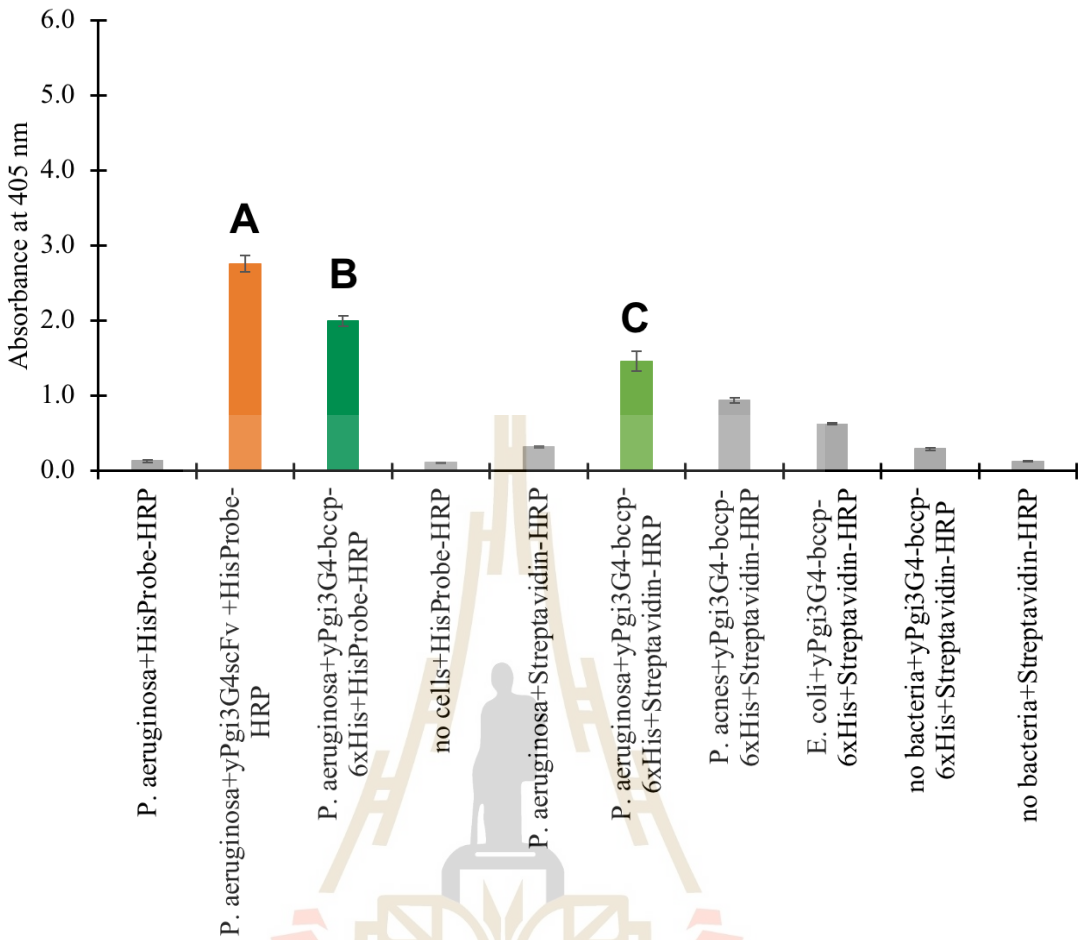


**Figure 5.9 Biotinylated yPgi3G4 scFv (yPgi3G4-bccp-6xHis) ELISA.**

Bar A (orange) is positive control, which is 6xHis-tagged scFv detected by HisProbe-HRP. Bar B (dark green) is yPgi3G4-bccp-6xHis detected by HisProbe-HRP. Bar C (light green) is yPgi3G4-bccp-6xHis detected by Streptavidin-HRP. The remaining bars are bacterial controls and secondary antibody controls. ELISA is performed in triplicates and error bars represent SEM.

In this study, two biotinylated scFv forms, with and without 6xHistidine tag are constructed. Biotin carboxyl carrier protein of *E. coli* is conjugated to scFv. When BCCP is attached with biotin at its lysine residue by biotin ligase of *E. coli*, our

scFv gets biotinylated at the known site, that is lysine. The integrity of DNA sequence of both forms has been confirmed. By using 6xHistidine tag system, scFv-BCCP-6xHistidine constructs are successfully purified and tested by biotin-streptavidin ELISA. Among three scFv constructs, yPac1A8-BCCP-6xHistidine conjugate binds the best with streptavidin-HRP. Both yPac1A8-BCCP-6xHistidine and yPgi3G4-BCCP-6xHistidine are detectable by streptavidin-HRP as well as by HisProbe-HRP. The construct, yPac1E4-BCCP-6xHistidine is the least responsive one to streptavidin-HRP.

Biotin-streptavidin coupling reaction and biotinylated antibodies have been widely used in molecular biology. Biotin ligase of *E. coli* has been engineered to biotinylate wide range of proteins (Choi-Rhee, Schulman, & Cronan, 2004). Non-enzymatic biotinylation of BCCP has been proposed (Streaker & Beckett, 2006). Biotin ligase of *E. coli* has been used in vitro (H. Wang, Zhao, Han, & Yang, 2016). Thus, scFv-BCCP constructs and their applicability are interesting topic. The BCCP vector of this study can be used to biotinylate other scFv of interest by substituting the scFv sequence by restriction enzyme-based cloning.

มหาวิทยาลัยเทคโนโลยีสุรนารี

## 5.4 EmGFP and scFv conjugation

### 5.4.1 Restriction enzyme cloning of scFv-EmGFP conjugates

From phagemid pMOD 1.1 of MY LAB, yPac1A8 and yPgi3G4 scFv DNA sequences were subcloned into pWS-EmGFP of MY LAB (derived from pET15b) by restriction digestion with NcoI-HF (NEB#R3193S, U.S.A) and NotI-HF (NEB#R3189S, U.S.A). The 3'end of scFv sequence was linked to EmGFP by $(Gly)_4$ linker and 3' end of EmGFP was equipped with FLAG and 6xHistidine tag systems.

Recombinant plasmids carrying scFv-EmGFP genes against *P. acnes* and *P. aeruginosa* were designated as pWS-EmGFP /yPac1A8 and pWS-EmGFP /yPgi3G4, respectively. The integrity of the constructs was confirmed by DNA sequencing at Macrogen, Inc., South Korea by using universal T7 promotor and T7 terminator primers. The length of vectors, inserts and recombinant products are shown in **Table 5.10**. The arrangement of gene segments in the construct is shown in **Figure 5.10**.

**Table 5.10 Length of recombinant products of scFv-EmGFP cloning**

| | |
|---|---|
| **Donor plasmid** | pMOD 1.1/yPac1A8 (5275 bp)<br>pMOD 1.1/yPgi3G4 (5260 bp) |
| **Recipient plasmid** | pWS-EmGFP of MY LAB (6447 bp) |
| **Insert** | yPac1A8 scFv (761 bp)<br>yPgi3G4 scFv (746 bp) |
| **Insert:Vector ratio** | 3:1 |
| **competent cells** | chemically competent TOP10 strain *E. coli* |
| **Recombinant plasmids** | pWS-EmGFP /yPac1A8 (7184 bp)<br>pWS-EmGFP /yPgi3G4 (7169 bp) |
| **Recombinant scFv-EmGFP proteins** | yPac1A8-EmGFP (55.69 kDa)<br>yPgi3G4-EmGFP (55.05 kDa) |

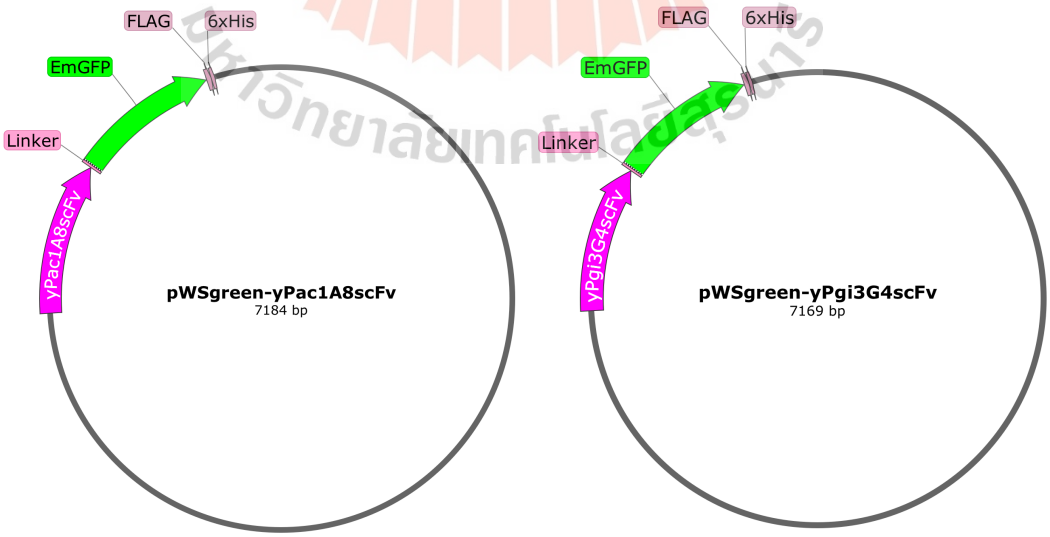


**Figure 5.10 The vector maps of scFv-EmGFP constructs.**

The maps are made by using Snapgene software version 5.2.

### 5.4.2 Expression of EmGFP conjugates

The scFv-EmGFP genes were expressed in SHuffle T7 B strain *E. coli* (NEB#C3029J, U.S.A) according to previous publications (Bezabeh et al., 2017; Lobstein et al., 2012) with some optimization. Briefly, a colony of SHuffle *E. coli* C3029 harboring pWS-EmGFP /yPac1A8 or pWS-EmGFP /yPgi3G4 was inoculated into Terrific broth (Tryptone 12 g/L, yeast extract 24 g/L, glycerol 4 mL/L, 0.17 M monobasic potassium phosphate 50 mL/L and 0.72 M dibasic potassium phosphate 50 mL/L) containing 100 µg/mL ampicillin and incubated overnight at 30°C at 225 rpm. It was sub-cultured (1:100 dilution) in fresh Terrific broth containing 100 µg/mL ampicillin and incubated at 30°C in a baffled flask at 225 rpm for 5 h ($OD_{600}$ reached 0.5). Protein expression was induced with 0.85 mM IPTG for 24 h at 25°C. The culture was kept on ice for 5 min and centrifuged (3000 *g*, 30 min, 4°C). The obtained *E. coli* cell pellet was used for scFv-EmGFP purification.

### 5.4.3 Purification of scFv-EmGFP conjugates

The *E. coli* cell pellet was resuspended in lysis buffer (pH 7.5 containing 50 mM Tris-HCl, 0.5 M NaCl, 5 mM imidazole, 1mg/mL lysozyme) and sonicated with 500Watt Ultrasonic Processor (CV334, Thomas Scientific, U.S.A) for 30 sec followed by incubation on ice for 30 sec alternatively for 5 min. Supernatant was separated from cell debris and unbroken cells by centrifugation (3000 *g*, 30 min, 4°C). That supernatant was centrifuged again after adding equal amount of equilibration buffer (pH 7.5 containing 50 mM Tris-HCl, 0.5 M NaCl, 5 mM imidazole) and transferred into a gravity flow column containing Ni-NTA (Nickel-Nitrilotriacetic acid) agarose affinity chromatography matrix (Qiagen#30230, Germany), pre-equilibrated with equilibration

buffer, and incubated for 45 min at 4°C. The agarose resin was washed with washing buffer (pH 7.5 containing 50 mM Tris-HCl, 0.5 M NaCl, 20 mM imidazole) and scFv was eluted with elution buffer (pH 7.5 containing 50 mM Tris-HCl, 0.5 M NaCl, 250 mM imidazole) (**Figure 5.11**).

Purity of eluted scFv was checked by SDS-PAGE (sodium dodecyl sulfate-polyacrylamide gel electrophoresis). Desalting and buffer exchange was performed by dialysis in SnakeSkin Dialysis Tubing with 10 kDa MWCO (ThermoScientific#68100, U.S.A) against PBS at 4°C overnight. Concentration of purified scFv-EmGFP was determined by Nanodrop 2000 spectrophotometer (ThermoScientific, U.S.A) and kept at -80°C in 250 mg/mL BSA (bovine serum albumin).

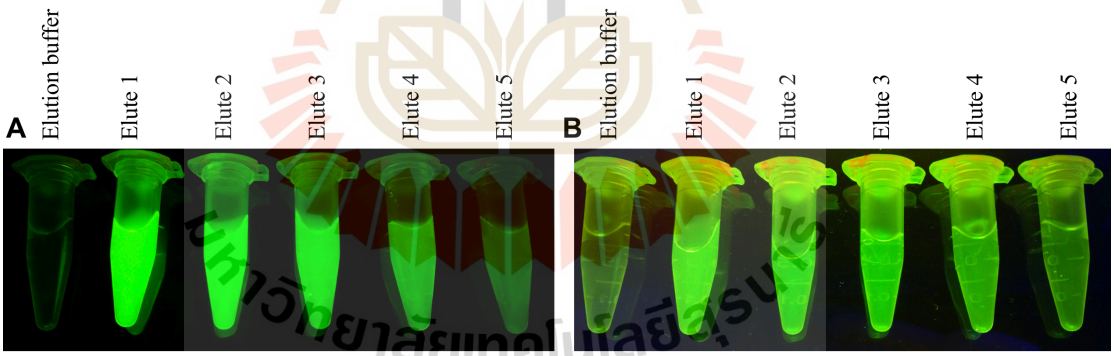


**Figure 5.11 Examination of scFv-EmGFP elutes.**

(A) Five elute tubes of yPac1A8-EmGFP and (B) yPgi3G4-EmGFP. The elutes were examined with with B-BOX Blue Light LED epiilluminator (SMOBiO#VE0100, U.S.A). The elution buffer only was used as negative control.

### 5.4.4 Western Blot analysis of scFv-EmGFP conjugates

Equal amount (1 μg) of purified yPac1A8 scFv, yPgi3G4 scFv, yPac1A8-EmGFP, and yPgi3G4-EmGFP in SDS sample buffer were heat-treated at 90°C for 10 min and electrophoresed in 12.5% SDS-PAGE gel for 5 min at 50 V followed by 90 min at 100 V. Transfer of proteins from the gel to PVDF (polyvinylidene difluoride) membrane (Cytiva#10600021, U.S.A), which was activated with absolute methanol, was done at 30 V for 15 h at 4°C by wet-blotting, where, tris-glycine transfer buffer (25 mM Tris, 192 mM glycine, 20% (v/v) methanol) and Mini Trans-Blot electrophoretic transfer cell (Biorad#1703930, U.S.A) were used. The membrane was blocked with 3% (w/v) BSA in TBST (20 mM Tris-150 mM NaCl buffer containing 0.1% (v/v) Tween-20) for 1 h at room temperature followed by 3 times TBST washing, 5 min each. Then, the membrane was incubated with 1:5000 diluted HisProbe-HRP (ThermoScientific# 15165, U.S.A) in blocking buffer for 1 h at room temperature followed by 3 times TBST washing. The presence of scFv and scFv-EmGFP (**Figure 5.12**) was checked by chemiluminescence, using Amersham ECL Prime reagent (GE Healthcare#RPN2232, UK). Image analysis was performed by using ChemiDoc XRS Gel Documentation System (Bio-Rad, U.S.A).

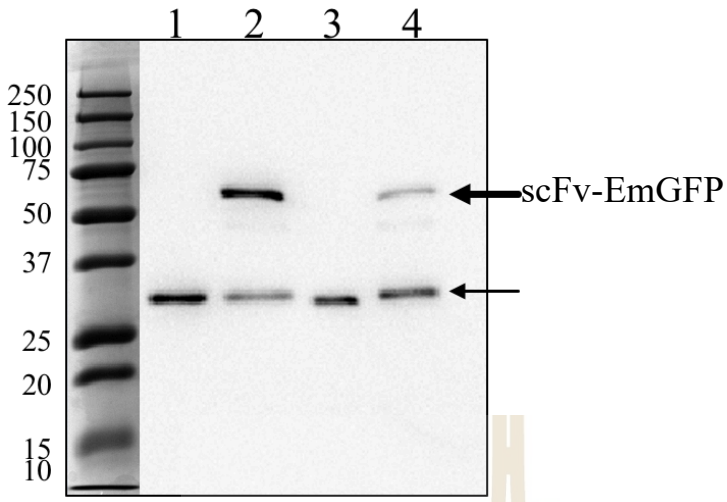


**Figure 5.12 Analysis of scFv and scFv-EmGFP by Western Blot.**

All Blue Prestained Protein Standards (BioRad#1610373, U.S.A) is used. The yPac1A8 scFv (lane 1), yPac1A8-EmGFP (lane 2), yPgi3G4 scFv (lane 3), and yPgi3G4-EmGFP (lane 4) are detected by HisProbe-HRP and Amersham ECL Prime chemiluminescence reagent.

Two bands (thick and thin arrow-pointed) are seen in scFv-EmGFP recombinant products (lane 2 and 4). Recombinant construct yPac1A8-EmGFP is 55.7 kDa protein and yPgi3G4-EmGFP is 55.1 kDa. The thick-arrowed bands in **Figure 5.12** are scFv-EmGFP constructs at expected size. ScFv alone, yPac1A8 (lane 1) and yPgi3G4 (lane 3), has molecular weight of 26.7 kDa and 26.1 kDa, respectively. EmGFP unit is made up of 240 amino acids (26.9 kDa). One extra band (thin-arrowed bands) in scFv-EmGFP lanes is located slightly higher than the level of scFv alone control. That extra band is thought to be EmGFP unit from the construct. Whether it is expressed as stand-alone EmGFP unit inside SHuffle *E. coli* expression host or is detached from the scFv-EmGFP construct during WB sample preparation has to be examined in the future.

### 5.4.5 Predicted 3D-structure of scFv-EmGFP constructs

The three-dimensional models of yPac1A8-EmGFP and yPgi3G4-EmGFP are constructed by using Protein Homology/analogY Recognition Engine V 2.0 (Kelley et al., 2015) and visualized by PyMOL molecular visualization system (www.pymol.org) from Schrödinger, LLC, U.S.A (DeLano & Bromberg, 2004). The models are shown in **Figure 5.13** below. The scFv unit of the models are gray and EmGFP unit are bright green. The two units are joined together by a (Gly)4 linker which are seen as pink unit in the models. The two tag systems are 6xHistidine (red) and FLAG (yellow).

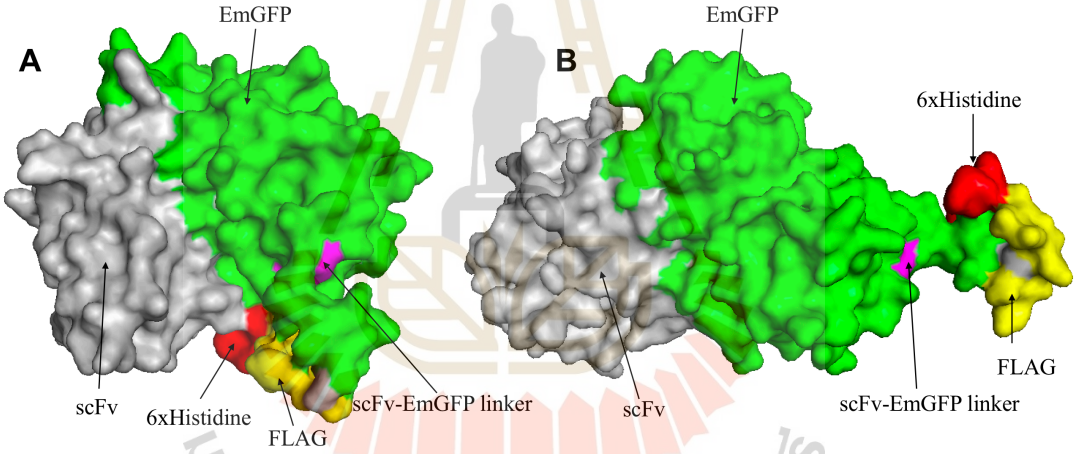


**Figure 5.13 3D model of (A) yPac1A8-EmGFP and (B) yPgi3G4-EmGFP.**

### 5.4.6 Fluorometric detection of yPac1A8-EmGFP

In order to evaluate the functionality of yPac1A8-EmGFP conjugate, serial dilutions of *P. acnes* (from $1.6 \times 10^9$ to $1.6 \times 10^2$ cells/mL) were incubated with various concentrations of yPac1A8-EmGFP (from 10 µg/mL to 0.1µg/mL) in one-step procedure. Briefly, a black 96-well immuno plate (ThermoScientific#437111, U.S.A) was coated with 10-fold dilutions of heat-inactivated *P. acnes* in PBS from row A to

H, where row A had the highest concentration ($1.6x10^9$ cells/mL), while row H had the lowest (160 cells/mL). Target immobilization was performed overnight at 37 °C. The wells were blocked with PBSM (2 % (w/v) skimmed milk protein in PBS) for 1 h followed by three times PBS washing. Then, the wells were incubated with six different dilutions of yPac1A8-EmGFP scFv in duplicate format. Column 1 and 2 had the highest scFv concentration (yPac1A8-EmGFP 10 μg/mL), while column 11 and 12 had the lowest (yPac1A8-EmGFP 0.1 μg/mL) for 1 h at room temperature in a dark place.

After that, the fluorescence intensity was measured using Varioskan LUX multimode microplate reader (ThermoScientific, U.S.A) with filter pair excitation 478 nm and emission 506 nm. Presence of immunoconjugates was determined by measuring EmGFP fluorescence intensity ( $\lambda_{ex}$=478 nm, $\lambda_{em}$=506 nm). The measured fluorescence intensity was plotted against *P. acnes* concentration (cells/mL) (**Figure 5.14**).

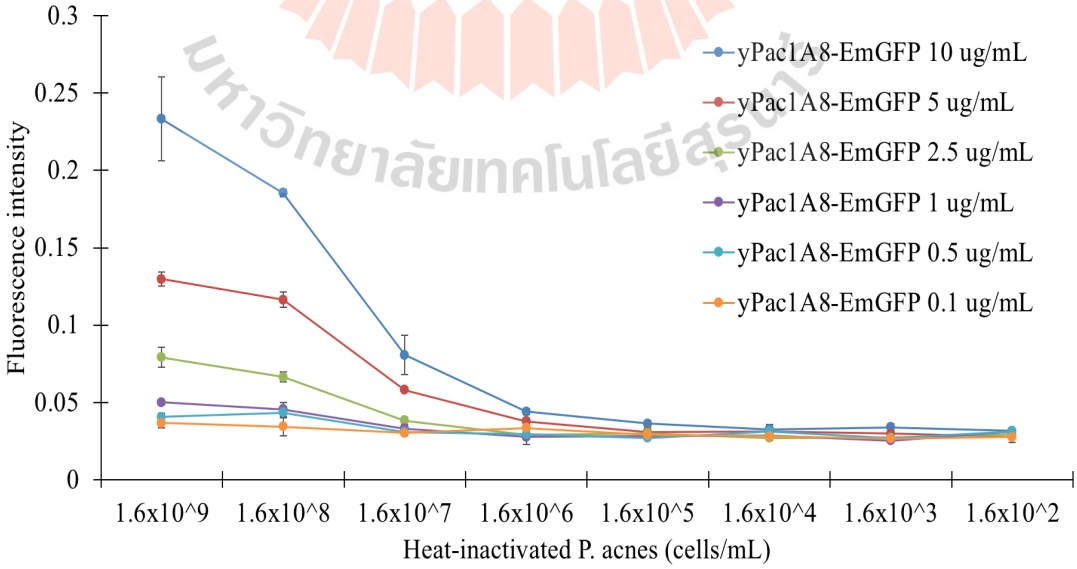


**Figure 5.14 Fluorometric immunoassay of yPac1A8-EmGFP.**

In **Figure 5.14**, the lines represent the average value of duplicate samples and error bars represent the standard error of the mean. For yPac1A8-EmGFP, the highest scFv concentration tested (10 μg/mL) could detect $1.6x10^7$ cells/mL and 2.5 μg/mL yPac1A8-EmGFP could detect $1.6x10^8$ cells/mL. Concentrations below 2.5 μg/mL could not give positive signal. In chapter III, yPac1A8 scFv 10 μg/mL could detect $1.6x10^5$ *P. acnes* cells/mL and 0.1 μg/mL could detect $1.6x10^9$ *P. acnes* cells/mL. In comparison, the limit of detection of yPac1A8-EmGFP is not as low as yPac1A8 scFv. For yPgi3G4-EmGFP, fluorometric immunoassay has not done, yet.

### 5.4.7 Direct immunofluorescence staining with scFv-EmGFP

About 1 mL of bacterial broth culture was centrifuged (3000 *g*, 5 min), washed with PBS for two times and resuspended in PBS. About 5 μL of that was spread into a smear on a glass slide and dried completely at 37°C. The smear was fixed with 4% PFA (paraformaldehyde) in PBS (pH 7.4) for 30 min, blocked with 1%BSA-300 mM glycine-0.1% PBST for 30 min, treated with 2 μg of scFv-EmGFP conjugates for 1 h in dark place, and counterstained with 300 μM DAPI (4′,6-diamidino-2-phenylindole) for 5 min. The smear was washed three times with PBS between above steps. The stained smear was covered with slow fade gold mountant (Invitrogen#S36936, U.S.A) and examined with confocal microscope (**Figure 5.15**).

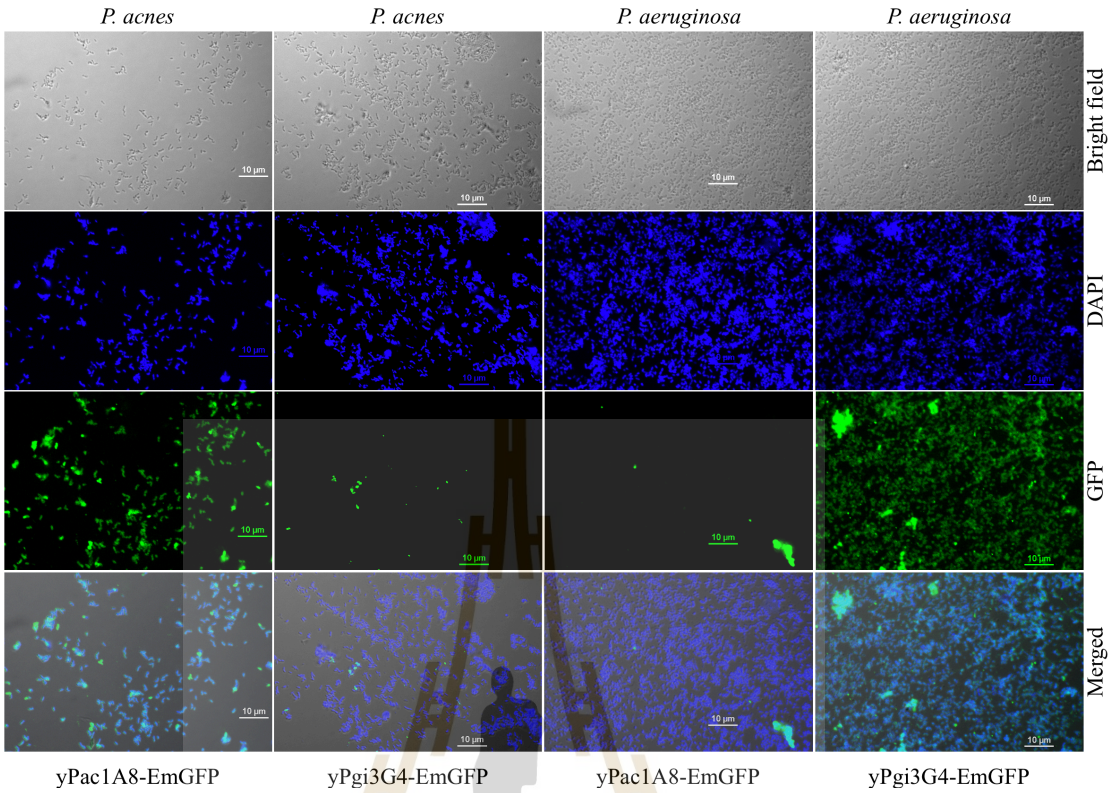


**Figure 5.15 Confocal microscopy of *P. acnes* and *P. aeruginosa*.**

Pictures are taken with Apo TIRF 60x Oil DIC N2 objective of Nikon A1R confocal laser microscope. Scale bars represent 10 µm. Planktonic cells of *P. acnes* DMST 14916 and *P. aeruginosa* DMST 37186 were incubated with yPac1A8-EmGFP and yPgi3G4 scFv-EmGFP as indicated in the figure and counterstained with DAPI. In bright field panel, bacterial cells are seen. In DAPI panel, nucleoids of bacteria are blue. In GFP panel, *P. acnes* cells are stained green by yPac1A8-EmGFP and *P. aeruginosa* cells are stained green by yPgi3G4-EmGFP.

GFP (green fluorescence protein) is about 27 kDa protein consisting of 238 amino acids. It is originated from the jellyfish *Aequorea victoria*. GFP has been

used as fusion tag, biosensors, cell marker, selection marker and so on (Addgene, 2017; Kumar & Pal, 2016). In this study, Emerald GFP is used to conjugate with scFv and usefulness of scFv-EmGFP constructs in bioimaging of bacteria has been tested. ScFv-EmGFP can be used as a one-step detection agent for immunofluorescence staining of target bacteria. The scFv-EmGFP conjugates also have 6xHistidine tag and FLAG at their carboxy terminal. By using 6xHistidine tag, scFv-EmGFP are easily purified. By Western Blot analysis, two bands are seen in purified conjugates. One line corresponds to the expected size of the scFv-EmGFP conjugate (55 kDa). The other line is likely to be the EmGFP unit without scFv part.

## 5.5 Antimicrobial peptide LL-37 and scFv conjugation

### 5.5.1 LL-37

LL-37 is a potent human host-defense antimicrobial peptide and is a component of innate immune system. It is encoded by a single cathelicidin gene on chromosome 3p21.3 and contains 37 amino acids which starts with a pair of leucines. It has a broad-spectrum antimicrobial and anti-biofilm activities, but its actions are non-specific (Dürr et al., 2006; G. Wang et al., 2014). We are interested to conjugate it with scFv and find out how to modify human origin, non-specific and short-lived LL-37 to non-immunogenic, target-directed potent therapeutic agent for infectious diseases.

### 5.5.2 scFv-LL-37 constructs

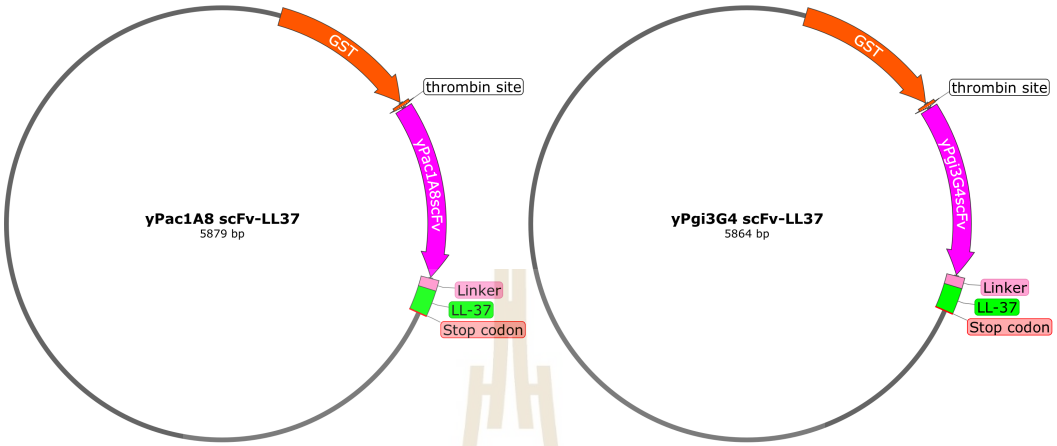


**Figure 5.16 The vector maps of scFv-LL37 constructs.**

Vector maps are made by using Snapgene software version 5.2.

The scFv-LL-37 constructs are planned to be expressed and purified by GST (Glutathione S-Transferase) gene fusion system. The empty vector (GST-LL37) construction has been finished. Next is to subclone yPac1A8 scFv and yPgi3G4 scFv sequences into the vector. The vector maps of the final constructs are shown in **Figure 5.16**. The effect of LL-37 and scFv-LL37 on target bacteria will be studied and the preliminary studies will use scFv-LL37 expressed in *E. coli* system. The predicted three-dimensional structures of scFv-LL37 constructs are shown in **Figure 5.17**. The expected properties of the final constructs are shown in **Table 5.11**.

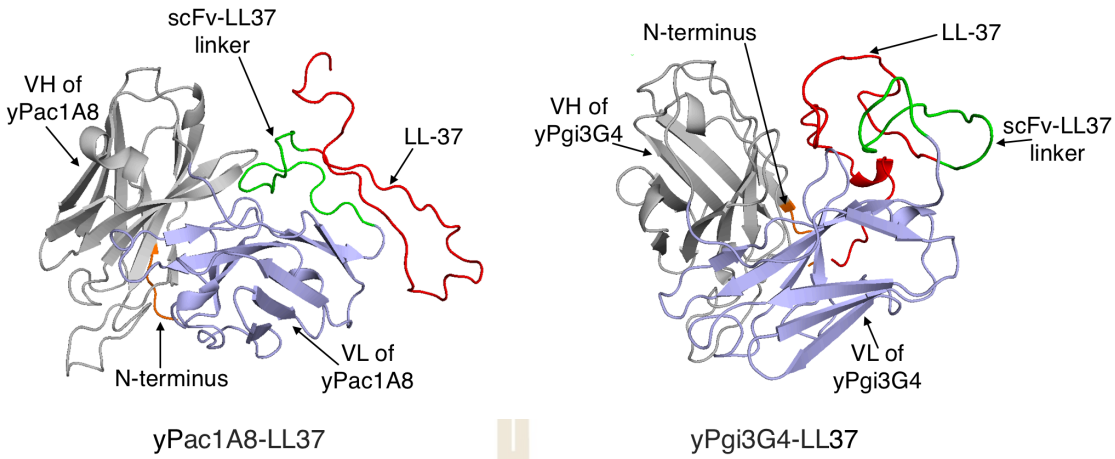


**Figure 5.17 Predicted 3D structure of (A) yPac1A8-LL37 (B) yPgi3G4-LL37.** The models are built by using Protein Homology/analogY Recognition Engine V 2.0 (Kelley et al., 2015) and visualized by PyMOL molecular visualization system (www.pymol.org) from Schrödinger, LLC, U.S.A (DeLano & Bromberg, 2004). In both models; N-terminus of the construct is orange, VH domain of scFv is gray, VL domain of scFv is light blue, the linker that connects scFv and LL37 units is green, and LL-37 unit is bright red.

**Table 5.11 Properties of scFv-LL37 recombinant proteins**

| | **yPac1A8-LL37** | **yPgi3G4-LL37** |
|---|---|---|
| length (amino acid residues) | 312 residues | 307 residues |
| molecular weight | 32.68 kDa | 32.05 kDa |
| charge at pH 7 | 6.96 | 2.96 |

## 5.6 Conclusion and future perspectives

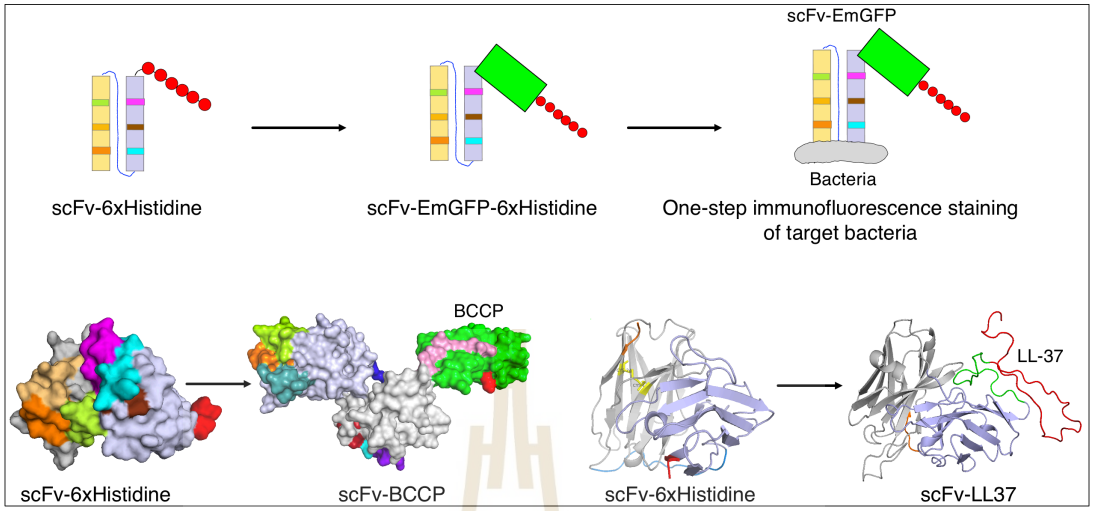


**Figure 5.18 Summary of chapter V.**

The summary of chapter V is illustrated in **Figure 5.18**. In this study, two biotinylated scFv forms, with and without 6xHistidine tag, are constructed. Biotin carboxyl carrier protein of *E. coli* is conjugated to scFv. When BCCP is attached with biotin at its lysine residue by biotin ligase of *E. coli*, our scFv gets biotinylated at the known site. Biotinylation of scFv is confirmed by means of biotin-streptavidin ELISA. Next, scFv is tagged with Emerald GFP and their usefulness in bioimaging of bacteria has been tested. The scFv-EmGFP constructs can be used as a one-step detection agent for immunofluorescence staining of target bacteria. Thirdly, scFv are attached to human anti-microbial peptide (LL-37). It is still an ongoing process, and the empty vector (GST-LL37) construction has been finished. After subcloning of yPac1A8 scFv and yPgi3G4 scFv sequences into the vector, the effect of LL-37 and scFv-LL37 on target bacteria will be studied and the preliminary studies will use scFv-LL37 expressed in *E. coli* system.

# CHAPTER VI

# FROM SINGLE CHAIN FRAGMENT VARIABLE (SCFV) TO FULL-LENGTH IMMUNOGLOBULIN G (IGG)

## 6.1 Abstract

A recombinant scFv antibody fragment is a single protein which contains antigen binding domains joined covalently by a peptide linker. One full-length IgG molecule is a tetramer and is five times larger than scFv. ScFv mainly conveys the target binding function, whereas full-length antibody like IgG has antigen binding function via its variable fragment (Fab) and also has to mediate downstream effector functions via its constant fragment (Fc). Fc part of IgG interacts with Fc-receptors on cells of the immune system and initiates antibody-dependent cellular phagocytosis and antibody-dependent cell-mediated cytotoxicity. Moreover, Fc fragment of IgG activates the complement system which is an important innate defence mechanism against infections. To broaden the horizon of their applicability, yPac1A8 and yPgi3G4 scFv are converted into full-length IgG by using the IgG expression platform of MY LAB. The binding activity of IgG constructs to their corresponding target bacteria is confirmed by slide agglutination test. Activation of complement system by yPgi3G4 IgG and subsequent complement-mediated killing of its target, *P. aeruginosa,* is tested. Activation of human macrophage cells by yPac1A8 and yPgi3G4 IgG for antibody-dependent cellular phagocytosis of target bacteria is tested.

The preliminary results of this study strongly suggested that yPac1A8 and yPgi3G4 IgG have potential to become antibody therapeutics in the future.

## 6.2 Introduction

Single chain fragment variable (scFv) is a monomer which contains antigen binding domains ($V_H$ and $V_L$) of lgG, covalently linked by a flexible peptide linker. One scFv fragment is 5 nm in diameter and about 30 kDa (Vallet-Courbin et al., 2017). One IgG molecule is a tetramer, having two heavy chains and two light chains. It is 20-40 nm in diameter and 2 nm in height. It has a molecular weight of approximately 150 kDa (Chen et al., 2004; Murphy, 2012; Saber et al., 2011).

Full-length antibodies have two structural regions: a variable fragment (Fab) and a constant fragment (Fc). Fab mediates antigen binding property of antibody and Fc mediates downstream effector functions by interacting with Fc-receptors on immune cells, such as, macrophages, monocytes, dendritic cells, neutrophils, eosinophils, basophils, natural killer cells and B lymphocytes. Some of the human IgG receptors, (hFcγRI, hFcγRIIA, hFcγRIIC, and hFcγRIIIA), function as activating receptors. Some, such as hFcγRIIB, are inhibitors. Some receptors, such as hFcRn, are responsible for recycling and transport of IgG. In addition, Fc fragment of IgG can bind with C1q protein of the complement system which is an essential non-specific defence mechanism in our body (Bournazos, Gupta, & Ravetch, 2020; Bruhns, 2012; Erp, Luytjes, Ferwerda, & van Kasteren, 2019).

The affinity and binding specificity of the Fc domain of IgG for different FcγR receptors not only depend on the differences in the primary amino acid sequence of the IgG subclasses but also on the structure and composition of the Fc-associated glycan

structures (Bournazos et al., 2020). In human, there are four IgG subclasses, namely, IgG1, IgG2, IgG3 and IgG4. In human serum, IgG1 is the most abundant antibody, followed by IgG2, IgG3, and IgG4 subclasses. IgG1 and IgG3 are strong inducers of antibody-dependent cellular cytotoxicity (ADCC), complement dependent cytotoxicity (CDC), and antibody-dependent cellular phagocytosis (ADCP) (Erp et al., 2019; Taeye, Rispens, & Vidarsson, 2019).

In this study, Single Chain Fragment Variable (scFv) recombinant antibodies, yPac1A8 and yPgi3G4, targeting *P. acnes* and *P. aeruginosa*, respectively, are engineered to become full-length IgG1 subclass in order to study their complement dependent cytotoxicity (CDC) and antibody-dependent cellular phagocytosis (ADCP) properties. Chapter VI is the paradigm of engineering scFv antibody fragments to full-length IgG and application of IgG constructs for therapeutic purposes.

## 6.3 Materials and methods

### 6.3.1 Generation of IgG heavy chain and light chain plasmids

#### 6.3.1.1 Preparation of VH and VL DNA sequences

To prepare VH (variable region of IgG heavy chain) and VL (variable region of IgG light chain) DNA sequences of yPac1A8 and yPgi3G4 recombinant antibodies by polymerase chain reaction (PCR), the scFv sequence carrying vectors (pMOD1.1-yPac1A8 and pMOD1.1-yPgi3G4) were used as templates. The following primers (**Table 6.1**) were designed so that VH PCR products had NheI cutting sites at their 5’ and 3’ ends both, and VL PCR products had NheI cutting site at their 5’ ends and BsiWI cutting site at 3’ ends.

PCR components were prepared according to **Table 6.2** and PCR cycles were performed according to **Table 6.3** by using T-100 Thermal cycler (Bio-Rad#186-1096, U.S.A). PCR products were purified with Wizard SV Gel and PCR Clean-Up System (Promega#A9282, U.S.A).

**Table 6.1 Primers for VH, VL insert PCR**

| Primer name | Sequences | Length and Tm |
|---|---|---|
| 1A8 VH FW | 5′-CTGTGCGCTAGCCAGGTACAGCTGCAGCAGTCAGGT-3′ | 36-mer, Tm 66°C |
| 1A8 VH RV | 5′-GCACAGGCTAGCTGAAGAGACGGTGACCATTGTCCC-3′ | 36-mer, Tm 63°C |
| 1A8 VL FW | 5′-CTGTGCGCTAGCCAGTCTGCCCTGACTCAGCCTGCC-3′ | 36-mer, Tm 68°C |
| 1A8 VL RV | 5′-GCACAGCGTACGACGTAGGACGGTGACCTTGGT-3′ | 33-mer, Tm 63°C |
| 3G4 VH FW | 5′-CTGTGCGCTAGCGAGGTGCAGCTGGTGGAGTC-3′ | 32-mer, Tm 68°C |
| 3G4 VH RV | 5′-GCACAGGCTAGCTGAGGAGACGGTGACCAGGG-3′ | 32-mer, Tm 68°C |
| 3G4 VL FW | 5′-CTGTGCGCTAGCCAGTCTGCCCTGACTCAG-3′ | 30-mer, Tm 59°C |
| 3G4 VL RV | 5′-GCACAGCGTACGTAGGACGGTCAGCTTGG-3′ | 29-mer, Tm 61°C |

**Table 6.2 VH, VL insert PCR components**

| Reaction components | Volume added per reaction | Concentration per reaction |
|---|---|---|
| 10x Pfx amplification buffer | 5 µL | 1x |
| Ultrapure deionized water | X µL | |
| 10x PCR enhancer solution | 2.5 µL | 0.5x |
| 10 mM dNTP mixture | 1.5 µL | 0.3 mM each |
| 50 mM $MgSO_4$ | 1 µL | 1 mM |
| Forward Primer (10 µM) | 1.5 µL | 0.3 µM |
| Reverse Primer (10 µM) | 1.5 µL | 0.3 µM |
| Template | 200 ng | |
| Platinum Pfx DNA polymerase (Invitrogen#11708-013, U.S.A) | 1 µL | 2.5 units |
| Total reaction volume | 50 µL/reaction | |

**Table 6.3 VH, VL insert PCR cycles**

| PCR steps | Temperature | duration |
|---|---|---|
| Denaturation | 94°C | 2 min |
| Denaturation | 94°C | 15 sec |
| Annealing | 60-61°C | 30 sec 34 cycles repeat |
| Extension | 68°C | 1 min |

#### 6.3.1.2 Restriction enzyme digestion of IgG heavy chain and IgG light chain vectors, and VH, VL inserts

The IgG heavy chain vector (HC pTT28) of this study was derived from KR-CH-yAFB1.c3, which was constructed by Kuntalee Rangnoi (former PhD student of MY LAB) (Kuntalee, 2016). The IgG light chain vector (LC pTT28) was derived from TS-152VL-lamda2MY of Thitima Sumphanapuy (PhD student of MY LAB). The PCR products of section 6.3.1.1 (1A8 VH, 1A8 VL, 3G4 VH and 3G4 VL) were used as VH and VL inserts.

NheI restriction digestion reaction of HC pTT28 vector and VH inserts was set up according to **Table 6.4** and was performed at 37°C overnight. It was followed by NheI inactivation at 65°C for 20 min. Then, 5 units of CIP (alkaline phosphatase, calf intestinal) (NEB# M0290S, U.S.A) was added and incubated at 37°C for 30 min. The gel purification of restriction digestion products was performed by using ultrapure agarose (ThermoScientific#16500100, U.S.A) 1% gel at 100V for 75 min.

**Table 6.4 Restriction digestion reaction for HC pTT28 vector and VH inserts**

| Reaction components | Volume added per reaction | Concentration per reaction |
|---|---|---|
| 10x NEB buffer 2.1 | 5 µL | 1x |
| Ultrapure deionized water | X µL | |
| DNA (vector or insert) | 2 µg | |
| NheI (NEB#R0131S, U.S.A) | 1 µL | 10 units |
| Total reaction volume | 50 µL/reaction | |

Serial restriction digestion reaction of LC pTT28 vector and VL inserts by NheI and BsiWI was set up as shown in **Table 6.5**. NheI digestion was performed at 37°C for 3 h. Then, 1.0 µL of 2.5 M NaCl was added in order to increase the salt concentration of reaction mixture to 100 mM. After that, 10 units of BsiWI (NEB#R0553S, U.S.A) was added and digestion was performed at 55°C water bath for 3 h. Enzyme inactivation was done at 65°C for 20 min. After that, 5 units of CIP (NEB# M0290S, U.S.A) was added and incubated at 37°C for 30 min. The gel purification of restriction digestion products was performed as above.

**Table 6.5 Restriction digestion reaction for LC pTT28 vector and VL inserts**

| Reaction components | Volume added per reaction | Concentration per reaction |
|---|---|---|
| 10x NEB buffer 2.1 | 5 µL | 1x |
| Ultrapure deionized water | X µL | |
| DNA (vector or insert) | 2 µg | |
| NheI (NEB#R0131S, U.S.A) | 1 µL | 10 units |
| Total reaction volume | 50 µL/reaction | |

#### 6.3.1.3 Ligation of HC pTT28 vector and VH inserts, and LC pTT28 vector and VL inserts

Required mass of insert (g) = (desired insert/vector molar ratio) x mass of vector (g) x ratio of insert to vector lengths (NEBioCalculator version 1.12.0, NEB, U.S.A)

The above formula were used to calculate the required mass of inserts while vector : insert molar ratio was fixed at 1:3 and the mass of vector at 100 ng. Ligation reaction set up was shown in **Table 6.6**. Ligation reaction was performed at 16°C for 16 h and enzyme inactivation was done at 65°C for 10 min. Ligation reaction products were kept at 4°C until transformation was performed.

**Table 6.6 Ligation reaction for HC pTT28 vector and VH inserts, and LC pTT28 vector and VL inserts**

| Ligation reaction components | Volume added per reaction | Concentration per reaction |
|---|---|---|
| 10x ligase reaction buffer | 2 µL | 1x |
| Ultrapure deionized water | X µL | |
| vector DNA | X µL | 100 ng |
| insert DNA | X µL | X ng |
| T4 DNA ligase (NEB#M0202S, U.S.A) | 1 µL | 400 units |
| Total reaction volume | 20 µL/reaction | |

#### 6.3.1.4 Transformation of IgG constructs

About 5 µL of each ligation product was mixed gently with 50 µL of chemically competent Top 10 *E. coli* and kept on ice for 30 min. It was exposed to 42°C for 30 sec and kept back on ice for 2 min. After that, 950 µL of SOC (Super Optimal broth with Catabolites repression) medium (pH 7.0, 0.5% (w/v) yeast extract,

2% (w/v) tryptone, 10 mM NaCl, 2.5 mM KCl, 20 mM $MgSO_4$, 20 mM glucose and 10 mM $MgCl_2$) was added and incubated at 37°C, 250 rpm for 1 h. Transformed *E. coli* were collected by centrifuging at 2000*g* for 5 min. They were spread onto LB agar plate containing 100 µg/mL ampicillin and incubated at 37°C overnight. Presence of *E. coli* colonies was checked on the next day.

#### 6.3.1.5 Confirmation of presence of inserts in IgG constructs

On next day of transformation, *E. coli* colonies were picked up as shown in **Table 6.7** and overnight broth cultures in LB medium containing 100 µg/mL ampicillin were prepared. From those cultures, IgG constructs/plasmids were prepared by using QIAprep Spin Miniprep Kit (Qiagen# 27106, Germany). Presence of VH inserts in IgG heavy chain constructs (HC pTT28 + 1A8VH construct and HC pTT28 + 3G4VH construct) was checked by NheI digestion. Presence of VL inserts in IgG light chain constructs (LC pTT28 + 1A8VL construct and LC pTT28 + 3G4VL construct) was checked by NheI and BsiWI digestion. Restriction digestion was performed as described in section 6.3.1.2 except that 250-300 ng of plasmid DNA was used to digest.

**Table 6.7 IgG constructs DNA sequence check**

| IgG constructs | no. of colony picked for cut and check | no. of clone sent for sequencing |
|---|---|---|
| HC pTT28 + 1A8VH construct | 6 colonies | 6 clones |
| LC pTT28 + 1A8VL construct | 3 colonies | 2 clones |
| HC pTT28 + 3G4VH construct | 6 colonies | 6 clones |
| LC pTT28 + 3G4VL construct | 3 colonies | 2 clones |

#### 6.3.1.6 DNA sequence checking of IgG constructs

As shown in **Table 6.7**, 6 clones of yPac1A8 IgG heavy chain, 2 clones of yPac1A8 IgG light chain, 6 clones of yPgi3G4 IgG heavy chain and 2 clones of yPgi3G4 IgG light chain were sent for DNA sequencing at 1st BASE sequencing service, Malaysia. The pTT28 FW 157 primer (5'-CACAGGTGTCCACTCCCAGGT-3', 21-mer, Tm 62°C) was used for sequencing. The integrity of IgG constructs was checked by using Vector NTI software (ThermoScientific, U.S.A).

### 6.3.2 Recombinant full-length IgG expression system

#### 6.3.2.1 Preparation of recombinant IgG plasmids for expression

Plasmids for IgG expression were prepared by using PureLink HiPure Plasmid Midiprep Kit (Invitrogen# K210005, U.S.A) and were filter-sterilized by using 0.2 µm pore size Johnson Polyethersulfone syringe filters (Johnson#SFP25P020S, UK).

#### 6.3.2.2 Recombinant IgG expression in 2 mL transfection volume

Recombinant IgG were expressed in suspension-adapted Human Embryonic Kidney (HEK) cells of Expi293F Expression System (Gibco#A14635, U.S.A). As for the first trial, 2 mL cultures were performed in 6-well non-treated cell culture plate (NEST# 703001, China). New Brunswick $CO_2$ incubator (shaker orbit 2.5 cm) (Eppendorf#S41I230011, Germany) was used. Two different heavy chain (HC)/light chain (LC) plasmid ratios, 1:2 and 1:3 were tested. The expression procedure was carried out according to the Expi293F Expression System user guideline.

Briefly, HEK Expi 293F cells (passage 5 vial) were thawed and subcultured in Expi 293 expression medium (Gibco# A1435101, U.S.A) at 37°C, 150 rpm, 8% $CO_2$. It was passage 10 ($3.9 \times 10^6$ viable cells/mL and 95.79% viability) when transient transfection with IgG plasmids was performed. ExpiFectamine 293 reagent was diluted in Opti-MEM 1 medium. HC (heavy chain) and LC (light chain) plasmid DNA were mixed in Opti-MEM 1 medium. Complexation of ExpiFectamine 293 reagent and plasmid DNA was performed gently at room temperature. Obtained lipid/DNA complexes were incubated for 10-20 min and added slowly to the cells while the culture plate was swirled gently (transfection day 0).

At 18 h after transfection (transfection day 1), ExpiFectamine 293 transfection enhancer-1 and enhancer-2 were added to the transfected cells slowly while the culture plate was swirled gently. The culture was continued at 37°C, 150 rpm, 8% $CO_2$. On transfection day 5, cell culture supernatant was collected by centrifuging at 3000 *g* for 30 min at 4°C. The crude supernatant containing expressed recombinant IgG was kept at 4°C. The detain description of IgG expression system components were shown in **Table 6.8**.

**Table 6.8 IgG expression system (2 mL transfection volume)**

| **IgG expression components** | **amount per well** |
|---|---|
| HEK Expi 293F cells | 2 mL ($2.5 \times 10^6$ cells/mL) |
| HC and LC Plasmid DNA mixture | 2 μg containing (HC/LC ratio of 1:2 or 1:3) in 100 μL Opti-MEM 1 medium |
| ExpiFectamine 293 reagent | 5.4 μL diluted in 100 μL Opti-MEM 1 medium |
| ExpiFectamine 293 transfection enhancer-1 | 10 μL |
| ExpiFectamine 293 transfection enhancer-2 | 100 μL |
| Final culture volume | about 2.3 mL |

#### 6.3.2.3 Recombinant IgG expression in 30 mL transfection volume

Plasmids for recombinant IgG (yPac1A8 IgG and yPgi3G4 IgG) expression were prepared and filter-sterilized in the same way as above. Recombinant IgG (yPac1A8 IgG and yPgi3G4 IgG) were expressed in suspension-adapted HEK cells of Expi293F Expression System (Gibco#A14635, U.S.A) as above. This time, the transfection volume was scaled up to 30 mL by using 125 mL Erlenmeyer cell culture flask with Vent Cap (Corning Life Sciences#CLS431143, U.S.A). Heavy chain (HC)/light chain (LC) plasmid ratio of 1:2 was used.

**Table 6.9 IgG expression system (30 mL transfection volume)**

| IgG expression components | amount per flask |
|---|---|
| HEK Expi 293F cells | 25.5 mL ($3x10^6$ cells/mL) |
| HC and LC Plasmid DNA mixture | 30 µg containing (HC/LC ratio of 1:2) in 100 µL Opti-MEM 1 medium |
| ExpiFectamine 293 reagent | 80 µL diluted in 1.5 mL Opti-MEM 1 medium |
| ExpiFectamine 293 transfection enhancer-1 | 150 µL |
| ExpiFectamine 293 transfection enhancer-2 | 1.5 mL |
| Final culture volume | about 30 mL |

HEK Expi 293F cells (passage 6 vial) was thawed in Expi 293 expression medium (Gibco# A1435101, U.S.A) and incubated at 37°C, 125 rpm, 8% $CO_2$ in New Brunswick $CO_2$ incubator (shaker orbit 2.5 cm) (Eppendorf#S41I230011, Germany). Transient transfection with yPac1A8 IgG and yPgi3G4 IgG plasmids was performed on passage 11 cells ($4.2x10^6$ viable cells/mL and 95.3% viability). Like previous 2 mL expression, ExpiFectamine 293 transfection enhancer-1 and enhancer-2 were added to the cells at 18 h after transfection (transfection day 1) and the culture

was continued at 37°C, 125 rpm, 8% $CO_2$. The number of cells, amount of plasmid DNA, ExpiFectamine 293 reagent, enhancer-1 and enhancer-2 added per flask were shown in **Table 6.9** above. At transfection day 6, cell culture supernatant was collected by centrifuging at 3000 *g* for 30 min at 4°C.

### 6.3.3 Quantitation of IgG in crude supernatant by using ForteBio Octet K2 Platform

Purified yPgi3G4 IgG (2.4 mg/mL) was used as a standard to generate a standard curve. Altogether, eight serial dilution samples of standard in PBS-Expi 293 expression medium (two-parts PBS + one-part medium mixture) containing yPgi3G4 IgG at final concentration of 100, 50, 25, 12.5, 6.25, 3.13, 1.56 and 0.78 µg/mL were prepared. PBS-Expi 293 expression medium (two-parts PBS + one-part medium mixture) alone was used as blank sample. One-part of test samples (crude supernatant containing yPac1A8 IgG or yPgi3G4 IgG) were diluted with two-parts of PBS. Concentration of IgG in blank, standard and test samples were quantified by ForteBio Octet K2 2-channel system (ForteBio, U.S.A) by using Protein A Dip and Read Biosensors (ForteBio#18-5012, U.S.A). Two replicas were measured, and the results were averaged.

### 6.3.4 Recombinant IgG purification

#### 6.3.4.1 yPac1A8 IgG purification

The materials used for yPac1A8 IgG purification were described in **Table 6.10**. Recombinant yPac1A8 IgG, transiently expressed in Expi293F Expression System by using HC:LC plasmid ratio of 1:2, was purified with Protein A

HP antibody purification column. About 25 mL of IgG containing crude supernatant was diluted with 75 mL of IgG binding buffer (dilution ratio of 1:3) for purification. The gradient purification method template in ÄKTA start protein purification system was used (GE-Healthcare-Life-Sciences, 2013) and the flow rate during sample feed, washing and elution steps was checked to be 0.5 mL/min. The elute was collected as 1 ml fractions.

The elute tubes representing the peak area were neutralized with IgG neutralization buffer (100 mL per 1 mL elute). Desalting and buffer exchange of the elute was performed by dialyzing overnight in SnakeSkin Dialysis Tubing against cold PBS buffer at 4°C. The purified yPac1A8 IgG was filter-sterilized and stored at 4ºC. The purity of yPac1A8 IgG elute was checked by SDS-PAGE and purified IgG concentration was measured by using Pierce BCA Protein assay kit.

**Table 6.10 Materials used for yPac1A8 IgG purification**

| **Materials used for yPac1A8 IgG purification** | **Specifications** |
|---|---|
| IgG purification column | HiTrap Protein A HP antibody purification column 1 mL (Cytiva#29048576, U.S.A) |
| Chromatography system | ÄKTA start protein purification system (Cytiva#29022094-ECOMINS, U.S.A) |
| IgG binding buffer | 20 mM sodium phosphate (pH 7.0) |
| IgG elution buffer | 0.1 M citric acid (pH 3.0) |
| IgG neutralization buffer | 1.0 M Tris-HCl (pH 9.0) |
| IgG buffer exchange system | SnakeSkin Dialysis Tubing with 10KDa MWCO (ThermoScientific#68100, U.S.A),<br>1xPBS |
| IgG filter-sterilization | 0.2 µm Minisart Cellulose Acetate syringe Filter (Sartorius#16534-GUK, Germany) |
| SDS-PAGE system | Handmade (5%-12.5%) SDS gel,<br>2xSDS sample buffer,<br>Precision Plus All Blue Prestained Protein Standards (BioRad#1610373, U.S.A) |
| Protein concentration measurement kit | Pierce BCA Protein assay kit (ThermoScientific#23225, U.S.A) |

#### 6.3.4.2 yPgi3G4 IgG purification

The materials used for yPgi3G4 IgG purification were described in **Table 6.11**. Recombinant yPgi3G4 IgG, transiently expressed in Expi293F Expression System by using HC:LC plasmid ratio of 1:2, was purified with HiTrap MabSelect PrismA column. About 25 mL of IgG containing crude supernatant was diluted with 75 mL of IgG binding buffer (dilution ratio of 1:3) for purification. The same purification, neutralization, dialysis, and filter-sterilization steps as yPac1A8 IgG purification were applied here except that the HiTrap MabSelect PrismA column was cleaned with 0.5 M NaOH after use. The purity of yPgi3G4 IgG elute was checked by SDS-PAGE and purified IgG concentration was measured by using Pierce BCA Protein assay kit.

**Table 6.11 Materials used for yPgi3G4 IgG purification**

| **Materials used for yPgi3G4 IgG purification** | **Specifications** |
|---|---|
| IgG purification column | HiTrap MabSelect PrismA 1 mL column Lot: 10276396, Exp 2021-12, (Cytiva#17549851, U.S.A), |
| Column cleaning reagent | 0.5 M NaOH |
| Chromatography system | ÄKTA start protein purification system (Cytiva#29022094-ECOMINS, U.S.A) |
| IgG binding buffer | 20 mM sodium phosphate (pH 7.0) |
| IgG elution buffer | 0.1 M citric acid (pH 3.0) |
| IgG neutralization buffer | 1.0 M Tris-HCl (pH 9.0) |
| IgG buffer exchange system | SnakeSkin Dialysis Tubing with 10KDa MWCO (ThermoScientific#68100, U.S.A), 1xPBS |
| IgG filter-sterilization | 0.2 µm Minisart Cellulose Acetate syringe Filter (Sartorius#16534-GUK, Germany) |
| SDS-PAGE system | Handmade (5%-12.5%) SDS gel, 2xSDS sample buffer, Precision Plus All Blue Prestained Protein Standards (BioRad#1610373, U.S.A) |
| Protein concentration measurement kit | Pierce BCA Protein assay kit (ThermoScientific#23225, U.S.A) |

### 6.3.5 Crude supernatant IgG ELISA

To test the functionality of recombinant IgG in culture supernatant, bacteria whole cell ELISA using the heat-inactivated (60°C for 45min at 130 rpm in water bath) bacteria ($10^9$ cells/mL) as target was performed. The counterpart scFv formats of IgG were used as positive control. Namely, yPac1A8 scFv (20 µg/mL) served as control for yPac1A8 IgG and yPgi3G4 scFv (20 µg/mL) served as control for yPgi3G4 IgG. Non-transfected HEK Expi 293F cells culture supernatant was used as negative control.

The detail ELISA procedure was the same as scFv ELISA which was described in Chapter III. About 100 µL of IgG containing or negative control HEK cell culture supernatant was added per well. HisProbe-HRP (ThermoScientific#15165, U.S.A) diluted at 1:5000 in PBS was used as secondary detection agent for scFv and $F(ab')_2$ fragment goat anti-human IgG (H+L)-HRP (Jackson ImmunoResearch Inc.#109-036-088, U.S.A) diluted at 1:5000 in PBS was used as secondary detection agent for IgG. ABTS substrate (Amresco#0400-10G, U.S.A) in citric acid-$H_2O_2$ buffer (0.05%$H_2O_2$ in 50 mM citric acid pH 4.0) was used as indicator system. The absorbance was measured at $OD_{405nm}$ with Tecan's Sunrise absorbance microplate reader (Tecan, Switzerland).

### 6.3.6 Slide agglutination test using crude supernatant IgG

To test the functionality of recombinant IgG further, agglutination of live bacteria by specific IgG was tested. For yPac1A8 IgG, 15 mL of *P. acnes* (DMST 14916) 72 h-culture in BHI broth was centrifuged at 5000 *g* for 15min at 4°C. *P. acnes* cells were resuspended in 1 mL of PBS and 10 µL of that *P. acnes* suspension was

dropped onto a clean glass slide. About 20 μL of yPac1A8 IgG containing crude supernatant was added to *P. acnes* drop and it was mixed gently by using sterilized wooden toothpick. Within 2 min time, agglutination or clumping of *P. acnes* cells was checked by naked eyes. Crude supernatant containing yPgi3G4 IgG and MY LAB Adalimumab IgG were used as isotype control. Similarly, for yPgi3G4 IgG, 15 mL of *P. aeruginosa* (DMST 37186) overnight-culture in LB broth was centrifuged and cells were resuspended in 1 mL of PBS. Slide agglutination test was carried out in the same way as above and crude supernatant containing yPac1A8 IgG and MY LAB Adalimumab IgG were used as isotype control.

**6.3.7 Slide agglutination test using purified IgG**

Agglutination of live bacteria by specific IgG was tested again by using purified yPac1A8 IgG and yPgi3G4 IgG. *P. acnes* (DMST 14916) and *P. aeruginosa* (DMST 37186) bacterial suspensions preparation and the assay procedure remained the same as section 6.3.6. Purified IgG 7 μg was used to agglutinate the target bacteria.

**6.3.8 Complement-mediated bacteriolysis of *P. aeruginosa* enhanced by yPgi3G4 IgG**

**6.3.8.1 Preparation of *P. aeruginosa* specific antibodies-depleted, diluted, and pooled human serum**

About 20 mL of blood from three healthy volunteers of MY LAB (Professor Montarop Yamabhai, Thitima Sumphanapuy and myself) were withdrawn by me. The blood was kept on ice until it clotted (about 3-4 h). Serum was collected by centrifuging the tube at 1200 *g* for 20 min at 4°C and it was stored as small

aliquots at -80°C. On preparation day, serum was thawed on ice and equal volume of serum from all three donors were pooled into one eppendorf tube. Each 100 µL of pooled serum was then mixed with 900 µL of PBS (1:10 diluted pooled serum in PBS).

Overnight LB broth culture of *P. aeruginosa* DMST 37186 (1.9 x $10^9$ cfu/mL) was distributed into eppendorf tubes (1 mL/tube) and spinned for 5 min at 4°C. Cells were resuspended in PBS 1 mL and spinned again for 5 min at 4°C. Then, the cells were resuspended in 1 mL of diluted pooled serum (1:10 in PBS) from above and rotated at 9-10 rpm for 90 min at 4°C. After that, the supernatant was collected by centrifuging at 10000 *g* x 5 min and filter-sterilized by 0.2 µm Minisart Cellulose Acetate syringe Filter (Sartorius#16534-GUK, Germany). Finally, filter-sterilized, *P. aeruginosa* specific antibodies-depleted, diluted (1:10 in PBS), and pooled human serum was obtained and was kept in 100 µL aliquots at -80°C. This serum was used as the source of complement system proteins.

**6.3.8.2 Preparation of *P. aeruginosa* seed cultures**

*P. aeruginosa* DMST 37186 from LB agar plate was inoculated into 5 mL LB broth and incubated at 37°C, 220 rpm for 17 h. About 1 mL of that overnight culture was spinned for 2 min at 4°C. Cells were resuspended in PBS 1 mL and spinned again for 2 min at 4°C. Then, the cells were resuspended in PBS 1 mL and 100 µL of it was diluted in 900 µL of PBS (1:10 dilution). About 10 µL of these diluted *P. aeruginosa* cells were used as input bacteria (inoculum) in complement-mediated bacteriolysis assay.

#### 6.3.8.3 Preparation of recombinant IgG antibodies

Recombinant IgG, yPac1A8 (0.7 mg/mL) and yPgi3G4 (2.4 mg/mL), which were expressed in MY LAB and Adalimumab/Humira (1 mg/mL) (AbbVie, U.S.A) were used. *P. aeruginosa* specific yPgi3G4 IgG is the one under testing and the remaining two served as isotype control. Working stocks (60 µg/mL in PBS) of all three IgG were prepared so that the final concentration of IgG in the assay would be 24 µg/mL.

#### 6.3.8.4 Complement-mediated bacteriolysis reaction set up

The four eppendorf tubes for one set of assay were labeled as described in **Table 6.12.** *P. aeruginosa* seed culture, IgG preparation or PBS, and serum were added according to the serial number in the table and the reaction tubes were incubated at 37°C, 400 rpm for 3 h in Eppendorf Thermomixer comfort (Eppendorf#5355, Germany). The final concentration of reaction components in the assay were shown in **Table 6.13**.

**Table 6.12 Complement-mediated bacteriolysis assay set up**

| No. | no IgG or no mAb tube | Adalimumab IgG tube | 3G4 IgG tube | 1A8 IgG tube |
|---|---|---|---|---|
| 1. | 10 µL of seed culture | 10 µL of seed culture | 10 µL of seed culture | 10 µL of seed culture |
| 2. | 40 µL of PBS | 40 µL of PBS-Adalimumab IgG | 40 µL of PBS-3G4 IgG | 40 µL of PBS-1A8 IgG |
| 3. | 50 µL of depleted, diluted, and pooled serum | 50 µL of depleted, diluted, and pooled serum | 50 µL of depleted, diluted, and pooled serum | 50 µL of depleted, diluted, and pooled serum |

**Table 6.13 Final concentration of reaction components in one reaction tube**

| No. | Reaction component | Volume added per tube | Final concentration |
|---|---|---|---|
| 1. | *P. aeruginosa* seed culture | 10 µL (approx. $10^7$ cfu/mL) | approx. $10^6$ cfu/mL |
| 2. | Adalimumab IgG or yPgi3G4 IgG or yPac1A8 IgG | 40 µL (60 µg/mL) | 24 µg/mL |
| 3. | depleted, diluted, and pooled serum | 50 µL (1:10 diluted serum) | 1:20 diluted serum |
| Total reaction volume | | | 100 µL per tube |

**6.3.8.5 Determination of number of colony forming units (viable count) in seed cultures**

Number of colony forming units (cfu/mL) in each seed culture were determined by Miles and Misra method (Miles et al., 1938). The procedure was depicted in **Figure 6.1** below. Briefly, serial dilutions of seed cultures were prepared in LB-T20 medium (LB broth containing 0.025% Tween-20) and triplicates of 10 µL drop of each dilution were placed on LB agar plate and incubated at 37°C overnight. Colonies were counted manually, and calculations were made to determine the viable count of seed cultures, from which the number of input bacteria (inoculum) added into the assay was calculated.

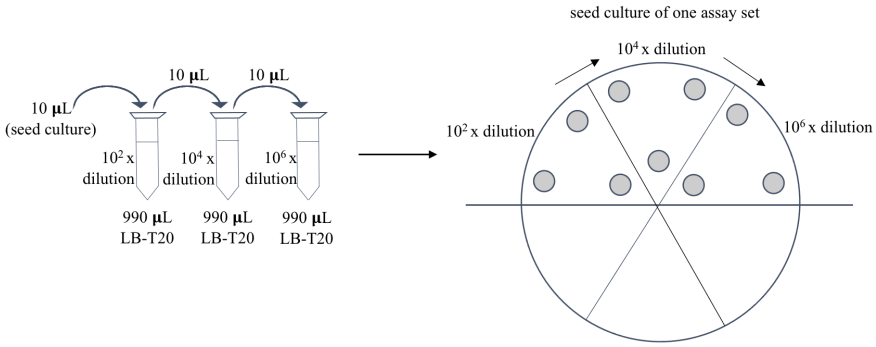


**Figure 6.1 Determination of viable count (cfu/mL) in *P. aeruginosa* seed cultures**

#### 6.3.8.6 Determination of number of colony forming units in reaction tubes

At the end of 3 h incubation of complement-mediated bacteriolysis assay, the number of colony forming units (viable count) in reaction tubes were determined according to the procedure shown in **Figure 6.2**. Two dilutions (10 x and $10^2$ x) in LB-T20 medium were prepared from each reaction tube. Triplicates of 10 µL drop of each dilution were placed on LB agar plate and incubated at 37°C overnight. Colonies were counted manually and calculations were made to determine the number of viable *P. aeruginosa* left in each reaction tube.

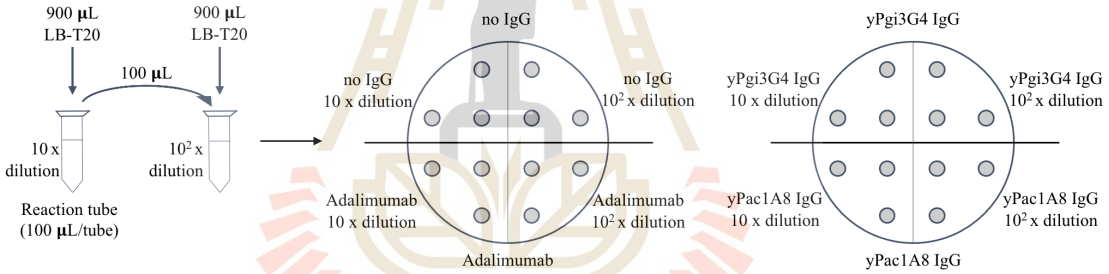


**Figure 6.2 Determination of viable count (cfu/mL) in reaction tubes**

### 6.3.9 Antibody-dependent cellular phagocytosis assay

#### 6.3.9.1 Heat-inactivation of *P. acnes* and *P. aeruginosa*

About 10 mL of overnight LB broth culture of *P. aeruginosa* DMST 37186 (2.1 x $10^9$ cfu/mL) was centrifuged at 5000 *g* for 15 min at 4°C. The cell pellet was washed with 1xPBS for two times and resuspended in equal volume of 1xPBS. The cells were heat-inactivated at 60°C for 45 min at 130 rpm in WNB series shaking water bath (Memmert#10573693, Germany). The cells were then cooled down, centrifuged at 5000 *g* for 10 min at 4°C, and resuspended in 2 mL of RPMI 1640

medium (see in section 6.3.9.2) so that the concentration of the cells was 1.05 x $10^{10}$ cells/mL. It was kept at 4°C. This heat-inactivated *P. aeruginosa* cells (1.05 x $10^{10}$ cells/mL) was used for THP-1 experiment.

About 10 mL of 72 h BHI broth culture of *P. acnes* DMST 14916 (1.09 x $10^9$ cfu/mL) was heat-inactivated in the same way as *P. aeruginosa* cells except that the cells were resuspended in 1 mL of RPMI 1640 medium at the final step so that the concentration of the cells was 1.09 x $10^{10}$ cells/mL. Both *P. acnes* and *P. aeruginosa* cells were diluted in RPMI 1640 medium to obtain $10^8$ cells/mL preparations just before the experiment was started.

**6.3.9.2 THP-1 cells treated with vitamin $D_3$**

THP-1 (Tohoku Hospital Pediatrics-1) cell line, originated from childhood acute monocytic leukemia cells of one-year old male patient, was purchased from CLS Cell Lines Service (CLS# 300356-1714SF, Germany). RPMI 1640 medium prepared from RPMI-1640 powder (ThermoScientific#31800022, U.S.A) supplemented with 10% FBS (fetel bovine serum), 2 mM L-glutamine, 1 mM sodium pyruvate, 100 units/mL penicillin-100 µg/mL streptomycin, and sodium bicarbonate buffer system (2.0 g/L) was used as THP-1 cells culture medium.

THP-1 cells (passage-28 having cell viability 98.4%) cultured in 75 mL filter cap flask (SPL Life Sciences#1SPL-70075, South Korea) were centrifuged at 100 *g* for 5 min. The cells were resuspended at a concentration of 1x$10^6$ viable cells/mL in fresh RPMI 1640 medium containing 0.24 µM Vitamin $D_3$ (Merck#679101-50UG, U.S.A). This THP-1 cell suspension was seeded (400 µL/well) into 24 well, non-treated, cell culture plate (Nest Biotech#702011, China).

Altogether, three 24 well plates were prepared and labelled as 30 min, 4 h and 24 h. For immunoflurescence staining of the cells, autoclaved No.1.0 cover glass of 12 mm diameter (HAD, China) were placed at the bottom of the wells before the cells were added. The culture plates were incubated at 37°C, 5% $CO_2$ in Forma Steri-Cycle i160 $CO_2$ incubator (ThermoScientific#51030303, U.S.A) for 72 h.

#### 6.3.9.3 yPac1A8 and yPgi3G4 IgG

Recombinant IgG, yPac1A8 (0.7 mg/mL) and yPgi3G4 (2.4 mg/mL), which were expressed and purified in MY LAB, were used. Both IgG were diluted in RPMI 1640 medium to obtain 20 µg/mL preparations just before the experiment was started.

#### 6.3.9.4 THP-1 cells challenged with bacteria

At the end of Vitamin $D_3$ treatment for 72 h, THP-1 cells were challenged with heat-inactivated *P. aeruginosa* or *P. acnes* cells with or without yPac1A8 IgG or yPgi3G4 IgG. The reaction set up was summerized in **Table 6.14** and **Table 6.15**. The final concentration of reaction components were shown in **Table 6.16**. Eppendorf tubes were labeled according to **Table 6.14** and **Table 6.15**. The components were mixed gently with pipette and the tubes were incubated at room temperature for 10 min during which the tubes were tapped gently by hand for one time. Then, the contents of the tubes were added into THP-1 cells in 24 well plate and mixed by moving the plate. The plates were incubated at 37°C, 5% $CO_2$. The final reaction volume in each well became 500 µL. The experiment plan for three reaction sets was depicted in **Figure 6.3.**

**Table 6.14 Antibody-dependent cellular phagocytosis (*P. acnes* experiment)**

| No. | no bacteria, no IgG | *P. acnes* only | *P. acnes* and yPac1A8 IgG | *P. acnes* and yPgi3G4 IgG |
|---|---|---|---|---|
| 1. | 100 µL of RPMI medium | 50 µL of RPMI medium | - | - |
| 2. | - | 50 µL of *P. acnes* in RPMI ($1.09 \times 10^8$ cells/mL) | 50 µL of *P. acnes* in RPMI ($1.09 \times 10^8$ cells/mL) | 50 µL of *P. acnes* in RPMI ($1.09 \times 10^8$ cells/mL) |
| 3. | - | - | 50 µL of yPac1A8 IgG in RPMI (20 µg/mL) | 50 µL of yPgi3G4 IgG in RPMI (20 µg/mL) |

**Table 6.15 Antibody-dependent cellular phagocytosis (*P. aeruginosa* experiment)**

| No. | no bacteria, no IgG | *P. aeruginosa* only | *P. aeruginosa* and yPac1A8 IgG | *P. aeruginosa* and yPgi3G4 IgG |
|---|---|---|---|---|
| 1. | 100 µL of RPMI medium | 50 µL of RPMI medium | - | - |
| 2. | - | 50 µL of *P. aeruginosa* in RPMI ($1.05 \times 10^8$ cells/mL) | 50 µL of *P. aeruginosa* in RPMI ($1.05 \times 10^8$ cells/mL) | 50 µL of *P. aeruginosa* in RPMI ($1.05 \times 10^8$ cells/mL) |
| 3. | - | - | 50 µL of yPac1A8 IgG in RPMI (20 µg/mL) | 50 µL of yPgi3G4 IgG in RPMI (20 µg/mL) |

มหาวิทยาลัยเทคโนโลยีสุรนารี

**Table 6.16 Final concentration of reaction components**

| No. | Reaction component | Final concentration |
|---|---|---|
| 1. | THP-1 cells | $1 \times 10^6$ cells/mL |
| 2. | Heat inactivated *P. acnes* | $1.09 \times 10^7$ cells/mL |
| 3. | Heat inactivated *P. aeruginosa* | $1.05 \times 10^7$ cells/mL |
| 4. | yPac1A8 IgG or yPgi3G4 IgG | 2 µg/mL |

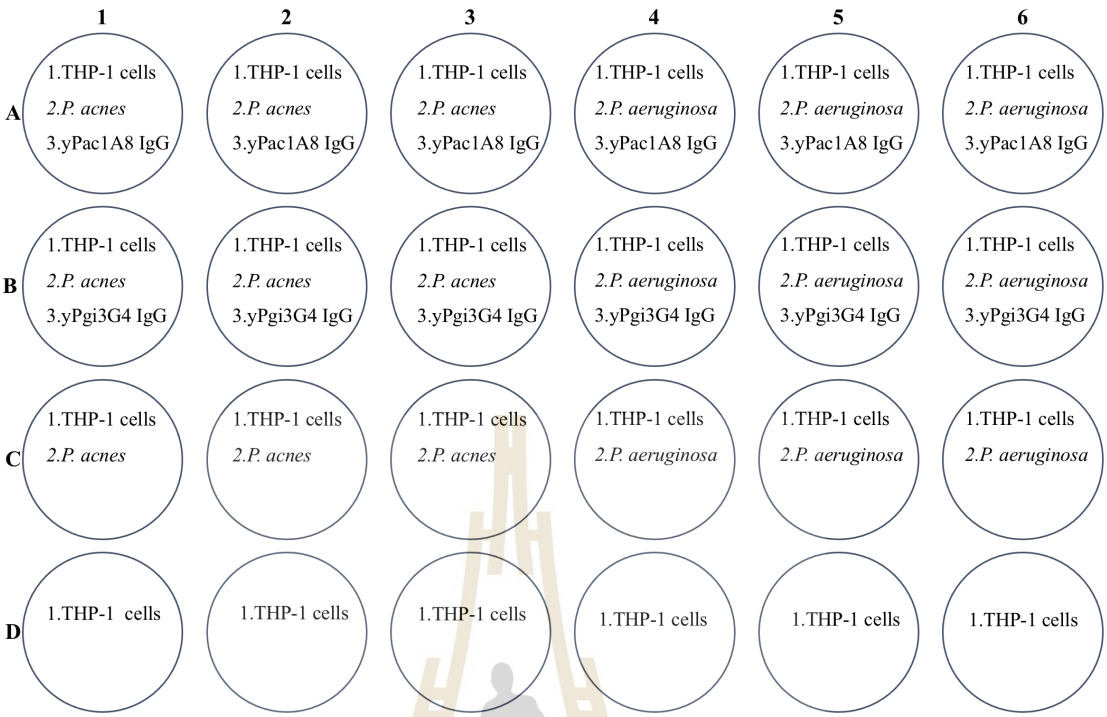


**Figure 6.3 Bird-eye view of experiment plan for 3 reaction sets**

#### 6.3.9.5 Duration of bacterial challenge and sample collection

The plate labelled as 30 min was taken out of the $CO_2$ incubator at 30 min after bacterial challenge was started. Likewise, the plates labelled 4 h and 24 h were taken out at 4 h and 24 h after the challenge, respectively. Pictures of cells were taken with Achro 20X LWD PH objective of EVOS XL Core imaging system (ThermoScientific#AMEX 1000, U.S.A). Then, 24 well plate was centrifuged at 560 *g* at 4°C with refrigerated centrifuge (Biosan#LMC-4200R, Latvia). The supernatants were collected and kept at -80°C for chemokine analysis. The cover glasses at the bottom of the wells underwent scFv immunofluorescence staining (see section 6.3.9.6).

#### 6.3.9.6 Immunofluorescence staining of THP-1 cells and bacteria

THP-1 cells, differentiated with vitamin $D_3$ and challenged with bacteria in the presence or absence of specific IgG, were stained as follows. The cells attached on cover glasses in 24 well plate were washed with 1xPBS for two times, fixed with 4%PFA (paraformaldehyde) in PBS (pH 7.4) for 30 min, and washed again with PBS for two times. The cells were permeabilized with 0.1% Triton X-100 (Calbiochem#9410, U.S.A) for 10 min and were washed with ice cold PBS for two times. The cell smear was blocked with 1%BSA-300 mM glycine-0.1% PBST for 30 min and washed with PBS for two times.

Then, *P. acnes* and *P. aeruginosa* inside or outside of THP-1 cells were incubated with yPac1A8 scFv (50 µg/mL) and yPgi3G4 scFv (50 µg/mL), respectively, at room temperature for 1 h. The smear was washed with PBS for two times and stained with 1:500 dilution of Dylight 488-labelled anti-hexa-histidine mouse monoclonal antibody (Abcam#ab117512, UK) in PBS for 1 h in a dark place. After that, the smear was washed with PBS for two times, counterstained with 50 µM DAPI (4′,6-diamidino-2-phenylindole) for 5 min and washed again with PBS for two times. The stained cover glasses were taken out of the 24 well plate and placed onto the clean glass slide in such a way that the stained cell smear faced the slow fade gold mountant (Invitrogen#S36936, U.S.A) drop on the glass slide. The stained smears were fixed and examined with Apo TIRF 60x Oil DIC N2 objective of Nikon A1R confocal laser microscope.

### 6.3.10 Interleukin-8 (IL-8) ELISA

The presence of IL-8 in culture supernatant of THP-1 cells, differentiated with vitamin $D_3$ and challenged with bacteria in the presence or absence of specific IgG, was checked by human IL-8 ELISA (Abcam#ab48481, UK). The reagents described in **Table 6.17** were prepared.

**Table 6.17 Reagents for IL-8 ELISA**

| **Reagents prepared** | **composition of reagents** |
|---|---|
| Reconstitution buffer | 1x PBS + 0.09% azide |
| Coating buffer | 1x PBS (pH 7.2-7.4) |
| Wash buffer | 1x PBS + 0.05% Tween-20 |
| Blocking buffer | 1x PBS + 5% BSA |
| Standard and secondary antibody dilution buffer | 1x PBS + 1% BSA |
| HRP diluent buffer | 1x PBS + 1% BSA + 0.1% Tween-20 |
| Stop reagent | 1 M sulfuric Acid |

The ELISA procedure was according to the protocol provided by the manufacturer (Abcam, 2019). Briefly, IL-8 capture antibody in coating buffer was immobilized in Maxisorp 96-well plate (ThermoScientific#44-2404-21, U.S.A) at 37°C overnight. The wells were washed with washing buffer for 2 times, blocked with blocking buffer for 2 h and washed for 3 times. About 100 µL/well of supernatant sample, thawed from -80°C, was added and secondly, detection antibody in antibody dilution buffer was added. The plate was incubated for 1 h. The wells were washed for 2 times, streptavidin-HRP (horseradish peroxidase) in HRP diluent buffer was added, and incubated for 30 min. The wells were washed for 2 times and TMB (3,3',5,5'-tetramethylbenzidine) substrate provided in the kit was added and incubated in a dark place for 10 min. Finally, the stop reagent was added and the absorbance value at 450 nm wavelength was measured with Sunrise microplate reader (Tecan, Switzerland).

## 6.4 Results and discussion

### 6.4.1 Generation of IgG heavy chain and light chain plasmids

#### 6.4.1.1 Preparation of VH and VL DNA sequences

By using scFv sequence carrying vectors of biopanning, (pMOD1.1-yPac1A8 and pMOD1.1-yPgi3G4) as templates for PCR, VH (variable region of IgG heavy chain) and VL (variable region of IgG light chain) DNA sequences of yPac1A8 and yPgi3G4 recombinant antibodies were amplified. Detail description of PCR products is made in **Table 6.18** and PCR products can be seen in **Figure 6.4**.

**Table 6.18 VH, VL PCR products**

| Lane no. in Figure 6.4 | PCR products | expected length (base pair) | DNA concentration after PCR clean up | 260/280 | 260/230 |
|---|---|---|---|---|---|
| Lane 2 | 1A8 VH | 387 bp | 134.1 ng/µL | 1.89 | 2.10 |
| Lane 3 | 1A8 VL | 360 bp | 122.4 ng/µL | 1.88 | 2.00 |
| Lane 4 | 3G4 VH | 378 bp | 83.9 ng/µL | 1.87 | 1.85 |
| Lane 5 | 3G4 VL | 354 bp | 106.0 ng/µL | 1.90 | 1.82 |

มหาวิทยาลัยเทคโนโลยีสุรนารี

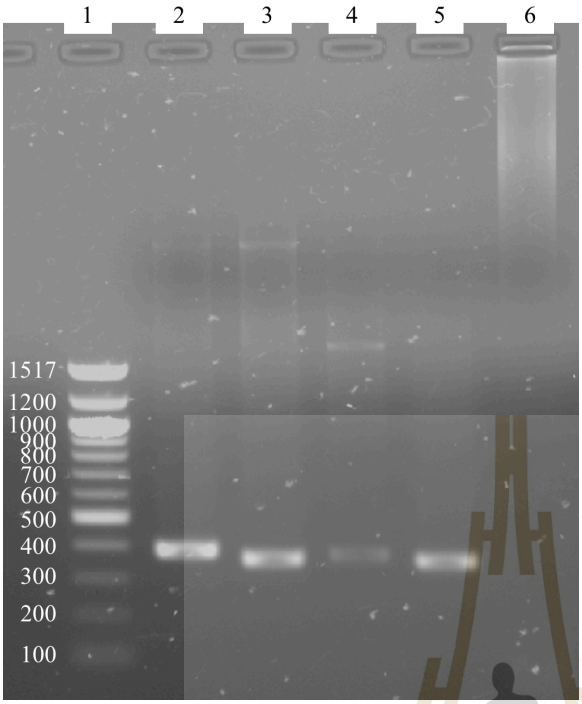


**Figure 6.4** **VH and VL PCR products.**

Lane 1 is 100 bp DNA ladder (NEB#N3231L, U.S.A). Lane 2 to 5 are VH, VL PCR products. Lane 6 is deionized water which served as PCR negative control where 1A8 VH primer pair was used.

#### 6.4.1.2 Restriction enzyme digestion of HC and LC vectors, and VH, VL inserts

The VH PCR products were designed to be cut by NheI at their 5' and 3' ends, both, in order to be cloned into HC vector. The VL PCR products were designed to be cut by NheI at their 5' ends and by BsiWI at their 3'ends in order to be cloned into LC vector. After restriction enzyme digestion, VH, VL inserts and HC, LC vectors with compatible overhangs/sticky ends were obtained (**Table 6.19**).

**Table 6.19 Concentration of restriction enzyme digested vectors and inserts after gel-purification**

| gel-purified restriction digestion products | DNA concentration | 260/280 | 260/230 |
|---|---|---|---|
| 1A8 VH insert | 14.6 ng/µL | 1.90 | 0.86 |
| 1A8 VL insert | 10.3 ng/µL | 2.01 | 0.74 |
| 3G4 VH insert | 4.0 ng/µL | 2.12 | 0.17 |
| 3G4 VL insert | 10.5 ng/µL | 2.23 | 0.88 |
| HC pTT28 vector | 39.8 ng/µL | 1.97 | 1.56 |
| LC pTT28 vector | 47.6 ng/µL | 1.97 | 1.67 |

**6.4.1.3 Ligation of HC pTT28 vector and VH inserts, and LC pTT28 vector and VL inserts**

The restriction digested and gel-purified 1A8 VH insert and HC pTT28 vector were ligated. 1A8 VL insert and LC pTT28 vector were ligated. 3G4 VH insert and HC pTT28 vector were ligated. 3G4 VL insert and LC pTT28 vector were ligated. The length of vectors, inserts and ligated IgG constructs are shown in **Table 6.20**. The vector maps are shown in **Figure 6.5**. The IgG light chain vector used in this study has λ constant region sequence of Professor Montarop Yamabhai and it is designated as MY- λ constant region (MY λ CL).

**Table 6.20 Length of vectors, inserts and ligated IgG constructs**

| Name of vectors and inserts | length (base pair) |
|---|---|
| HC pTT28 vector | 5425 bp |
| LC pTT28 vector | 4754 bp |
| 1A8VH insert | 369 bp |
| 1A8VL insert | 342 bp |
| 3G4VH insert | 360 bp |
| 3G4VL insert | 336 bp |
| HC pTT28 + 1A8VH construct | 5794 bp |
| LC pTT28 + 1A8VL construct | 5096 bp |
| HC pTT28 + 3G4VH construct | 5785 bp |
| LC pTT28 + 3G4VL construct | 5090 bp |

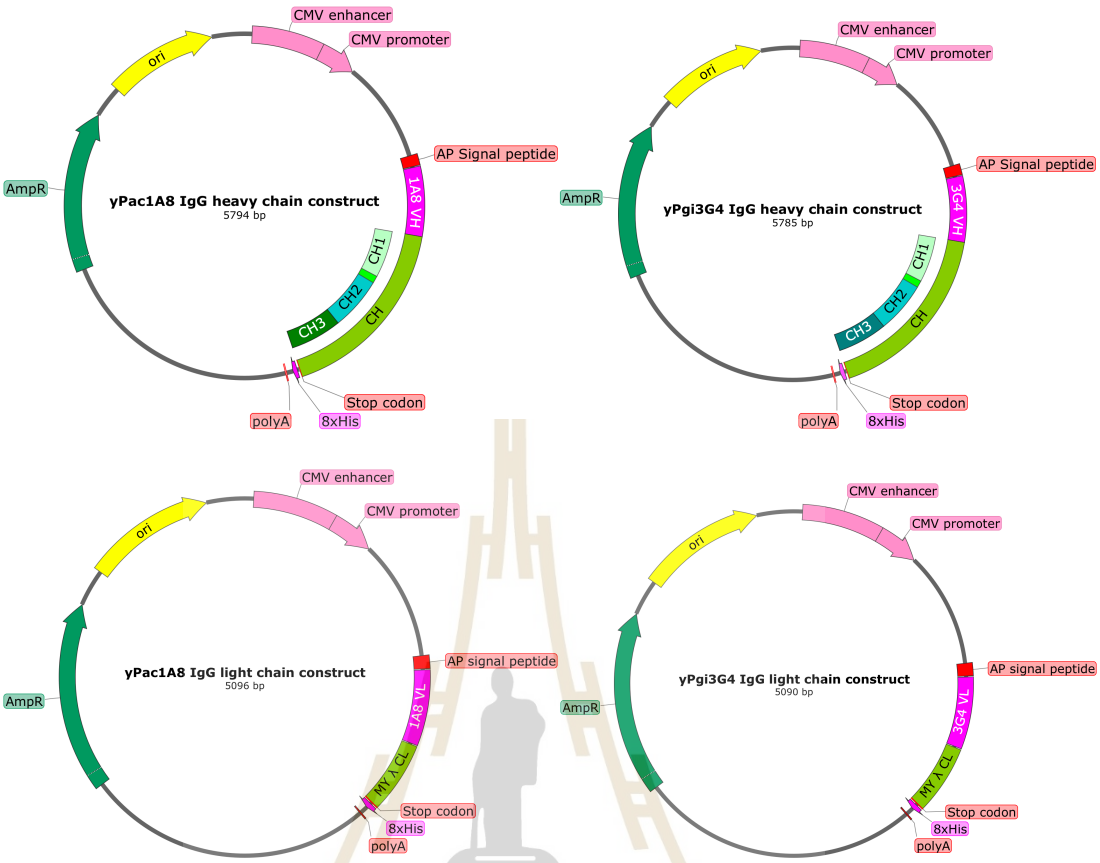


**Figure 6.5** **IgG heavy chain and light chain vector maps of yPac1A8 and yPgi3G4.**

The IgG vector maps are made by using Snapgene software version 5.2. Light chain vectors have MY λ CL (Montarop Yamabhai - λ constant region).

#### 6.4.1.4 Transformation of IgG constructs

Ligated IgG constructs and ligation controls were transformed into chemically competent Top 10 *E. coli* and the results were shown in **Table 6.21** and **Figure 6.6**.

**Table 6.21 Transformation results of ligation controls and IgG constructs**

| Transformation of IgG constructs | plate no. in Figure 6.6 | colony obtained | colony picked | clones sent for sequencing |
|---|---|---|---|---|
| uncut IgG heavy chain vector | plate 1 | uncountable colonies | - | - |
| NheI cut IgG heavy chain vector (HC pTT28) | plate 2 | 3 colonies | - | - |
| uncut IgG light chain vector | plate 3 | uncountable colonies | - | - |
| NheI and BsiWI cut IgG light chain vector (LC pTT28) | plate 4 | no colony | - | - |
| HC pTT28 + 1A8VH construct | plate 5 | 33 colonies | 6 colonies | 6 clones |
| LC pTT28 + 1A8VL construct | plate 6 | 127 colonies | 3 colonies | 2 clones |
| HC pTT28 + 3G4VH construct | plate 7 | 29 colonies | 6 colonies | 6 clones |
| LC pTT28 + 3G4VL construct | plate 8 | 137 colonies | 3 colonies | 2 clones |

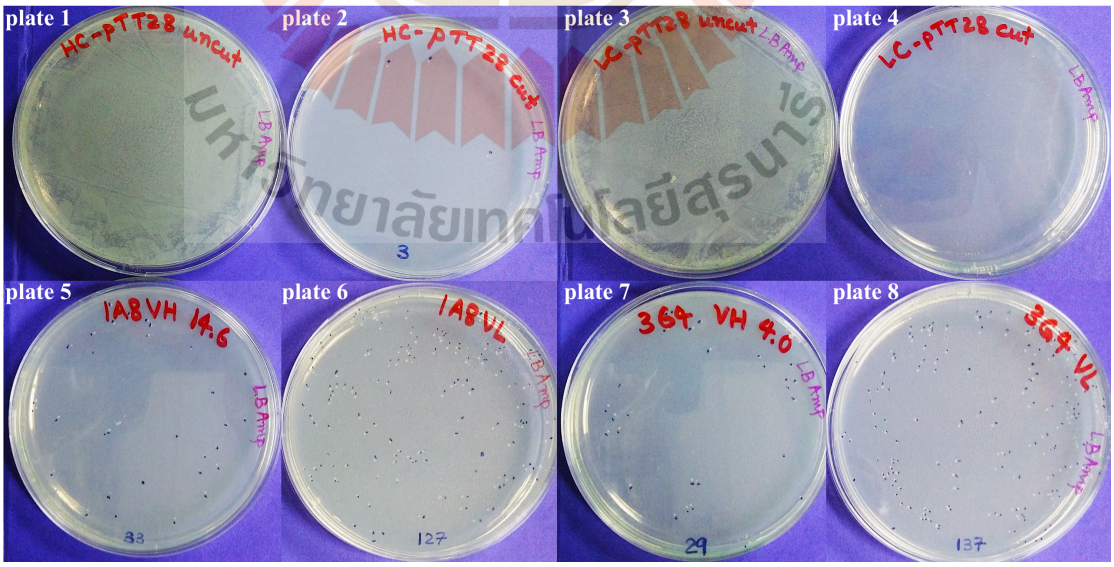


**Figure 6.6 Transformation results of ligation controls and IgG constructs**

#### 6.4.1.5 Confirmation of presence of inserts in IgG constructs

Colonies picked to check the presence of inserts were restriction digested and analysed by agarose gel electrophoresis. The restriction enzyme cut-check result of yPac1A8 and yPgi3G4 heavy chain vectors is shown in **Figure 6.7**. All of the clones checked have inserts of expected length (369-360 bp).

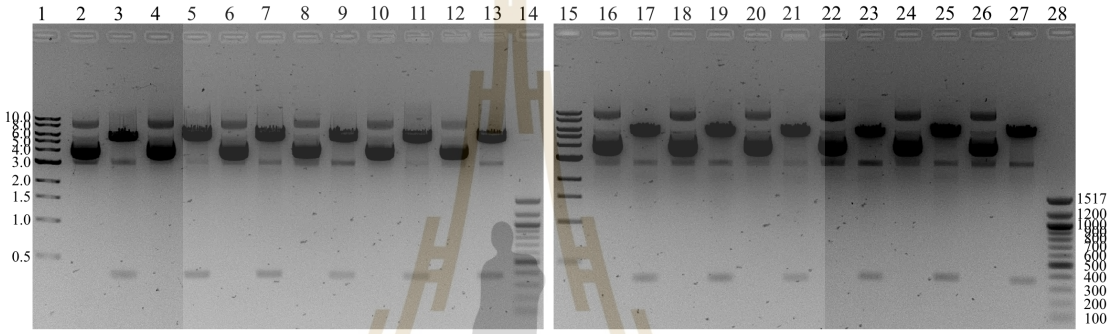


**Figure 6.7 Restriction enzyme cut-check result of yPac1A8 and yPgi3G4 heavy chain vectors (6 clones each)**

1 = 1 kbp DNA ladder (NEB#N3232L, U.S.A)
2 = uncut yPac1A8 HC vector clone 1
3 = cut yPac1A8 HC vector clone 1
4 = uncut yPac1A8 HC vector clone 2
5 = cut yPac1A8 HC vector clone 2
6 = uncut yPac1A8 HC vector clone 3
7 = cut yPac1A8 HC vector clone 3
8 = uncut yPac1A8 HC vector clone 4
9 = cut yPac1A8 HC vector clone 4
10 = uncut yPac1A8 HC vector clone 5
11 = cut yPac1A8 HC vector clone 5
12 = uncut yPac1A8 HC vector clone 6
13 = cut yPac1A8 HC vector clone 6
14 = 100 bp DNA ladder

15 = 1 kbp DNA ladder
16 = uncut yPgi3G4 HC vector clone 1
17 = cut yPgi3G4 HC vector clone 1
18 = uncut yPgi3G4 HC vector clone 2
19 = cut yPgi3G4 HC vector clone 2
20 = uncut yPgi3G4 HC vector clone 3
21 = cut yPgi3G4 HC vector clone 3
22 = uncut yPgi3G4 HC vector clone 4
23 = cut yPgi3G4 HC vector clone 4
24 = uncut yPgi3G4 HC vector clone 5
25 = cut yPgi3G4 HC vector clone 5
26 = uncut yPgi3G4 HC vector clone 6
27 = cut yPgi3G4 HC vector clone 6
28=100 bp DNA ladder (NEB#N3231L, U.S.A)

The restriction enzyme cut-check result of yPac1A8 and yPgi3G4 light chain vectors is shown in **Figure 6.8**. All of the clones checked have inserts of expected length (342-336 bp).

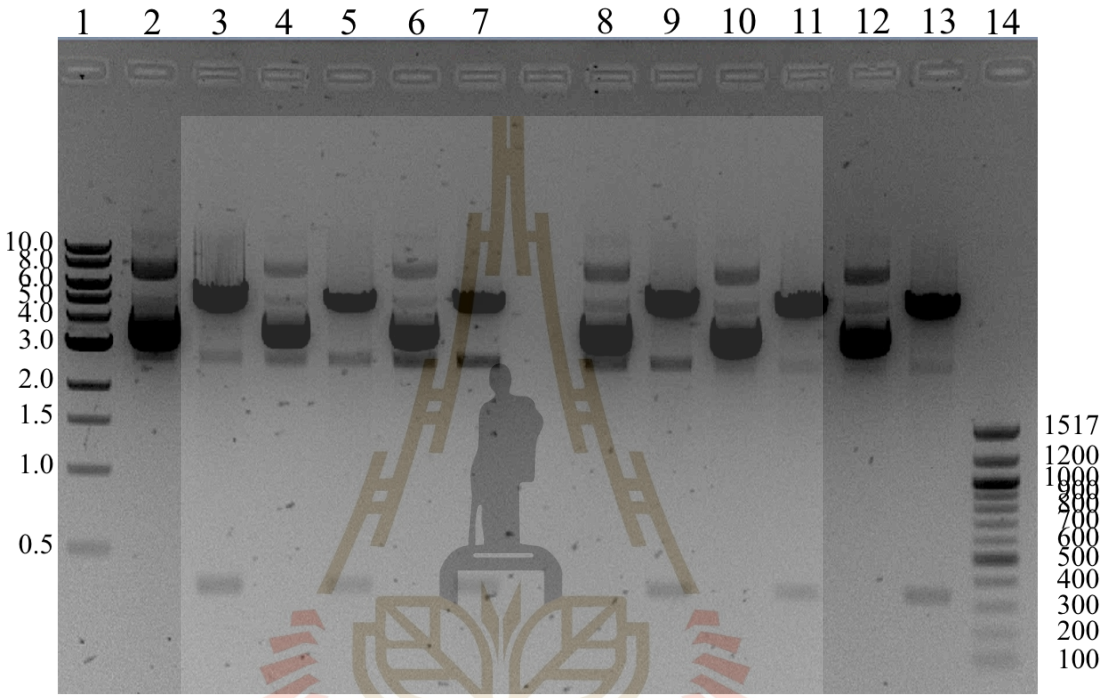


**Figure 6.8 Restriction enzyme cut-check result of yPac1A8 and yPgi3G4 light chain vectors (3 clones each)**

1 = 1 kbp DNA ladder (NEB#N3232L, U.S.A)
2 = uncut yPac1A8 LC vector clone 1
3 = cut yPac1A8 LC vector clone 1
4 = uncut yPac1A8 LC vector clone 2
5 = cut yPac1A8 LC vector clone 2
6 = uncut yPac1A8 LC vector clone 3
7 = cut yPac1A8 LC vector clone 3
8 = uncut yPgi3G4 LC vector clone 1
9 = cut yPgi3G4 LC vector clone 1
10 = uncut yPgi3G4 LC vector clone 2
11 = cut yPgi3G4 LC vector clone 2
12 = uncut yPgi3G4 LC vector clone 3
13 = cut yPgi3G4 LC vector clone 3
14 = 100 bp DNA ladder (NEB#N3231L, U.S.A)

#### 6.4.1.6 DNA sequence checking of IgG constructs

Altogether, 6 clones of yPac1A8 IgG heavy chain (yPac1A8 HC), 2 clones of yPac1A8 IgG light chain (yPac1A8 LC), 6 clones of yPgi3G4 IgG heavy chain (yPgi3G4 HC) and 2 clones of yPgi3G4 IgG light chain (yPgi3G4 LC) were sent for insert DNA sequencing. The results were checked for orientation of the insert, reading frames of insert and signal peptide, and the sequence similarity between insert and original scFv template (**Table 6.22**). There are chances of disoriented ligation in heavy chain constructs because heavy chain cloning used only one restriction enzyme (NheI). Out of six yPac1A8 HC vectors sequenced, four have correct orientation of insert. Out of six yPgi3G4 HC vectors sequenced, only two have correct orientation of insert. The perfect heavy chain and light chain clones for IgG expression are highlighted in gray in **Table 6.22**.

**Table 6.22 IgG constructs DNA sequence check result**

| Plasmid name | orientation of insert | insert in the same reading frame with signal peptide | similarity between insert and original template sequences |
|---|---|---|---|
| yPac1A8 HC 1 | correct | yes | 100% |
| yPac1A8 HC 2 | correct | no | one base deletion detected between NheI and FR1 site |
| yPac1A8 HC 3 | inverted | | |
| yPac1A8 HC 4 | correct | yes | 100% |
| yPac1A8 HC 5 | correct | yes | 100% |
| yPac1A8 HC 6 | inverted | | |
| yPgi3G4 HC 1 | correct | yes | 100% |
| yPgi3G4 HC 2 | correct | yes | 100% |
| yPgi3G4 HC 3 | inverted | | |
| yPgi3G4 HC 4 | inverted | | |
| yPgi3G4 HC 5 | inverted | | |
| yPgi3G4 HC 6 | inverted | | |
| yPac1A8 LC 1 | correct | yes | 100% |
| yPac1A8 LC 2 | correct | yes | 100% |
| yPgi3G4 LC 1 | correct | yes | 100% |
| yPgi3G4 LC 2 | correct | yes | 100% |

### 6.4.2 Recombinant full-length IgG expression system

#### 6.4.2.1 Preparation of recombinant IgG plasmids for expression

One pair of yPac1A8 IgG plasmids (yPac1A8 IgG HC and yPac1A8 IgG LC) and one pair of yPgi3G4 IgG plasmids (yPgi3G4 IgG HC and yPgi3G4 IgG LC) were selected for IgG expression. They are copied in chemically competent Top 10 *E. coli* cells and purified with PureLink HiPure Plasmid Midiprep Kit to obtain transfection-grade plasmid DNA.

#### 6.4.2.2 Recombinant IgG expression in 2 mL transfection volume

The first time IgG expression was performed at 2 mL volume and two heavy chain/light chain ration (1:2 and 1:3) were tested. Crude supernatant was collected on transfection day 5 and checked for the presence of functioning yPac1A8 IgG and yPgi3G4 IgG by performing crude supernatant IgG ELISA and slide agglutination test (see section 6.4.5 and 6.4.6 below).

#### 6.4.2.3 Recombinant IgG expression in 30 mL transfection volume

Taken into account of crude supernatant IgG ELISA result, heavy chain/light chain ratio of 1:2 was used in 30 mL scale-up IgG expression. Crude supernatant was collected on transfection day 6 and at that time, the viability of transfected cells in both yPac1A8 IgG and yPgi3G4 IgG expression systems dropped to 16%.

มหาวิทยาลัยเทคโนโลยีสุรนารี

### 6.4.3 Quantitation of IgG in crude supernatant by using ForteBio Octet K2 Platform

The yPac1A8 IgG and yPgi3G4 IgG in crude supernatant were quantified by using ForteBio Octet K2 2-channel system and Protein A Dip and Read Biosensors. Purified yPgi3G4 IgG (2.4 mg/mL) was used as the standard IgG. The raw data (binding curve graph) of both standard and samples is shown in **Figure. 6.9**.

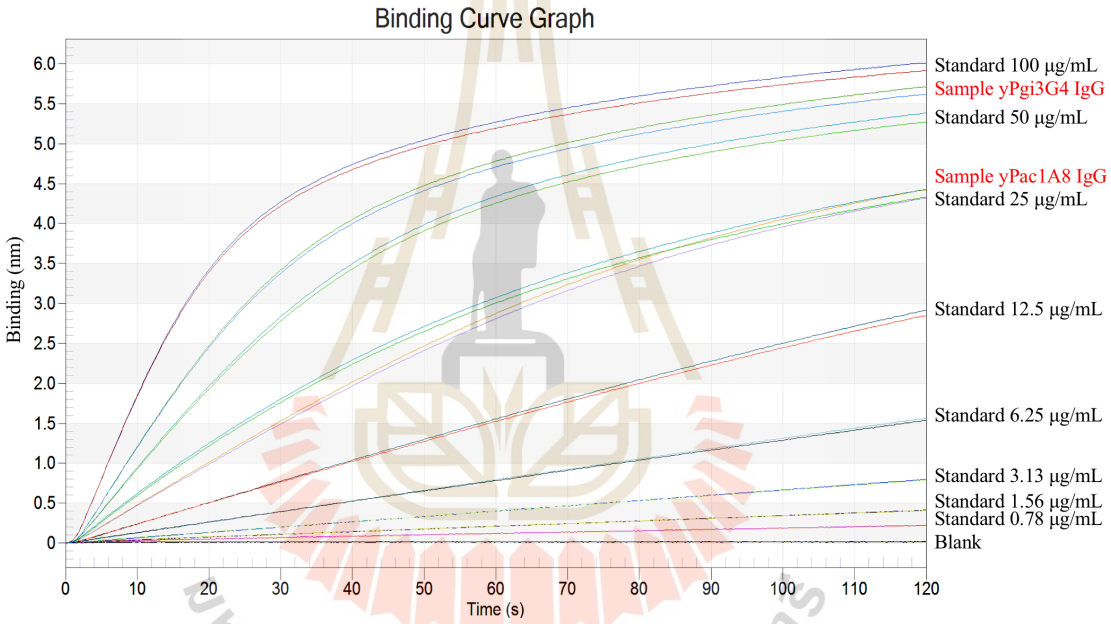


**Figure 6.9 Binding curve graph of standard IgG and samples**

Based on the binding rate of standard IgG to protein A biosensors and its known concentration, standard curve was generated and subsequently, the concentration of IgG in the samples was interpolated. Duplicates of both standard and samples were measured, and the average value was taken into calculation by Octet system. The standard curve obtained is shown in **Figure 6.10** and the calculations are shown in **Table 6.23** where samples are highlighted in gray.

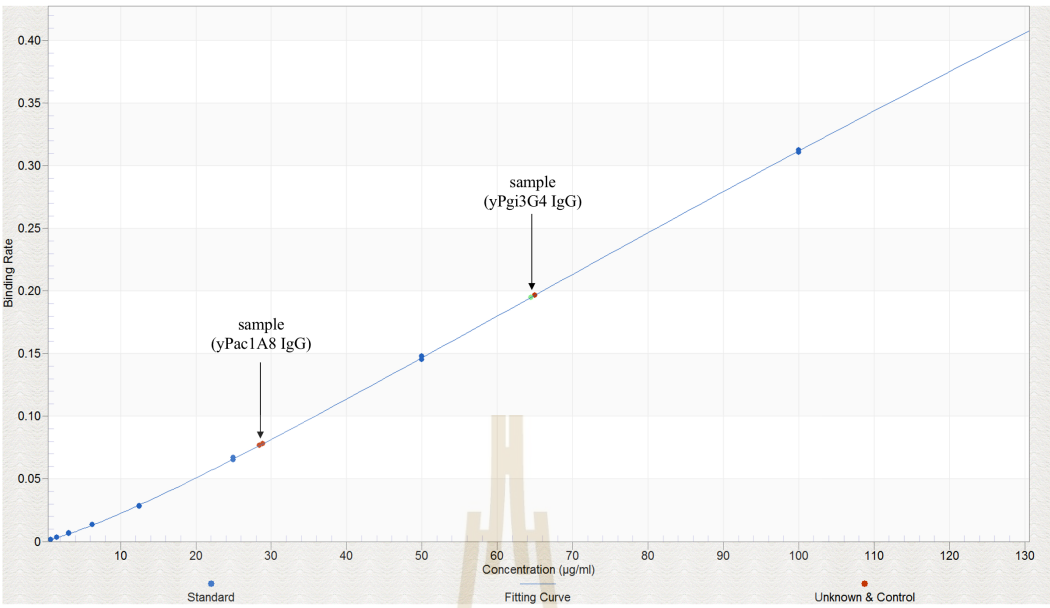


**Figure 6.10 Standard curve showing standard IgG (blue) and samples (red)**

**Table 6.23 Calculation of IgG concentration in crude supernatant**

| Sample ID | Type | Conc. (µg/ml) | Well Conc. | Dilution Factor | Calculated Conc. | Conc. average |
|---|---|---|---|---|---|---|
| yPac1A8 crude | Unknown | N/A | 28.9 | 3 | 86.6 | 86 |
| yPac1A8 crude | Unknown | N/A | 28.5 | 3 | 85.4 | 86 |
| yPgi3G4 crude | Unknown | N/A | 65 | 3 | 195 | 194.2 |
| yPgi3G4 crude | Unknown | N/A | 64.5 | 3 | 193.4 | 194.2 |
| Std yPgi3G4 | Standard | 100 | 100.3 | | 100.3 | 100 |
| Std yPgi3G4 | Standard | 100 | 99.7 | | 99.7 | 100 |
| Std yPgi3G4 | Standard | 50 | 50.4 | | 50.4 | 50 |
| Std yPgi3G4 | Standard | 50 | 49.6 | | 49.6 | 50 |
| Std yPgi3G4 | Standard | 25 | 25.3 | | 25.3 | 25.1 |
| Std yPgi3G4 | Standard | 25 | 24.8 | | 24.8 | 25.1 |
| Std yPgi3G4 | Standard | 12.5 | 12.3 | | 12.3 | 12.2 |
| Std yPgi3G4 | Standard | 12.5 | 12.1 | | 12.1 | 12.2 |
| Std yPgi3G4 | Standard | 6.25 | 6.49 | | 6.49 | 6.44 |
| Std yPgi3G4 | Standard | 6.25 | 6.39 | | 6.39 | 6.44 |
| Std yPgi3G4 | Standard | 3.13 | 3.47 | | 3.47 | 3.44 |
| Std yPgi3G4 | Standard | 3.13 | 3.42 | | 3.42 | 3.44 |
| Std yPgi3G4 | Standard | 1.56 | 1.81 | | 1.81 | 1.81 |
| Std yPgi3G4 | Standard | 1.56 | 1.81 | | 1.81 | 1.81 |
| Std yPgi3G4 | Standard | 0.78 | 0.7818 | | 0.7818 | 0.78 |
| Std yPgi3G4 | Standard | 0.78 | 0.7782 | | 0.7782 | 0.78 |
| Std yPgi3G4 | Standard | 0 | 0 | | 0 | 0 |
| Std yPgi3G4 | Standard | 0 | 0 | | 0 | 0 |

Therefore, 86 µg/mL of yPac1A8 IgG is present in crude supernatant. It means that 86 mg/L of yPac1A8 IgG is produced by the expression system applied in this study. About 194.2 µg/mL of yPgi3G4 IgG is present in the crude supernatant and so, 194.2 mg/L of yPgi3G4 IgG can be produced by the expression system of this study.

### 6.4.4 Recombinant IgG purification

#### 6.4.4.1 yPac1A8 IgG purification

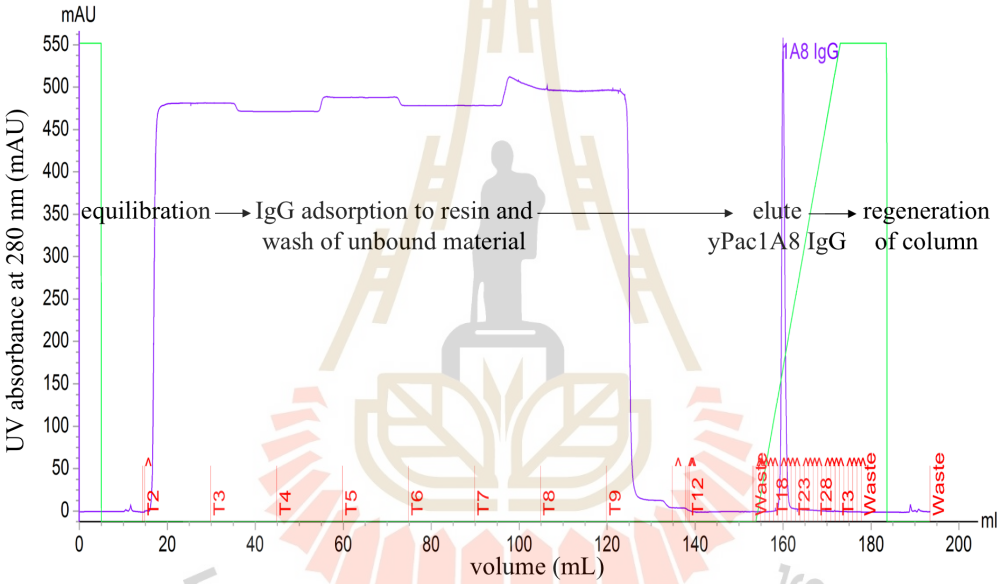


| No | Peak name | Retention ml | Area ml*mAU | Height mAU |
|---|---|---|---|---|
| 1 | - | 17.57 | 581.8821 | 215.663 |
| 2 | - | 122.52 | 208.6609 | 196.545 |
| 3 | - | 124.04 | 268.5184 | 267.777 |
| 4 | - | 124.40 | 234.7866 | 274.480 |
| 5 | 1A8 IgG | 159.97 | 482.6084 | 551.302 |

**Figure 6.11 Chromatogram showing the purification profile of yPac1A8 IgG.** The purple line represents the UV absorbance at 280 nm. A single peak, named as 1A8 IgG, represents the fraction containing purified yPac1A8 IgG. The green line represents the gradient concentration of the buffers. The red line represents the fraction volume and the collection tube

numbers. The peak area calculations are shown at the bottom of the graph.

The yPac1A8 IgG was purified by using HiTrap Protein A HP antibody purification (1 mL) column and ÄKTA start protein purification system with UNICORN start software and Frac30 fraction collector. Protein concentration of yPac1A8 IgG elute was measured by Pierce BCA Protein assay kit and calculated as follows:

eluted yPac1A8 IgG = (0.72 mg/mL x 1.5 mL)+(0.268 mg/mL x 450 μL) = 1.2006 mg

Therefore, 1.2 mg of yPac1A8 IgG was eluted from 25 mL crude supernatant.

The chromatogram of yPac1A8 IgG purification is shown in **Figure 6.11** above. SDS-PAGE analysis of purified yPac1A8 IgG is shown in **Figure 6.13** together with purified yPgi3G4 IgG.

#### 6.4.4.2 yPgi3G4 IgG purification

The yPgi3G4 IgG was purified by using HiTrap MabSelect PrismA (1 mL) column. MabSelect PrismA is a next-generation protein A resin that can be cleaned with 0.5-1.0 M NaOH. It has optimized high-flow agarose base matrix and a genetically engineered protein A-derived ligand that can bind to about 80 mg human IgG/mL of resin (Cytiva, 2020; GE-Healthcare, 2009, 2018). Protein concentration of yPgi3G4 IgG elute was measured by Pierce BCA Protein assay kit and calculated as follows:

eluted yPgi3G4 IgG = 2.443 mg/mL x 1.6 mL = 3.9088 mg

Therefore, 3.9 mg of yPgi3G4 IgG was eluted from 25 mL crude supernatant.

The chromatogram of yPgi3G4 IgG purification is shown in **Figure 6.12** below. SDS-PAGE analysis of purified yPgi3G4 IgG is shown in **Figure 6.13**.

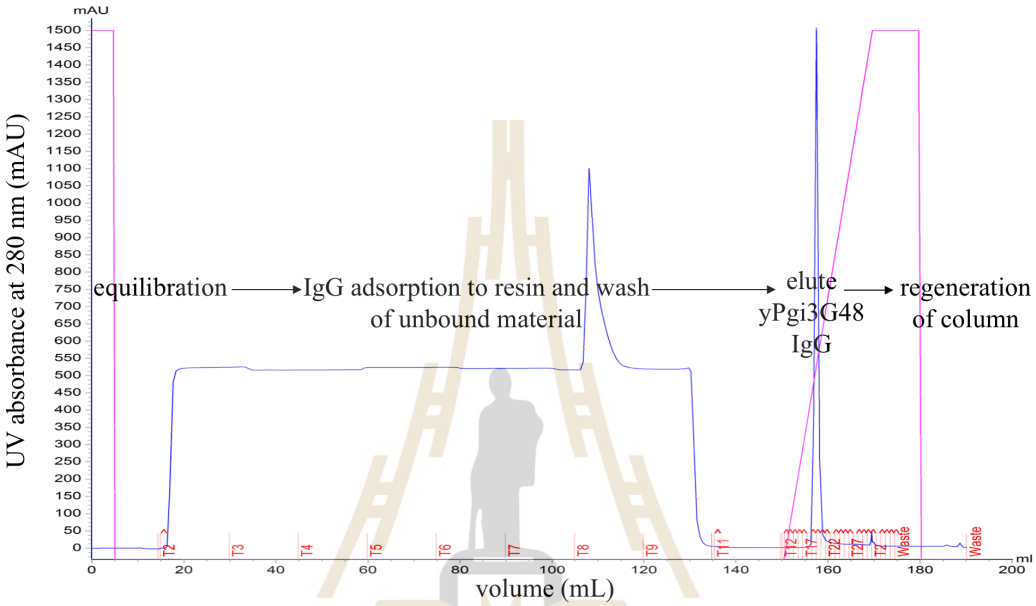


| No | Peak name | Retention ml | Area ml*mAU | Height mAU |
|---|---|---|---|---|
| 1 | - | 18.02 | 1969.1680 | 280.286 |
| 2 | - | 108.09 | 1593.1590 | 582.610 |
| 3 | - | 127.95 | 448.5012 | 218.911 |
| 4 | - | 130.15 | 466.4935 | 295.401 |
| 5 | 3G4 IgG | 157.48 | 1468.3530 | 1496.017 |

**Figure 6.12 Chromatogram showing the purification profile of yPgi3G4 IgG.** The purple line represents the UV absorbance at 280 nm. A single elute peak represents the fraction containing purified yPgi3G4 IgG. The pink line represents the gradient concentration of the buffers. The red line represents the fraction volume and the collection tube numbers. The peak calculations are shown at the bottom of the table.

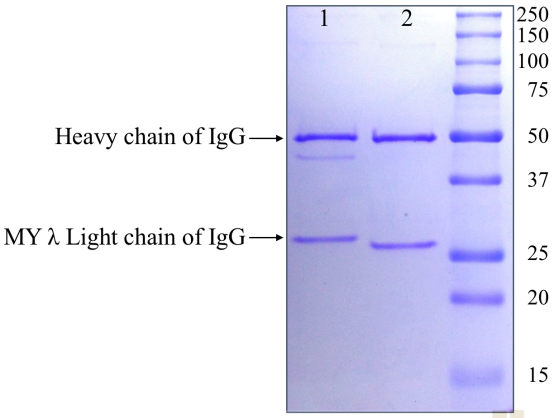


**Figure 6.13 Reduced SDS-PAGE analysis of purified IgG.**

Lane 1: yPac1A8 IgG (2.0 µg). Lane 2: yPgi3G4 IgG (2.0 µg). All Blue Prestained Protein Standards (BioRad#1610373, U.S.A) is used.

The summary of the IgG yield in this study was shown in **Table 6.24**. About 86 µg/mL of yPac1A8 IgG is present in crude supernatant. About 1.2 mg of yPac1A8 IgG is eluted from 25 mL crude supernatant. Therefore, 55.8% of expressed yPac1A8 IgG is purified by HiTrap Protein A HP antibody purification column. About 194.2 µg/mL of yPgi3G4 IgG is present in the crude supernatant. As 3.9 mg of yPgi3G4 IgG is eluted from 25 mL crude supernatant, 80.3% of expressed yPgi3G4 IgG is purified by HiTrap MabSelect PrismA column.

**Table 6.24 Summary of recombinant IgG yield in this study**

| IgG | IgG in crude supernatant | purification column | purified IgG | % purified |
|---|---|---|---|---|
| yPac1A8 IgG | 86 µg/mL | HiTrap Protein A HP antibody purification column | 1.2 mg from 25 mL crude supernatant | 55.8% of expressed yPac1A8 IgG is purified |
| yPgi3G4 IgG | 194.2 µg/mL | HiTrap MabSelect PrismA column | 3.9 mg from 25 mL crude supernatant | 80.3% of expressed yPgi3G4 IgG is purified |

### 6.4.5 Crude supernatant IgG ELISA

To examine the target binding ability of yPac1A8 IgG and yPgi3G4 IgG in crude supernatant, *P. acnes* and *P. aeruginosa* whole cell ELISA was performed. As shown in **Figure 6.14**, both IgG in crude supernatant can bind to heat-inactivated targets like their counterpart scFv positive control (purified scFv 20 µg/mL). HEK 293 cells supernatant was used as negative control.

In case of *P. aeruginosa* ELISA, the absorbance signal of both IgG and scFv formats are below 1.0. It could be due to the use of *P. aeruginosa* target stored at -40°C for more than 6 months and scFv stored at -80°C for more than one year. Nevertheless, both IgG ELISA results indicated that heavy chain/light chain ratio 1:2 is better than 1:3 for yPac1A8 and yPgi3G4 IgG expression.

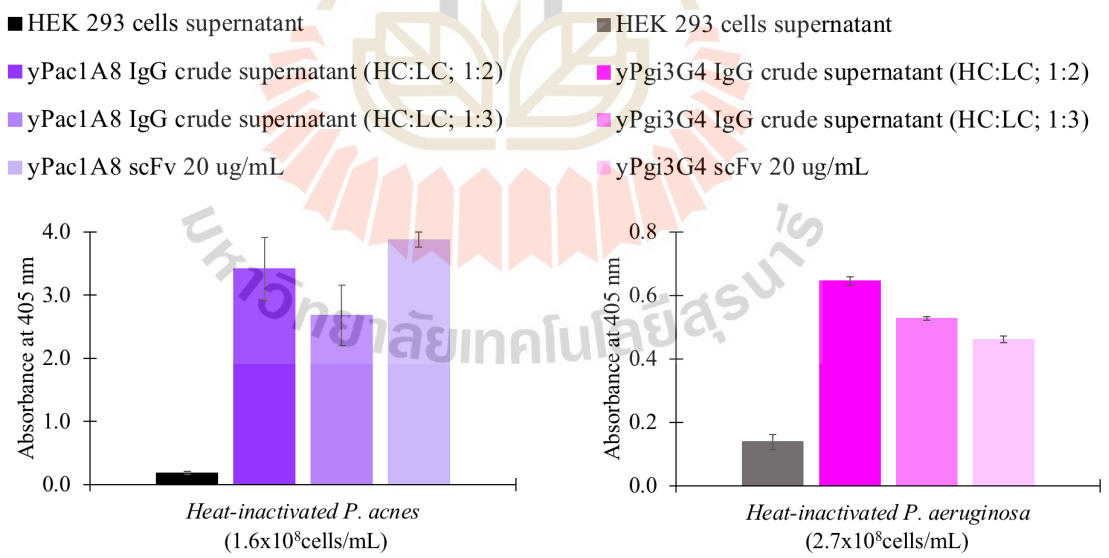


**Figure 6.14** ***P. acnes* and *P. aeruginosa* and crude supernatant IgG ELISA**

In both *P. acnes* and *P. aeruginosa* ELISA, purified scFv (20 µg/mL) is positive control and HEK 293 cells supernatant is negative control.

### 6.4.6 Slide agglutination test using crude supernatant IgG

IgG in crude supernatant was added to live cell suspension of *P. acnes*. The clumping of *P. acnes* caused by yPac1A8 IgG in crude supernatant could be seen clearly within 2 min which didn't happen with MY LAB adalimumab and yPgi3G4 IgG (**Figure 6.15**). With yPgi3G4 IgG in crude supernatant, clumping of *P. aeruginosa* within 2 min was not obvious enough to take pictures.

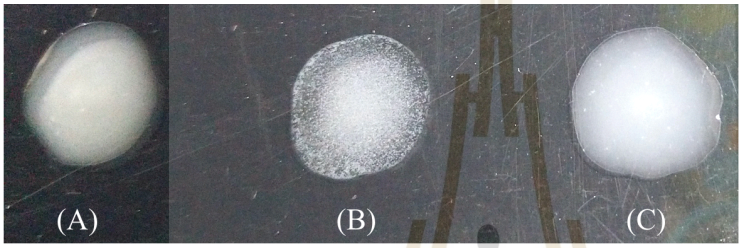


**Figure 6.15** ***P. acnes* slide agglutination test using crude supernatant IgG**

(A) *P. acnes* in PBS 10 µL and crude supernatant Adalimumab 20 µL.

(B) *P. acnes* in PBS 10 µL and crude supernatant yPac1A8 IgG 20 µL.

(C) *P. acnes* in PBS 10 µL and crude supernatant yPgi3G4 IgG 20 µL.

### 6.4.7 Slide agglutination test using purified IgG

Agglutination of live *P. acnes* (DMST 14916) by purified yPac1A8 IgG was visible within two min (**Figure 6.16**). This time, purified IgG isotype control was not available to use.

**Figure 6.16** ***P. acnes* slide agglutination test using purified IgG**

(A) *P. acnes* (DMST 14916) in PBS. (B) *P. acnes* (DMST 14916) in PBS agglutinated by purified yPac1A8 IgG (7 µg).

In section 6.4.6, agglutination of live *P. aeruginosa* (DMST 37186) by crude supernatant yPgi3G4 IgG was not clear enough to take picture. The same test was tried again with purified yPgi3G4 IgG and agglutination of *P. aeruginosa* was seen as shown in **Figure 6.17**. There was no agglutination of *P. aeruginosa* with IgG isotype control (purified yPac1A8 IgG).

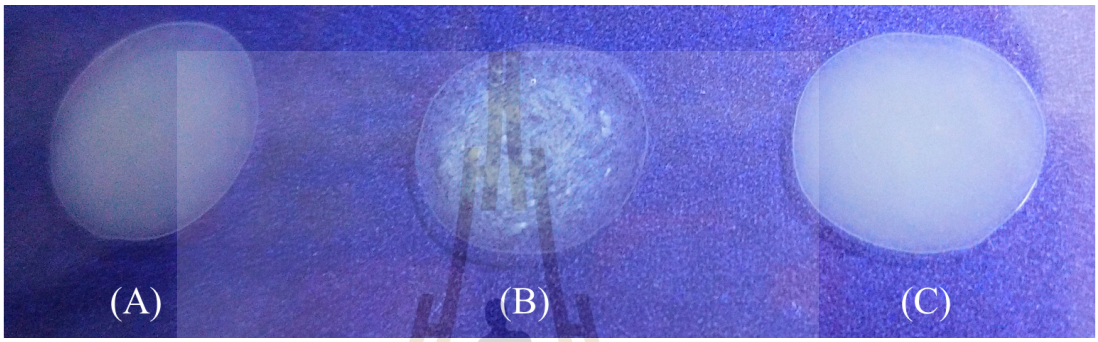


**Figure 6.17** ***P. aeruginosa* slide agglutination test using purified IgG**

(A) *P. aeruginosa* (DMST 37186) in PBS. (B) *P. aeruginosa* (DMST 37186) in PBS agglutinated by purified yPgi3G4 IgG (7 µg). (C) *P. aeruginosa* (DMST 37186) in PBS mixed with yPac1A8 IgG (7 µg).

### 6.4.8 Complement-mediated bacteriolysis of *P. aeruginosa* enhanced by yPgi3G4 IgG

#### 6.4.8.1 *P. aeruginosa* specific antibodies-depleted, diluted, and pooled human serum

The filter-sterilized, *P. aeruginosa* specific antibodies-depleted, diluted (1:10 in PBS), and pooled human serum, which were kept in 100 µL aliquots at -80°C, was used as the source of complement proteins in complement-mediated bacteriolysis assay.

#### 6.4.8.2 Preparation of *P. aeruginosa* seed cultures

*P. aeruginosa* (DMST 37186) seed cultures were freshly prepared from overnight broth culture for each and every set of bacteriolysis assay. About 10 µL of seed culture became *P. aeruginosa* inoculum in every assay tube.

#### 6.4.8.3 Preparation of recombinant antibodies

Recombinant IgG intermediate stocks (60 µg/mL in PBS) of all three IgG were prepared in order to obtain 24 µg/mL final concentration of IgG in assay tubes.

#### 6.4.8.4 Complement-mediated bacteriolysis reaction set up

One set of bacteriolysis assay has four reaction tubes. In no IgG (no mAb) tube, *P. aeruginosa* inoculum are incubated with the depleted-diluted-pooled serum only. In Adalimumab tube, *P. aeruginosa* is incubated with serum plus adalimumab (IgG isotype control). In yPgi3G4 IgG tube, *P. aeruginosa* is incubated with serum plus yPgi3G4 IgG (*P. aeruginosa* specific IgG under testing). In yPac1A8 IgG tube, *P. aeruginosa* is incubated with serum plus yPac1A8 IgG (antibacterial IgG isotype control).

#### 6.4.8.5 Colony forming units (viable count) in seed cultures

Colonies obtained from three replicates of 10 µL drop were counted as shown in **Figure 6.18** and **Figure 6.19**. Viable count in 1 mL of seed culture was calculated. From viable count of seed cultures, the input bacterial number

(inoculum) into reaction tubes was calculated. Calculation and results obtained were collectively shown in **Table 6.25**.

**Figure 6.18 Culture plates and colony counts of seed cultures of assay set 1, 2, and 3**

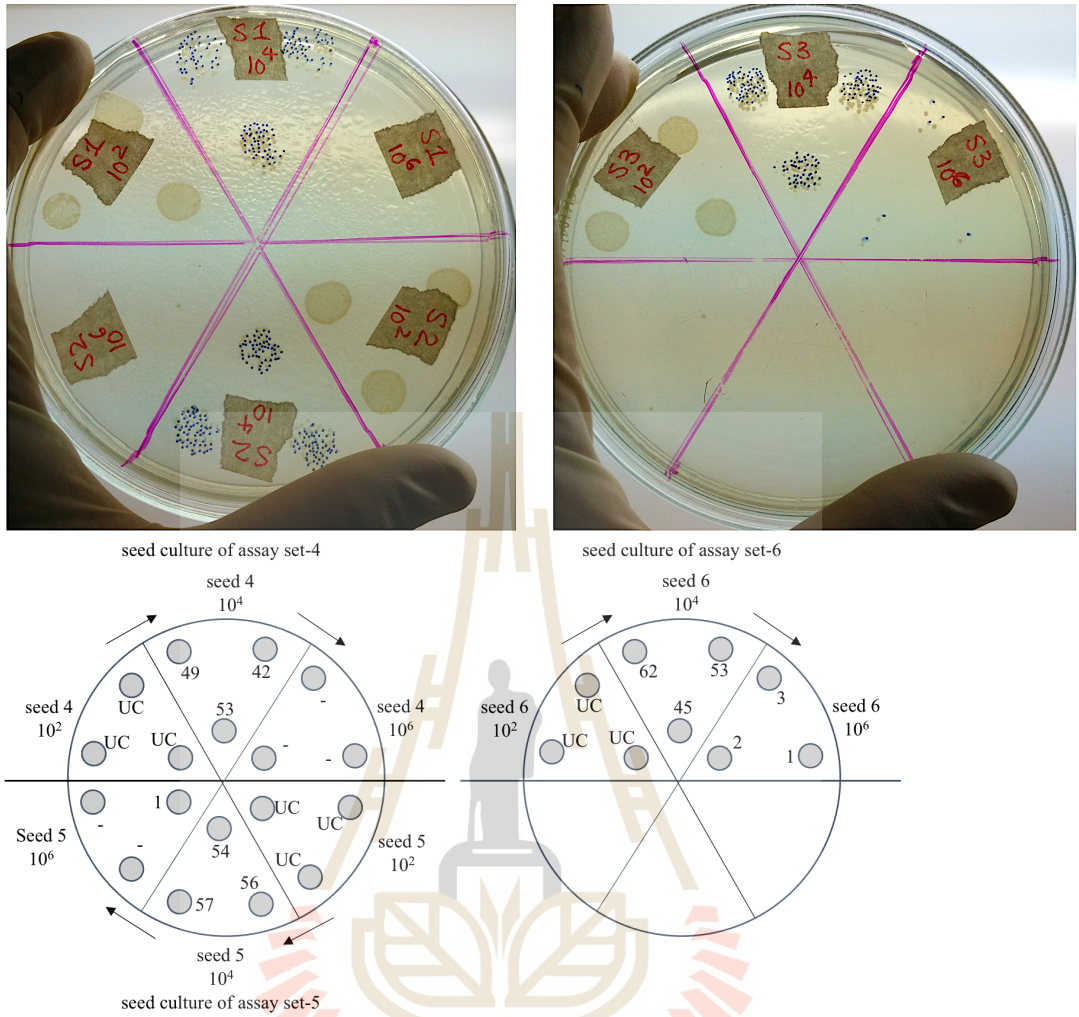


**Figure 6.19** **Culture plates and colony counts of seed cultures of assay set 4, 5, and 6**

**Table 6.25** **Number of viable *P. aeruginosa* in seed cultures and input bacterial number (inoculum) in each assay set**

| Seed cultures | Calculation based on obtained colony counts | viable count (cfu/mL) of seed cultures | input bacterial number (inoculum) in reaction tubes |
|---|---|---|---|
| assay set 1 | $((50+45+46)/3)*10^4*10^2$ | $4.7*10^7$ cfu/mL | $4.7*10^6$ cfu/mL |
| assay set 2 | $((35+30+28)/3)*10^4*10^2$ | $3.1*10^7$ cfu/mL | $3.1*10^6$ cfu/mL |
| assay set 3 | $((20+18+27)/3)*10^4*10^2$ | $2.16*10^7$ cfu/mL | $2.16*10^6$ cfu/mL |
| assay set 4 | $((49+42+53)/3)*10^4*10^2$ | $4.8*10^7$ cfu/mL | $4.8*10^6$ cfu/mL |
| assay set 5 | $((54+57+56)/3)*10^4*10^2$ | $5.6*10^7$ cfu/mL | $5.6*10^6$ cfu/mL |
| assay set 6 | $((62+53+45)/3)*10^4*10^2$ | $5.3*10^7$ cfu/mL | $5.3*10^6$ cfu/mL |

#### 6.4.8.6 Colony forming units left in reaction tubes

At the end of 3 h incubation of complement-mediated bacteriolysis assay, the number of colony forming units in reaction tubes was determined. Colonies obtained from triplicates of 10 µL drop were counted (**Figure 6.20 to 6.25)**. Calculations made and results obtained were shown in **Table 6.26**.

**Table 6.26 Number of *P. aeruginosa* left in reaction tubes (six assay sets)**

| **Complement-mediated bacteriolysis assay** | **Calculation based on obtained colony counts** | **viable *P. aeruginosa* (cfu/mL) left in reaction tubes** |
|---|---|---|
| Assay set 1 | | |
| no IgG | $((63+70+52)/3)*10^2*10^2$ | $6.2*10^5$ |
| Adalimumab | $((82+89)/2)*10^2*10^2$ | $8.6*10^5$ |
| yPgi3G4 IgG | $((60+61+51)/3)*10*10^2$ | $5.7*10^4$ |
| yPac1A8 IgG | $((73+80+76)/3)*10^2*10^2$ | $7.6*10^5$ |
| Assay set 2 | | |
| no IgG | $((52+52+44)/3)*10^2*10^2$ | $4.9*10^5$ |
| Adalimumab | $((62+72+86)/3)*10^2*10^2$ | $7.3*10^5$ |
| yPgi3G4 IgG | $((43+44+26)/3)*10*10^2$ | $3.8*10^4$ |
| yPac1A8 IgG | $((60+62+73)/3)*10^2*10^2$ | $6.5*10^5$ |
| Assay set 3 | | |
| no IgG | $((44+47+37)/3)*10^2*10^2$ | $4.3*10^5$ |
| Adalimumab | $((78+81+95)/3)*10^2*10^2$ | $8.5*10^5$ |
| yPgi3G4 IgG | $((35+49+36)/3)*10*10^2$ | $4.0*10^4$ |
| yPac1A8 IgG | $((79+76+74)/3)*10^2*10^2$ | $7.6*10^5$ |
| Assay set 4 | | |
| no IgG | $((109+90+125)/3)*10^2*10^2$ | $1.1*10^6$ |
| Adalimumab | $((108+135+122)/2)*10^2*10^2$ | $1.2*10^6$ |
| yPgi3G4 IgG | $((67+69+80)/3)*10*10^2$ | $7.2*10^4$ |
| yPac1A8 IgG | $((143+117+140)/3)*10^2*10^2$ | $1.3*10^6$ |
| Assay set 5 | | |
| no IgG | $((124+126+133)/3)*10^2*10^2$ | $1.3*10^6$ |
| Adalimumab | $((145+141+131)/3)*10^2*10^2$ | $1.4*10^6$ |
| yPgi3G4 IgG | $((100+101+97)/3)*10*10^2$ | $9.9*10^4$ |
| yPac1A8 IgG | $((152+115+132)/3)*10^2*10^2$ | $1.3*10^6$ |
| Assay set 6 | | |
| no IgG | $((140+148+147)/3)*10^2*10^2$ | $1.5*10^6$ |
| Adalimumab | $((177+196+145)/3)*10^2*10^2$ | $1.7*10^6$ |
| yPgi3G4 IgG | $((101+118+127)/3)*10*10^2$ | $1.2*10^5$ |
| yPac1A8 IgG | $((157+173+176)/3)*10^2*10^2$ | $1.7*10^6$ |

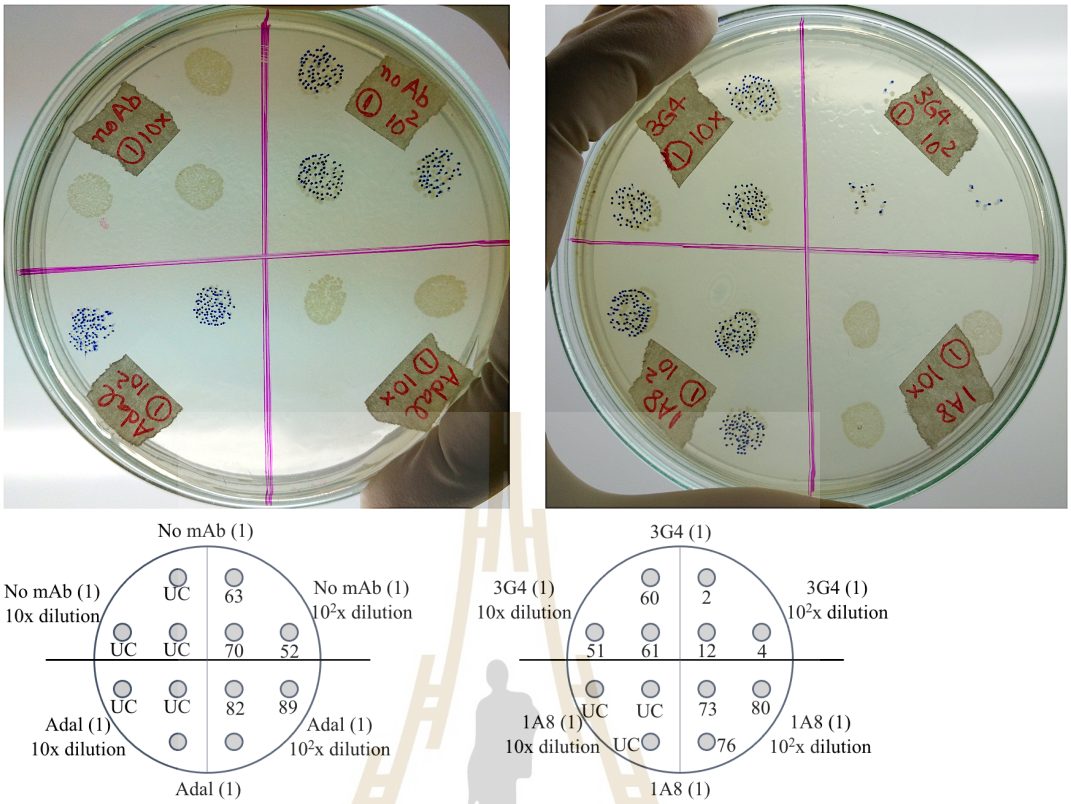


**Figure 6.20 Culture plates and colony counts of assay set 1**

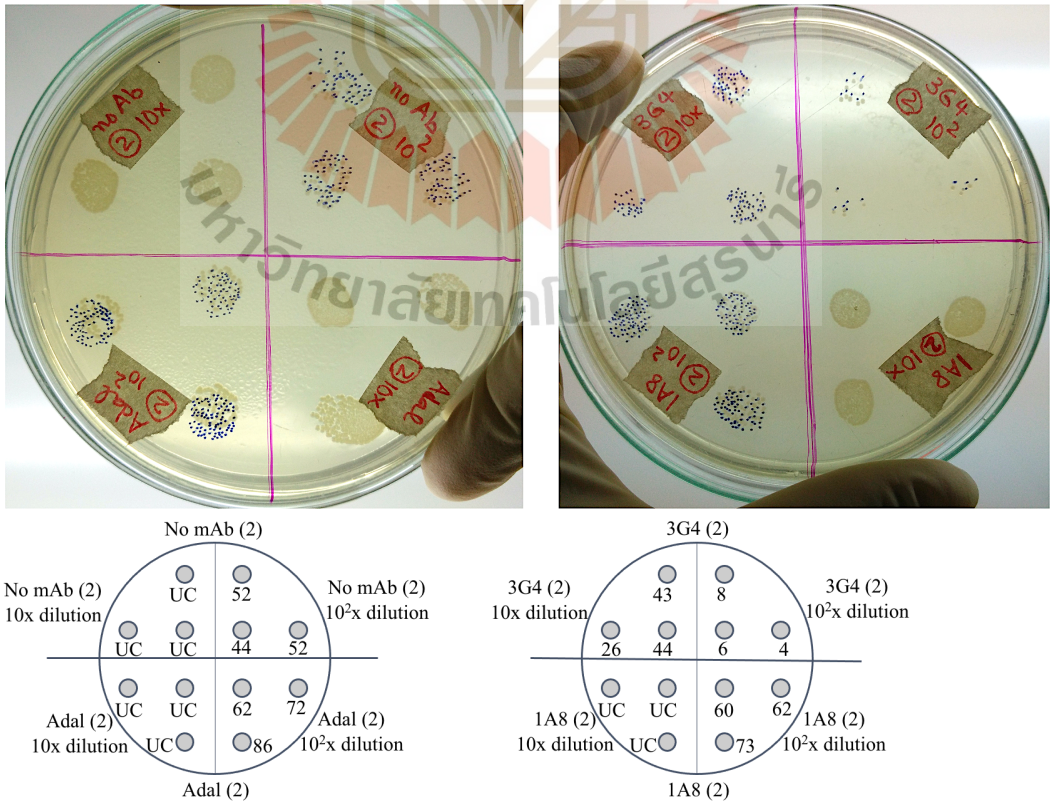


**Figure 6.21 Culture plates and colony counts of assay set 2**

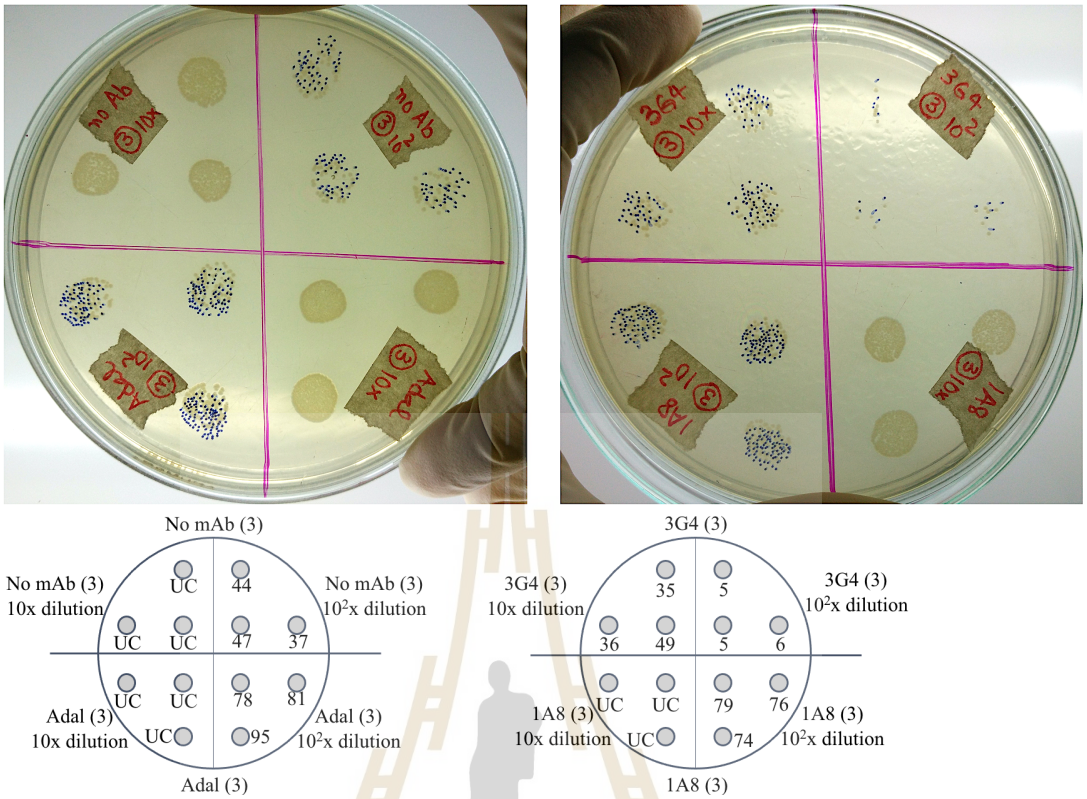


**Figure 6.22 Culture plates and colony counts of assay set 3**

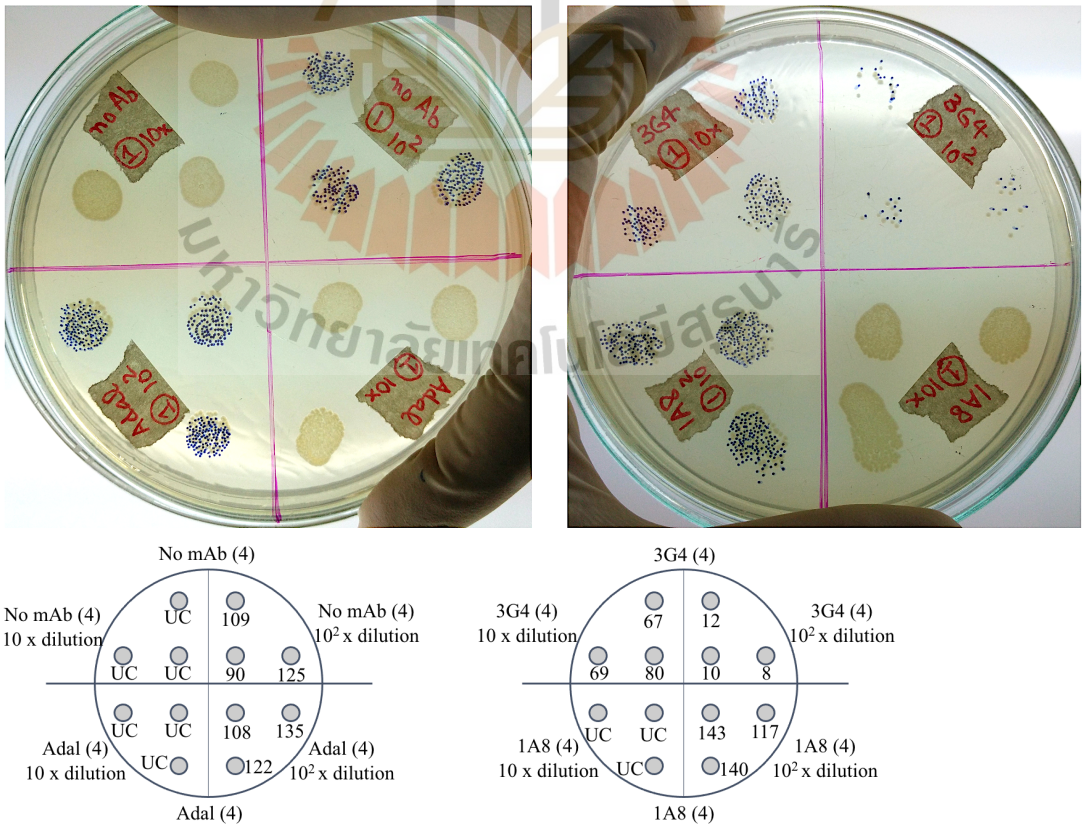


**Figure 6.23 Culture plates and colony counts of assay set 4**

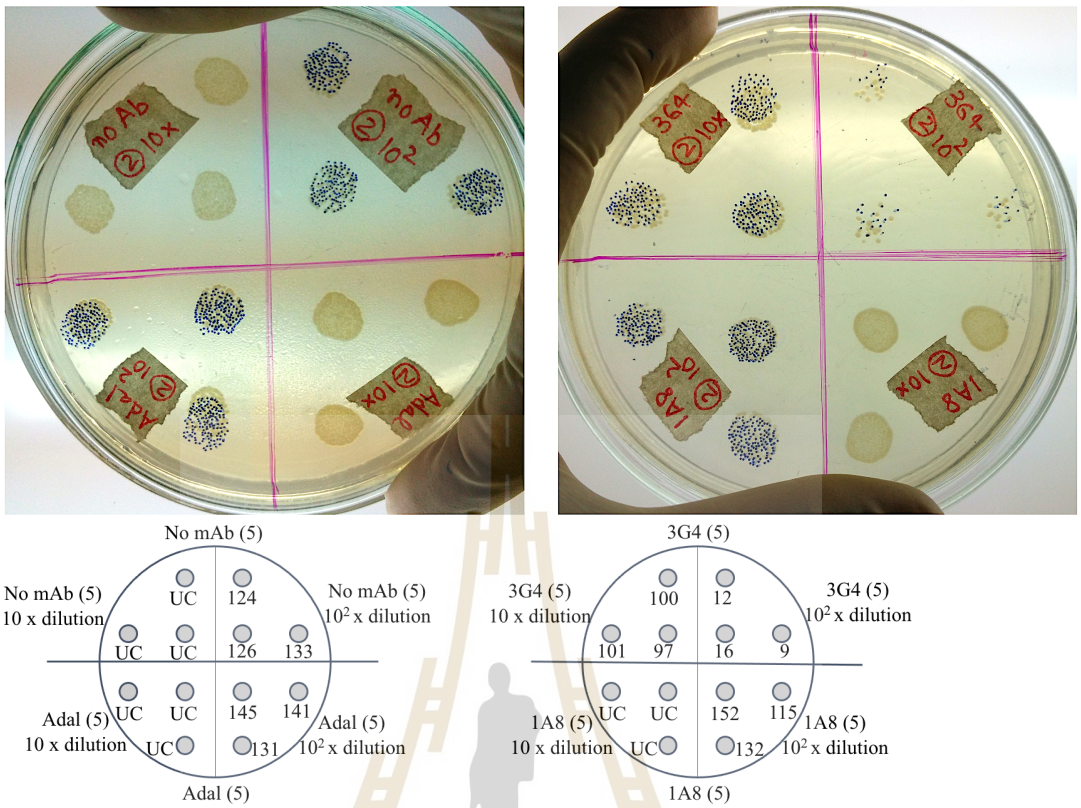


**Figure 6.24 Culture plates and colony counts of assay set 5**

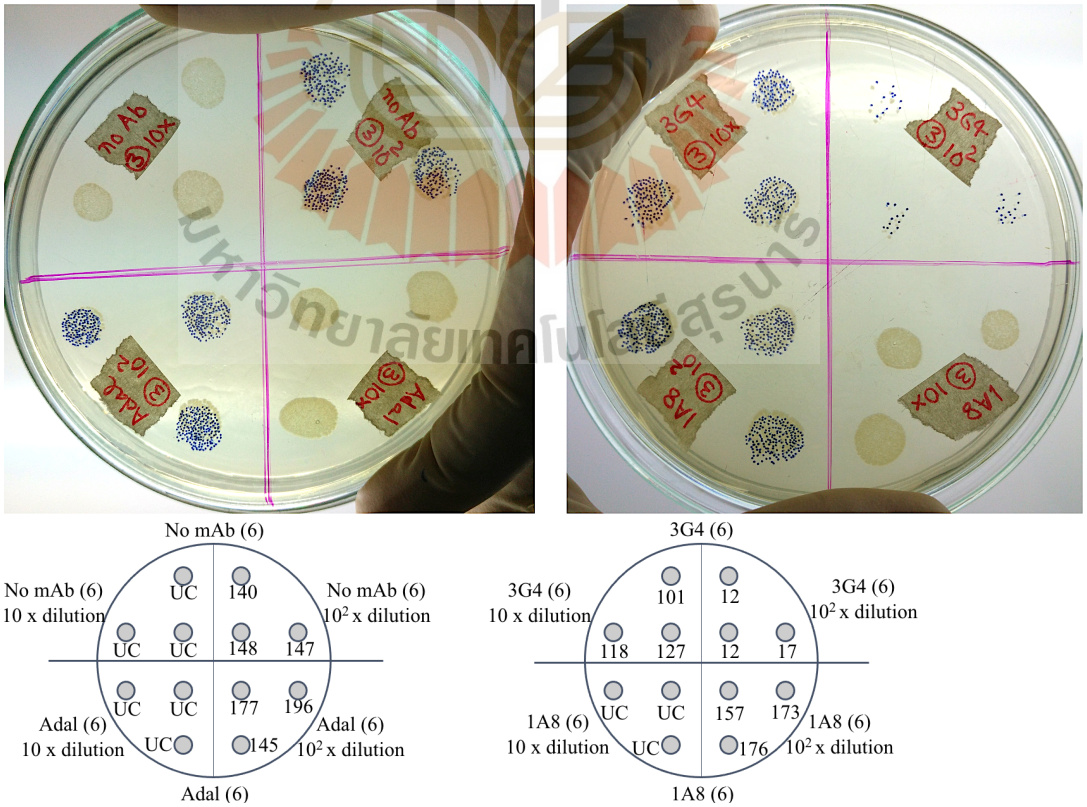


**Figure 6.25 Culture plates and colony counts of assay set 6**

The percentage of viable *P. aeruginosa* left in reaction tubes, in relation to the number of input bacteria (inoculum) were calculated according to Guachalla group (Guachalla et al., 2017). The results were shown in **Table 6.27**.

**Table 6.27** ***P. aeruginosa*** **survival relative to input (inoculum)**

| **Complement-mediated bacteriolysis assay** | **viable *P. aeruginosa* (cfu/mL) left in reaction tube** | **Survival relative to input *P. aeruginosa* (%)** | **Log values of survival (%) relative to input *P. aeruginosa*** |
|---|---|---|---|
| **Assay set (1)** (number of input *P. aeruginosa* = $4.7*10^6$ cfu/mL) | | | |
| no IgG | $6.2*10^5$ | 13.11 | 1.12 |
| Adalimumab | $8.6*10^5$ | 18.19 | 1.26 |
| yPgi3G4 IgG | $5.7*10^4$ | 1.22 | 0.09 |
| yPac1A8 IgG | $7.6*10^5$ | 16.23 | 1.21 |
| **Assay set (2)** (number of input *P. aeruginosa* = $3.1*10^6$ cfu/mL) | | | |
| no IgG | $4.9*10^5$ | 15.90 | 1.20 |
| Adalimumab | $7.3*10^5$ | 23.65 | 1.37 |
| yPgi3G4 IgG | $3.8*10^4$ | 1.21 | 0.08 |
| yPac1A8 IgG | $6.5*10^5$ | 20.97 | 1.32 |
| **Assay set (3)** (number of input *P. aeruginosa* = $2.16*10^6$ cfu/mL) | | | |
| no IgG | $4.3*10^5$ | 19.77 | 1.30 |
| Adalimumab | $8.5*10^5$ | 39.21 | 1.59 |
| yPgi3G4 IgG | $4.0*10^4$ | 1.85 | 0.27 |
| yPac1A8 IgG | $7.6*10^5$ | 35.32 | 1.55 |
| Assay set (4) (number of input *P. aeruginosa* = $4.8*10^6$ cfu/mL) | | | |
| no IgG | $1.1*10^6$ | 22.50 | 1.35 |
| Adalimumab | $1.2*10^6$ | 25.42 | 1.41 |
| yPgi3G4 IgG | $7.2*10^4$ | 1.50 | 0.18 |
| yPac1A8 IgG | $1.3*10^6$ | 27.71 | 1.44 |
| **Assay set (5)** (number of input *P. aeruginosa* = $5.6*10^6$ cfu/mL) | | | |
| no IgG | $1.3*10^6$ | 22.86 | 1.36 |
| Adalimumab | $1.4*10^6$ | 24.82 | 1.39 |
| yPgi3G4 IgG | $9.9*10^4$ | 1.77 | 0.25 |
| yPac1A8 IgG | $1.3*10^6$ | 23.75 | 1.38 |
| **Assay set (6)** (number of input *P. aeruginosa* = $5.3*10^6$ cfu/mL) | | | |
| no IgG | $1.5*10^6$ | 27.36 | 1.44 |
| Adalimumab | $1.7*10^6$ | 32.64 | 1.51 |
| yPgi3G4 IgG | $1.2*10^5$ | 2.17 | 0.34 |
| yPac1A8 IgG | $1.7*10^6$ | 31.89 | 1.50 |

Statistical analysis of data from six independent complement-mediated bacteriolysis assays was performed by using Prism version 8 (GraphPad Software, U.S.A). Ordinary one-way ANOVA with Tukey's multiple comparisons test was performed. The number of viable *P. aeruginosa* cells was significantly less when they were exposed to specific antibody-depleted human serum and yPgi3G4 IgG than when exposed to serum alone or serum together with non-specific IgG, such as, yPac1A8 IgG or adalimumab. The Tukey's multiple comparisons test result was shown in **Table 6.28**.

**Table 6.28 Tukey's multiple comparisons test result of complement-mediated bacteriolysis assay**

| Tukey's multiple comparisons test | Mean Difference | 95.00% CI of difference | Significant? | Summary | Adjusted P Value |
|---|---|---|---|---|---|
| no IgG vs. Adalimumab | -0.1296 | -0.3156 to 0.05639 | No | ns | 0.2397 |
| no IgG vs. yPgi3G4 IgG | 1.094 | 0.9083 to 1.280 | Yes | **** | <0.0001 |
| no IgG vs. yPac1A8 IgG | -0.1064 | -0.2924 to 0.07952 | No | ns | 0.3999 |
| Adalimumab vs. yPgi3G4 IgG | 1.224 | 1.038 to 1.410 | Yes | **** | <0.0001 |
| Adalimumab vs. yPac1A8 IgG | 0.02314 | -0.1628 to 0.2091 | No | ns | 0.9851 |
| yPgi3G4 IgG vs. yPac1A8 IgG | -1.201 | -1.387 to -1.015 | Yes | **** | <0.0001 |

By using Prism version 8, the log values of survival (%) relative to input *P. aeruginosa* numbers were plotted against the type of IgG added into the assay system. The resultant graph was shown at **Figure 6.26**.

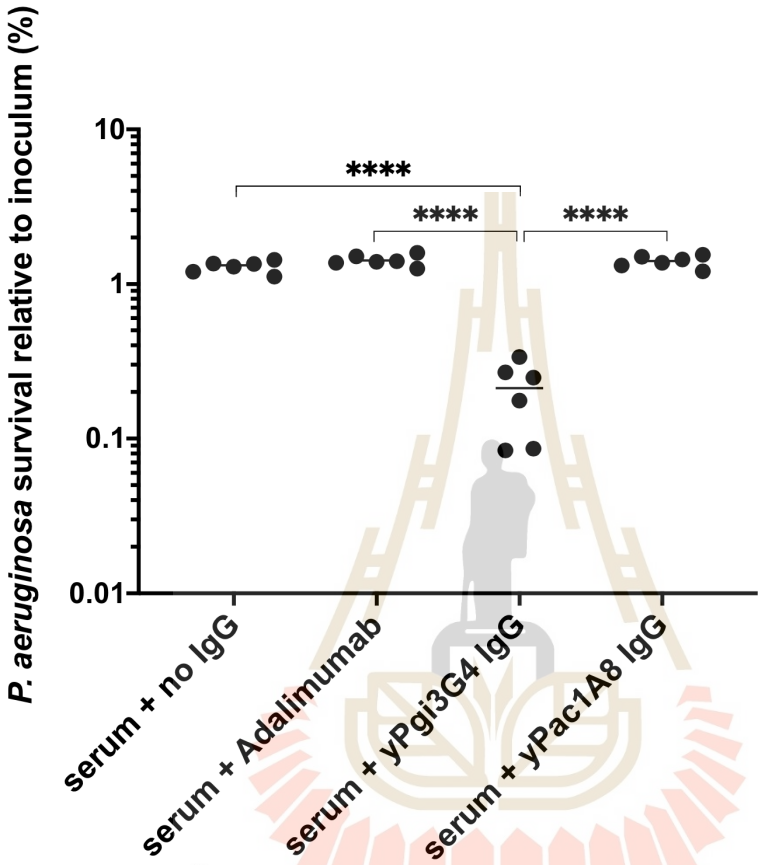


**Figure 6.26** ***P. aeruginosa* survival relative to inoculum (%) in four different treatment settings.**

The treatment settings are: (1) depleted-diluted-pooled human serum alone and no IgG, (2) depleted-diluted-pooled human serum and non-specific IgG control (Adalimumab), (3) depleted-diluted-pooled human serum and *P. aeruginosa*-specific IgG (yPgi3G4 IgG), and (4) depleted-diluted-pooled human serum and non-specific antibacterial IgG control (yPac1A8 IgG). P values were <0.0001 when confidence level was set at 0.05.

Enhancement of complement-mediated bacterial clearance by recombinant IgG has been documented previously (Guachalla et al., 2017). Guachalla group used humanized murine mAb IgG (κ) and tested its action on complement-mediated bacteriolysis of *E. coli*.

### 6.4.9 Antibody-dependent cellular phagocytosis assay

#### 6.4.9.1 Heat-inactivation of *P. aeruginosa* and *P. acnes*

Heat-inactivated *P. aeruginosa* DMST 37186 (1.05 x $10^{10}$ cells/mL) and *P. acnes* DMST 14916 (1.09 x $10^{10}$ cfu/mL) are used as bacterial challenge. Intermediate stocks of $10^8$ cells/mL *P. acnes* and *P. aeruginosa* are prepared so that the final concentration of *P. acnes* and *P. aeruginosa* in the assay is $10^7$ cells/mL.

#### 6.4.9.2 THP-1 cells treated with vitamin $D_3$

In this study, THP-1 (Tohoku Hospital Pediatrics-1) cell line is used as the source of human macrophage. THP-1 cells are stimulated with 0.24 µM Vitamin $D_3$ for 72 h to differentiate into macrophages.

มหาวิทยาลัยเทคโนโลยีสุรนารี

#### 6.4.9.3 yPac1A8 and yPgi3G4 IgG

Recombinant full-length IgG, yPac1A8 (*P. acnes* specific) and yPgi3G4 (*P. aeruginosa* specific) are tested. They serve as IgG isotype control for each other. The intermediate stocks of 20 µg/mL are used to get 2 µg/mL concentration in the assay.

#### 6.4.9.4 THP-1 cells challenged with bacteria

At the end of Vitamin $D_3$ treatment, THP-1 cells have viable count of 1.95 x $10^6$ cells/mL and 82.3% viability. One assay set uses seven THP-1 containing wells for seven different treatment settings which are (1) THP-1 cells incubated in RPMI 1640 medium without any challenge (negative control), (2) THP-1 cells incubated with *P. aeruginosa* $10^7$ cells/mL (positive control), (3) THP-1 cells incubated with *P. aeruginosa* $10^7$ cells/mL and yPac1A8 IgG (IgG isotype control), (4) THP-1 cells incubated with *P. aeruginosa* $10^7$ cells/mL and yPgi3G4 IgG, (5) THP-1 cells incubated with *P. acnes* $10^7$ cells/mL (positive control), (6) THP-1 cells incubated with *P. acnes* $10^7$ cells/mL and yPac1A8 IgG, and (7) THP-1 cells incubated with *P. acnes* $10^7$ cells/mL and yPgi3G4 IgG (IgG isotype control).

#### 6.4.9.5 Duration of bacterial challenge and sample collection

Incubation of the first 24-well plate is stopped at 30 min, the second one at 4 h and the last one at 24 h, respectively. Phase-contrast pictures of cells are taken with 20X PH objective of EVOS XL Core imaging system (see section 6.4.9.6). Culture supernatant are kept for chemokine analysis. Cover glasses at the bottom of the wells are immunostained (see section 6.4.9.7).

#### 6.4.9.6 Phase contrast microscopy of THP-1 cells

Phase-contrast pictures of THP-1 cells are arranged as three columns (30 min, 4 h and 24 h incubations) in **Figure 6.27** and **Figure 6.28**. The incubation times are written on the top of the columns and the treatment conditions are written on the left of the columns.

In **Figure 6.27**, there is less *P. acnes* cells in intercellular spaces in the middle panel (THP-1 cells+*P. acnes*+ yPac1A8 IgG) than the upper and lower panels. That decrease in *P. acnes* cells was visible at 4 h and 24 h incubations. It suggests that starting from 4 h time point, the clearance of *P. acnes* by THP-1 cells is obviously greater in the presence of specific IgG (yPac1A8) than *P. acnes* alone or *P. acnes* with non-specific IgG (yPgi3G4) conditions.

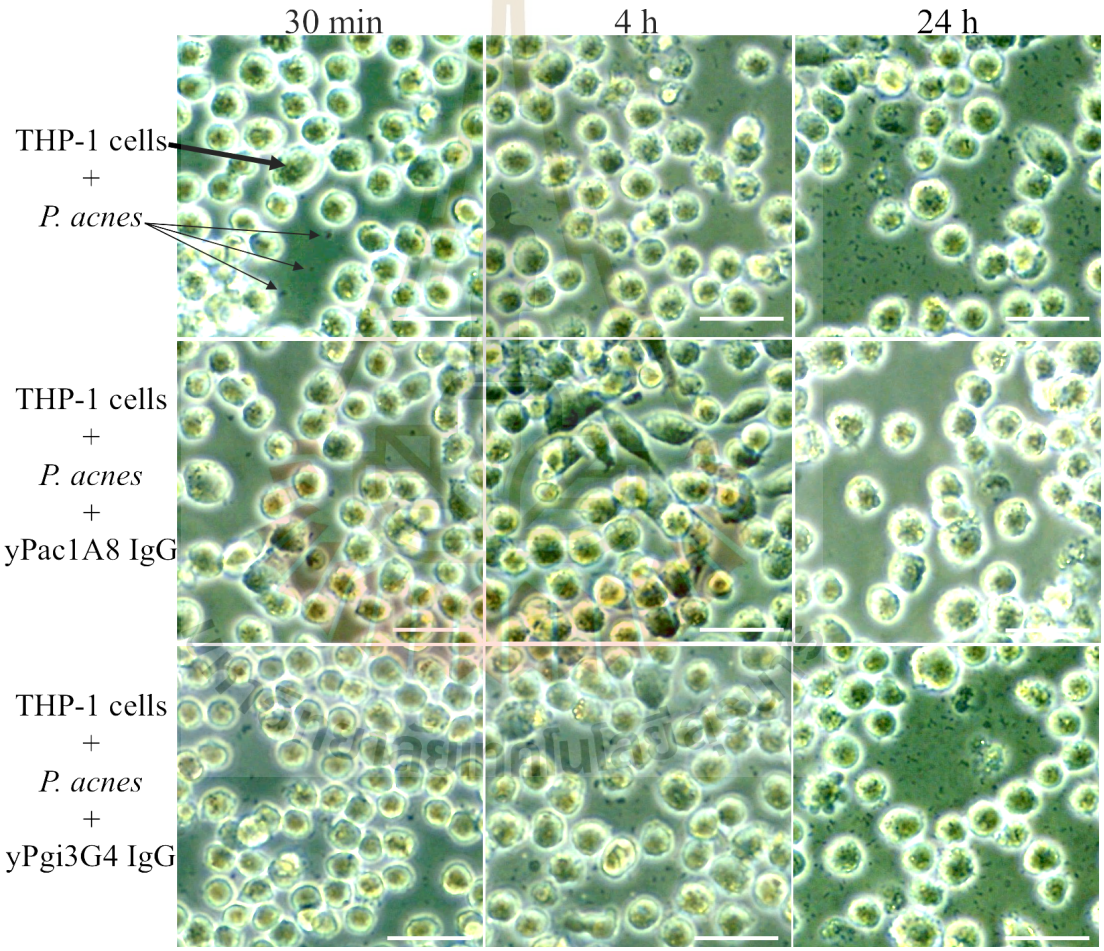


**Figure 6.27 Phase-contrast pictures of THP-1 cells (thick arrow) challenged with *P. acnes* (thin arrows).**

Pictures are taken with 20X PH objective of EVOS XL Core imaging system. Scale bars represent 50 μm.

In **Figure 6.28**, there is less *P. aeruginosa* cells in intercellular spaces in the lowest panel (THP-1 cells+*P. aeruginosa*+ yPgi3G4 IgG) than the upper two panels. That decrease in *P. aeruginosa* cells is visible at 24 h incubation. It suggests that starting from 24 h time point, the clearance of *P. aeruginosa* by THP-1 cells is obviously greater in the presence of specific IgG (yPgi3G4) than *P. aeruginosa* alone or *P. aeruginosa* with non-specific IgG (yPac1A8) conditions.

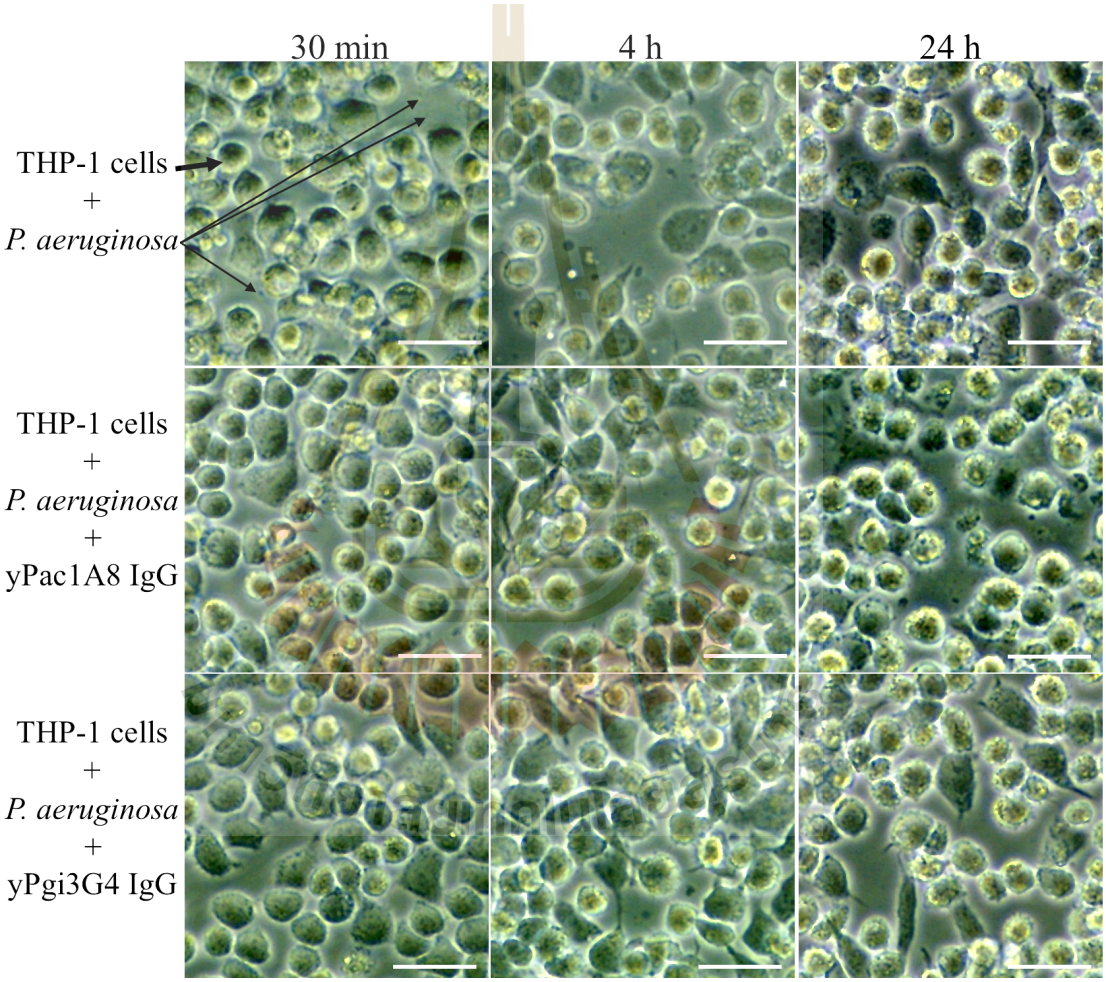


**Figure 6.28 Phase-contrast pictures of THP-1 cells (thick arrow) challenged with *P. aeruginosa* (thin arrows).**

Pictures are taken with 20X PH objective of EVOS XL Core imaging system. Scale bars represent 50 μm.

#### 6.4.9.7 Immunofluorescence staining of THP-1 cells and bacteria

Cover glasses at the bottom of the wells, which are added before THP-1 cell seeding, are seen attached with THP-1 cell layer from 30 min time point onwards. THP-1 cells on cover glasses are checked for the presence of *P. aeruginosa* or *P. acnes* by scFv immunofluorescent staining as previously described in chapter III. *P. aeruginosa* cells are detected by 6xHis-tagged yPgi3G4 scFv and *P. acnes* cells by 6xHis-tagged yPac1A8 scFv, respectively. The cells-scFv complexes are stained with Dylight 488-labelled anti-hexa-histidine mouse monoclonal antibody. The nuclei of THP-1 cells are stained with DAPI. The cover glasses are examined by confocal laser scanning microscopy.

Three sets of confocal microscpy pictures of THP-1 cells challenged with *P. acnes* are arranged into **Figure 6.29, 6.30** and **6.31**. The three columns represent three incubation time points (30 min, 4 h, and 24 h) which are written on the top of the columns. The treatment conditions are written on the left of the columns. Three sets of confocal microscpy pictures of THP-1 cells challenged with *P. aeruginosa* are arranged into **Figure 6.32, 6.33** and **6.34**. The columns are arranged in the same way as written above.

In **Figure 6.29, 6.30** and **6.31**, there is more *P. acnes* cells (green structures) in THP-1 cells treated with *P. acnes* in the presence of yPac1A8 IgG (middle panel) than the controls (upper and lower panels), particularly at 4 h incubation. It suggests that yPac1A8 IgG-dependent phagocytosis of *P. acnes* cells by THP-1 macrophages is best seen around 4 h incubation. This finding is supportive to the phase contrast microscopy result of **Figure 6.27**. The phase contrast microscopy and confocal microscopy results strongly suggest that yPac1A8 IgG-dependent phagocytosis of *P.*

*acnes* cells by THP-1 macrophages has taken place and that can be documented around 4 h incubation time.

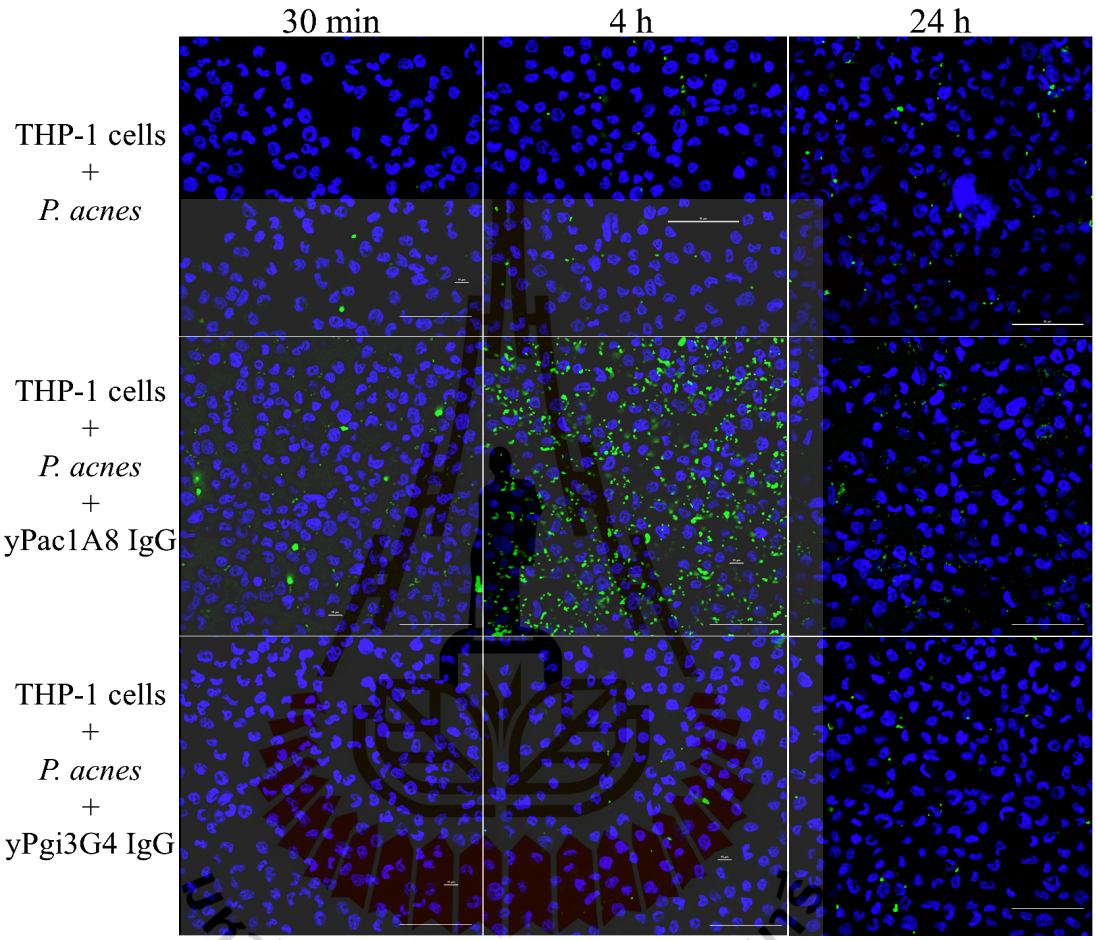


**Figure 6.29 First set of confocal microscopy images of THP-1 and *P. acnes* experiment.**

Three challenge conditions (stated on left side of pictures) are compared at three time points (30 min, 4 h and 24 h). Nucleus of THP-1 cells are stained blue by DAPI. *P. acnes* are stained green by yPac1A8 scFv and Dylight 488-labelled anti-hexa-histidine antibody. Pictures are taken with Apo TIRF 60x Oil DIC N2 objective of Nikon A1R confocal laser microscope. Scale bars represent 50 μm.

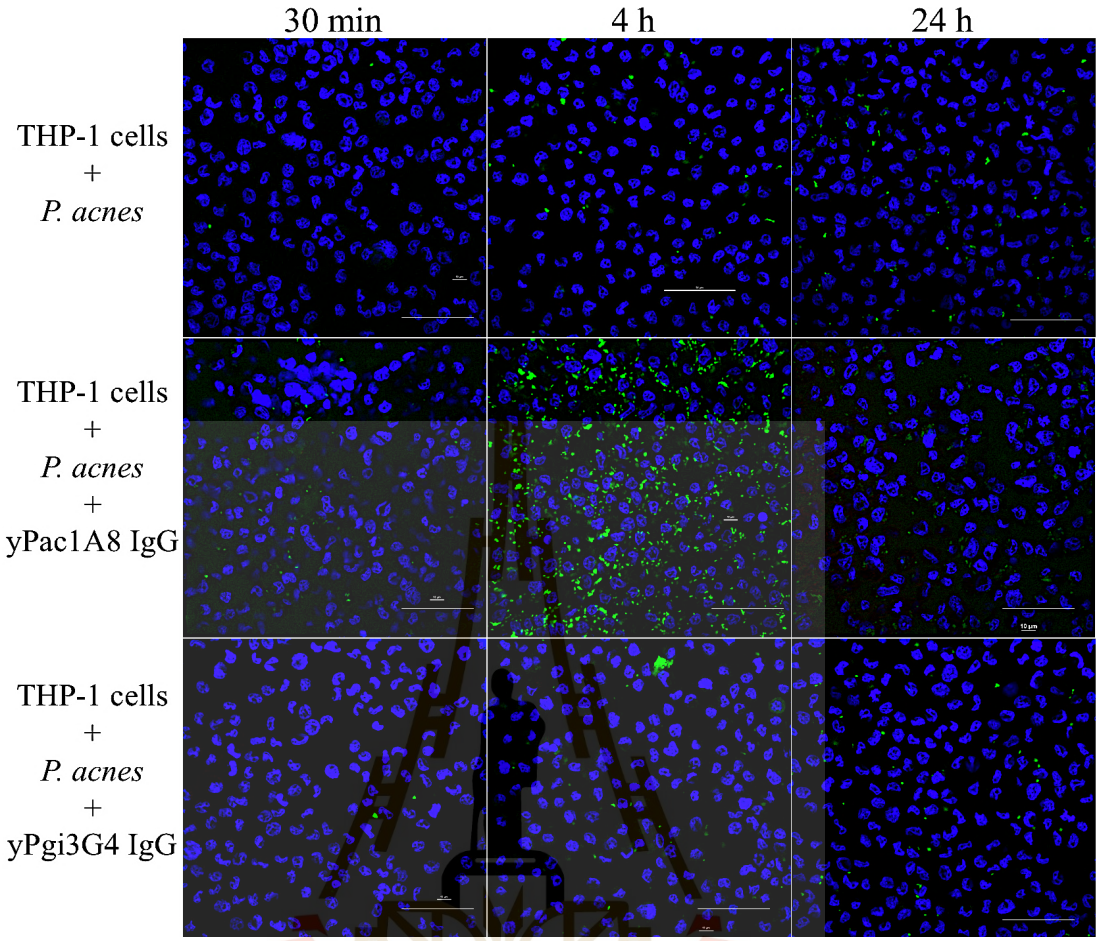


**Figure 6.30 Second set of confocal microscopy images of THP-1 and *P. acnes* experiment.**

Three challenge conditions (stated on left side of pictures) are compared at three time points (30 min, 4 h and 24 h). Nucleus of THP-1 cells are stained blue by DAPI. *P. acnes* are stained green by yPac1A8 scFv and Dylight 488-labelled anti-hexa-histidine antibody. Pictures are taken with Apo TIRF 60x Oil DIC N2 objective of Nikon A1R confocal laser microscope. Scale bars represent 50 µm.

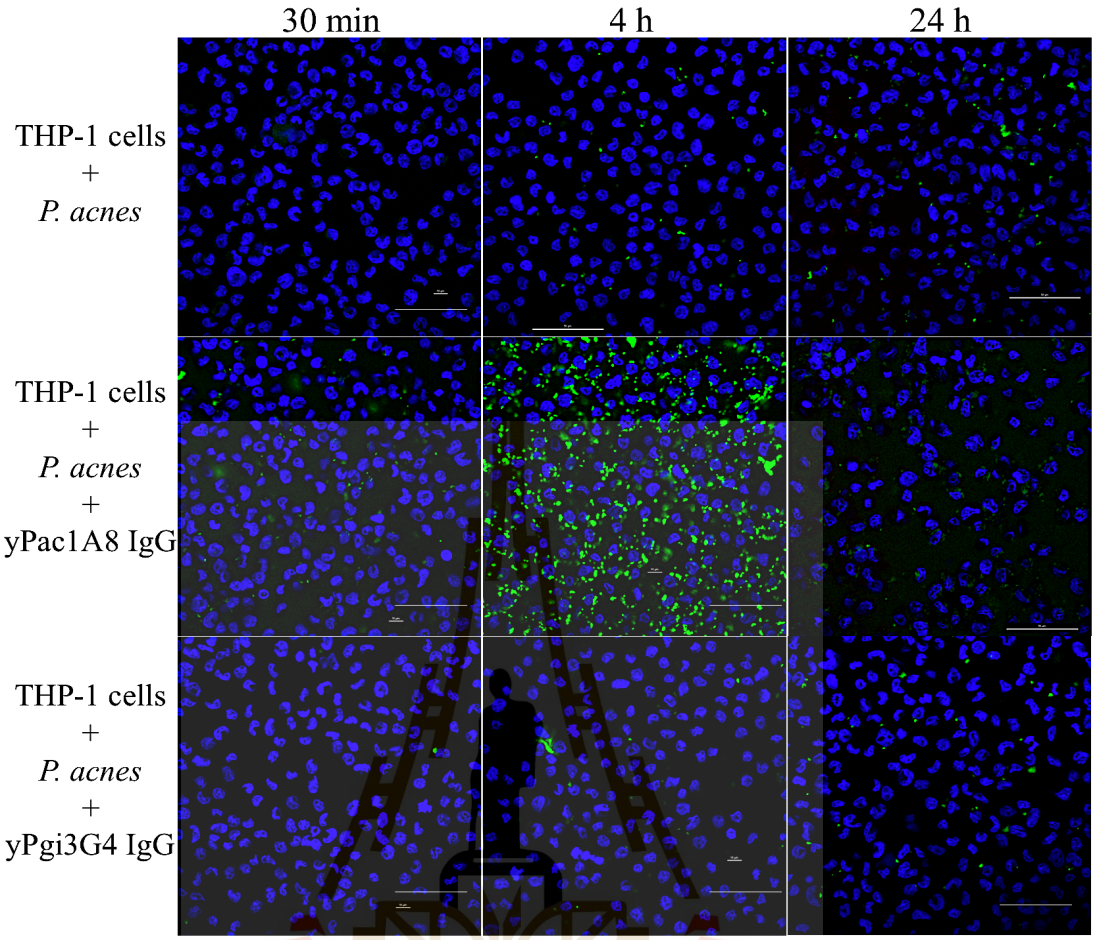


**Figure 6.31 Third set of confocal microscopy images of THP-1 and *P. acnes* experiment.**

Three challenge conditions (stated on left side of pictures) are compared at three time points (30 min, 4 h and 24 h). Nucleus of THP-1 cells are stained blue by DAPI. *P. acnes* are stained green by yPac1A8 scFv and Dylight 488-labelled anti-hexa-histidine antibody. Pictures are taken with Apo TIRF 60x Oil DIC N2 objective of Nikon A1R confocal laser microscope. Scale bars represent 50 µm.

In **Figure 6.32, 6.33** and **6.34**, there is more *P. aeruginosa* cells (green structures) in THP-1 cells treated with *P. aeruginosa* in the presence of yPgi3G4 IgG (lowest panel) than the controls (upper two panels), particularly at 24 h incubation. This finding is supportive to the phase contrast microscopy result of **Figure 6.28**. The phase contrast microscopy and confocal microscopy results strongly suggest that yPgi3G4 IgG-dependent phagocytosis of *P. aeruginosa* cells by THP-1 macrophages has taken place and that can be documented around 24 h incubation time.

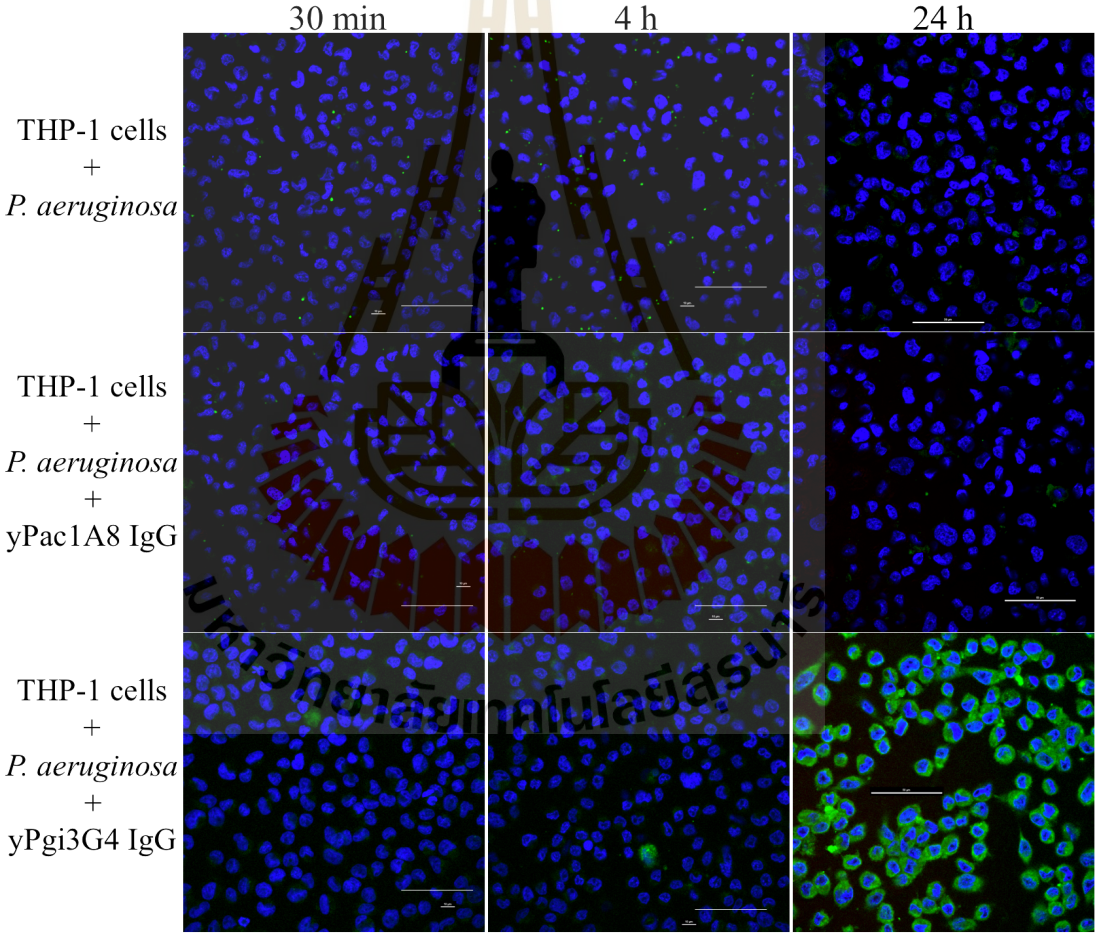


**Figure 6.32 First set of confocal microscopy images of THP-1 and *P. aeruginosa* experiment.**

Three challenge conditions (stated on left side of pictures) are compared at three time points (30 min, 4 h and 24 h). Nucleus of THP-1 cells are

stained blue by DAPI. *P. aeruginosa* are stained green by yPgi3G4 scFv and Dylight 488-labelled anti-hexa-histidine antibody. Pictures are taken with Apo TIRF 60x Oil DIC N2 objective of Nikon A1R confocal laser microscope. Scale bars represent 50 µm.

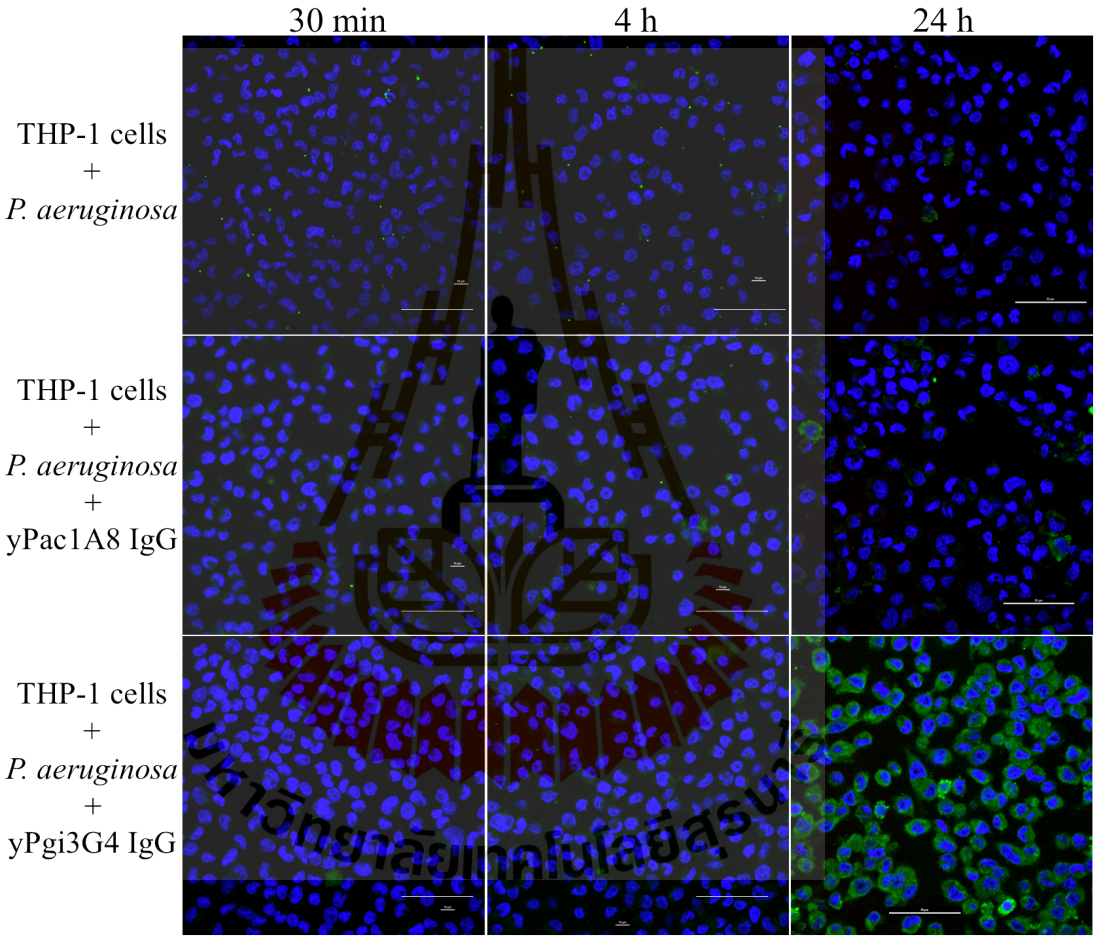


**Figure 6.33 Second set of confocal microscopy images of THP-1 and *P. aeruginosa* experiment.**

Three challenge conditions (stated on left side of pictures) are compared at three time points (30 min, 4 h and 24 h). Nucleus of THP-1 cells are stained blue by DAPI. *P. aeruginosa* are stained green by yPgi3G4 scFv and Dylight 488-labelled anti-hexa-histidine antibody. Pictures are

taken with Apo TIRF 60x Oil DIC N2 objective of Nikon A1R confocal laser microscope. Scale bars represent 50 µm.

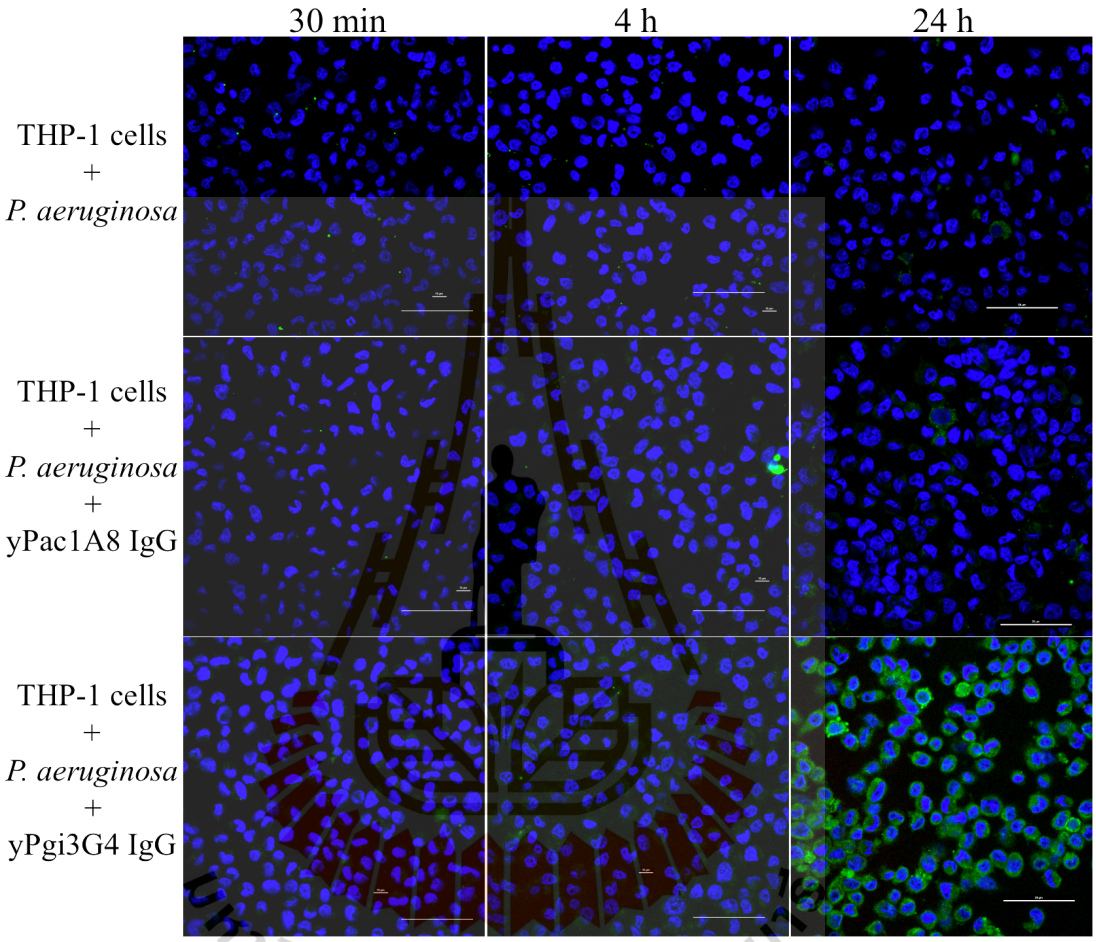


**Figure 6.34 Third set of confocal microscopy images of THP-1 and *P. aeruginosa* experiment.**

Three challenge conditions (stated on left side of pictures) are compared at three time points (30 min, 4 h and 24 h). Nucleus of THP-1 cells are stained blue by DAPI. *P. aeruginosa* are stained green by yPgi3G4 scFv and Dylight 488-labelled anti-hexa-histidine antibody. Pictures are taken with Apo TIRF 60x Oil DIC N2 objective of Nikon A1R confocal laser microscope. Scale bars represent 50 µm.

The immunofluorescence results are supportive of phase contrast microscopy results. Phagocytosis of *P. acnes* and *P. aeruginosa* by THP-1 macrophages is enhanced by specific recombinant full-length IgG, yPac1A8 and yPgi3G4, respectively. According to the immunostain patten obtained, the phagocytosis pathway and intracellular fate of *P. acnes* and *P. aeruginosa* in THP-1 macrophages seem to be different. *P. acnes* clearance starts much earlier than that of *P. aeruginosa*.

Guachalla group used murine macrophage cells (RAW 264.7), human serum, humanized murine IgG under testing and alive *E. coli* cells to perform opsonophagocytosis assay. They measured the outcome by performing viable count and suggested the possible complement receptor mediated opsonophagocytosis (Guachalla et al., 2017). We didn't use complement proteins or serum and studied the direct involvement of yPac1A8 and yPgi3G4 IgG in *P. acnes* and *P. aeruginosa* clearance by human macrophage cells (THP-1). The outcome was checked qualitatively by immunoflourescence staining and the result is suggestive of IgG receptor mediated enhancement of phagocytosis.

Rossmann group identified complement enhancing mAb against *Enterococcus faecalis* by human B cell selection (Rossmann et al., 2015). Complement is a complex protein cascade of the innate immune system. Complement activation results in the rapid clearance of bacteria in two ways. The activated complement complex can make large pores in bacteria cell wall. Complement components can opsonize bacteria for immune cells (Heesterbeek, Angelier, Harrison, & Rooijakkers, 2018). Antibodies that can augment complement-dependent bacteriolysis are of interest for treatment of antibiotic-resistant bacteria.

### 6.4.10 Interleukin-8 (IL-8) ELISA

Cell culture supernatant of THP-1 experiments (24 h incubation) in section 6.4.9 are tested for the presence of human IL-8. In IL-8 ELISA, duplicates of each sample are tested and the average values are used for data analysis. Statistical analysis of data was performed by using Prism version 8 (GraphPad Software, U.S.A). Ordinary one-way ANOVA with Tukey's multiple comparisons test was performed. The IL-8 ELISA result of THP-1 and *P. acnes* experiments are shown in **Figure 6.35** and **Table 6.29**. The IL-8 ELISA result of THP-1 and *P. aeruginosa* experiments can be seen in **Figure 6.36** and **Table 6.30**.

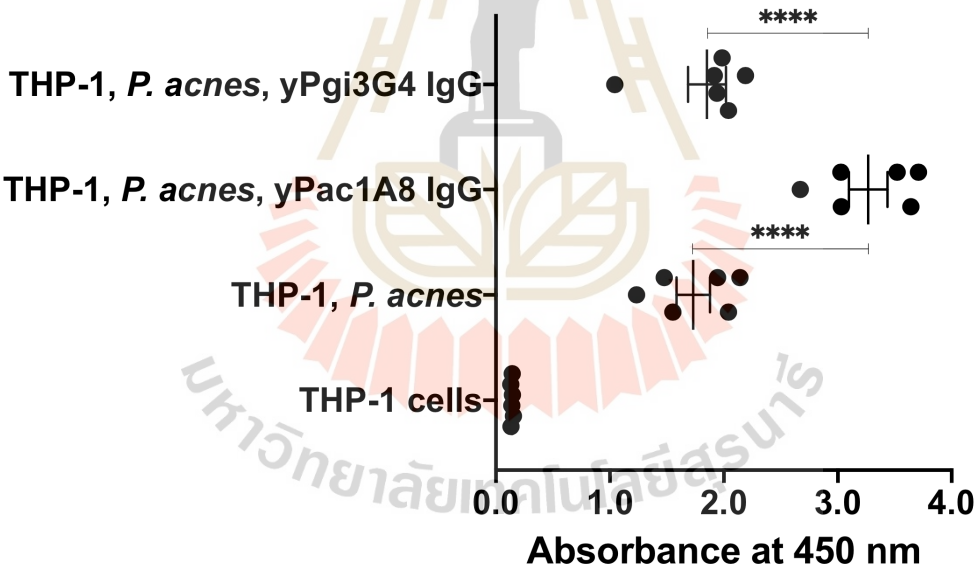


**Figure 6.35 Comparison of IL-8 response (*P. acnes* experiment).**

IL-8 ELISA was performed for six samples. Duplicates of each sample are tested for the presence of IL-8 and the average values are used for data analysis. The error bars indicate the standard error of the mean (SEM).

**Table 6.29 Tukey's multiple comparisons test result of THP-1 and *P. acnes* experiment (six repeats)**

| Tukey's multiple comparisons test | Mean Diff. | 95.00% CI of diff. | Signifi-cant | Summary | Adjusted P Value |
|---|---|---|---|---|---|
| THP-1 cells vs. (THP-1, *P. acnes*) | -1.591 | -2.146 to -1.036 | Yes | **** | <0.0001 |
| THP-1 cells vs. (THP-1, *P. acnes*, yPac1A8 IgG) | -3.126 | -3.681 to -2.571 | Yes | **** | <0.0001 |
| THP-1 cells vs. THP-1, *P. acnes*, yPgi3G4 IgG) | -1.711 | -2.266 to -1.157 | Yes | **** | <0.0001 |
| (THP-1, *P. acnes*) vs. (THP-1, *P. acnes*, yPac1A8 IgG) | -1.535 | -2.090 to -0.9802 | Yes | **** | <0.0001 |
| (THP-1, *P. acnes*) vs. (THP-1, *P. acnes*, yPgi3G4 IgG) | -0.1206 | -0.6754 to 0.4342 | No | ns | 0.9282 |
| (THP-1, *P. acnes*, yPac1A8 IgG) vs. (THP-1, *P. acnes*, yPgi3G4 IgG) | 1.414 | 0.8596 to 1.969 | Yes | **** | <0.0001 |

IL-8 level is significantly higher when THP-1 cells are exposed to *P. acnes* in the presence of specific IgG, that is yPac1A8 than when THP-1 faced *P. acnes* alone or in the presence of non-specific IgG, that is yPgi3G4.

มหาวิทยาลัยเทคโนโลยีสุรนารี

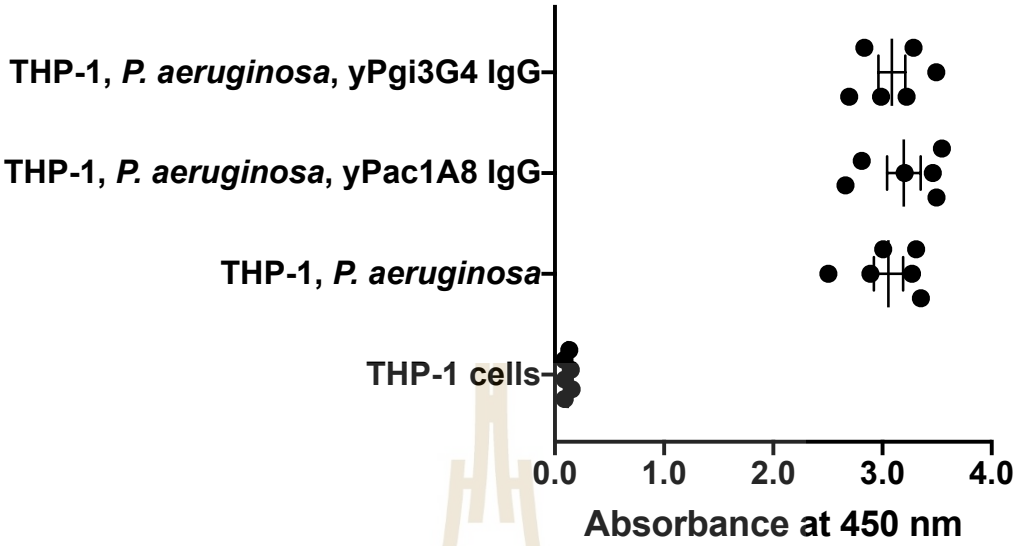


**Figure 6.36 Comparison of IL-8 response (*P. aeruginosa* experiment).** IL-8 ELISA was performed for six samples. Duplicates of each sample are tested for the presence of IL-8 and the average values are used for data analysis. The error bars indicate the standard error of the mean (SEM).

มหาวิทยาลัยเทคโนโลยีสุรนารี

**Table 6.30 Tukey's multiple comparisons test result of six THP-1 and *P. aeruginosa* experiment (six repeats)**

| Tukey's multiple comparisons test | Mean Diff. | 95.00% CI of diff. | Signifi-cant | Summary | Adjusted P Value |
|---|---|---|---|---|---|
| THP-1 cells vs. (THP-1, *P. aeruginosa*) | -2.938 | -3.410 to -2.467 | Yes | **** | <0.0001 |
| THP-1 cells vs. (THP-1, *P. aeruginosa*, yPac1A8 IgG) | -3.079 | -3.551 to -2.607 | Yes | **** | <0.0001 |
| THP-1 cells vs. (THP-1, *P. aeruginosa*, yPgi3G4 IgG) | -2.969 | -3.441 to -2.497 | Yes | **** | <0.0001 |
| (THP-1, *P. aeruginosa*) vs. (THP-1, *P. aeruginosa*, yPac1A8 IgG) | -0.1408 | -0.6125 to 0.3309 | No | ns | 0.8369 |
| (THP-1, *P. aeruginosa*) vs. (THP-1, *P. aeruginosa*, yPgi3G4 IgG) | -0.03058 | -0.5023 to 0.4411 | No | ns | 0.9978 |
| (THP-1, *P. aeruginosa*, yPac1A8 IgG) vs. (THP-1, *P. aeruginosa*, yPgi3G4 IgG) | 0.1103 | -0.3614 to 0.5819 | No | ns | 0.9128 |

Unlike *P. acnes* experiment result, there is no significant difference in IL-8 level in THP-1 and *P. aeruginosa* experiments. It remains high in all three experiment conditions, which are (1) THP-1 cells exposed to *P. aeruginosa* in the presence of specific IgG, that is yPgi3G4, (2) THP-1 cells exposed to *P. aeruginosa* in the presence of non-specific IgG, that is yPac1A8, and (3) THP-1 cells exposed to *P. aeruginosa* only. Possibly, IL-8 production in *P. aeruginosa* infection is stimulated by several antigens through different receptors and IL-8 level is highly independent of the presence of specific IgG (yPgi3G4).

As it has been confirmed in chapter III, yPac1A8 and yPgi3G4 bind to cell surface antigen of *P. acnes* and *P. aeruginosa*, respectively. Antibodies that can directly bind to bacterial cell surfaces are favourable for antibody-based interventions. They can be blocking antibodies and interfere the colonization or be opsonizing

antibodies and augment the bacterial clearance by immune system (Bebbington & Yarranton, 2008). Considering the experiments, we have done so far, yPac1A8 and yPgi3G4 IgG could work as opsonizing antibodies in between target bacteria and human macrophage cells. In case of yPgi3G4 IgG, it can enhance the complement-mediated bacteriolysis of *P. aeruginosa* cells.

## 6.5 Conclusion and future perspectives

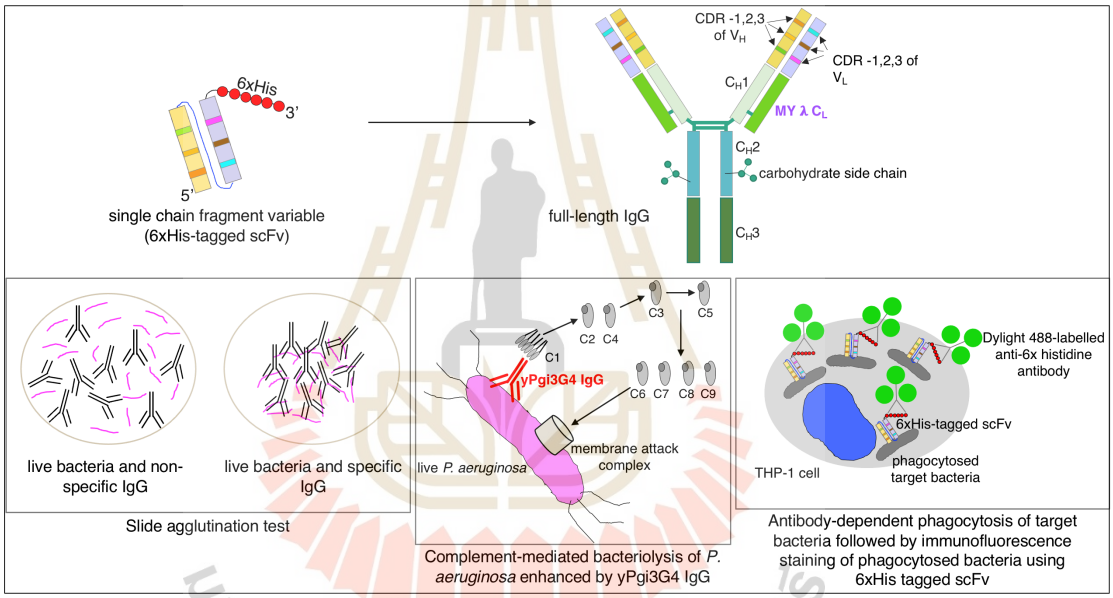


**Figure 6.37 Summary of chapter VI**

The summary of chapter VI is illustrated in **Figure 6.37**. In this chapter, two Single Chain Fragment Variable (scFv), yPac1A8 and yPgi3G4, targeting *P. acnes* and *P. aeruginosa*, respectively, are engineered into full-length IgG1 subclass antibodies. IgG heavy chain and light chain vectors and IgG expression platform of MY LAB are used to produce yPac1A8 and yPgi3G4 IgG. The unique characteristic of MY LAB IgG light chain plasmid is that it contains the λ light chain constant region of Professor

Montarop Yamabhai, the director of MY LAB. The full-length IgG1 yPac1A8 and yPgi3G4 are successfully expressed with the production range of 85-195 mg/L. Their functionality is confirmed by using them to aggregate the live target bacteria in slide agglutination test. Anti-*P. aeruginosa* IgG (yPgi3G4 IgG) is used to augment the complement-mediated bacteriolysis of *P. aeruginosa* which is an important non-specific defence arm of our body. Both, anti-*P. aeruginosa* yPgi3G4 IgG and anti-*P. acnes* yPac1A8 IgG are used to initiate the antibody-dependent phagocytosis of target bacteria by human macrophage cells (THP-1). Overall, the results suggest that (1) both IgG can do opsonization of target bacteria and facilitate the phagocytosis pathway, (2) the two IgG might not use the same IgG receptor type and (3) the intracellular fate of *P. acnes* and *P. aeruginosa* in human macrophage might be different. In order to prove these facts, a number of experiments have to be done. Opsonophagocytosis mechanism should be clarified more by using macrophage cell surface stains and intracellular compartment tracking. It is really two different intracellular pathways or two different time points of the same pathway has to be confirmed by checking at several time points, especially between 4 h and 24 h incubation or even beyond 24 h. The fact that *P. acnes* and yPac1A8 IgG can induce THP-1 cells to produce extra IL-8, and *P. aeruginosa* and yPgi3G4 IgG can’t is also another important information to consider.

# CHAPTER VII

# CONCLUSION

*P. acnes* DMST 14916 and *P. aeruginosa* DMST 37186 were used as targets and Yamo-I human scFv display phage library of MY LAB was used as source of scFv antibody fragments for affinity selection (biopanning). Three scFv clones for *P. acnes* were identified and the best of them (yPac1A8 scFv) was further characterized. One scFv clone for *P. aeruginosa* (yPgi3G4) was identified and it was further analysed. Usefulness of scFv in bioimaging of bacteria was demonstrated. The yPac1A8 scFv could immunoprecipitate its target antigen, CAMP factor 1 from *P. acnes* cells as well as soluble CAMP factor 1 from *P. acnes* broth culture supernatant. Both yPac1A8 and yPgi3G4 scFv were successfully biotinylated and Em-GFP coupled. Both were constructed into full-length IgG antibodies carrying light chain (λ) constant region sequence. The yPgi3G4 IgG could enhance complement-mediated bacteriolysis of *P. aeruginosa*. Both yPgi3G4 and yPac1A8 IgG could agglutinate live target cells, and both could augment the antibody-dependent phagocytosis of *P. aeruginosa* and *P. acnes* by human macrophage cells, respectively. Both yPgi3G4 and yPac1A8 IgG have potential to be developed into antibody therapeutics in the future.

# REFERENCES


Abcam. (2019). Ab48481 human IL-8 ELISA set (without plates). Retrieved from https:// www.abcam.com/human-IL-8-elisa-set-without-plates-ab48481.html

Achermann, Y., Goldstein, E. J., Coenye, T., & Shirtliff, M. E. (2014). *Propionibacterium acnes*: From commensal to opportunistic biofilm-associated implant pathogen. **Clin Microbiol Rev***, 27*(3), 419-440. doi:10.1128/CMR. 000 92-13

Achermann, Y., Sahin, F., Schwyzer, H. K., Kolling, C., Wust, J., & Vogt, M. (2013). Characteristics and outcome of 16 periprosthetic shoulder joint infections. **Infection***, 41*(3), 613-620. doi:10.1007/s15010-012-0360-4

Addgene (2017). Fluorescent Proteins 101: A Desktop Resource. pp1-160.

Ali, S. O., Yu, X. Q., Robbie, G. J., Wu, Y., Shoemaker, K., Yu, L., DiGiandomenico A., Keller A. E., Anude C., Hernandez-Illas M., Bellamy T., Falloon J., Dubovsky F., Jafri, H. S. (2019). Phase 1 study of MEDI3902, an investigational anti-*Pseudomonas aeruginosa* pcrv and psl bispecific human monoclonal antibody, in healthy adults. **Clin Microbiol Infect***, 25*(5), 629 e621-629 e626. doi:10.1016/j.cmi. 2018.08.004

Armstrong, R. R., & Johnson, R. S. (1931). Concentrated antipneumococcal serum in the treatment of lobar pneumonia. **British Medical Journal***, 25*(1), 701-703.

Babb, R., & Pirofski, L. A. (2017). Help is on the way: Monoclonal antibody therapy for multi-drug resistant bacteria. **Virulence**, 8(7), 1055-1058. doi:10.1080/ 21505594.2017.1306620

Backmann, N., Zahnd, C., Huber, F., Bietsch, A., Pluckthun, A., Lang, H. P., Guntherodt, H. J., Hegner, M.Gerber, C. (2005). A label-free immunosensor array using single-chain antibody fragments. **Proc Natl Acad Sci U S A**, *102*(41), 14587-14592. doi:10.1073/ pnas.0504917102

Banzon, J. M., Rehm, S. J., Gordon, S. M., Hussain, S. T., Pettersson, G. B., & Shrestha, N. K. (2017). *Propionibacterium acnes* endocarditis: A case series. **Clin Microbiol Infect**, *23*(6), 396-399. doi:10.1016/j.cmi.2016.12.026

Bassan, H. F. (1905). Tuberculosis treated by marmorek's serum. **Hospital**, *39*(998), 100.

Bebbington, C., & Yarranton, G. (2008). Antibodies for the treatment of bacterial infections: Current experience and future prospects. **Curr Opin Biotechnol**, *19*(6), 613-619. doi:10.1016/j.copbio.2008.10.002

Berkmen, M. (2012). Production of disulfide-bonded proteins in *Escherichia coli*. **Protein Expression and Purification**, *82*, 240-251. doi:10.1016/j.pep.2011. 10. 009

Bezabeh, B., Fleming, R., Fazenbaker, C., Zhong, H., Coffman, K., Yu, X. Q., Leow C. C., Gibson N., Wilson S., Stover C. K., Wu H., Gao C., Dimasi, N. (2017). Insertion of scfv into the hinge domain of full-length IgG1 monoclonal antibody results in tetravalent bispecific molecule with robust properties. **MAbs**, *9*(2), 240-256. doi:10.1080/19420862.2016.1270492

Bio-Rad. (2017). ELISA basics guide. Retrieved from https://www.bio-rad-antibodies .com

Boster-Bio. (2017). ELISA handbook. Retrieved from https://www.bosterbio.com/ newsletter-archive/20170616-checkerboard-titration#

Bournazos, S., Gupta, A., & Ravetch, J. V. (2020). The role of IgG Fc receptors in antibody-dependent enhancement. **Nat Rev Immunol**, *20*(10), 633-643. doi:10. 1038/s41577-020-00410-0

Brochet, X., Lefranc, M.-P., & Giudicelli, V. r. (2008). IMGT/V-Quest: The highly customized and integrated system for IG and TR standardized V-J and V-D-J sequence analysis. **Nucleic Acids Research**, *36*, 503-508.

Bronfenbrenner, J. J., & Weiss, H. (1923). The effect of anesthesia and of sedatives on the serum therapy of experimental botulism. **Journal of Experimental medicine**, *39*(4), 517-532.

Bruce, R. M. (1909). Note on five cases of typhoid fever treated with anti-endotoxic serum. **Proceedings of the Royal Society of Medicine**, *2*, 262-264.

Bruhns, P. (2012). Properties of mouse and human IgG receptors and their contribution to disease models. **Blood**, *119*(24), 5640-5649. doi:10.1182/blood-2012-01-380 121

Buckland, D. (2017). Antimicrobial resistance and the race to find new antibiotics. **Analysis** (January), 12-15.

Calmette, A. (1900). Professor calmette on anti-plague serum therapy. **The Lancet**, *156* (4029), 1454-1455.

Cardinale, A., Filesi, I., Mattei, S., & Biocca, S. (2004). Intracellular targeting and functional analysis of single-chain fv fragments in mammalian cells. **Methods**, *34*(2), 171-178. doi:10.1016/j.ymeth.2004.04.006

CDC. (2019). Antibiotic resistance threats in the united states, 2019.

Cecil, R. L. (1937). Effects of very early serum treatment in Pneumococcus type I pneumonia. **The Journal of the American Medical Association**, *108*(9), 689-692.

Chen, Y., Cai, J., Xu, Q., & Chen, Z. W. (2004). Atomic force bio-analytics of polymerization and aggregation of phycoerythrin-conjugated immunoglobulin G molecules. **Mol Immunol**, *41*(12), 1247-1252. doi:10.1016/j.molimm.2004.05.012

Choi-Rhee, E., Schulman, H., & Cronan, J. E. (2004). Promiscuous protein biotinylation by *Escherichia coli* biotin protein ligase. **Protein Sci**, *13*(11), 3043-3050. doi:10.1110/ps.04911804

Christie, K., Atkins, N. E., & Munch-Petehsen, E. (1944). A note on a lytic phenomenon shown by group b streptococci. **Australian journal of experimental biology and medical science**, *22*, 197-200.

Chuzeville, S., Puymege, A., Madec, J. Y., Haenni, M., & Payot, S. (2012). Characterization of a new camp factor carried by an integrative and conjugative element in streptococcus agalactiae and spreading in streptococci. **PLOS ONE**, *7*(11), e48918. doi:10.1371/journal.pone.0048918

Clackson, T., Hoogenboom, H. R., Griffiths, A. D., & Winter, G. (1991). Making antibody fragments using phage display libraries. **Nature**, *352*.

Coates, A. R., Halls, G., & Hu, Y. (2011). Novel classes of antibiotics or more of the same? **British Journal of Pharmacology**, *163*, 184-194. doi:10.1111/j.1476-5381.2011.01250.x

Conen, A., Walti, L. N., Merlo, A., Fluckiger, U., Battegay, M., & Trampuz, A. (2008). Characteristics and treatment outcome of cerebrospinal fluid shunt-associated infections in adults: A retrospective analysis over an 11-year period. **Clin Infect Dis**, *47*(1), 73-82. doi:10.1086/588298

Cubitt, A. B., Heim, R., Adams, S. R., goyd, A. E., A.Gross, L., & Tsien, R. Y. (1995). Understanding, improving using green fluorescent proteins. **Trends in Biochemical Sciences**, *20*, 448-455.

Cubitt, A. B., Woollenweber, L. A., & Heim, R. (1999). Chapter 2: Understanding structure-function relationships in the aequorea victoria green fluorescent protein. In **Green fluorescent proteins**. pp. 19-30.

Cyagen (2020). Choosing a fluorescent protein. *Molecular Biology Resources.* Retrieved from https://www.cyagen.com/us/en/resources/molecular-biology-resource.html

Cytiva. (2020). Mabselect PrismA affinity chromatography.

Darling, C. L. (1975). Standardization and evaluation of the CAMP reaction for the prompt, presumptive identification of *Streptococcus agalactiae* (Lancefield group B) in clinical material. **Journal Of Clinical Microbiology**, *Feb*, 171-174.

Dawson, A. S. (1927). The treatment of bubonic plague by intravenous injections of anti-plague serum. **Indian Medical Gazette**, *62*(12), 691-692.

Day, R. N., & Davidson, M. W. (2009). The fluorescent protein palette: Tools for cellular imaging. **Chem Soc Rev**, *38*(10), 2887-2921. doi:10.1039/b901966a

Dekio, I., Culak, R., Misra, R., Gaulton, T., Fang, M., Sakamoto, M., Ohkuma, M., Oshima, K., Hattori, M., Klenk, H. P., Rajendram, D., Gharbia, S. E., Shah, H. N. (2015). Dissecting the taxonomic heterogeneity within *Propionibacterium acnes*: Proposal for *Propionibacterium acnes* subsp. acnes subsp. nov. and *Propionibacterium acnes* subsp. elongatum subsp. nov. **Int J Syst Evol Microbiol**, *65*(12), 4776-4787. doi:10.1099/ijsem.0.000648

DeLano, W. L., & Bromberg, S. (2004). *Pymol user's guide*. San Carlos, CA, USA: DeLano Scientific.

Dietrich, T., Perlitz, C., Licha, K., Stawowy, P., Atrott, K., Tachezy, M., Meyborg, H., Stocker, C., Grafe, M., Fleck, E., Schirner, M., Graf, K. (2007). ED-B fibronectin (ED-B) can be targeted using a novel single chain antibody conjugate and is associated with macrophage accumulation in atherosclerotic lesions. **Basic Res Cardiol**, *102*(4), 298-307. doi:10.1007/ s00395-007-0652-5

DiGiandomenico, A., Keller, A. E., Gao, C., Rainey, G. J., Warrener, P., Camara, M. M., Bonnell, J., Fleming, R., Bezabeh, B., Dimasi, N., Sellman, B. R., Hilliard, J., Guenther, C. M., Datta, V., Zhao, W., Gao, C., Yu, X. Q., Suzich, J. A., Stover, C. K. (2014). A multifunctional bispecific antibody protects against *Pseudomonas aeruginosa*. **Sci Transl Med**, *6*(262), 1-12. doi:10.1126/scitrans lmed.3009655

DiGiandomenico, A., & Sellman, B. R. (2015). Antibacterial monoclonal antibodies: The next generation? **Curr Opin Microbiol**, *27*, 78-85. doi:10.1016/j.mib. 2015.07.014

DiGiandomenico, A., Warrener, P., Hamilton, M., Guillard, S., Ravn, P., Minter, R., Camara, M. M., Venkatraman, V., Macgill, R. S., Lin, J., Wang, Q., Keller, A. E., Bonnell, J. C., Tomich, M., Jermutus, L., McCarthy, M. P., Melnick, D. A., Suzich, J. A., Stover, C. K. (2012). Identification of broadly protective human antibodies to *Pseudomonas aeruginosa* exopolysaccharide psl by phenotypic screening. **J Exp Med**, *209*(7), 1273-1287. doi:10.1084/jem.20120033

Doern, G. V. (2001). Antimicrobial use and the emergence of antimicrobial resistance with *Streptococcus pneumoniae* in the united states. **Clinical Infectious diseases**, *33*, 187-192.

Dürr, U. H. N., Sudheendra, U. S., & Ramamoorthy, A. (2006). LL-37, the only human member of the cathelicidin family of antimicrobial peptides. **Biochimica et Biophysica Acta**, *1758*, 1408-1425. doi:10.1016/j.bbamem.2006.03.030

Eason, J. (1935). Anti-streptococcal serum for "rheumatic" affections. **British Medical Journal**, *1*, 176.

ECDC. (2019). Surveillance of antimicrobial resistance in europe: Annual report of the european antimicrobial resistance surveillance network (EARS-NET).

El Zoeiby, A., Sanschagrin, F., Darveau, A., Brisson, J. R., & Levesque, R. C. (2003). Identification of novel inhibitors of *Pseudomonas aeruginosa* murc enzyme derived from phage-displayed peptide libraries. **Journal of Antimicrobial Chemotherapy**, *51*(3), 531-543. doi:10.1093/jac/dkg010

Elsevier. (2018). On the horizon: An acne vaccine. **ScienceDaily**. Retrieved from https://www.sciencedaily.com/releases/2018/08/180829115522.htm

Erp, E. A. V., Luytjes, W., Ferwerda, G., & van Kasteren, P. B. (2019). Fc-mediated antibody effector functions during respiratory syncytial virus infection and disease. **Front Immunol**, *10*, 548. doi:10.3389/fimmu.2019.00548

Evans, M. J., Rollins, L. S. A., Wolff, D. W., Rother, R. P., Norin, A. J., Therrien, D. M., G. A. Grijalva, J. P. Mueller, S. H. Nye, S. P. Squinto, Wilkinss, J. A. (1995). In vitro and in invo inhibition of complement activity by a single-chain Fv fragment recognizing human C5. **Molecular Immunology**, *32*, 1183-1195.

Faber, H. K. (1941). Serum therapy and vaccination. **Journal of the American Medical Association**, *117*(4), 275-278.

Fathi-Roudsari, M., Akhavian-Tehrani, A., & Maghsoudi, N. (2016). Comparison of three *Escherichia coli* strains in recombinant production of Reteplase. **Avicenna Journal of Medical Biotechnology**, *8*(16-22).

Felix, A. (1954). The provisional international standard antityphoid serum. **Bulletin of the World Health Organization**, *10*, 911-917.

Fernebro, J. (2011). Fighting bacterial infections-future treatment options. **Drug Resist Updat**, *14*(2), 125-139. doi:10.1016/j.drup.2011.02.001

Fischer, N., Mak, T. N., Shinohara, D. B., Sfanos, K. S., Meyer, T. F., & Bruggemann, H. (2013). Deciphering the intracellular fate of *Propionibacterium acnes* in macrophages. **Biomed Res Int**, *2013*, 603046. doi:10.1155/2013/603046

Fitch, J. C. K., Rollins, S., Matis, L., Alford, B., Aranki, S., Collard, C. D., Dewar M., Elefteriades J., Hines R., Kopf G., Kraker P., Li L., Hara R. O., Rinder C., Rinder H., Shaw R., Smith B., Stahl G., Shernan, S. K. (1999). Pharmacology and biological efficacy of a recombinant, humanized, single-chain antibody C5 complement inhibitor in patients undergoing coronary artery bypass graft

surgery with cardiopulmonary bypass. **Circulation** (December 21/28), 2499-2506.

Fitzgerald. (2020). ELISA optimization protocol. Retrieved from www.fitzgerald-fii.com

Fleming, A. (1929). On the antibacterial action of cultures of a penicillium, with special reference to their use in the isolation of *B. Influenzae*. **British Journal Of Experimental Pathology**, *X*(3), 226-236.

Flexner, S., & Jobling, W. (1908). Serum treatment of epidemic cerebro-spinal meningitis. **Journal of Experimental medicine**, *10*(1), 141-203.

Francois, B., Barraud, O., & Jafri, H. S. (2017). Antibody-based therapy to combat *Staphylococcus aureus* infections. **Clin Microbiol Infect**, *23*(4), 219-221. doi: 10.1016/j.cmi.2017.02.035

Gaciarz, A., & Ruddock, L. W. (2017). Complementarity determining regions and frameworks contribute to the disulfide bond independent folding of intrinsically stable scFv. **PLOS ONE**, *12*(12), e0189964. doi:10.1371/journal.pone.0189964

Gandelman, G., Frishman, W. H., Wiese, C., Green-Gastwirth, V., Hong, S., Aronow, W. S., & Horowitz, H. W. (2007). Intravascular device infections: Epidemiology, diagnosis, and management. **Cardiol Rev**, *15*(1), 13-23. doi:10.1097/01.crd.0000197966.53529.67

GE-Healthcare. (2009). Hitrap affinity columns instructions.

GE-Healthcare. (2018). Hitrap mabselect prisma hiscreen mabselect PrismA.

GE-Healthcare. (2013). AKTA-start. *Chromatography systems.* Retrieved from https://www.cytivalifesciences.com/en/us/shop/chromatography/chromatographysystems/akta-start-p-05773#related-documents

Ghosh, H. (1935). Treatment of cholera with a new anti-cholera serum. **British Medical Journal**, *1*(3862), 56-65.

Glockshuber, R., Schmidt, T., & Pliickthun, A. (1992). The disulfide bonds in antibody variable domains: Effects on stability, folding in vitro, and functional expression in *Escherichia coli*. **Biochemistry**, *31*(5), 1270-1279.

Guachalla, L. M., Hartl, K., Varga, C. l., Stulik, L., Mirkina, I., Malafa, S., Nagy E., Nagy G., Szijártó, V. (2017). Multiple modes of action of a monoclonal antibody against multidrug-resistant *Escherichia coli* sequence type 131-H30. **Antimicrobial Agents and Chemotherapy**, *61*(11), 1-11. doi:10.1128/AAC .01428-17

Guo, D., Xi, Y., Wang, S., & Wang, Z. (2019). Is a positive christie-atkinson-munch-peterson (camp) test sensitive enough for the identification of *Streptococcus agalactiae*? **BMC Infectious Diseases**, *19*(1), 7. doi:10.1186/s12879-018-3561 -3

Gutiérrez-Díaz, E., Montero-Rodríguez, M., Mencía-Gutiérrez, E., Fernández-González, M. C., & Pérez-Blázquez, E. (2001). *Propionibacterium acnes* endophthalmitis in Ahmed glaucoma valve. **European Journal of Ophthalmology**, *11*(4), 383-385.

Hall, G. S., Pratt-Rippin, K., Meisler, D. M., Washington, J. A., Roussel, T. J., & Mille, D. (1994). Growth curve for *Propionibacterium acnes*. **Current Eye Research**, *13*, 465-466.

Hansen, S. M., & Sorensen, U. B. (2003). Method for quantitative detection and presumptive identification of group B streptococci on primary plating. **Journal**

**Of Clinical Microbiology**, *41*(4), 1399-1403. doi:10.1128/jcm.41.4.1399-1403.2003

Hauser, A. R., Mecsas, J., & Moir, D. T. (2016). Beyond antibiotics: New therapeutic approaches for bacterial infections. **Clin Infect Dis**, *63*(1), 89-95. doi:10.1093/cid/ciw200

Heesterbeek, D. A. C., Angelier, M. L., Harrison, R. A., & Rooijakkers, S. H. M. (2018). Complement and bacterial infections: From molecular mechanisms to therapeutic applications. **J Innate Immun**, *10*(5-6), 455-464. doi:10.1159/000491439

Hemsted, H. (1909). A case of disseminated tuberculosis treated with marmorek's serum. **British Medical Journal**, *2*(2549), 1337-1338.

Hewlett, R. T. (1910). *Serum and vaccine therapy* (2 ed.). London: J. and A. Churchill.

Hoefnagel, D., Dammers, R., Ter Laak-Poort, M. P., & Avezaat, C. J. (2008). Risk factors for infections related to external ventricular drainage. **Acta Neurochir (Wien)**, *150*(3), 209-214; discussion 214. doi:10.1007/s00701-007-1458-9

Huang, C. M. (2015). Acne vaccines targeting a surface sialidase and a secreted CAMP factor toxin. In: **National Institute of Health**.

Ilagan, R. P., Rhoades, E., Gruber, D. F., Kao, H. T., Pieribone, V. A., & Regan, L. (2010). A new bright green-emitting fluorescent protein-engineered monomeric and dimeric forms. **FEBS** *J, 277*(8), 1967-1978. doi:10.1111/j.17424658.2010.07618.x

Jung, Y. S., Matsumoto, S. E., Katakura, Y., Yamashita, M., Tomimatsu, K., Kabayama, S., Teruya, K., Shirahata, S. (2008). Generation of human monoclonal antibodies against *Propionibacterium acnes* by applying the phage

display method to human peripheral blood mononuclear cells immunized in vitro. **Cytotechnology**, *57*(2), 169-175. doi:10.1007/s10616-008-9138-z

Kadler, B. K., Mehta, S. S., & Funk, L. (2015). *Propionibacterium acnes* infection after shoulder surgery. **Int J Shoulder Surg**, *9*(4), 139-144. doi:10.4103/09736042.167957

Kelley, L. A., Mezulis, S., Yates, C. M., Wass, M. N., & Sternberg, M. J. (2015). The phyre2 web portal for protein modeling, prediction and analysis. **Nat Protoc**, *10*(6), 845-858. doi:10.1038/nprot.2015.053

Khafri, A., & Nazari, A. (2004). The rapid camp test for identification of *Streptococcus agalactiae* using alpha toxin. **National Digital Archives of Iranian Scholarly Journals**, *58*, 119-124.

Kitidee, K., Nangola, S., Gonzalez, G., Boulanger, P., Tayapiwatana, C., & Hong, S.-S. (2010). Baculovirus display of single chain antibody (scFv) using a novel signal peptide. **BMC Biotechnology**, *10*(1). doi:10.1186/1472-6750-10-80

Klein, B. G. (1919). Notes on serum treatment of bacillary dysentery and on dysentery arthritis. **Journal of the Royal Army Medical Corps**, *33*(4), 343-352.

Kleymann, G., Ostermeier, C., Heitmann, K., Haase, W., & Michel, H. (1995). Use of antibody fragments (Fv) in immunocytochemistry. **Journal of Histochemistry and Cytochemistry**, *43*, 607-614.

Knudson, G. B. (1986). Treatment of anthrax in man: Historical and current concepts. **Military Medicine**, *151*(2), 71-77.

Kohler, G., & Milstein, C. (1975). Continuous cultures of fused cells secreting antibody of predefined specificity. **Nature**, *256*, 495-497.

Köhler, W. (1988). CAMP-like phenomena of vibrios. Series A: **Medical Microbiology, Infectious Diseases, Virology, Parasitology**, *270*(1-2), 35-40. doi:10.1016/s01766724 (88)80139-1

Kulkeaw, K., Sakolvaree, Y., Srimanote, P., Tongtawe, P., Maneewatch, S., Sookrung, N., Tungtrongchitr, A., Tapchaisri, P., Kurazono, H., Chaicumpa, W. (2009). Human monoclonal scFv neutralize lethal thai cobra, *Naja kaouthia*, neurotoxin. **J Proteomic***s, 72*(2), 270-282. doi:10.1016 /j.jprot.2008.12.007

Kumar, A., & Pal, D. (2016). Green fluorescent protein and their applications in advance research. **Journal of Research in Engineering and Applied Sciences**, *01*(01), 42-46. doi:10.46565/jreas.2016.v01i01.007

Kuntalee, R. (2016). Development of recombinant antibody for the detection of aflatoxin.

Kurien, B. T., & Scofield, R. H. (2012). Extraction of proteins from gels: A brief review. In B. T. Kurien & R. H. Scofield (Eds.), *Protein electrophoresis methods and protocols*.1 ed., pp. 403-406. London: Springer Science Business Media.

Ladwig, V. (1943). Anthrax in iowa. **Iowa State University Veterinarian**, *6*(2), 79-100.

Lajcak, M., Heidecke, V., Haude, K. H., & Rainov, N. G. (2013). Infection rates of external ventricular drains are reduced by the use of silver-impregnated catheters. **Acta Neurochir (Wien)**, *155*(5), 875-881. doi:10.1007/s00701-013-16379

Lamppa, J. W., Tanyos, S. A., & Griswold, K. E. (2013). Engineering *Escherichia coli* for soluble expression and single step purification of active human lysozyme.

**Journal of Biotechnology** *164 (2013) 1–8, 164*, 1-8. doi:10.1016/j.jbiotec. 2012.11.007

Latham, A. (1904). Marmorek's antituberculous serum. **British Medical Journal,** *1*(2258), 857-858.

Lensen, J. F. M., Rops, A. L. W. M. M., Wijnhoven, T. J. M., Hafmans, T., Feitz, W. F. J., Oosterwijk, E., Banas B., Bindels R. J. M., Heuvel L.P. W. J., Vlag J., Berden J. H. M., Kuppevelt, T. H. (2005). Localization and functional characterization of glycosaminoglycan domains in the normal human kidney as revealed by phage display-derived single chain antibodies. **Journal of the American Society of Nephrology**, *16*(5), 1279-1288. doi:10.1681/asn.2004 050413

Levy, O., Iyer, S., Atoun, E., Peter, N., Hous, N., Cash, D., Musa, F., Narvani, A. A. (2013). *Propionibacterium acnes*: An underestimated etiology in the pathogenesis of osteoarthritis? **J Shoulder Elbow Surg**, *22*(4), 505-511. doi:10.1016/j.jse.2012. 07.007

Li, Y., Li, X., Li, H., Lockridge, O., & Wang, G. (2007). A novel method for purifying recombinant human host defense cathelicidin LL-37 by utilizing its inherent property of aggregation. **Protein Expression and Purification** *54*, 157-165. doi:10.1016/j.pep.2007.02.003

Lim, S. A., Na, K. S., & Joo, C. K. (2017). Clinical features of infectious keratitis caused by *Propionibacterium acnes*. **Eye Contact Lens**, *43*(5), 330-333. doi:10.1097/ICL.0000000000000281

Lindsay, H. F. S. (1933). The treatment of puerperal streptococal sepsis. **Ulster Medical Journal**, *2*(2), 86-98.

Linton, D. S. (2005). Emil von behring: Infectious disease, immunology, serum therapy: American Philosophical Society.

Liu, P. F., Nakatsuji, T., Zhu, W., Gallo, R. L., & Huang, C. M. (2011). Passive immunoprotection targeting a secreted camp factor of *Propionibacterium acnes* as a novel immunotherapeutic for acne vulgaris. **Vaccine**, *29*(17), 3230-3238. doi:10.1016/j.vaccine.2011.02.036

Lobstein, J., Emrich, C. A., Jeans, C., Faulkner, M., Riggs, P., & Berkmen, M. (2012). Shuffle, a novel *Escherichia coli* protein expression strain capable of correctly folding disulfide bonded proteins in its cytoplasm. **Microbial Cell Factories**, *11*, 1-16. doi:10.1186/1475-2859-11-56

Lu, R. M., Hwang, Y. C., Liu, I. J., Lee, C. C., Tsai, H. Z., Li, H. J., & Wu, H. C. (2020). Development of therapeutic antibodies for the treatment of diseases. **J Biomed Sci**, *27*(1), 1. doi:10.1186/s12929-019-0592-z

Macleod, C. M. (1939). Treatment of pneumonia with antipneumococcal rabbit serum. **Bulletin of the New York Academy of Medicine**, *15*(2), 116-124.

Mahaffey, K. W., Van de Werf, F., Shernan, S. K., Granger, C. B., Verrier, E. D., Filloon, T. G., Todaro, T. G., Adams, P. X., Levy, J. H., Hasselblad, V., Armstrong, P. W. (2006). Effect of pexelizumab on mortality in patients with acute myocardial infarction or undergoing coronary artery bypass surgery: A systematic overview. **Am Heart J**, *152*(2), 291-296. doi:10.1016/j.ahj.2006.03.027

Mahon, C. R., & Lehman, D. C. (2018). Textbook of diagnostic microbiology (6 ed.): Elsevier Saunders.

Market-Data-Forecast. (2019). Cancer monoclonal antibodies market.

Marston, H. D., Paules, C. I., & Fauci, A. S. (2018). Monoclonal antibodies for emerging infectious diseases - borrowing from history. **The New England Journal of Medicine**, *378*, 1469-1472.

Maynard, E. F., & Bushnell, F. G. (1905). General staphylococcic infection treatment by antistaphylococcic serum and hetol: Death. **The Lancet**, *166*(4277), 520-522.

McCafferty, J., Griffiths, A. D., Winter, G., & Chiswell, D. J. (1990). Phage antibodies: Filamentous phage displaying antibody variable domains. **Nature**, *348*, 552-554.

McCafferty, J., & Johnson, K. S. (1996). Construction and screening of antibody display libraries. In B. K. Kay, J. Winter, & J. McCafferty (Eds.), *Phage display of peptides and proteins* (pp. 79-110). USA: Academic Press, Inc.

Miles, A. A., Misra, S. S., & Irwin, J. (1938). The estimation of the bactericidal power of the blood. **Journal of hygiene**, *38*, 732-749. doi:10.1017/s00221724000 1158x

Mitchell, J. P. (1912). Notes on clinical trials with marmorek's antituberculous serum. **British Medical Journal**, *1*(2667), 299.

Molina-Lopez, J., Sanschagrin, F., & Levesque, R. C. (2006). A peptide inhibitor of Mura UDP-N-acetylglucosamine enolpyruvyl transferase: The first committed step in peptidoglycan biosynthesis. **Peptides**, *27*(12), 3115-3121. doi:10.1016 /j.peptides.2006.08.023

Montoliu-Gaya, L., Martinez, J. C., & Villegas, S. (2017). Understanding the contribution of disulfide bridges to the folding and misfolding of an anti-abeta scFv. **Protein Sci**, *26*(6), 1138-1149. doi:10.1002/pro.3164

Motley, M. P., Banerjee, K., & Fries, B. C. (2019). Monoclonal antibody-based therapies for bacterial infections. **Curr Opin Infect Dis**, *32*(3), 210-216. doi:10.1097/QCO.0000000000000539

Murphy, K. (2012). Janeway's immunobiology. United States of America: Garland Science.

Nakatsuji, T., Tang, D. C., Zhang, L., Gallo, R. L., & Huang, C. M. (2011). *Propionibacterium acnes* CAMP factor and host acid sphingomyelinase contribute to bacterial virulence: Potential targets for inflammatory acne treatment. **PLOS ONE**, *6*(4), e14797. doi:10.1371/journal.pone.0014797

Nattan-larrier, L., & Noyer, B. (1931). Activity of anti-trypanosomal serums according to channel of introduction. from Centre for Agriculture and Bioscience International

Nazipi, S., Stodkilde-Jorgensen, K., Scavenius, C., & Bruggemann, H. (2017). The skin bacterium *Propionibacterium acnes* employs two variants of hyaluronate lyase with distinct properties. **Microorganisms**, *5*(3). doi:10.3390/microorganisms 5030057

Nguyen, J. T., Fong, J., Fong, D., Fong, T., Lucero, R. M., Gallimore, J. M., Burata O. E., Parungao K., Rascon, A. A. (2018). Soluble expression of recombinant midgut zymogen (native propeptide) proteases from the *Aedes aegypti* mosquito utilizing *E. coli* as a host. **BMC Biochemistry,** *19*, 1-14. doi:10.1186/s12858-018-0101-0

Nobel-Prize-Organisation. (1901). Emil von behring - nobel lecture: Serum therapy in therapeutics and medical science.

Nobel-Prize-Organisation. (2008). The nobel prize in chemistry 2008 - press release. Retrieved from https://www.nobelprize.org/prizes/chemistry/2008/pressrelease

Nobel-Prize-Organization. (1984). The nobel prize press release.

Nobel-Prize-Organization. (2018). The nobel prize in chemistry 2018.

O'Neill, J. (2014). Antimicrobial resistance: Tackling a crisis for the health and wealth of nations.

O'Neill, J. (2016). Tackling drug-resistant infections globally: Final report and recommendations (Vol. May). UK: Wellcome Trust and UK Government.

Oren, Z., Lerman, J. C., Gudmundsson, G. H., Agerberth, B., & Shai, Y. (1999). Structure and organization of the human antimicrobial peptide LL-37 in phospholipid membranes: Relevance to the molecular basis for its non-cell-selective activity. **Biochem. J**., *341*, 501-513.

Pakshir, K., Bordbar, M., Zomorodian, K., Nouraei, H., & Khodadadi, H. (2017). Evaluation of CAMP-like effect, biofilm formation, and discrimination of candida africana from vaginal *Candida albicans* species. **J Pathog**, 2017, 7126 258.doi:10.1155/2017/7126258

Pansri, P., Jaruseranee, N., Rangnoi, K., Kristensen, P., & Yamabhai, M. (2009). A compact phage display human scFv library for selection of antibodies to a wide variety of antigens. **BMC Biotechnology**, *9*(6), 1-16.

Papadopoulos, J. S., & Agarwala, R. (2007). Cobalt: Constraint-based alignment tool for multiple protein sequences. **Bioinformatics**, *23*(9), 1073-1079. doi:10.1093/ bioinformatics/btm076

Paradis-Bleau, C., Lloyd, A., Sanschagrin, F., Clarke, T., Blewett, A., Bugg, T. D., & Levesque, R. C. (2008). Phage display-derived inhibitor of the essential cell

wall biosynthesis enzyme murf. **BMC Biochem**, *9*, 1-11. doi:10.1186/1471-2091-9-33

Paradis-Bleau, C., Lloyd, A., Sanschagrin, F., Maaroufi, H., Clarke, T., Blewett, A., Dowson, C., Roper, D. I., Bugg, T. D., Levesque, R. C. (2009). *Pseudomonas aeruginosa* Mure amide ligase: Enzyme kinetics and peptide inhibitor. **Biochem J**, *421*(2), 263-272. doi:10.1042/BJ2008 1395

Paradis-Bleau, C., Sanschagrin, F., & Levesque, R. C. (2005). Peptide inhibitors of the essential cell division protein ftsa. **Protein Eng Des Sel**, *18*(2), 85-91. doi:10. 1093/protein/gzi008

Parmley, S. F., & Smith, G. P. (1988). Antibody-selectable filamentous fd phage vectors: Affinity purification of target genes. **Gene**, *73*, 305–318.

Petrenko, V. A., & Smith, G. P. (2015). Vectors and modes of display. In S. S. Sidhu & C. R. Geyer (Eds.), *Phage display in biotechnology and drug discovery*. 2 ed., pp. 43-74: Taylor & Francis Group, LLC.

Pini, A., Giuliani, A., Falciani, C., Runci, Y., Ricci, C., Lelli, B., Malossi, M., Neri, P., Rossolini, G. M., Bracci, L. (2005). Antimicrobial activity of novel dendrimeric peptides obtained by phage display selection and rational modification. **Antimicrobial Agents and Chemotherapy**, *49*(7), 2665-2672. doi:10.1128/ AAC.49.7.2665-2672.2005

Piper, K. E., Jacobson, M. J., Cofield, R. H., Sperling, J. W., Sanchez-Sotelo, J., Osmon, D. R., McDowell, A., Patrick, S., Steckelberg, J. M., Mandrekar, J. N., Sampedro, M. F., Patel, R. (2009). Microbiologic diagnosis of prosthetic shoulder infection by use of implant sonication. **J Clin Microbiol**, *47*(6), 1878-1884. doi:10.1128/JCM.01686-08

Platsidaki, E., & Dessinioti, C. (2018). Recent advances in understanding *Propionibacterium acnes* (*Cutibacterium acnes*) in acne. **F1000Res**, *7*. doi:10. 12688/f1000research.15659.1

Pozo, J. L. D., Tran, N. V., Petty, P. M., Johnson, C. H., Walsh, M. F., Bite, U., Clay, R. P., Mandrekar, J. N., Piper, K. E., Steckelberg, J. M., Patel, R. (2009). Pilot study of association of bacteria on breast implants with capsular contracture. **J Clin Microbiol**, *47*(5), 1333-1337. doi:10.1128/JCM. 00096-09

Proba, K., WoÈrn, A., Honegger, A., & PluÈckthun, A. (1998). Antibody scFv fragments without disulfide bonds made by molecular evolution. **Journal of Molecular Biology**, *275*, 245-253.

Rajpal, A., Beyaz, N., Haber, L., Cappuccilli, G., Yee, H., Bhatt, R. R., Takeuchi, T., Lerner, R. A., Crea, R. (2005). A general method for greatly improving the affinity of antibodies by using combinatorial libraries. **Proc Natl Acad Sci U S A**, *102*(24), 8466-8471. doi:10.1073/pnas.0503543102

Rangnoi, K., Choowongkomon, K., O'Kennedy, R., Ruker, F., & Yamabhai, M. (2018). Enhancement and analysis of human antiaflatoxin β1 (AFB1) scFv antibody-ligand interaction using chain shuffling. **J Agric Food Chem**, *66*(22), 5713-5722.doi:10.1021/acs.jafc.8b01141

Rangnoi, K., Jaruseranee, N., O'Kennedy, R., Pansri, P., & Yamabhai, M. (2011). One-step detection of aflatoxin- β (1) using scFv-alkaline phosphatase-fusion selected from human phage display antibody library. **Mol Biotechnol**, *49*(3), 240-249. doi:10.1007/s12033-011-9398-2

Rao, S. S., Mohan, K. V., & Atreya, C. D. (2013). A peptide derived from phage display library exhibits antibacterial activity against *E. coli* and *Pseudomonas aeruginosa*. **PLOS ONE**, *8*(2), 1-11. doi:10.1371/journal.pone.0056081

Ratner, H. B., Weeks, L. S., & Stratton, A. W. (1986). Evaluation of spot CAMP test for identification of group B streptococci. **Journal Of Clinical Microbiology**, *Aug.*, 296-297.

Reenstierna, J. (1942). A short account of an anti-leprosy serum and its therapeutic value. **Journal of the American Medical Association**, *118*(4), 336.

Ren, G., Ke, N., & Berkmen1, M. (2016). Use of the shuffle strains in production of proteins. **Current Protocols in Protein Science**, *5.26.1*, 1-21. doi:10.1002/cpps.11

Ren, G., Ke, N., & Berkmen, M. (2016). Use of the shuffle strains in production of proteins. **Current Protocols in Protein Science**, *85*(5.26), 5.26.21-25.26.21.

Rieger, U. M., Mesina, J., Kalbermatten, D. F., Haug, M., Frey, H. P., Pico, R., Frei, R., Pierer, G., Luscher, N. J., Trampuz, A. (2013). Bacterial biofilms and capsular contracture in patients with breast implants. **Br J Surg**, *100*(6), 768-774. doi:10.1002/bjs.9084

Rieger, U. M., Pierer, G., Luscher, N. J., & Trampuz, A. (2009). Sonication of removed breast implants for improved detection of subclinical infection. **Aesthetic Plast Surg**, *33*(3), 404-408. doi:10.1007/s00266-009-9333-0

Rodet, A., & Galavielle. (1902). Antirabies serum therapy. In E. W. Allen (Ed.), *Experiment station record 1901-1902*, Vol. XIII, pp. 96. Washington government printing office.

Rohacek, M., Weisser, M., Kobza, R., Schoenenberger, A. W., Pfyffer, G. E., Frei, R., Erne, P., Trampuz, A. (2010). Bacterial colonization and infection of electrophysiological cardiac devices detected with sonication and swab culture. **Circulation**, *121*(15), 1691-1697. doi:10.1161/CIRCULATIONAHA.109.906461

Rossmann, F. S., Laverde, D., Kropec, A., Romero-Saavedra, F., Meyer-Buehn, M., & Huebner, J. (2015). Isolation of highly active monoclonal antibodies against multiresistant gram-positive bacteria. **PLOS ONE**, *10*(2), e0118405.doi:10.1371/journal.pone.0118405

Roy, D. M. (1935). Treatment of acute bacillary dysentery with anti-dysenteric serum and bacteriophage. **Indian Medical Gazette**, *70*(1), 26.

Russel, M., Lowman, H. B., & Clackson, T. (2004). Introduction to phage biology and phage display. In T. Clackson & H. B. Lowman (Eds.), *Phage display.* pp.1-24: Oxford University Press.

Saber, R., Sarkar, S., Gill, P., Nazari, B., & Faridani, F. (2011). High resolution imaging of igg and igm molecules by scanning tunneling microscopy in air condition. **Scientia Iranica**, *18*(6), 1643-1646. doi:10.1016/j.scient.2011.11.028

Santajit, S., Seesuay, W., Mahasongkram, K., Sookrung, N., Ampawong, S., Reamtong, O., Diraphat, P., Chaicumpa, W., Indrawattana, N. (2019). Human single-chain antibodies that neutralize *Pseudomonas aeruginosa*-exotoxin A-mediated cellular apoptosis. **Sci Rep**, *9*(1), 1-15. doi:10.1038/s41598-019-51089-w

Santala, V., & Lamminmaki, U. (2004). Production of a biotinylated single-chain antibody fragment in the cytoplasm of *Escherichia coli*. **J Immunol Methods**, *284*(1-2), 165-175. doi:10.1016/j.jim.2003.10.008

Schlapp, G., Scavone, P., Zunino, P., & Hartel, S. (2011). Development of 3D architecture of uropathogenic proteus mirabilis batch culture biofilms-a quantitative confocal microscopy approach. **J Microbiol Methods**, *87*(2), 234-240. doi:10.1016/j.mimet.2011.07.021

Schouten, A., Roosien, J., Bakker, J., & Schots, A. (2002). Formation of disulfide bridges by a single-chain Fv antibody in the reducing ectopic environment of the plant cytosol. **J Biol Chem**, *277*(22), 19339-19345. doi:10.1074/jbc.M201245200

Shen, Z., Mernaugh, R. L., Yan, H., Yu, L., Zhang, Y., & Zeng, X. (2005). Engineered recombinant single-chain fragment variable antibody for immunosensors. **Anal Chem**, *77*(21), 6834-6842. doi:10.1021/ac0507690

Sheplar, A. E., Spence, M. J., & Macneal, W. J. (1934). Therapeutic use of concentrated antistreptococcus serum of New York state department of health. **Archives of Surgery**, *29*(5), 858-865.

Singh, J. A., Sperling, J. W., Schleck, C., Harmsen, W., & Cofield, R. H. (2012). Periprosthetic infections after shoulder hemiarthroplasty. **J Shoulder Elbow Surg**, *21*(10), 1304-1309. doi:10.1016/j.jse.2011.08.067

Smyth, H. F., & Higgins, W. D. (1945). Anthrax in the United States, 1939-1943. **American Journal of Public Health and the Nation's Health**, *35*(8), 850-858.

Sohail, M. R., Uslan, D. Z., Khan, A. H., Friedman, P. A., Hayes, D. L., Wilson, W. R., Steckelberg, J. M., Stoner, S., Baddour, L. M. (2007). Management and outcome of permanent pacemaker and implantable cardioverter-defibrillator infections. **J Am Coll Cardiol**, *49*(18), 1851-1859. doi:10.1016/j.jacc.2007.01.072

Sompungaa, P., Pruksametanana, N., Rangnoia, K., Choowongkomonb, K., & Yamabhai, M. (2019). Generation of human and rabbit recombinant antibodies for the detection of zearalenone by phage display antibody technology. **Talanta**, *201*, 397-405.

Sowmiya, M., Malathi, J., Swarnali, S., Priya, J. P., Therese, K. L., & Madhavan, H. N. (2015). A study on the characterization of *Propionibacterium acnes* isolated from ocular clinical specimens. **Indian J Med Res**, *142*(4), 438-449. doi:10.4103/0971-5916.169209

Speziale, P., Rindi, S., & Pietrocola, G. (2018). Antibody-based agents in the management of antibiotic-resistant *Staphylococcus aureus* diseases. **Micro-organisms**, *6*(1). doi:10.3390/microorganisms6010025

Stableforth, A. W. (1954). The international standard for anti-*Brucella abortus* serum. **Bull. Wld Hlth Org**., *10*, 927-935.

Streaker, E. D., & Beckett, D. (2006). Nonenzymatic biotinylation of a biotin carboxyl carrier protein: Unusual reactivity of the physiological target lysine. **Protein Sci**, *15*(8), 1928-1935. doi:10.1110/ps.062187306

Tabor, D. E., Oganesyan, V., Keller, A. E., Yu, L., McLaughlin, R. E., Song, E., Warrener, P., Rosenthal, K., Esser, M., Qi, Y., Ruzin, A., Stover, C. K., DiGiandomenico, A. (2018). *Pseudomonas aeruginosa* pcrv and psl, the molecular targets of bispecific antibody MEDI3902, are conserved among diverse global clinical isolates. **J Infect Dis**, *218*(12), 1983-1994. doi:10.1093/infdis/jiy438

Taeye, S. W. D., Rispens, T., & Vidarsson, G. (2019). The ligands for human IgG and their effector functions. **Antibodies (Basel)**, *8*(2). doi:10.3390/antib8020030

Tami, J. A., Parr, M. D., Brown, S. A., & Thompson, J. S. (1986). Monoclonal antibody technology. **Americam Journal of Hospital Pharmacy**, *43*, 2816-2825.

Thanabalasuriar, A., Surewaard, B. G., Willson, M. E., Neupane, A. S., Stover, C. K., Warrener, P., Wilson, G., Keller, A. E., Sellman, B. R., DiGiandomenico, A., Kubes, P. (2017). Bispecific antibody targets multiple *Pseudomonas aeruginosa* evasion mechanisms in the lung vasculature. **J Clin Invest**, *127*(6), 2249-2261. doi:10.1172/JCI89652

Theroux, P., Armstrong, P. W., Mahaffey, K. W., Hochman, J. S., Malloy, K. J., Rollins, S., Nicolau, J. C., Lavoie, J., Luong, T. M., Burchenal, J., Granger, C. B. (2005). Prognostic significance of blood markers of inflammation in patients with ST-segment elevation myocardial infarction undergoing primary angioplasty and effects of pexelizumab, a C5 inhibitor: A substudy of the comma trial. **Eur Heart J**, *26*(19), 1964-1970. doi:10.1093/ eurheartj/ehi292

Thomas, B. A. (1913). The preparation and employment, in a series of cases, of a potent polyvalent antistaphylococcic serum. **Journal of the American Medical Association**, *60*(14), 1070-1073.

Thomas, C. P. (1897). Anti-streptococcus serum. **Journal of the American Medical Association**, *XXIX*(25), 1259-1260.

Townsend, C. L., Laffy, J. M., Wu, Y. B., Silva O'Hare, J., Martin, V., Kipling, D., Fraternali, F., Dunn-Walters, D. K. (2016). Significant differences in physicochemical properties of human immunoglobulin kappa and lambda CDR3 regions. **Front Immuno***l*, *7*, 1-12. doi:10.3389/fimmu.2016.00388

Turnbull, P. C. B., & Shadomy, S. V. (2011). Anthrax from 5000 BC to AD 2010. In N. H. Bergman (Ed.), *Bacillus anthracis and anthrax*. pp.1-14: John Wiley & Sons, Inc.

UniProt. (2020). Taxonomy - *Cutibacterium acnes* (*Propionibacterium acnes*). Retrieved from https://www.uniprot.org/taxonomy/1747#

Valanne, S., McDowell, A., Ramage, G., Tunney, M. M., Einarsson, G. G., O'Hagan, S., Wisdom, G. B., Fairley, D., Bhatia, A., Maisonneuve, J. F., Lodes, M., Persing, D. H., Patrick, S. (2005). CAMP factor homologues in *Propionibacterium acnes*: A new protein family differentially expressed by types I and II. **Microbiology**, *151*(Pt 5), 1369-1379. doi:10.1099/mic.0.277880

Valen, R. V., Wijngaarden, R. A. D. L. V., Verkaik, N. J., Mokhles, M. M., & Bogers, A. J. (2016). Prosthetic valve endocarditis due to *Propionibacterium acnes*. **Interact Cardiovasc Thorac Surg**, *23*(1), 150-155. doi:10.1093/icvts/ivw087

Vallet-Courbin, A., Lariviere, M., Hocquellet, A., Hemadou, A., Parimala, S. N., Laroche-Traineau, J., Santarelli, X.. Clofent-Sanchez, G., Jacobin-Valat, M. J., Noubhani, A. (2017). A recombinant human anti-platelet scFv antibody produced in *Pichia pastoris* for atheroma targeting. **PLOS ONE**, *12*(1), 1-18. doi:10.1371/journal.pone.0170305

Vestby, L. K., Gronseth, T., Simm, R., & Nesse, L. L. (2020). Bacterial biofilm and its role in the pathogenesis of disease. **Antibiotics**, *9*(2), 1-29. doi:10.3390/antibiotics9020059

Vu, N. X., Pruksametanan, N., Srila, W., Yuttavanichakul, W., Teamtisong, K., Teaumroong, N., Boonkerd, N., Tittabutr, P., Yamabhai, M. (2017). Generation of a rabbit single-chain fragment variable (scFv) antibody for specific detection

of *Bradyrhizobium* sp. DOA9 in both free-living and bacteroid forms. **PLOS ONE**, *12*(6), 1-21. doi: https://doi.org/10.1371/journal.pone.0179983

Waller, W. E., & Oxon, B. C. (1919). The use of anti-dysentery serum in the treatment of bacillary dysentery. **The Lancet**, *194*(5018), 778-780.

Walti, L. N., Conen, A., Coward, J., Jost, G. F., & Trampuz, A. (2013). Characteristics of infections associated with external ventricular drains of cerebrospinal fluid. **J Infect**, *66*(5), 424-431. doi:10.1016/j.jinf.2012.12.010

Wang, G., Mishra, B., Epand, R. F., & Epand, R. M. (2014). High-quality 3D structures shine light on antibacterial, anti-biofilm and antiviral activities of human cathelicidin LL-37 and its fragments. **Biochimica et Biophysica Acta**, *1838*, 2160-2172. doi:10.1016/j.bbamem.2014.01.016

Wang, H., Zhao, F., Han, X., & Yang, Z. (2016). Production and characterization of a biotinylated single-chain variable fragment antibody for detection of parathion-methyl. **Protein Expr Purif**, *126*, 1-8. doi:10.1016/j.pep.2016.05.005

Wang, Y., Hata, T. R., Tong, Y. L., Kao, M. S., Zouboulis, C. C., Gallo, R. L., & Huang, C. M. (2018). The anti-inflammatory activities of *Propionibacterium acnes* CAMP factor-targeted acne vaccines. **J Invest Dermatol**, *138*(11), 2355-2364. doi:10.1016/j.jid.2018.05.032

Wang-Lin, S. X., & Balthasar, J. P. (2018). Pharmacokinetic and pharmacodynamic considerations for the use of monoclonal antibodies in the treatment of bacterial infections. **Antibodies** *(Basel), 7*(1). doi:10.3390/antib7010005

Warrener, P., Varkey, R., Bonnell, J. C., DiGiandomenico, A., Camara, M., Cook, K., Peng, L., Zha, J., Chowdury, P., Sellman, B., Stover, C. K. (2014). A novel anti-pcrv antibody providing enhanced protection against *Pseudomonas aeruginosa*

in multiple animal infection models. **Antimicrobial Agents and Chemotherapy**, *58*(8), 4384-4391. doi:10. 1128/AAC.02643-14

Waterhouse, A., Bertoni, M., Bienert, S., Studer, G., Tauriello, G., Gumienny, R., Heer, F. T., de Beer, T. A. P., Rempfer, C., Bordoli, L., Lepore, R., Schwede, T. (2018). SWISS-model: Homology modelling of protein structures and complexes. **Nucleic Acids Research**, *46*(W1), 296-303.

Weatherill, E. E., Cain, K. L., Heywood, S. P., Compson, J. E., Heads, J. T., Adams, R., & Humphreys, D. P. (2012). Towards a universal disulphide stabilised single chain Fv format: Importance of interchain disulphide bond location and VL-VH orientation. **Protein Eng Des Sel**, *25*(7), 321-329. doi:10.1093/protein/gzs021

WHO. (2017). Global priority list of antibiotic-resistant bacteria to guide research, discovery, and development of new antibiotics.

WHO. (2019a). 2019 antibacterial agents in clinical development. 1-48.

WHO. (2019b). 2019 antibacterial agents in clinical development: An analysis of the antibacterial clinical development pipeline.

Williams, K. J. (2009). The introduction of 'chemotherapy' using arsphenamine - the first magic bullet. **J R Soc Med**, *102*(8), 343-348. doi:10.1258/jrsm.2009.09k036

Ye, J., Ma, N., Madden, T. L., & Ostell, J. M. (2013). Igblast: An immunoglobulin variable domain sequence analysis tool. **Nucleic Acids Res,** *41*(Web Server issue), 34-40. doi:10.1093/nar/gkt382

Yuan, Y., Zhou, Z., Jia, Y., Li, C., Zheng, Y., Lin, Y., Xiao J., Chen Z., Cao, P. (2017). Histological identification of *Propionibacterium acne*s in nonpyogenic

degenerated intervertebral discs. **BioMed Research International**, 1-7. doi:10.1155/2017/ 6192935

Zárate, M. S., Vargas, L. J., Pacheco, M. V., Canigia, L. F. n., & Smayevsky, J. (2005). Modified spot CAMP test: A rapid, inexpensive and accurate method for identification of group B streptococci. **Revista Argentina de Microbiología**, *37*, 126-128.

Zarschler, K., Witecy, S., Kapplusch, F., Foerster, C., & Stephan, H. (2013). High-yield production of functional soluble single-domain antibodies in the cytoplasm of *Escherichia coli.* **Microbial Cell Factories**, *12*(97), 1-13.

Zeller, V., Ghorbani, A., Strady, C., Leonard, P., Mamoudy, P., & Desplaces, N. (2007). *Propionibacterium acnes*: An agent of prosthetic joint infection and colonization. **J Infect**, *55*(2), 119-124. doi:10.1016/j.jinf.2007.02.006

Zhao, J. X., Yang, L., Gu, Z. N., Chen, H. Q., Tian, F. W., Chen, Y. Q., Zhang, H., Chen, W. (2010). Stabilization of the single-chain fragment variable by an interdomain disulfide bond and its effect on antibody affinity. **Int J Mol Sci**, *12*(1), 1-11. doi:10.3390/ijms12010001

Zurawski, D. V., & McLendon, M. K. (2020). Monoclonal antibodies as an antibacterial approach against bacterial pathogens. **Antibiotics**, *9*(4), 1-12. doi:10.3390/ antibiotics9040155

# APPENDIX

## Publication

Thae Thae Min and Montarop Yamabhai. Human hexa-histidine-tagged single-chain variable fragments (scFv) for bioimaging of bacterial infections. **ACS Omega** (manuscript accepted for publication)

## Patents

Recombinant human anti-bacterial scFv antibodies against *Propionibacterium acnes*. Patent file number 1901005235

Recombinant human anti-bacterial scFv antibodies against *Pseudomonas aeruginosa*. Patent file number 1901005236

## Presentation at conferences

Thae Thae Min and Montarop Yamabhai. Human scFv antibody against *Propionibacterium acnes*. **The 13th Asian Congress on Biotechnology (ACB 2017)**: *Bioinnovation and Bioeconomy*. 23-27 July 2017, Pullman Khon Kaen Raja Orchid Hotel, Khon Kaen, Thailand. (Poster)

Thae Thae Min and Montarop Yamabhai. Identification of Human Antibody against *Pseudomonas aeruginosa* by Phage Display Technology. **The 14th Asian Congress on Biotechnology (ACB 2019)**: *Biotechnology 20/20 and Beyond*. 1-4 July 2019, Fullon Hotel, Tamsui Fishermen's Wharf, Taipei, Taiwan. (Oral)

Thae Thae Min, Kuntalee Rangnoi, and Montarop Yamabhai. From scFv antibody fragment to monoclonal **λ** IgG by recombinant antibody technology. **The 31st Annual Meeting of the Thai Society for Biotechnology and International Conference (TSB 2019)**: *BIO innovation for sustainability*. 10-12 November 2019, Duangjitt Resort & Spa, Patong, Phuket, Thailand. (Poster)

Thae Thae Min and Montarop Yamabhai. Application of hexa-histidine-tagged scFv antibody fragments in immunofluorescence staining and immunoelectron microscopy of bacteria. **The 37th International Conference of the Microscopy Society of Thailand (MST 37)**: *Brilliant Synchrotron Light Towards Microscopic World*. 25-28 February 2020, Kantary Hotel, Nakhon Ratchasima, Thailand. (Oral)

มหาวิทยาลัยเทคโนโลยีสุรนารี

This is an open access article published under a Creative Commons Non-Commercial No Derivative Works (CC-BY-NC-ND) Attribution License, which permits copying and redistribution of the article, and creation of adaptations, all for non-commercial purposes.

ACS AUTHORCHOICE

ACS OMEGA

http://pubs.acs.org/journal/acsodf

Article

# Human Hexa-Histidine-Tagged Single-Chain Variable Fragments for Bioimaging of Bacterial Infections

Thae Thae Min and Montarop Yamabhai*

Cite This: *ACS Omega* 2021, 6, 762−774

Read Online

ACCESS | Metrics & More | Article Recommendations | Supporting Information

**ABSTRACT:** The single-chain variable fragment (scFv) of monoclonal antibodies is a promising recombinant nanostructure for various medical applications, including bioimaging and targeted therapy. While numerous scFv antibodies against eukaryotic cell surface proteins (especially cancer biomarkers) have been generated and engineered to suit various purposes, only a few specific scFv against bacterial cell surfaces have been developed, especially those of human origin. Recent incidents of emerging multidrug-resistant pathogenic bacteria and the realization of the importance of a balanced microbiota on the health of the host has led to more interests in the development of recombinant antibacterial antibodies as a detection probe or targeted therapy for bacterial infections. This study reports the generation of two specific human antibacterial scFv using phage display antibody technology. The recombinant scFv fragments of about 30 kDa and a diameter of 5 nm were produced and purified from engineered *Escherichia coli* that can enhance cytosolic disulfide bond formation. As a proof of principle, *Propionibacterium acnes* and *Pseudomonas aeruginosa* were used as model Gram-positive and Gram-negative bacteria, respectively. Specificity at the strain and species level to both planktonic and biofilm forms of these bacteria were demonstrated in various assay formats, namely, ELISA, flow cytometry, western blot, immunofluorescence, and electron microscopy via the hexa-histidine tag. This recombinant scFv generation platform can be applied for other bacteria, and since the scFv obtained has a benefit of being a human origin, it could be conveniently engineered for various therapeutic or theranostic applications with minimized adverse immunoreaction.

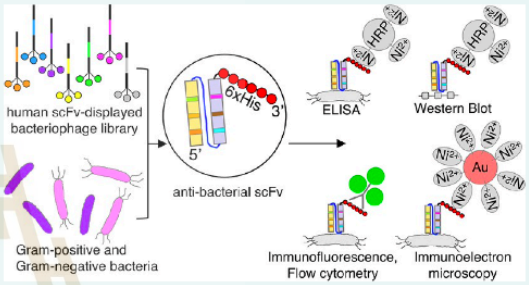


## INTRODUCTION

Phage display antibody technology, one of the most popular methods for the generation of recombinant antibodies, has recently been awarded the Nobel Prize in Chemistry for the year 2018.[1] The key advantage of this technology relies on the simplicity but powerful affinity selection (bio-panning) procedure and the direct linkage between the displayed antibody and its encoding gene within the virion genome.[2] Recombinant antibodies against a desired target can be identified directly from diverse repertoires of antibody genes, generating high-affinity binding sites without the constraint imposed by classical methods for generating either polyclonal or monoclonal antibodies.[3] Since this method does not depend on an animal's immune system, antibodies to a wide variety of antigens, including molecules that cannot stimulate the immune system of animals, such as small molecule haptens and self-antigens have been successfully isolated using this technology.[4] Various forms of antigen-binding fragments, including Fab and scFv have been cloned and displayed on the filamentous bacteriophage M13.[5] ScFv is a nanostructure that consists of light and heavy chain variable domains of immunoglobulins of mammals, linked with a peptide linker $(G_4S)_3$. One scFv fragment has a molecular weight of about 30 kDa and a diameter of 5 nm, which is about one-fifth the size of the parental IgG molecule.[6,7] Once the sequence of scFv against any target has been identified, it can be further engineered into various formats including whole immunoglobulin (IgG) monoclonal antibodies and bispecific antibodies or fabricated into various nanoparticles for both therapeutic and diagnostic purposes.[8]

Most of the research and development on recombinant antibodies mainly focuses on cancer. Several hundred monoclonal antibodies have been approved or are in clinical trial stages for the treatment of cancer and autoimmune diseases.[9] Until now, only a handful of publications regarding the generation of recombinant antibodies against infectious micro-organisms have been published.[10,11] The emergence of multidrug-resistant pathogenic bacteria as well as the concern

Received: November 2, 2020
Accepted: December 11, 2020
Published: December 22, 2020

ACS Publications

© 2020 The Authors. Published by American Chemical Society

for a balanced microbiota have led to more interest in generating recombinant antibodies against pathogenic bacteria.[12]

The model Gram-negative bacteria in this study, *P. aeruginosa*, is one of the WHO prioritized pathogens for which research and development of new antibiotics are critically needed.[13] Some research groups used molecular targets, such as purified recombinant proteins of *P. aeruginosa*,[14−18] whereas others used whole bacterial cells in suspension as targets for affinity selection.[19,20] All carried out affinity selection using peptide display phage libraries, and from this, anti-*P. aeruginosa* peptides were identified. On the other hand, a study group from MedImmune Ltd., UK,[21,22] used *P. aeruginosa* whole cells as a target for affinity selection against a human scFv library derived from patients who had recently recovered from *P. aeruginosa* infections and identified a scFv against *P. aeruginosa* exopolysaccharide residue (Psl). Another study group used the recombinant exotoxin A of *P. aeruginosa* to do affinity selection against a human scFv phage display library based on 60 Thai blood donors and isolated anti-exotoxin A scFv clones.[23,24] To the best of our knowledge, only the anti-Psl scFv of MedImmune Ltd. group has been developed into an anti-pseudomonal drug candidate.

The model Gram-positive bacteria of this study, *P. acnes*, have been used as an affinity selection target by one study group.[25] They generated a scFv display phage library from human peripheral blood mononuclear cells, which were immunized *in vitro* with heat-killed *P. acnes* and three anti-*P. acnes* scFv clones were identified, but there was no known further development from those clones.

Biopharmaceuticals could become a reliable resource to fight back multidrug- and pandrug-resistant bacteria, which has been a global concern. In 2017, multidrug-resistant *P. aeruginosa* caused an estimated 32,600 infections among hospitalized patients and 2700 estimated deaths in the US alone. It has been estimated that human deaths attributable to antimicrobial resistance (AMR) will surpass that of cancer in 2050 and the global GDP loss related to AMR will be trillions of USD.[26,27] Recently, cartography of opportunistic pathogens and antibiotic resistance genes in a tertiary hospital environment, from genomic and metagenomic analysis, has been reported.[28,29] Therefore, obtaining scFv nanostructures against living bacteria, which could be further engineered to be used as alternative diagnostic and therapeutic strategies to combat deadly bacterial infections, is highly attractive.

This study reports an efficient method for the generation of specific human scFvs against both Gram-positive and Gram-negative bacteria using phage display technology.

## ■ RESULTS AND DISCUSSION

Two opportunistic bacteria with different cell surface structures were used as model bacteria in this study because they have important clinical relevance and are easier to handle with a standard biosafety level in a general laboratory. The procedures presented in this study could be adopted for the generation of scFvs to other important pathogenic bacteria with no current effective treatment.

**Affinity Selection against *P. acnes* and *P. aeruginosa*.** A summary of the affinity selection results is shown in Table 1. After the first round of selection against *P. acnes* (DMST 14916), 844 colonies of TG1 strain *E. coli* infected with eluted virions were obtained. Then, 576 colonies were manually picked and were subjected to monoclonal phage ELISA. Three virion clones, eventually designated as yPac1A8, yPac1E4, and yPac1E7, which showed a two-fold higher OD signal against *P. acnes* than the negative control (1% BSA), were selected for binding re-confirmation by phage ELISA and DNA sequence analysis. The result revealed that they possessed unique scFv sequences; however, the clone yPac1E7 had an amber stop codon (TAG) within its open reading frame. Binding confirmation by scFv ELISA of two soluble scFv clones (yPac1A8 and yPac1E4) produced from the non-suppressor strain of *E. coli* (HB2151) proved that only clone yPac1A8 showed good binding (OD value was two times higher than 1% BSA control, data not shown). Therefore, yPac1A8 was selected for expression in pET-21d (+) for further analysis.

**Table 1. Summary of Affinity Selection Results against *P. acnes* and *P. aeruginosa***

| affinity selection step | *P. acnes* DMST 14916 | *P. aeruginosa* DMST 37186 |
|---|---|---|
| rounds of selection | 1 | 3 |
| colonies obtained | 844 colonies | $2.2 \times 10^4$ colonies |
| colonies picked up | 576 colonies | 96 colonies |
| positive clones at monoclonal phage ELISA | 3 clones | 61 clones |
| positive clones at scFv ELISA expressed in HB2151 *E. coli* | 1 out of 2 clones tested | 4 out of 15 clones tested |
| clones sent for DNA sequencing | 3 clones | 4 clones |
| DNA sequencing result | 3 different scFv sequences | all 4 clones have same scFv sequence |
| scFv clone identity | yPac1A8, yPac1E4, yPac1E7 | yPgi3G4 |

For *P. aeruginosa* (DMST 37186), 3 rounds of affinity selection were carried out and 96 colonies were randomly picked for monoclonal phage ELISA. Sixty-one virion clones showed two-fold higher OD values against *P. aeruginosa* than the negative control (1% BSA). After binding confirmation, 15 clones were selected to generate soluble scFv from the non-suppressor strain of *E. coli* (HB2151). Out of 15, 4 clones that showed a high signal by scFv ELISA (data not shown) were sent for DNA sequencing, and the result revealed that all clones possessed the same scFv sequence. This clone, designated yPgi3G4, was further expressed in the pET-21d (+) system.

The affinity selection data confirms the previous observation that a compact non-immunized phage display human scFv library, generated from blood of healthy individuals in the rural regions of Thailand,[4] can be used as a good resource for the generation of specific antibodies against a wide variety of external antigens, including both the Gram-positive and Gram-negative pathogenic bacteria used in this study. It is worth noting that the immobilization of the desired targets is one of the important steps in the affinity selection process of phage display technology. In this report, we have optimized various parameters of the affinity selection procedure.[30] In particular, we have prepared bacterial targets in several ways. These include whole, boiled and sonicated bacterial cells. The effective method which yields positive clones came from using boiled bacterial antigens as described in the materials and methods section.

**DNA and Amino Acid Sequence Analysis of Selected Virion Clones.** A diagram of recombinant scFv in this study is depicted in Figure 1A. The variable region of the heavy chain ($V_H$) at the N-terminus is connected to the variable region of the light chain ($V_L$) by a GGGGSGGGGSGGGGS peptide



https://dx.doi.org/10.1021/acsomega.0c05340
ACS Omega 2021, 6, 762−774

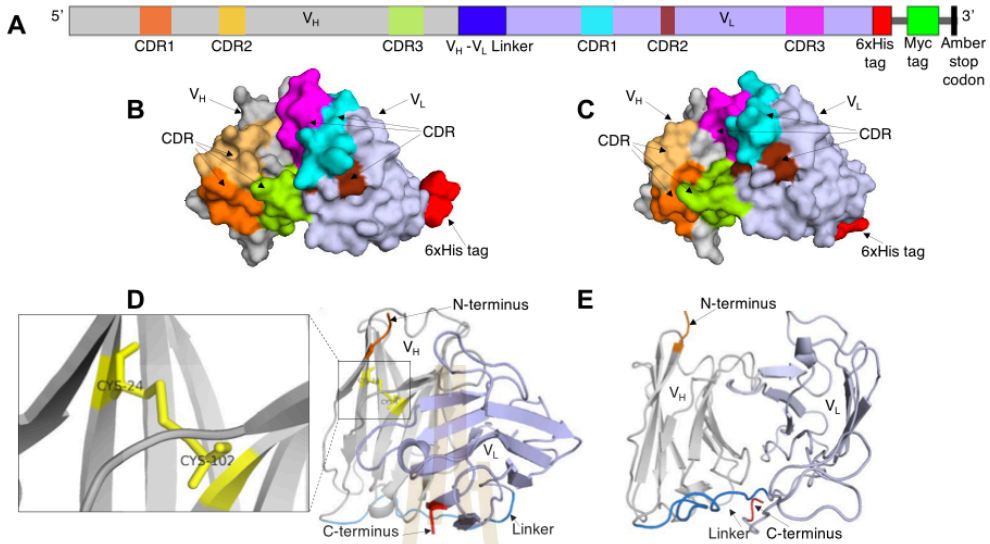


**Figure 1.** Structural analysis of 6xHis-tagged scFv. (A) Schematic arrangement of scFv primary structure from the N-terminus (5′) to C-terminus (3′): CDR regions of $V_H$ domain, $V_H$-$V_L$ linker (blue), CDR regions of $V_L$ domain, 6xHis tag (red), Myc tag (green), and Amber stop codon (black). 3D modeling structures based on scFv (PDB ID code 1f3r.1.B) are shown in (B)−(E). Surface view of yPac1A8 scFv (B) and yPgi3G4 scFv (C), with the same color coding as in diagram (A). A ribbon model showing the $\alpha$-helix and $\beta$-sheet of yPac1A8 scFv (D) and yPgi3G4 scFv (E): N-terminus (orange), $V_H$ domain (gray), disulfide bridge (yellow), linker (blue), $V_L$ domain (violet), and C-terminus (red). Only yPac1A8 possesses intra-domain disulfide bridge (shown in inset) between Cysteine 24 and Cysteine 102 residues of the $V_H$ domain.

**Table 2. Analysis of DNA and Amino Acid Sequences of Isolated scFv Fragments against Gram-Positive and Gram-Negative Bacteria**[a]

| scFv clone | germline | identity to germline (%) | amino acid differences from germline | CDR3 sequence |
|---|---|---|---|---|
| $V_H$ genes | | | | |
| yPac1A8 | Homsap IGHV6-1*01 | 92.59 | 13 | TRGKYSGFDM |
| yPac1E4 | Homsap IGHV6-1*01 | 92.59 | 13 | TRGKYSGFDM |
| yPac1E7 | Homsap IGHV6-1*01 | 91.92 | 17 | VRGQHSAFDM |
| yPgi3G4 | Homsap IGHV3-7*01 | 93.40 | 15 | ARVLWGFPFDL |
| $V_L$ genes | | | | |
| yPac1A8 | Homsap IGLV2-18*02 | 94.44 | 9 | SSFTSTISPSYV |
| yPac1E4 | Homsap IGLV2-14*01 | 98.96 | 1 | SSYTSSSPNWV |
| yPac1E7 | Homsap IGLV2-18*02 | 93.75 | 12 | SSYTSSSTWV |
| yPgi3G4 | Homsap IGLV2-8*01 | 97.57 | 8 | SSYGGSNNLV |

[a]Homsap, Homosapien; IGHV, immunoglobulin heavy variable; IGLV, immunoglobulin lambda variable; V-domain, variable domain.

linker sequence. The C-terminus of scFv is linked with a hexa-histidine tag (6 x His tag) followed by a Myc tag. The gene of scFv and the gene III protein sequence of the bacteriophage are intervened by an Amber stop codon (TAG), which is recognized by the non-suppressor strain of *E. coli*, HB2151, as a stop signal.[4] DNA and amino acid sequences of isolated clones in comparison with those of human germline antibody variable region gene sequences are presented in Table 2. Out of the seven existing IGHV (human immunoglobulin heavy variable) gene subgroups, isolated scFv clones from this study belong to subgroups 3 and 6. Clones active against *P. acnes* (yPac1A8, yPac1E4, yPac1E7) are from IGHV subgroup 6 and are derived from the same germline gene and allele IGHV6-1*01 with >91% sequence identity. Their sequences differ from that in the germline by 13−17 amino acids. Three clones share one CDR3 amino acid sequence pattern ("-RG-S-FDM"). The clone active against *P. aeruginosa* (yPgi3G4) is from the IGHV subgroup 3 and derived from germline gene and allele IGHV3-7*01 with >90% sequence identity. Its sequence is different from that in the germline by 15 amino acids.

All isolated scFv clones, either active against *P. acnes* or *P. aeruginosa*, are members of IGLV (human immunoglobulin $\lambda$) gene subgroup 2 out of the existing 11 (IGLV1 to 11). The immunoglobulin light chain $\kappa$ to $\lambda$ ratio has been estimated to be 1.5−2, and the chance of isolating $\kappa$ light chain antibodies is higher than that of the $\lambda$.[31] However, in our study, all four scFv clones have $\lambda$. Two of them (yPac1A8, yPac1E7) are derived from the germline gene and allele IGLV2-18*02 with >93% sequence identity, with 9−12 amino acids difference. Another clone (yPac1E4) originates from the germline gene and allele IGLV2-14*01 with nearly 99% sequence identity and has only one amino acid difference. The last clone (yPgi3G4) is a derivative of the germline gene and allele IGLV2-8*01 with



https://dx.doi.org/10.1021/acsomega.0c05340
ACS Omega 2021, 6, 762−774

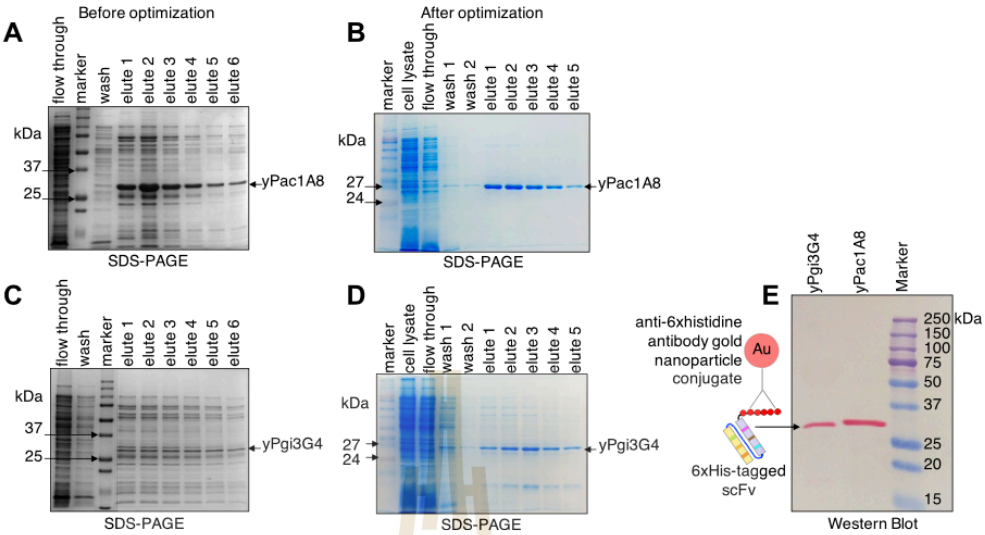


**Figure 2.** Expression and purification of 6xHis-tagged scFv. SDS-PAGE of 6xHis-tagged scFv samples before and after optimization of expression and purification steps. All gels were Coomassie Brilliant Blue-stained. (A) yPac1A8 scFv before optimization. (B) yPac1A8 scFv after optimization. (C) yPgi3G4 scFv before optimization and (D) yPgi3G4 scFv after optimization. Precision Plus All Blue Prestained Protein Standards (BioRad #1610373, U.S.A.) were used as a molecular weight marker in (A) and (C). Prestained Protein Standards (Enzmart #APC-001, Thailand) were used as a molecular weight marker for (B) and (D). (E) Purified yPac1A8 and yPgi3G4 scFv were resolved by SDS-PAGE and immunoblotted with anti-histidine antibody-gold nanoparticle conjugate. Solid arrow indicates scFv bands at a correct size (about 29 kDa).

>97% sequence identity and has eight amino acids difference. The amino acid sequence of the light chain CDR3 region of all isolated clones starts with "SS" and ends with "V". Sequence analysis of the two scFv genes showed a high number of amino acid differences from germline genes, indicating that the genes were isolated from plasma B cells in the blood after affinity maturation.

The predicted three-dimensional structure of the two scFv clones that were selected for further study, i.e., anti-*P. acnes* clone (yPac1A8) and anti-*P. aeruginosa* clone (yPgi3G4), are illustrated in Figure 1B–E. Anti-*P. acnes* (yPac1A8) scFv was a 29.4 kDa protein of 279 amino acids, while anti-*P. aeruginosa* (yPgi3G4) scFv was a 28.7 kDa protein of 274 amino acids. The surface view of important structures of yPac1A8 and yPgi3G4 is illustrated in Figure 1B and C, respectively. In addition, the $\alpha$-helix and $\beta$-sheet of both clones are shown in Figure 1D and E. The intra-domain disulfide bond of yPac1A8 $V_H$ region was zoomed in and is shown in Figure 1D.

**Cloning and Expression of scFv Antibody Fragments.** To further characterize the two identified recombinant scFvs against model Gram-positive and Gram-negative bacteria, DNA sequences of yPac1A8 and yPgi3G4 scFvs were subcloned into pET-21d (+), expressed in SHuffle T7 B strain *E. coli*, and purified by one-step $Ni^{2+}$-NTA agarose affinity chromatography. Optimization of expression and purification processes was carried out, and SDS-PAGE of the purification process of both scFvs, before and after optimization, is demonstrated in Figure 2A–D. The majority of unwanted protein fractions could be removed after optimization. Elution fractions contained protein bands of scFv at the expected molecular weight of approx. 29 kDa. About 3.0 mg of purified yPac1A8 scFv and 2.3 mg of purified yPgi3G4 scFv are routinely obtained from a 1 L Terrific broth by the baffled flask culture system. A discrepancy between the purity of the two scFv clones was observed under the same scFv expression and purification protocols (Figure 2A–E), of which clone yPac1A8, which has a higher scFv yield, appeared purer than clone yPgi3G4.

The two scFv clones were also observed by western blotting (WB) as shown in Figure 2E. About 1 $\mu$g of each scFv could be detected by an anti-histidine antibody gold nanoparticle conjugate, indicating that hexa-histidine tag of both scFv fragments could interact with the anti-6xhistidine detection system. Both yPac1A8 and yPgi3G4 scFvs could be observed as bright red bands at the expected size. Although equal amounts of scFv were loaded as estimated by the Bradford standard microtiter plate assay, the yPgi3G4 WB band appeared slightly thinner than that of yPac1A8.

**Specific Binding of scFv Antibody by Whole Cell ELISA.** To evaluate the binding specificity of the two anti-bacterial scFv antibodies, an ELISA against whole cell bacteria was performed. The binding of yPac1A8 and yPgi3G4 scFv was tested against a panel of Gram-positive bacteria (*Propionibacterium acidipropionici*, *Propionibacterium freudenreichii*, *P. acnes*) and Gram-negative bacteria (*Pseudomonas putida*, *Pseudomonas fluorescens*, *P. aeruginosa*). Heat-inactivated whole cell bacteria ($10^9$ cells/mL) were immobilized and incubated with 10 $\mu$g/mL of the two scFv clones. Specific binding of yPac1A8 scFv to *P. acnes* and yPgi3G4 scFv to *P. aeruginosa*, respectively, at the species level could be obtained as demonstrated in Figure 3A and Figure S1. Anti-*P. acnes* scFv (yPac1A8) did not bind to five *P. acnes* strains tested, other than the target that was used for affinity selection. Anti-*P. aeruginosa* scFv (yPgi3G4) could bind to three out of four *P. aeruginosa* strains tested, in addition to its affinity selection target.

In this study, successful uses of scFv as a nanostructure for the specific detection of bacterial targets in various formats



https://dx.doi.org/10.1021/acsomega.0c05340
ACS Omega 2021, 6, 762−774

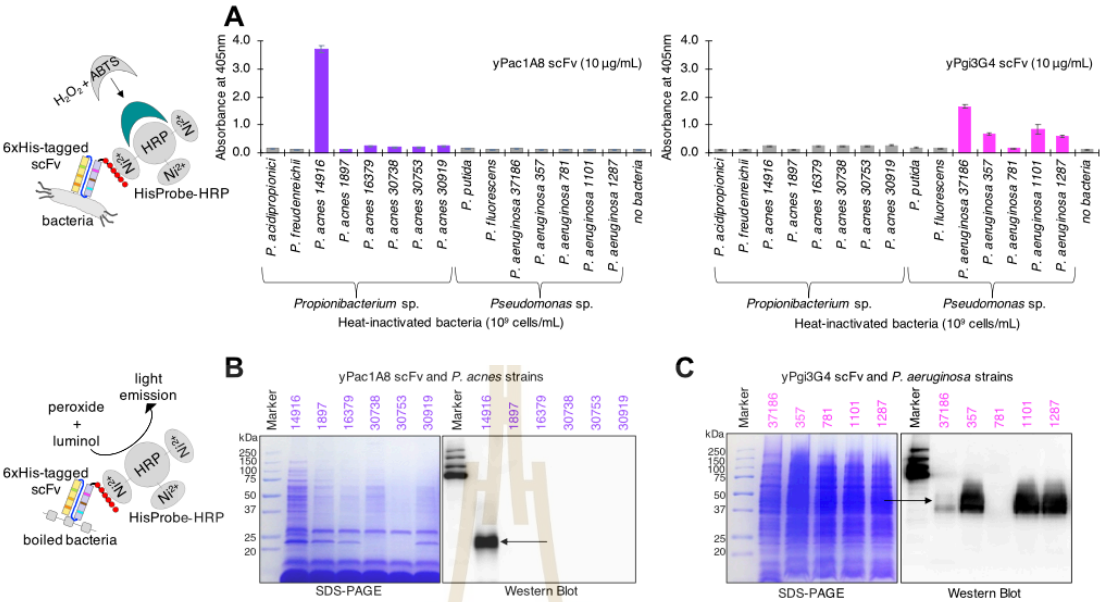


**Figure 3.** Cross-reactivity analysis of 6xHis-tagged scFv by whole-cell ELISA and WB. Binding activities of yPac1A8 and yPgi3G4 scFvs were determined by whole-cell ELISA on a plate coated with the indicated bacteria (A): *P. acidipropionici* TISTR 442, *P. freudenreichii* TISTR 446, *P. acnes* DMST 14916, *P. acnes* strains DSM 1897, DSM 16379, DSM 30738, DSM 30753, DSM 30919, *P. putida* TISTR 1522, *P. fluorescens* TISTR 358, *P. aeruginosa* DMST 37186, *P. aeruginosa* strains TISTR 357, TISTR 781, TISTR 1101, TISTR 1287, and wells without immobilized bacteria. The bars represent the average OD values of triplicate samples, and error bars represent the standard error of the mean. A picture of the ELISA plate is shown in the Supporting Information (Figure S1). (B) SDS-PAGE and WB of boiled antigen preparation of *P. acnes* strains, immunoblotted with yPac1A8 scFv: DMST 14916, DSM 1897, DSM 16379, DSM 30738, DSM 30753, and DSM 30919: Coomassie Brilliant Blue-stained SDS-PAGE gel. The *P. acnes* antigen is located between 20 and 25 kDa (arrow pointed) and was detected by yPac1A8 scFv. (C) SDS-PAGE and WB of boiled antigen preparation of *P. aeruginosa* strains, immunoblotted with yPgi3G4 scFv as indicated: DMST 37186, TISTR 357, TISTR 781, TISTR 1101, and TISTR 1287. The *P. aeruginosa* antigen located between 37 and 50 kDa (arrow pointed) was detected by yPgi3G4 scFv. Precision Plus All Blue Prestained Protein Standards (BioRad#1610373, U.S.A.) were used as a molecular weight marker.

have been demonstrated. The key to the success could be because (1) the phage display library was generated from plasma B cells of healthy individuals who might have been exposed to the bacteria and (2) the choice of affinity selection method used in this study. Boiled pathogenic bacterial antigens were used as a target for affinity selection. This is the same type of antigen preparation that is used to immunize animals for generating antibodies via the traditional method. The fact that the target antigen could resist heat denaturation and that the western blot bands were heterogeneous suggested that the epitopes are post-translationally modified, probably by glycosylation or the addition of a short linear epitope on the surface of the protein, but not a discontinuous epitope, which is a segment on the 3D structure of the protein that will not resist heat. Identification of the epitopes of these two scFv antibodies is beyond the scope of this study and will be explored in the next step.

**Detection of Bacterial Targets by WB.** In addition to ELISA, the target antigens of the two scFv clones were also detected by WB. As shown in Figure 3B, yPac1A8 scFv could detect its target antigen, located between 20 and 25 kDa regions, from denatured *P. acnes* DMST 14916 preparation, but not from other *P. acnes* strains tested. Similarly, as shown in Figure 3C, yPgi3G4 scFv could detect its target antigen, located between 37 and 50 kDa regions, out of the boiled *P. aeruginosa* DMST 37186 preparation. Moreover, yPgi3G4 scFv could detect its target from three other *P. aeruginosa* strains tested (TISTR 357, TISTR 1101, TISTR 1287), but not from TISTR 781. These results are similar to the patterns obtained from ELISA assay. Identification of these bacterial target antigens is beyond the scope of this study and will be carried out in the future.

It has been shown that the level of expression and folding of different scFv fragments varied, depending on the amino acid sequence and intracellular disulfide bond formation.[32] In this report, while there was one intra-domain disulfide in clone yPac1A8 scFv, there was no detectable disulfide bond formation in yPgi3G4; consequently, we observed that the clone yPgi3G4 was less stable and this could be because the folding was disulfide-independent.[33] Even though both scFv antibodies could be expressed at a relatively good yield from *E. coli* SHuffle strain, which favors disulfide bond formation inside the cytoplasm,[34,35] it is possible to improve the stability and hence the binding affinity, by introducing inter-domain disulfide bonds.[36,37]

**Checkerboard Titration (CBT) ELISA.** In order to determine the optimal concentration of target bacteria and corresponding scFv antibody to be used in the ELISA, a checkerboard titration was performed.[38] This method could be used to estimate the binding affinity of the two recombinant antibodies to their target bacteria,[39] and the results are shown in Figure 4A and C and Figures S2 and S3. For yPac1A8, the



https://dx.doi.org/10.1021/acsomega.0c05340
ACS Omega 2021, 6, 762−774

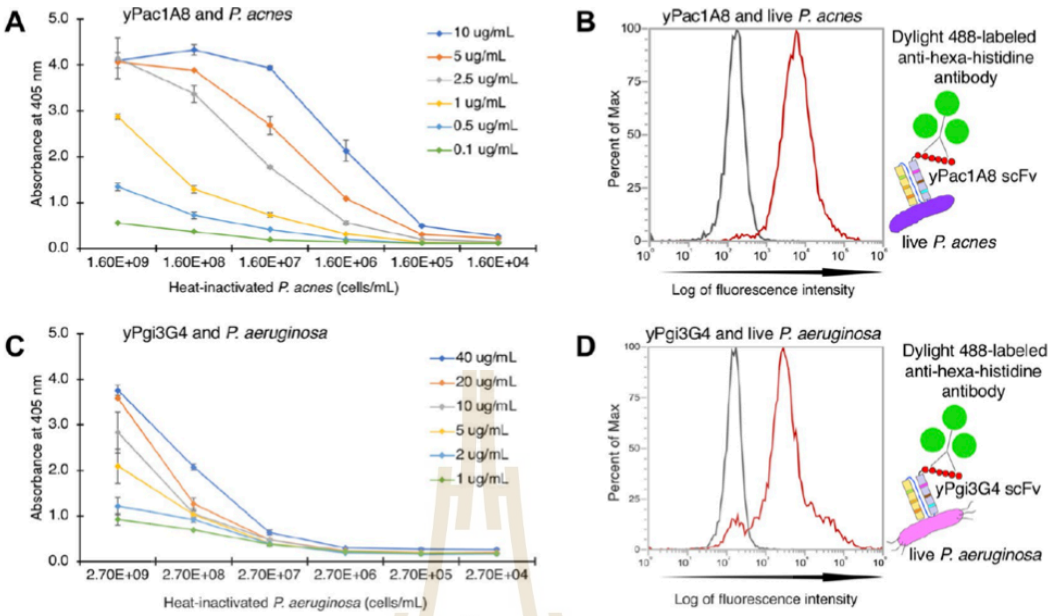


**Figure 4.** Checkerboard titration and flow cytometry analysis against whole cell bacteria. The limit of detection of yPac1A8 for *P. acnes* DMST 14916 (A) and yPgi3G4 for *P. aeruginosa* DMST 37186 (C) was determined by checkerboard titration of whole-cell ELISA, using a dilution series of scFv and serial dilutions of bacteria as indicated. The lines represent the average absorbance values of duplicate samples, and error bars represent the standard error of the mean. Pictures of ELISA plates are shown in the Supporting Information (Figures S2 and S3). Flow cytometry analysis of yPac1A8 (B) and yPgi3G4 scFv (D) binding to live *P. acnes* DMST 14916 and *P. aeruginosa* DMST 37186, respectively. Reactivity of 6xHis-tagged scFv is indicated by the red line. The secondary antibody alone (control) is indicated by the black line.

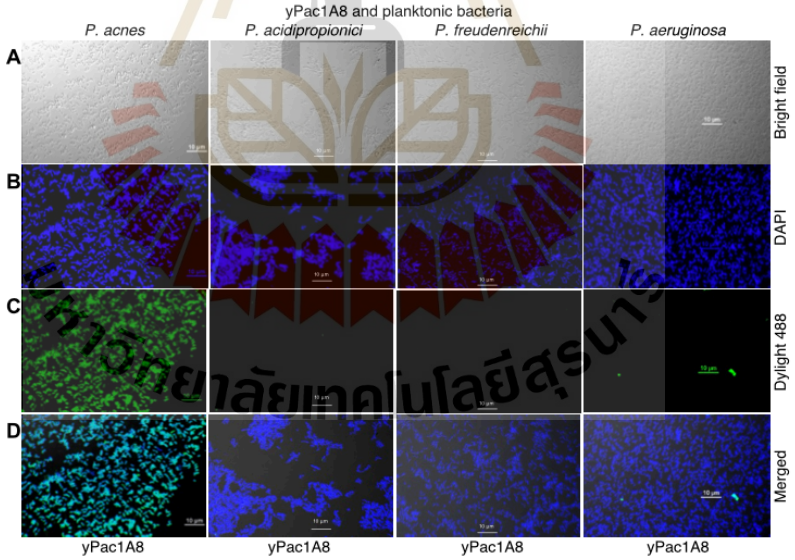


**Figure 5.** CLSM of yPac1A8 and planktonic bacteria. *P. acnes* DMST 14916, *P. acidipropionici* TISTR 442, *P. freudenreichii* TISTR 446, and *P. aeruginosa* DMST 37186 were incubated with yPac1A8 scFv, detected by Dylight 488-labeled anti-hexa-histidine mouse monoclonal antibody, and counterstained with DAPI. Photos were taken by an Apo TIRF 60x Oil DIC N2 objective of Nikon A1R confocal laser microscope. Scale bars represent 10 $\mu$m. In bright field panel (A), individual bacterial cells were seen. In DAPI panel (B), nucleoids of bacteria were stained blue. In Dylight 488 panel (C), only *P. acnes* DMST 14916 was stained green. In merged panel (D), the blue nucleoids and the green cell surfaces of *P. acnes* overlapped. In the case of *P. acidipropionici*, *P. freudenreichii*, and *P. aeruginosa*, only the blue nucleoids were stained.



https://dx.doi.org/10.1021/acsomega.0c05340
ACS Omega 2021, 6, 762−774

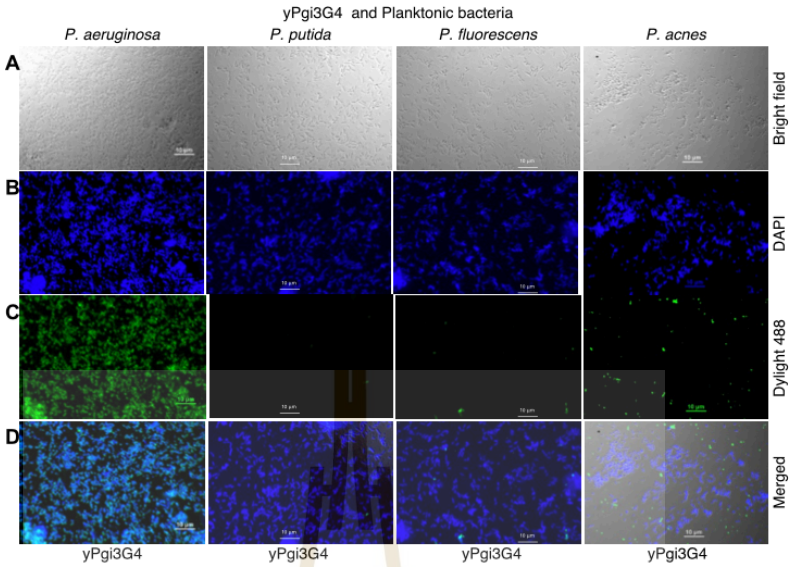


**Figure 6.** CLSM of yPgi3G4 and planktonic bacteria. Photos of *P. aeruginosa* DMST 37186, *P. putida* TISTR 1522, *P. fluorescens* TISTR 358, and *P. acnes* DMST 14916 were taken at the same specifications as in Figure 5. Scale bars represent 10 $\mu$m. In bright field panel (A), bacterial cells are seen. In DAPI panel (B), nucleoids of bacteria are blue. In Dylight 488 panel (C), only *P. aeruginosa* are green. In merged panel (D), the blue nucleoids and the green cell surfaces of *P. aeruginosa* overlapped. In the case of *P. putida*, *P. fluorescens* and *P. acnes*, only the blue nucleoids were stained.

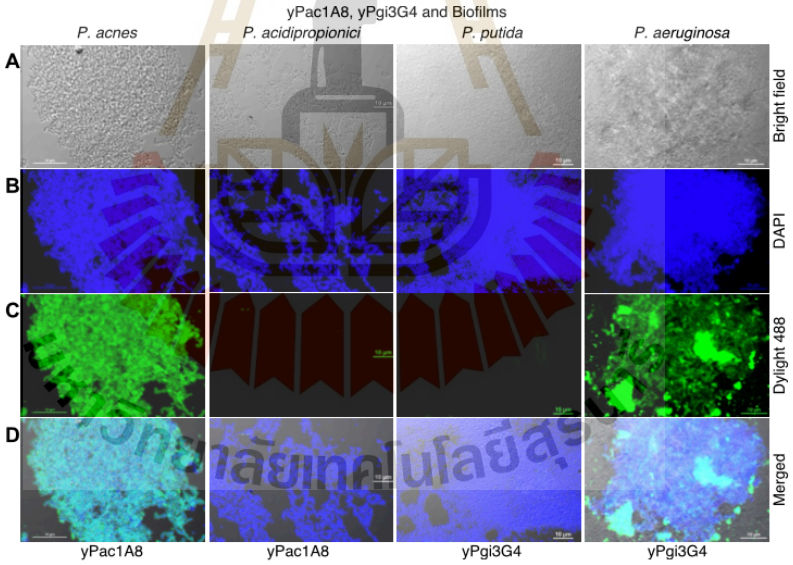


**Figure 7.** CLSM of biofilms stained by indicated scFv. Biofilms of *P. acnes* DMST 14916, *P. acidipropionici* TISTR 442, *P. putida* TISTR 1522, and *P. aeruginosa* DMST 37186 were stained by yPac1A8 and yPgi3G4 scFvs as indicated. Scale bars represent 10 $\mu$m. In bright field panel (A), bacterial cell clusters were seen. In DAPI panel (B), nucleoids of bacteria were stained blue. In Dylight 488 panel (C), *P. acnes* were stained green by yPac1A8 scFv but not *P. acidipropionici*. Likewise, *P. aeruginosa* were stained green by yPgi3G4 scFv but not *P. putida*. In merged panel (D), the blue nucleoids and the green cell surfaces of *P. acnes* and *P. aeruginosa* overlapped. In the case of *P. acidipropionici* and *P. putida*, only the blue nucleoids were stained.

highest scFv concentration tested (10 $\mu$g/mL) could detect 1.6 $\times$ $10^5$ cells/mL and the lowest scFv concentration tested (0.1 $\mu$g/mL) could detect 1.6 $\times$ $10^9$ cells/mL. For yPgi3G4, as much as 40 $\mu$g/mL scFv could detect 2.7 $\times$ $10^7$ cells/mL. These results indicated that the binding affinity of scFv clone yPac1A8 to its target (*P. acnes*) is higher than that of the clone



https://dx.doi.org/10.1021/acsomega.0c05340
ACS Omega 2021, 6, 762−774

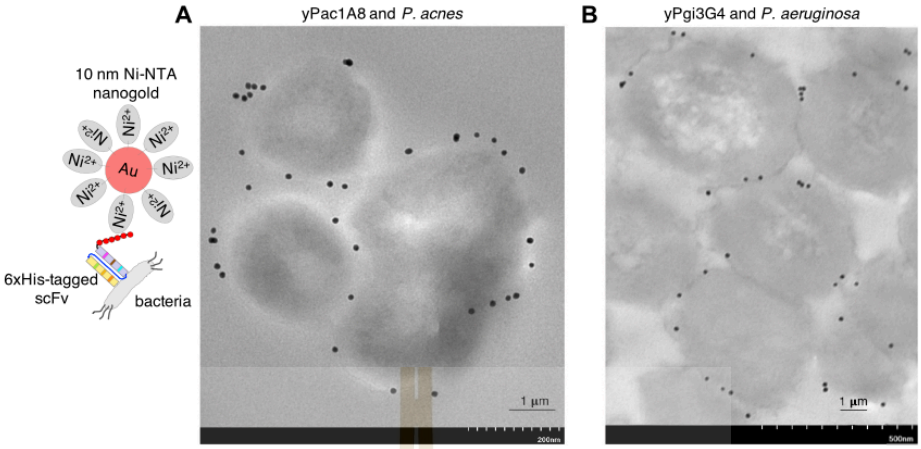


**Figure 8.** TEM of *P. acnes* and *P. aeruginosa*. Four *P. acnes* DMST 14916 cells (A) and six *P. aeruginosa* DMST 37186 cells (B) were treated with yPac1A8 and yPgi3G4 scFvs, respectively. Photos were taken by the Hitachi Hi-Tech HT7700 transmission electron microscope at x25.0 k magnification with Zoom-1 lens mode at the accelerating voltage of 80.0 kV. Scale bars represent 1.0 $\mu$m. The large round structures are bacterial cells, and small dense black dots are 10 nm Ni-NTA nanogold particles.

yPgi3G4 against its target (*P. aeruginosa*). While the apparent binding characteristics of the two isolated antibodies seems sufficient for various assay formats, further improvement of binding affinity or specificity could be performed by different affinity maturation techniques as previously described.[40,41]

**Detection of Live Bacteria by Flow Cytometry.** To demonstrate the binding of yPac1A8 and yPgi3G4 to living target bacteria, flow cytometry analysis was performed. *P. acnes* and *P. aeruginosa* cells were exposed to their corresponding specific scFv followed by anti-polyhistidine Dylight 488 secondary antibody. Cells stained only with anti-polyhistidine Dylight 488 monoclonal antibody were used as a negative control. From each sample, 10,000 events were collected and around 90% of them were bacteria, which were gated in hierarchy for their Dylight 488 fluorescence signal. About 96.9% and 83.3% of *P. acnes* and *P. aeruginosa* were stained with their corresponding antibodies. Data analysis was performed using the built-in Attune Cytometric Software. The results were presented in a histogram overlay format in Figure 4B and D.

**Immunofluorescent Staining of Whole Bacterial Cells and Biofilms.** In addition to ELISA, WB, and flow cytometry, the binding of scFv antibodies was also revealed by a confocal laser scanning microscopy (CLSM) technique as illustrated in Figures 5−7. For the species-specific binding of yPac1A8 to *P. acnes*, *P. acidipropionici*, *P. freudenreichii*, and *P. aeruginosa* were used as controls (Figure 5). In the bright field row, bacterial cells were seen dispersed throughout the field. In the DAPI row, the nucleoid regions of bacteria were stained blue. In the Dylight 488 row, only *P. acnes* cells were bound by yPac1A8 hexa-histidine-tagged scFv, which was detected by a Dylight 488-labeled secondary detection agent and the cells appeared green. Some *P. acnes* cells showed a green cell outline along an unstained center suggesting the cell surface localization of the yPac1A8 scFv-ligand. Similar species-specific binding could be observed between the binding of 6xHis-tagged yPgi3G4 against its target bacteria, *P. aeruginosa* cells (Figure 6). *P. putida*, *P. fluorescens*, and *P. acnes* were used as bacterial controls. These results corresponded well with the ELISA as described in the previous section.

Since bacterial biofilms may play a role in pathogenesis and chronic infection,[42] the binding of selected scFvs against target bacteria in biofilms was also investigated. As demonstrated in Figure 7, *P. acnes* and *P. aeruginosa* biofilms cultured on glass coverslips were stained by yPac1A8 and yPgi3G4, respectively. Biofilms of *P. acidipropionici* TISTR 442 and *P. putida* TISTR 1522 were used as controls. In the bright field row, bacterial cell clusters were seen. In the DAPI row, the nucleoid regions of bacteria were stained blue. In the Dylight 488 row, *P. acnes* and *P. aeruginosa* cells were observed as green bacilli with an obvious unstained central halo region. The results indicated that both scFvs could bind to their target bacteria inside a biofilm.

**Cell Surface Staining by Electron Microscopy.** Electron microscopy was carried out to further investigate the findings obtained by whole cell ELISA, flow cytometry, and CLSM, which suggested that the target antigens are located on the bacterial cell surface. Ni-NTA sensitized 10 nm nanogold particles were used as a detection probe. As expected, nanogold particles were seen as dark dots along the cell outline of *P. acnes* and *P. aeruginosa* under a transmission electron microscope (Figure 8). These results confirmed the cell surface localization of the two anti-bacterial scFv ligands.

The application of anti-bacterial scFvs as nanostructures is demonstrated in different binding assays. In these assays, the 6xHis tag at the C-terminus of the scFv was bound with anti-His antibody or nickel, conjugated with enzyme horseradish peroxidase (HRP), gold nanoparticle, or fluorescent dye. The data from this study indicated that the arrangement of domains comprising $V_H$-($G_4S$)3-$V_L$-6xHis-Myc, as depicted in Figure 1A, is an effective nanostructure. The predicted 3D structure of both scFv antibodies indicated that the CDR regions of yPac1A8 and yPgi3G4 scFv are located opposite to the 6xHis tag. This conformation seems to be favorable for specific antigen binding activity and for the poly-His tag recognition function to take place without structural constraint.



https://dx.doi.org/10.1021/acsomega.0c05340
ACS Omega 2021, 6, 762−774

The advantage of directional conjugation via the 6xHis-tag over random conjugation is that there is no interference with the antigen binding site. Histidine is strongly involved in the coordinate bond with metal ions and the polyhistidine tag has been used as one of the most popular tags for protein purification by metal chelate affinity chromatography. The $Ni^{2+}$ ion of Ni-NTA binds with two histidine residues of the 6xHis tag.[43] A stable attachment between one scFv and one gold particle is established when three adjacent Ni-NTA groups of the gold nanoparticle bind to the 6x-His tag of scFv. As for metal ions, copper has the highest affinity, and the affinity decreases in the order of nickel, zinc, and cobalt.[44] While nickel is often used for general purposes, the binding affinity between scFv and a detector or carrier can be increased by changing the type of metal ion or by introducing a type of tag, such as using streptavidin-biotin interactions, which are considered the strongest non-covalent natural bond.[45]

## ■ CONCLUSIONS AND FUTURE PERSPECTIVES

An efficient method for the identification of scFv nanostructures for the specific detection of two model Gram-positive and Gram-negative bacteria, *P. acnes* and *P. aeruginosa*, by the affinity selection of a non-immunized human phage scFv antibody library against boiled bacterial antigens is reported. The specific binding of 6xHis-tagged scFv fragments to a bacterial cell surface was demonstrated by ELISA, WB, flow cytometry, and confocal fluorescence and electron microscopy. These scFv antibody fragments could be further developed to be used as a point-of-care diagnostic or further engineered and used as novel therapeutic agents in many ways such as conversion into whole immunoglobulin (IgG) molecule for monoclonal antibody therapy, conjugation to nanoparticles loaded with antibiotics, or conjugation with nanoparticles for multiplex biosensor-based detection, which could be very useful for biofilm detection. In addition, genetic engineering can be used to improve the binding affinity or specificity, create bi-specific antibody to enhance the binding spectrum or creating sensitive detection probe by fusing with fluorescent proteins or enzymes such as alkaline phosphatase, horseradish peroxidase, or luciferase. These are examples of interesting research in the next step to be explored.

## ■ MATERIALS AND METHODS

**Bacterial Strains.** Affinity selection targets: *P. acnes* DMST 14916 and *P. aeruginosa* DMST 37186, were kindly provided by Dr. Griangsak Eumkeb, School of Sciences, Suranaree University of Technology, Thailand. The species identity of both strains was confirmed by 16S rRNA gene sequencing at Macrogen, Inc., South Korea. *P. acnes* strains DSM 1897, DSM 16379, DSM 30738, DSM 30753, and DSM 30919 were kindly provided by Professor Dietmar Haltrich, Department of Food Science and Technology, University of Natural Resources and Life Sciences, Vienna. *P. freudenreichii* TISTR 446, *P. fluorescens* TISTR 358, *P. putida* TISTR 1522, and *P. aeruginosa* strains TISTR 357, TISTR 781, and TISTR 1287 were purchased from the Thailand Institute of Scientific and Technological Research. *P. acidipropionici* TISTR 442 and *P. aeruginosa* TISTR 1101 were kindly provided by TISTR for academic research purposes. TG1 strain *E. coli* and HB2151 strain *E. coli* were obtained from the Medical Research Council (MRC) Laboratory, Cambridge, UK. SHuffle T7 B strain *E. coli* (NEB #C3029J, U.S.A.) was purchased from New England Biolabs, U.S.A. The source of materials used is described elsewhere.

**Affinity Selection (Biopanning) against *P. acnes* and *P. aeruginosa*.** *Antigen Preparation.* *P. aeruginosa* colonies were grown on LB broth and incubated overnight at 250 rpm, 37 °C. *P. acnes* colonies were cultured in BHI broth and incubated for 5 days at 37 °C anaerobically in a GasPak system. Bacterial cells were washed with PBS two times and resuspended in PBS at the $OD_{600}$ of 2.0. Cell suspensions were boiled for 1 h in a water bath, and the protein concentration was determined by Bradford standard microtiter plate assay (BioRad #500-0006, California, U.S.A.).

*Affinity Selection Procedure.* Affinity selection was carried out according to a previously published protocol.[30] Maxisorp immunotube (Nalgene Nunc International, Denmark) was coated overnight at 4 °C with 25 μg of boiled bacterial antigen in 100 mM $NaHCO_3$ (pH 8.5). The tube was blocked with 2% (w/v) skimmed milk protein in phosphate-buffered saline (PBSM) before incubation with $10^{12}$ plaque-forming units (pfu) of virion from the Yamo I human phage display scFv library[4] in 2% PBSM. The tube was washed five times with 0.05% (v/v) Tween-20 in PBS (PBST) followed by five more PBS washes. Then, the bound virions were eluted with 1 mg/mL trypsin in PBS followed by 100 mM glycine-HCl (pH 2.0), and neutralization was carried out with 200 mM $NaPO_4$ (pH 7.5). For the second and third round, eluted virions were pooled together, amplified, and purified by PEG precipitation, as previously described.[46]

*Amplification of the Individual Virion Clone.* Discrete colonies of *E. coli* TG1, infected with eluted virions from affinity selection, were randomly picked and cultured in U-shaped 96-well microplates (Nunclon delta surface, Thermo Fisher Scientific #163320, U.S.A.), containing 100 μL/well of 2×YT medium with 100 μg/mL ampicillin and 1.0% (w/v) glucose (2xYT-AmpGlu). The cultures were super-infected with helper phage KM13 to amplify the isolated virion as previously explained.[47] After incubation at 30 °C with shaking at 250 rpm for 20 h, supernatants containing the virions obtained after the centrifugation of a deep-well plate were used for monoclonal phage ELISA as described in the ELISA section.

*DNA and Amino Acid Sequence Analysis of Selected Virion Clones.* Phagemids from selected ELISA-positive virion clones were prepared and sent for automated DNA sequence analysis as previously described.[47] Contig alignment of the sequences was performed using Vector NTI software (Thermo Fisher Scientific, U.S.A.), and the aligned sequences were further analyzed with the IgBLAST tool from the National Center for Biotechnology Information[48] and IMGT/V-QUEST tool from the international ImMunoGeneTics information system.[49] Three-dimensional structures of selected scFvs were generated by using the SWISS-MODEL server from the Swiss Institute of Bioinformatics.[50] The template (PDB ID code: 1f3r.1.B) was chosen by sequence identity analysis. Models were built by target-template alignment using ProMod3 and visualized with the program PyMOL, a molecular visualization system from Schrödinger, LLC, U.S.A.[51]

*Small-Scale Production of Soluble scFv from E. coli HB2151.* Soluble scFv clones were produced from the non-suppressor strain of *E. coli* HB2151, which read the Amber codon between the scFv and geneIII protein gene sequences in the phagemid vector as a stop codon instead of glutamic acid



https://dx.doi.org/10.1021/acsomega.0c05340
ACS Omega 2021, 6, 762−774

in the TG1 strain, as previously described.[41] The culture supernatant containing soluble scFv fragments was used for scFv ELISA as described in the ELISA section.

**Production of Hexa-Histidine-Tagged scFv (6xHis-Tagged scFv).** *Cloning and Expression of scFv Genes.* The scFv genes against *P. acnes* and *P. aeruginosa* were cloned into pET-21d (+) expression vectors and designated as pET21d +/yPac1A8 and pET21d+/yPgi3G4, respectively, as previously described.[47] The scFv genes were expressed in the cytoplasm of protease deficient *E. coli*, SHuffle T7 B strain (NEB #C3029J, U.S.A.), according to a previous study[52] with some optimization. Briefly, a colony streaked from −80 °C stock of SHuffle *E. coli* C3029 harboring pET21d+/yPac1A8 or pET21d+/yPgi3G4 was inoculated into 5 mL of Terrific Broth (TB: Tryptone 12 g/L, yeast extract 24 g/L, glycerol 4 mL/L, 0.17 M $KH_2PO_4$, and 0.72 M $K_2HPO_4$) containing 100 μg/mL ampicillin and incubated overnight at 30 °C with 225 rpm shaking. On the next day, a starter culture was transferred into 500 mL of fresh TB containing 100 μg/mL ampicillin and cultured at 30 °C in a bench-top bioreactor system or in a baffled flask with 225 rpm shaking until the $OD_{600}$ reached about 1.0. Protein expression was induced with 0.85 mM IPTG for 24 h at 25 °C. The culture was cooled on ice for 5 min and centrifuged at 3000*g* for 30 min at 4 °C. The cell pellet was used directly for scFv purification or otherwise stored at −40 °C.

*Purification of Hexa-Histidine-Tagged scFv.* The 6xHis-tagged scFv was purified by immobilized metal affinity chromatography (IMAC), using a gravity flow column containing a Ni-NTA ($Ni^{2+}$ nitrilotriacetic acid) agarose affinity chromatography matrix, following the company's manual (Qiagen #30230, Germany). The resin was washed with washing buffer (50 mM Tris-HCl, 0.5 M NaCl, 100 mM imidazole, pH 7.5), and scFv was eluted with elution buffer (50 mM Tris-HCl, 0.5 M NaCl, 500 mM imidazole, pH 7.5). Desalting and buffer exchange was performed by dialysis overnight in SnakeSkin Dialysis Tubing with 10 kDa MWCO (Thermo Fisher Scientific #68100, U.S.A.) against cold PBS buffer at 4 °C. The purity of eluted scFvs was checked by SDS-PAGE, and the purified soluble scFv concentration was determined by a Bradford standard microtiter plate assay (BioRad #500-0006, California, U.S.A.). The samples were kept at −80 °C in 250 mg/mL BSA or at −40 °C in 20% glycerol.

**Western Blot Analysis.** *WB of Isolated scFv.* Equal amounts (1 μg) of purified scFv (yPac1A8 and yPgi3G4) were heat-treated at 90 °C for 10 min in SDS sample buffer containing β-mercaptoethanol. Then, samples were electrophoresed in 12.5% SDS-PAGE gel for 5 min at 50 V followed by 90 min at 100 V and were transferred to a polyvinylidene difluoride (PVDF) membrane (Cytiva #10600021, U.S.A.) by wet-blotting using a Mini Trans-Blot electrophoretic transfer cell (Biorad #1703930, U.S.A.) at 30 V for 15 h at 4 °C. To detect the scFv, the membrane was incubated with 10 mL of anti-histidine antibody-gold nanoparticle conjugate (Jena Bioscience# PS-110, Germany) for 3 h at room temperature with slight rocking. The scFv bands became visible due to antibody mediated gold nanoparticle accumulation.

*WB of Bacterial Targets Using Identified 6xHis-Tagged scFv.* About 30 μg of boiled bacterial antigen preparation (*P. acnes* and *P. aeruginosa*) was used as samples. The SDS-PAGE and wet-blotting procedures were the same as above. After blocking with 3% BSA-TBST, the membrane was incubated in 2 μg/mL 6xHis-tagged scFv (yPac1A8 and yPgi3G4) in TBST for 15 h at 4 °C followed by washing three times with TBST (5 min per wash). It was then incubated with 1:5000 diluted HisProbe-HRP (a nickel ($Ni^{2+}$)-activated derivative of horseradish peroxidase) (Thermo Fisher Scientific#15165, U.S.A.) in blocking buffer for 1 h at room temperature with slight rocking followed by washing three times with TBST. Finally, the protein band was detected by chemiluminescence using Amersham ECL Prime Western blotting detection reagent (GE Healthcare #RPN2232, UK). Image analysis was performed by CCD camera-based imaging, using the ChemiDoc XRS Gel Documentation System (Bio-Rad, U.S.A.).

**Enzyme-Linked Immunosorbent Assay (ELISA).** *Monoclonal Phage ELISA.* For phage ELISA, 5 μg of bacterial antigen in 100 mM $NaHCO_3$ (pH 8.5) was used as a target and 1% (w/v) BSA in PBS as a negative control. The phage ELISA was performed as previously described.[53] Virion clones that showed an OD value of at least two times higher than those of negative controls were selected for confirmation.

*scFv ELISA.* For scFv ELISA, 2 μg of bacterial antigen in 100 mM $NaHCO_3$ (pH 8.5) was used as a target and 1% (w/v) BSA in PBS as a negative control. The supernatant containing soluble scFv fragments (150 μL/well) was used as a primary detection agent. HisProbe-HRP (Thermo Fisher Scientific #15165, U.S.A.) diluted at 1:5000 in PBS was used as a secondary detection agent. The ELISA procedure was the same as the monoclonal phage ELISA.

*scFv ELISA against Whole Cell Bacteria.* For *Propionibacterium* species, colonies streaked from −80 °C stock on BHI agar were inoculated into BHI broth and incubated anaerobically for 5 days at 37 °C in the case of *P. acnes* and at 30 °C in the case of *P. acidipropionici* and *P. freudenreichii*. For *Pseudomonas* species, colonies streaked from −80 °C stock on LB agar were inoculated into LB broth and incubated overnight at 250 rpm at 37 °C in the case of *P. aeruginosa* and at 30 °C in the case of *P. fluorescens* and *P. putida*. Broth cultures were washed with PBS two times, and cells were resuspended in PBS. The $OD_{600}$ value of cell suspensions was adjusted to 2.0. Heat inactivation was carried out in a water bath for 30 min at 60 °C. Heat-inactivated bacteria were used for whole cell ELISA.

To check the specificity of 6xHis-tagged scFv, heat-inactivated bacteria ($10^9$ cells/mL) was used as a target. Purified hexa-histidine-tagged scFv (10 μg/mL) was used as a primary detection agent and HisProbe-HRP as a secondary detection agent. The ELISA procedure was the same as above except that the immobilization step was performed overnight at 37 °C.

*Checkerboard Titration (CBT).* To optimize the scFv ELISA and to determine the limit of detection of recombinant scFv, the ELISA plate was coated with serial dilutions of heat-inactivated bacterial suspension from rows A to F, where row A had the highest ($10^9$ cells/mL) bacterial concentration while row F had the lowest ($10^4$ cells/mL). The ELISA procedure was carried out as described above except that the wells were incubated with six different dilutions of scFv in duplicate format from columns 1 to 12, where columns 1 and 2 had the highest scFv concentration (yPac1A8 scFv 10 μg/mL or yPgi3G4 scFv 40 μg/mL) while columns 11 and 12 had the lowest (yPac1A8 scFv 0.1 μg/mL or yPgi3G4 scFv 1.0 μg/mL).

**Flow Cytometry.** A bacterial colony was suspended in 900 μL of PBS, and 300 μL of it was diluted with PBS to 1 mL and was centrifuged at 2000*g* for 5 min. The cells were resuspended



https://dx.doi.org/10.1021/acsomega.0c05340
ACS Omega 2021, 6, 762−774

in 1 mL of 1% BSA-0.1% PBST, blocked for 30 min at room temperature, and washed two times with PBS. The cells were incubated with specific 6xHis-tagged scFv (200 μg/mL) for 1 h at room temperature. *P. acnes* cells were exposed to yPac1A8 scFv and *P. aeruginosa* cells to yPgi3G4 scFv. After two PBS washes, the cells were stained with a 1:500 dilution of Dylight 488-labeled anti-hexa-histidine mouse monoclonal antibody (Abcam #ab117512, UK) in PBS for 1 h in a dark place at room temperature. The cells were washed with PBS two times and resuspended in 500 μL of PBS containing 4 μg/mL PI (propidium iodide) solution (Thermo Fisher Scientific #A28993, U.S.A.). Sample reading was performed using an Invitrogen Attune NxT Acoustic Focusing 3-Laser System Cytometer (Thermo Fisher Scientific# P3566, U.S.A.).

**Confocal Laser Scanning Microscopy (CLSM).** *CLSM of Planktonic Bacteria.* About 1 mL of broth culture was centrifuged (3000*g*, 5 min), washed with PBS two times, and resuspended in PBS. About 5 μL of the suspension was spread into a smear on a glass slide and dried completely at 37 °C. The smear was fixed with 4% PFA (paraformaldehyde) in PBS (pH 7.4) for 30 min, blocked with 1% BSA-300 mM glycine-0.1% PBST for 30 min, treated with 2 μg of 6xHis-tagged scFv for 1 h, incubated with 1:500 dilution of Dylight 488-labeled anti-hexa-histidine mouse monoclonal antibody (Abcam #ab117512, UK) in PBS for 1 h, and counterstained with 300 μM DAPI (4′,6-diamidino-2-phenylindole) for 5 min. The smear was washed three times with PBS between the above steps. The stained smear was covered with slow fade gold mountant (Invitrogen #S36936, U.S.A.) and examined with a confocal microscope (Nikon A1R, Japan).

*CLSM of Bacterial Biofilms.* Bacterial biofilm was grown by placing autoclaved glass coverslips at the air−liquid interface of broth cultures.[54] The incubation time for *P. acnes* and *P. aeruginosa* biofilms were 5 days anaerobically in the GasPak system and overnight aerobically, respectively. Before staining, the biofilm was washed with PBS three times and dried completely at 37 °C. The staining procedure was the same as above except that 20 μg of 6xHis-tagged scFv was used. One set of biofilms was used for crystal violet staining.

**Transmission Electron Microscopy (TEM).** The procedure was carried out in a microcentrifuge tube. Bacteria in broth culture were centrifuged at 3000*g* for 5 min, washed with 0.85% NaCl followed by PBS, and fixed with 4% PFA (pH 7.4) in PBS for 30 min at room temperature. After washing with PBS two times, the bacteria were blocked with 1% BSA-300 mM glycine in 0.1% PBST for 30 min at room temperature followed by two PBS washes. Then, 50 μg of 6xHis-tagged scFv in PBS was added and incubated for 60 min at room temperature. After washing two times with PBS, a 1:20 dilution of 10 nm Ni-NTA nanogold (Nanoprobes #2084, U.S.A.) in 0.05% TBST containing 1% BSA, which is the recommended dilution from the manufacturer, was added and incubated for 30 min at room temperature followed by two TBST-BSA washes. Then, the samples were resuspended in PBS, dehydrated by the graded ethanol dehydration method, and polymerized in LR White medium grade resin and accelerator (EMS #14380, U.S.A.) in a BEEM embedding capsule (EMS #69911-01, U.S.A.) by a cold curing method. Finally, ultra-thin sections were examined with a transmission electron microscope (Hitachi Hi-Tech HT7700, Japan).

## ■ ASSOCIATED CONTENT

### Supporting Information

The Supporting Information is available free of charge at https://pubs.acs.org/doi/10.1021/acsomega.0c05340.

Picture of an ELISA plate for the result shown in Figure 3A (Figure S1) and pictures of ELISA plates for the results shown in Figure 4A and C are provided as Figures S2 and S3 (PDF)

## ■ AUTHOR INFORMATION

### Corresponding Author

**Montarop Yamabhai** − *Molecular Biotechnology Laboratory, School of Biotechnology, Institute of Agricultural Technology, Suranaree University of Technology, Nakhon Ratchasima 30000, Thailand*; orcid.org/0000-0003-2674-2419; Email: montarop@g.sut.ac.th

### Author

**Thae Thae Min** − *Molecular Biotechnology Laboratory, School of Biotechnology, Institute of Agricultural Technology, Suranaree University of Technology, Nakhon Ratchasima 30000, Thailand*

Complete contact information is available at: https://pubs.acs.org/10.1021/acsomega.0c05340

### Author Contributions

T.T.M. performed all experiments and drafted the first draft. M.Y. conceived the study, designed the experiments, analyzed the results, and edited the manuscript. Both authors have given approval to the final version of the manuscript.

### Funding

This research was supported by the SUT-PhD scholarship for ASEAN students (2014), SUT, and Thailand Science Research and Innovation (TSRI) [grant number RTA6180012].

### Notes

The authors declare no competing financial interest.

## ■ ACKNOWLEDGMENTS

We thank Assoc. Professor Griangsak Eumkeb, School of Sciences, Suranaree University of Technology (SUT), Thailand and Professor Dietmar Haltrich, University of Natural Resources and Life Sciences, Vienna, Austria, for kindly sharing bacteria. We are thankful to Confocal microscopy and Electron microscopy sections of SUT and the Electron microscopy section of Chulalongkorn University and Kasetsart University for helping us with immunoelectron microscopy.

## ■ ABBREVIATIONS

ABTS, 2,2′-azino-bis(3-ethylbenzthiazoline-6-sulfonic acid) diammonium salt; DMST, Department of Medical Sciences Thailand; DSM, German Collection of Microorganisms and Cell Cultures; LR White, London Resin Company's Product; MWCO, molecular weight cutoff

## ■ REFERENCES

(1) Barderas, R.; Benito-Peña, E. The 2018 Nobel Prize in Chemistry: phage display of peptides and antibodies. *Anal. Bioanal. Chem.* **2019**, *411*, 2475−2479.

(2) Kehoe, J. W.; Kay, B. K. Filamentous phage display in the new millennium. *Chem. Rev.* **2005**, *105*, 4056−4072.

(3) McCafferty, J.; Griffiths, A. D.; Winter, G.; Chiswell, D. J. Phage antibodies: filamentous phage displaying antibody variable domains. *Nature* **1990**, *348*, 552−554.
(4) Pansri, P.; Jaruseranee, N.; Rangnoi, K.; Kristensen, P.; Yamabhai, M. A compact phage display human scFv library for selection of antibodies to a wide variety of antigens. *BMC Biotechnol.* **2009**, *9*, 6.
(5) Bradbury, A. R. M.; Sidhu, S.; Dübel, S.; McCafferty, J. Beyond natural antibodies: the power of in vitro display technologies. *Nat. Biotechnol.* **2011**, *29*, 245−254.
(6) Gavilondo, J. V.; Larrick, J. W. Antibody engineering at the millennium. *BioTechniques* **2000**, *29*, 128−145.
(7) Vallet-Courbin, A.; Larivière, M.; Hocquellet, A.; Hemadou, A.; Parimala, S.-N.; Laroche-Traineau, J.; Santarelli, X.; Clofent-Sanchez, G.; Jacobin-Valat, M. J.; Noubhani, A. A recombinant human anti-platelet scfv antibody produced in *Pichia pastoris* for atheroma targeting. *PLoS One* **2017**, *12*, No. e0170305.
(8) Kontermann, R. E. Bispecific diabodies and single-chain diabodies. In *Antibody Engineering*; Kontermann, R.; Dubel, S., Eds. Springer: 2010; Vol. 2, pp. 227−238.
(9) Marston, H. D.; Paules, C. I.; Fauci, A. S. Monoclonal antibodies for emerging infectious diseases - borrowing from history. *The New England Journal of Medicine* **2018**, *378*, 1469−1472.
(10) Martín-Galiano, A. J.; McConnell, M. J. Using omics technologies and systems biology to identify epitope targets for the development of monoclonal antibodies against antibiotic-resistant bacteria. *Front. Immunol.* **2019**, *10*, 1−8.
(11) Zurawski, D. V.; McLendon, M. K. Monoclonal antibodies as an antibacterial approach against bacterial pathogens. *Antibiotics* **2020**, *9*, 155.
(12) Langdon, A.; Crook, N.; Dantas, G. The effects of antibiotics on the microbiome throughout development and alternative approaches for therapeutic modulation. *Genome. Med.* **2016**, *8*, 39.
(13) WHO *Global priority list of antibiotic-resistant bacteria to guide research, discovery, and development of new antibiotics*. 2017.
(14) Molina-López, J.; Sanschagrin, F.; Levesque, R. C. A peptide inhibitor of MurA UDP-N-acetylglucosamine enolpyruvyl transferase: the first committed step in peptidoglycan biosynthesis. *Peptides* **2006**, *27*, 3115−3121.
(15) El Zoeiby, A.; Sanschagrin, F.; Darveau, A.; Brisson, J. R.; Levesque, R. C. Identification of novel inhibitors of *Pseudomonas aeruginosa* MurC enzyme derived from phage-displayed peptide libraries. *J. Antimicrob. Chemother.* **2003**, *51*, 531−543.
(16) Paradis-Bleau, C.; Lloyd, A.; Sanschagrin, F.; Clarke, T.; Blewett, A.; Bugg, T. D.; Levesque, R. C. Phage display-derived inhibitor of the essential cell wall biosynthesis enzyme MurF. *BMC Biochem* **2008**, *9*, 33.
(17) Paradis-Bleau, C.; Lloyd, A.; Sanschagrin, F.; Maaroufi, H.; Clarke, T.; Blewett, A.; Dowson, C.; Roper, D. I.; Bugg, T. D.; Levesque, R. C. *Pseudomonas aeruginosa* MurE amide ligase: enzyme kinetics and peptide inhibitor. *Biochem. J.* **2009**, *421*, 263−272.
(18) Paradis-Bleau, C.; Sanschagrin, F.; Levesque, R. C. Peptide inhibitors of the essential cell division protein FtsA. *Protein Eng., Des. Sel.* **2005**, *18*, 85−91.
(19) Pini, A.; Giuliani, A.; Falciani, C.; Runci, Y.; Ricci, C.; Lelli, B.; Malossi, M.; Neri, P.; Rossolini, G. M.; Bracci, L. Antimicrobial activity of novel dendrimeric peptides obtained by phage display selection and rational modification. *Antimicrob. Agents Chemother.* **2005**, *49*, 2665−2672.
(20) Rao, S. S.; Mohan, K. V. K.; Atreya, C. D. A peptide derived from phage display library exhibits antibacterial activity against *E. coli* and *Pseudomonas aeruginosa*. *PLoS One* **2013**, *8*, 1−259.
(21) DiGiandomenico, A.; Warrener, P.; Hamilton, M.; Guillard, S.; Ravn, P.; Minter, R.; Camara, M. M.; Venkatraman, V.; Macgill, R. S.; Lin, J.; Wang, Q.; Keller, A. E.; Bonnell, J. C.; Tomich, M.; Jermutus, L.; McCarthy, M. P.; Melnick, D. A.; Suzich, J. A.; Stover, C. K. Identification of broadly protective human antibodies to *Pseudomonas aeruginosa* exopolysaccharide Psl by phenotypic screening. *J Exp Med* **2012**, *209*, 1273−1287.
(22) DiGiandomenico, A.; Keller, A. E.; Gao, C.; Rainey, G. J.; Warrener, P.; Camara, M. M.; Bonnell, J.; Fleming, R.; Bezabeh, B.; Dimasi, N.; Sellman, B. R.; Hilliard, J.; Guenther, C. M.; Datta, V.; Zhao, W.; Gao, C.; Yu, X. Q.; Suzich, J. A.; Stover, C. K. A multifunctional bispecific antibody protects against *Pseudomonas aeruginosa*. *Sci. Transl. Med.* **2014**, *6*, 262ra155.
(23) Santajit, S.; Seesuay, W.; Mahasongkram, K.; Sookrung, N.; Ampawong, S.; Reamtong, O.; Diraphat, P.; Chaicumpa, W.; Indrawattana, N. Human single-chain antibodies that neutralize *Pseudomonas aeruginosa*-exotoxin A-mediated cellular apoptosis. *Sci. Rep.* **2019**, *9*, 14928.
(24) Kulkeaw, K.; Sakolvaree, Y.; Srimanote, P.; Tongtawe, P.; Maneewatch, S.; Sookrung, N.; Tungtrongchitr, A.; Tapchaisri, P.; Kurazono, H.; Chaicumpa, W. Human monoclonal scFv neutralize lethal Thai cobra, *Naja kaouthia*, neurotoxin. *J. Proteomics* **2009**, *72*, 270−282.
(25) Jung, Y. S.; Matsumoto, S. E.; Katakura, Y.; Yamashita, M.; Tomimatsu, K.; Kabayama, S.; Teruya, K.; Shirahata, S. Generation of human monoclonal antibodies against *Propionibacterium acnes* by applying the phage display method to human peripheral blood mononuclear cells immunized in vitro. *Cytotechnology* **2008**, *57*, 169−175.
(26) CDC *Antibiotic resistance threats in the United States, 2019*. 2019.
(27) O'Neill, J. *Tackling drug-resistant infections globally: final report and recommendations*. Wellcome Trust and UK Government: UK, 2016; *Vol.* May.
(28) Chng, K. R.; Li, C.; Bertrand, D.; Ng, A. H. Q.; Kwah, J. S.; Low, H. M.; Tong, C.; Natrajan, M.; Zhang, M. H.; Xu, L.; Ko, K. K. K.; Ho, E. X. P.; Av-Shalom, T. V.; Teo, J. W. P.; Khor, C. C.; Consortium, M.; Chen, S. L.; Mason, C. E.; Ng, O. T.; Marimuthu, K.; Ang, B.; Nagarajan, N. Cartography of opportunistic pathogens and antibiotic resistance genes in a tertiary hospital environment. *Nat. Med.* **2020**, *26*, 941−951.
(29) Haak, B. W.; Wiersinga, W. J. Uncovering hidden antimicrobial resistance patterns within the hospital microbiome. *Nat. Med.* **2020**, *26*, 826−828.
(30) McCafferty, J.; Johnson, K. S. Construction and screening of antibody display libraries. In *Phage Display of Peptides and Proteins*; Kay, B. K.; Winter, J.; McCafferty, J., Eds. Academic Press, Inc.: USA, 1996; pp. 79−110.
(31) Townsend, C. L.; Laffy, J. M. J.; Wu, Y.-C. B.; Silva O'Hare, J.; Martin, V.; Kipling, D.; Fraternali, F.; Dunn-Walters, D. K. Significant differences in physicochemical properties of human immunoglobulin kappa and lambda CDR3 regions. *Front Immunol.* **2016**, *7*, 388.
(32) Zarschler, K.; Witecy, S.; Kapplusch, F.; Foerster, C.; Stephan, H. High-yield production of functional soluble single-domain antibodies in the cytoplasm of *Escherichia coli*. *Microb. Cell Fact.* **2013**, *12*, 97.
(33) Proba, K.; Wörn, A.; Honegger, A.; Plückthun, A. Antibody scFv fragments without disulfide bonds made by molecular evolution. *J. Mol. Biol.* **1998**, *275*, 245−253.
(34) Berkmen, M. Production of disulfide-bonded proteins in *Escherichia coli*. *Protein Expression Purif.* **2012**, *82*, 240−251.
(35) Ren, G.; Ke, N.; Berkmen, M. Use of the SHuffle strains in production of proteins. *Curr. Protoc. Protein Sci.* **2016**, *85*, 5.26.1−5.26.21.
(36) Zhao, J. X.; Yang, L.; Gu, Z. N.; Chen, H. Q.; Tian, F. W.; Chen, Y. Q.; Zhang, H.; Chen, W. Stabilization of the single-chain fragment variable by an interdomain disulfide bond and its effect on antibody affinity. *Int. J. Mol. Sci.* **2010**, *12*, 1−11.
(37) Weatherill, E. E.; Cain, K. L.; Heywood, S. P.; Compson, J. E.; Heads, J. T.; Adams, R.; Humphreys, D. P. Towards a universal disulphide stabilised single chain Fv format: importance of interchain disulphide bond location and VL-VH orientation. *Protein Eng., Des. Sel.* **2012**, *25*, 321−329.
(38) *Fitzgerald ELISA optimization protocol*. www.fitzgerald-fii.com.



https://dx.doi.org/10.1021/acsomega.0c05340
*ACS Omega* 2021, 6, 762−774

(39) Eble, J. A. Titration ELISA as a method to determine the dissociation constant of receptor ligand interaction. *J. Visualized Exp.* **2018**, *132*, 1−9.
(40) Rajpal, A.; Beyaz, N.; Haber, L.; Cappuccilli, G.; Yee, H.; Bhatt, R. R.; Takeuchi, T.; Lerner, R. A.; Crea, R. A general method for greatly improving the affinity of antibodies by using combinatorial libraries. *Proc. Natl. Acad. Sci. U. S. A.* **2005**, *102*, 8466−8471.
(41) Rangnoi, K.; Choowongkomon, K.; O'Kennedy, R.; Rüker, F.; Yamabhai, M. Enhancement and analysis of human antiaflatoxin B1 (AFB1) scFv antibody-ligand interaction using chain shuffling. *J. Agric. Food Chem.* **2018**, *66*, 5713−5722.
(42) Vestby, L. K.; Gronseth, T.; Simm, R.; Nesse, L. L. Bacterial biofilm and its role in the pathogenesis of disease. *Antibiotics* **2020**, *9*, 59−29.
(43) Porath, J.; Carlsson, J.; Olsson, I.; Belfrage, G. Metal chelate affinity chromatography, a new approach to protein fractionation. *Nature* **1975**, *258*, 598−599.
(44) Todorova-Balvay, D.; Pitiot, O.; Bourhim, M.; Srikrishnan, T.; Vijayalakshmi, M. Immobilized metal-ion affinity chromatography of human antibodies and their proteolytic fragments. *J. Chromatogr. B Analyt Technol. Biomed. Life Sci.* **2004**, *808*, 57−62.
(45) Howarth, M.; Chinnapen, D. J.-F.; Gerrow, K.; Dorrestein, P. C.; Grandy, M. R.; Kelleher, N. L.; El-Husseini, A.; Ting, A. Y. A monovalent streptavidin with a single femtomolar biotin binding site. *Nat. Methods* **2006**, *3*, 267−273.
(46) Rangnoi, K.; Jaruseranee, N.; O'Kennedy, R.; Pansri, P.; Yamabhai, M. One-step detection of aflatoxin-B (1) using scFv-alkaline phosphatase-fusion selected from human phage display antibody library. *Mol. Biotechnol.* **2011**, *49*, 240−249.
(47) Sompunga, P.; Pruksametanan, N.; Rangnoi, K.; Choowongkomon, K.; Yamabhai, M. Generation of human and rabbit recombinant antibodies for the detection of Zearalenone by phage display antibody technology. *Talanta* **2019**, *201*, 397−405.
(48) Ye, J.; Ma, N.; Madden, T. L.; Ostell, J. M. IgBLAST: an immunoglobulin variable domain sequence analysis tool. *Nucleic Acids Res.* **2013**, *41*, W34−W40.
(49) Brochet, X.; Lefranc, M.-P.; Giudicelli, V. IMGT/V-QUEST: the highly customized and integrated system for IG and TR standardized V-J and V-D-J sequence analysis. *Nucleic Acids Res.* **2008**, *36*, W503−W508.
(50) Waterhouse, A.; Bertoni, M.; Bienert, S.; Studer, G.; Tauriello, G.; Gumienny, R.; Heer, F. T.; de Beer, T. A. P.; Rempfer, C.; Bordoli, L.; Lepore, R.; Schwede, T. SWISS-MODEL: homology modelling of protein structures and complexes. *Nucleic Acids Res.* **2018**, *46*, W296−W303.
(51) DeLano, W. L.; Bromberg, S. *PyMOL user's guide*; DeLano Scientific: San Carlos, CA, USA, 2004.
(52) Lobstein, J.; Emrich, C. A.; Jeans, C.; Faulkner, M.; Riggs, P.; Berkmen, M. SHuffle, a novel *Escherichia coli* protein expression strain capable of correctly folding disulfide bonded proteins in its cytoplasm. *Microb. Cell Fact.* **2012**, *11*, 753−716.
(53) Vu, N. X.; Pruksametanan, N.; Srila, W.; Yuttavanichakul, W.; Teamtisong, K.; Teaumroong, N.; Boonkerd, N.; Tittabutr, P.; Yamabhai, M. Generation of a rabbit single-chain fragment variable (scFv) antibody for specific detection of *Bradyrhizobium* sp. DOA9 in both free-living and bacteroid forms. *PLoS One* **2017**, *12*, e0179983.
(54) Schlapp, G.; Scavone, P.; Zunino, P.; Härtel, S. Development of 3D architecture of uropathogenic *Proteus mirabilis* batch culture biofilms-A quantitative confocal microscopy approach. *J. Microbiol. Methods* **2011**, *87*, 234−240.



https://dx.doi.org/10.1021/acsomega.0c05340
*ACS Omega* 2021, 6, 762−774

# BIOGRAPHY

Miss ThaeThae Min was born on January 31, 1975 in Mandalay, Union of Myanmar. She obtained MBBS from Institute of Medicine, Mandalay, Myanmar in 2000. She finished M.Med.Sc (Medical Microbiology) course at Institute of Medicine, Mandalay, Myanmar in 2005. She received a PhD degree in Medical Microbiology in 2012 at University of Medicine-1, Yangon, Myanmar. She has taken PhD (Molecular Biotechnology) course at School of Biotechnology, Institute of Agricultural Technology, Suranaree University of Technology, Thailand, since 2014. Until 2014, she worked as a lecturer at Department of Microbiology of University of Medicine-1, Yangon, Myanmar. She is interested in immunology, particularly in innate immune system components.

มหาวิทยาลัยเทคโนโลยีสุรนารี